THE EFFECTS OF THE CONDITIONS OF CHAR FORMATION ON THE PHYSICAL PROPERTIES OF CHARRED PHENOLIC-NYLON

by E. D. Smyly and C. D. Pears

Prepared under Contract NAS1-10517 by

SOUTHERN RESEARCH INSTITUTE
BIRMINGHAM, ALABAMA

for

NATIONAL AERONAUTICS AND SPACE ADMINISTRATION

FOREWORD

This report is submitted in accordance with the statement of work for Contract NAS1-10517.

The program was conducted by the Thermal Section of the Mechanical Engineering and Mechanics Division at the Southern Research Institute, Birmingham, Alabama, between January, 1971 and August, 1972. Mr. E. D. Smyly was Project Engineer and Dr. Ronald K. Clark of the Langley Research Center was the Technical Representative for this contract.

TABLE OF CONTENTS

TABLE OF CONTENTS - CONTINUED

LIST OF TABLES

LIST OF TABLES - CONTINUED

LIST OF ILLUSTRATIONS

LIST OF ILLUSTRATIONS - CONTINUED

LIST OF ILLUSTRATIONS - CONTINUED

LIST OF ILLUSTRATIONS - CONTINUED

LIST OF ILLUSTRATIONS - CONTINUED

LIST OF ILLUSTRATIONS - CONTINUED

LIST OF ILLUSTRATIONS - CONTINUED

LIST OF ILLUSTRATIONS - CONTINUED

LIST OF ILLUSTRATIONS - CONTINUED

LIST OF ILLUSTRATIONS - CONTINUED

SUMMARY

A study was made of the effects of the conditions of char formation on the physical properties of charred phenolic-nylon of 0.577 gm/cm^3 density. It was found that the thermal conductivity and several of the monitors correlate well with degradation conditions. The monitors included electrical resistivity, sonic velocity, porosity, lattice spacing and crystallite size.

Chars were prepared in the laboratory at controlled heating rates to various temperatures. The chars formed in the laboratory at heating rates above about 17 x 10^4 W/m^2 were found to be essentially the same as chars prepared at the "use" conditions in the arc-jet. The parameters varied were heating rate, residence time-at-temperature and maximum exposure temperature.

Chars prepared at very low heating rates but taken to high final temperature were found to be non-graphitizable and carbon-like even after subsequent exposures to 3000 K for relatively long times. At heating rates above about 17 x 10^4 W/m^2 and with any final temperature above 2000 K the chars were found to be quite graphitizable and graphite-like with further graphitization possible when exposed subsequently to, say, 3000 K.

For the chars prepared by rapid degradation, the crystalline nature and hence the thermal conductivity was found to be more dependent on residence time-at-temperature and the maximum exposure temperature. The monitors confirmed this behavior and provided quantitative results for these effects. The monitors which were found to be most sensitive to changes in the char as a function of thermal exposure were electrical resistivity, lattice spacing, crystallite size and thermal conductivity. The first three monitors also correlated well with thermal conductivity.

Dramatic effects were observed for the thermal conductivities of the rapidly formed chars as a function of the residence time-at-temperature and the maximum exposure temperature. The thermal conductivity shifted significantly upward as the residence time and maximum temperature were increased. These effects were most pronounced at temperatures above 2000 K. The typical shift to lower temperatures in the maximum of the thermal conductivity curve with increased crystalline order was observed.

Limited studies were also made on chars made from high-density phenolic-nylon and phenolic. The trends in the properties of these chars as a function of the degradation conditions were similar to those of the charred low-density phenolic-nylon. The char from the high-density phenolic-nylon was very much like that of the charred low-density phenolic-nylon except that it had a higher bulk density.

Data are also presented for properties other than those mentioned on the previous page. Measurements of weight loss, shrinkage, bulk density, true density, thermal expansion and sonic velocity are presented for the various chars.

An estimate was made of the thermal conductivity of the charred low-density phenolic-nylon as a function of temperature during ablation. The estimate was made by extrapolating the measured thermal conductivity values of the chars prepared at various formation temperatures. Then the locus of points of thermal conductivity at the formation temperature were connected. The values thus obtained were found to be somewhat lower than previous estimates for the charred low-density phenolic-nylon but in good agreement with chars formed in arc-jets.

INTRODUCTION

This is the final report to the National Aeronautics and Space Administration, Langley Research Center, for the work performed under Contract NAS1-10517. The purpose of this study was to investigate the effects of the conditions of char formation on the physical and structural properties of chars prepared from phenolic-nylon.

Specifically, the objective of this work was to investigate the relationships between physical and structural properties and the parameters which control degradation. The conditions of char formation considered were heating rate, time-at-temperature and maximum temperature. Chars were prepared in the laboratory from 0.577 gm/cm^3 phenolic-nylon at various heating rates to various maximum temperature levels. The chars were held at temperature for specific times and then cooled. The physical properties of the chars thus prepared were then measured at 300 K. The physical properties measured were electrical resistivity, ultrasonic velocity, bulk density, true density, lattice spacing, crystallite size, porosity, thermal expansion, weight loss and shrinkage. In addition, thermal conductivity measurements were made on selected chars over the temperature range from about 350 K to 1100 K.

Once a material is carbonized or graphitized and cooled rapidly from the maximum exposure temperature, the properties are essentially "locked-in" for the material as they were at the maximum condition. Then, if properties are measured at temperatures far below the maximum exposure temperature, one is characterizing the physical state of the material at the stage of carbonization or graphitization which was achieved by the high temperature exposure. Hence, the method of heating and cooling used in this program allowed a study of the

effects of the various exposure conditions on the physical state of the ablative chars formed at the various conditions. This provides one with quantitative measurements of the effects of the exposure conditions on the nature of the material (i.e., the degree of graphitization and the subsequent change in thermal conductivity). Such information should eventually allow one to predict the transient response of the thermal conductivity during ablation. However, the primary objective of this program was to see if correlations exist between the degradation conditions and the physical monitors and also between the physical monitors and the thermal conductivity.

When an ablative material is degraded, a carbonaceous structure is formed. At the formation temperature the structure is that of an amorphous or nongraphitized carbon. As the temperature is increased the structure becomes more ordered with a subsequent increase in thermal conductivity. The ordering of the structure is dependent upon at least the temperature level, the time-at-temperature, heating rate and probably environment. However, it is not known whether or not this effect is due to the basic way in which the polymer degrades as a function of heating rate or events induced by vapor deposition of carbon from the pyrolysis gases. Generally, phenolic-nylon is thought to be non-graphitizing. This conclusion was true at very low heating rates but not true for chars prepared at heating rates above those very low values.

The effective thermal conductivity of an ablation char formed from phenolic-nylon is controlled primarily by the thermal conductivity of the solid material in the char. Hence, the study concentrated on the effects of the degradation conditions on the nature of the char solid.

Most of the studies were performed on 0.577 gm/cm^3 phenolic-nylon which was degraded in the laboratory. However, limited studies were performed on arc-jet chars from the same material, high-density phenolic-nylon and phenolic.

SPECIMEN MATERIALS AND CUTTING PLANS

The materials used for the studies were supplied by the Langley Research Center. The standard material used was low-density phenolic-nylon with a virgin density of 0.577 gm/cm^3 and was manufactured by Hughes Aircraft Company. This material was supplied in panels about 38 cm x 46 cm x 3.2 cm thick. The panels used in this program were

designated as 1, 7 and 11. The panel number was used as a suffix before the specimen number in identifying the specimens. The composition of this material was as follows:

Constituent	Designation	Percent by Weight
Phenolic microballons	Union Carbide BJO-0930	23
Powdered phenolic resin	Union Carbide BRP-5549	37
Powdered nylon	6/6 Nylon, Dupont Zytel 103	40

In addition, a high density phenolic-nylon material was supplied. This material had a virgin density of about 1.202 gm/cm^3 and consisted of 50 weight percent of BRP-5549 phenolic powder and 50 weight percent of zytel 103 nylon. This material was supplied in a panel about 38 cm x 46 cm x 3.2 cm thick.

The phenolic used in the program was made from the same phenolic resin as was used in the low-density material and contained no filler. The density of the virgin phenolic was about 1.250 gm/cm^3. The phenolic which was supplied was a chord from a circular billet and was about 30 cm long x 8 cm wide x 6 cm thick.

Arc-jet chars were made by the NASA Langley Research Center. The arc-jet chars were made from the phenolic-nylon with a density of 0.577 gm/cm^3. Arc-jet specimens were 7.62 cm diameter by 2.54 cm thick. Charring was performed in an arc-jet at the following nominal conditions:

Test Gas	=	Nitrogen
Cold Wall Heat Flux	=	227×10^4 W/m^2 (200 Btu/sec ft^2)
Stream Enthalpy	=	23 258 J/gm (10 000 Btu/lb)
Model Pressure	=	5.1×10^3 N/M^2 (0.05 atmospheres)
Exposure Time	=	400-500 Seconds

Pictures of the arc-jet chars are presented in Figure 1.

Blanks for charring in the laboratory were cut from the panels which were supplied. The blank dimensions were 4.81 cm wide x 5.08 cm long x 0.952 cm thick. The thickness directions of the blank were taken in the thickness directions of the panels.

The cutting plans for specimens from the arc-jet chars are presented in Figures 2 and 3. Shown in Figure 2 is the cutting plans used to obtain specimens for thermal conductivity, electrical

resistivity, bulk density and sonic velocity. Shown in Figure 3 is the cutting plan for specimens for thermal expansion. Note that specimens were obtained at three different depths from the heated surface.

APPARATUSES AND PROCEDURES

Char Preparation

Chars were prepared in a high temperature furnace which employs an electrically heated graphite heater tube. The heater tube is cylindrical in shape. The heater tube temperature is controlled manually with a powerstat which drives a 25 kw transformer.

In most cases, chars were prepared by immersion of the char blanks in the furnace after it had been preheated to a selected temperature level. The char blanks which were 4.81 cm wide x 5.08 cm long x 0.952 cm thick were supported in a holder which could be rapidly inserted or extracted from the furnace. A picture of the specimen holder is given in Figure 4. Two blanks were charred at the same time. The blanks were placed back-to-back and were separated by graphite felt. Graphite felt insulation was also used around the edges of the specimen to prevent lateral heating. Thus, only one face of each blank was directly exposed to the heater tube. The back-to-back arrangement provided essentially one-dimensional heating of the char blanks by insulating the back surface of each blank.

The maximum temperature was measured for each char prepared. This was done by measuring the face temperature of the char through the sight port in the furnace. Temperatures were measured either with chromel/alumel thermocouples installed at the specimen surface through the sight port or by direct readings with an optical pyrometer. When using the optical pyrometer, appropriate corrections were made for the sight window.

Some specimens were left in the furnace to cool after the power had been turned off. These specimens have been designated as "in-furnace" cooling. The specimens made from the middle to the end of the program were rapidly cooled. This was done by withdrawing the specimens from the furnace at the end of the heating cycle and placing them inside a cold cylinder purged with helium. These specimens cooled rapidly by radiation and have been designated as rapid cooling by radiation.

A helium purge was used in the furnace during all of the char work. A helium purge also was inserted at the bottom of the heater tube and the gas traveled from bottom to top. This was used to

sweep the pyrolysis gases toward the top of the furnace.

The heating rate was specified as the radiant cold wall heat flux from the heater tube to a specimen with an emittance of 0.8. The correlation between furnace preheat temperature and cold wall heat flux is given in Table 1. The correlation is also rather good between the radiant cold wall heat flux and the convective cold-wall heat flux in a high enthalpy nitrogen gas stream. For example, at a furnace preheat temperature of 2500 K, the radiant cold wall heat flux is 177×10^4 W/m^2 and the surface quickly reaches a temperature of about 2500 K. In a nitrogen arc at high enthalpy the surface temperature is estimated to be about 2589 K at a convective cold wall heat flux of 227×10^4 W/m^2 (200 Btu/sec ft^2).

The thermal response of the chars prepared in the laboratory were defined from measurements of temperature at the surface and in-depth. Chromel/alumel thermocouples were installed in the char at a distance of 0.715 cm from the heated surface. The thermocouple wires were housed in double bore alumina tubing and were inserted in holes drilled parallel to the heated surface. The thermocouple wires melted at the point of exit from the specimen unless special provision was made to insulate them. The wires were insulated above the specimen with phenolic-nylon tubes placed around the insulator. These tubes were made to about the same thickness as the depth of the thermocouple from the surface.

The temperature measurements were used to define the heat treatment of specimens as to the time required for the front face and the in-depth thermocouple to achieve equilibrium. This aided in defining the uniformity of the char with regard to temperature exposure. Further, the time required to reach a uniform temperature at various furnace preheat conditions was utilized as a base for varying the residence time in the furnace. The results of the initial measurements which established the response were used throughout the program as being representative for all chars prepared.

Other specimen configurations were tried but the configuration described above was found to provide the most useable and geometrically stable char. For example, a very thin blank was used but was found to warp excessively. A blank was heated from both sides and contained a large central void. The specimen configuration selected seemed to provide the best tradeoff between geometric stability and a reasonable thickness for the subsequent physical measurements.

Special Char Handling Methods

Some special techniques were used to handle the ablative chars in order to make samples on which subsequent physical property measurements could be made. Most of the chars prepared at 2500 K and above were made into specimens by hand working. This involved careful sanding with 400 grit sandpaper to some thickness at which flat surfaces could be obtained. Then, the diameter was obtained by sanding on the edges of the blank after it was placed between two aligned steel references 1.905 cm in diameter. Extreme care was exercised in all sanding operations to prevent tearing the sample.

Some of the chars prepared at temperatures below 2500 K were also made into specimens by the sanding technique. However, most of these samples were extremely friable and an impregnation technique was used. The charred blanks were impregnated with Amoco resin 18-210 prior to a machining operation. Then, the samples were machined to the desired dimensions. The impregnant was removed by baking the machined sample in an inert environment for about 1 hour at 672 K. At this temperature the resin turns to a gas and leaves the specimen with essentially no residue.

An addition to the impregnation technique was added late in the program. Thin-walled rings made of transite were placed around the impregnated specimen after it had been machined. The rings were made about 0.075 cm thinner than the sample. These rings were left on during the bake-out operation and throughout subsequent electrical resistivity and sonic velocity measurement. This approach proved to be quite an aid in keeping the sample intact throughout the measurements. Of course, the rings were removed for thermal conductivity measurements.

Thermal Conductivity

A comparative rod apparatus was used for measurements to 1089 K. A complete description of the apparatus is given in Appendix I. The procedures for the evaluation were somewhat different from those given in the appendix. Since a thin sample was used the normal procedure of installing thermocouples inside the sample could not be used. Instead, the temperatures of the sample were measured at the surfaces. The technique used has been successfully employed in prior programs.

A schematic of the modified technique used for these measurements is given in Figure 5. A thin specimen was sandwiched between two sheets of Grafoil 0.025 cm thick and a "bare-wire" method was used to

measure the temperature of the Grafoil. The method consisted of pressing bare thermocouple wires against the surface of the Grafoil with a separation between wires of no more than 0.16 cm. This allowed the Grafoil to form the junction of the thermocouple. The thermocouple wires were inserted in double bore alumina insulators, and the ends of the wires were flattened to a thickness of 0.005 cm or less. The flattened ends of the wires were pressed against the surface by boron nitride discs which were slotted to the centerline to receive the insulator. The Grafoil was used on the surface of the sample because the specimen was highly porous. Had bare wires been used on the surface of the sample a surface temperature would probably not have been measured. Past experience has shown that Grafoil provides a good interface between two materials. In reducing the data, the temperature drop across the Grafoil was subtracted from the measured temperature difference. This correction normally was less than 2 percent of the total measured temperature difference.

The thermal conductivity of the specimens was reduced from the measurements as follows: the heat flux densities through the top and bottom references were calculated from the equation

$$\frac{Q}{A} = k \frac{\Delta T}{\Delta X} \tag{1}$$

where

$\frac{Q}{A}$ = heat flux density
k = thermal conductivity of reference
ΔT = temperature difference across gage length of reference
ΔX = gage length of reference

Under ideal conditions, the heat flux densities through the top and bottom references are identical. However, because of imperfect guarding and radial heat flow, this condition is seldom achieved in practice. Therefore, the heat flux through the specimen is taken as the average of the heat fluxes through the top and bottom references. Then the thermal conductivity of the specimen is calculated from the equation

$$k_s = \left| \frac{Q}{A} \right| \frac{\Delta X}{\Delta T} \tag{2}$$

The thermal conductivity of the specimen in terms of the thermal conductivities of the references and the temperature differences in the references can be derived by combining equations (1) and (2)

$$k_s = \left(\frac{k_1 \Delta T_1}{\Delta X_1} + \frac{k_2 \Delta T_2}{\Delta X_2} \right) \frac{\Delta X_s}{2 \Delta T_s} \qquad (3)$$

where subscripts s, 1, and 2 refer to the specimen, and lower and upper references, respectively.

All temperature measurements were made with Chromel Alumel thermocouples. Code 9606 Pyroceram was used as the reference material for the measurements. Thermatomic carbon was used as insulation in the annulus between the central column and the guard heater.

All measurements were made in a nitrogen environment.

There were two sources of error in the thermal conductivity measurements made in this program. The first error involves heat shunting around the sample which provides an erroneously high value when the thermal conductivity of the sample is below about 1.442 W/m-K (10 Btu in./hr ft^2 °F). This error decreases as the thermal conductivity of the sample increases. The second error is due to the interface resistance between the Grafoil and the sample which provides too high a measured temperature difference and hence an erroneously low value of thermal conductivity. Corrections were made for both of these sources of uncertainty.

The heat bypass error was defined from an analysis given by Flynn [1, 2][1]. According to Flynn the error is defined by

$$k_T = \frac{k_m}{1-\alpha} \qquad (4)$$

---

[1]Bracketed quantities refer to references cited at end of report.

where

k_T = corrected value of thermal conductivity

k_m = measured value of thermal conductivity

$$\alpha = k_i \left[\frac{1}{K_R} - \frac{1}{K_T} \right] F_g \qquad (5)$$

k_i = thermal conductivity of insulation around specimen

k_R = thermal conductivity of references

F_g = a geometric factor

The value of F_g depends upon the ratio of sample diameter to guard diameter and the temperature gradients in the guard relative to those in the central column [2]. For the experimental configuration used in this program, the specimen diameter was 1.905 cm and the diameter of the guard column was 5.08 cm. From prior studies here on thin samples, the value of F_g has been estimated to be 2.6. This value was used for the corrections in this program.

The thermal conductivity values used for the thermatomic carbon are given in Figure 6. The thermal conductivity values used for the Code 9606 Pyroceram references are given in Figure 7.

With the use of equations (4) and (5) and the thermal conductivity values given in Figures 6 and 7, a set of correction curves was developed which provided the corrected thermal conductivity in terms of the measured thermal conductivity for various mean temperatures. These curves are presented in Figures 8 and 9. Shown in Figure 8 are the correction curves for measured values up to 2.163 W/m-K. Shown in Figure 9 are the correction curves for measured values from 1.442 to 10.094 W/m-K.

In order to check the correction procedure an experimental measurement was made on FM5131 (phenolic-silica) which has a low value of thermal conductivity. The thermal conductivity of this material had previously been defined with the ASTM C-177 guarded hot plate apparatus. The results of this test are presented in Figure 10. The solid line shown in Figure 10 represents the values measured with the guarded hot plate. The circles are the values which were measured in the comparative rod apparatus. The X's given in Figure 10 are the values as corrected for heat bypass from Figure 9. Note that all of the corrected values agree within about 5 percent with the values defined from the guarded hot plate measurements. Hence, the correction procedure appears to be a logical analysis of the data.

The error due to interface resistance was defined from the equation

$$k_T = \frac{1}{\frac{1}{k_m} - \frac{1}{h\Delta\chi}} \qquad (6)$$

where

k_T = corrected value of thermal conductivity

k_m = measured value of thermal conductivity

h = combined interface heat transfer coefficient for both interfaces

$\Delta\chi$ = specimen thickness

A value for the interface coefficient of 1135 W/m^2-K was used for the correction analysis. This value was obtained from prior measurements between Grafoil and specimens with thermal conductivities ranging from 2.45 to 4.33 W/m-K. The corrected thermal conductivity is plotted versus the measured thermal conductivity in Figure 11 for various specimen thickness. Note that the correction is 14 percent for a measured thermal conductivity of 5.77 W/m-K and a sample thickness of 0.38 cm.

The correction for interface resistance was applied to the measured values after they had been corrected for heat bypass.

The uncertainty in measurements with the comparative rod apparatus is ±5 percent for the standard configuration. For the modified technique used in this program, the uncertainty is estimated to increase to ±10 percent. The increase in uncertainty is attributed to the uncertainties involved in the correction procedures.

Electrical Resistivity

Electrical resistivity measurements on the chars were very difficult because of the limited specimen thickness. The thinner samples introduced a problem with interface resistance because voltage probes could not be made inside the material. Several methods were tried in an attempt to overcome this problem and the best method was adopted.

The apparatus which was used to measure electrical resistivity is shown schematically in Figure 12. The sample was placed between

two discs of 0.0254 cm thick Grafoil and this was in turn placed between two stainless steel references to which the current leads were attached. The stainless steel references were electrically isolated from the support fixture and were dead weight loaded with a spherical joint under the bottom reference to facilitate alignment of the contact surface.

Voltage was measured with two aluminum foil voltage taps placed between the specimen and the Grafoil. The aluminum foil was about 0.001 cm thick and was cut into strips about 0.159 cm wide x 6.35 cm long. The voltage taps were placed diametrically across the sample and reached past the centerline.

A d.c. current was passed through the sample from a constant voltage power supply and was measured with a precision d.c. ammeter accurate to about 1 percent. Voltage was measured with a Leeds and Northrup Type K-3 potentiometer.

One would suppose that the measured values of electrical resistivity would be low because of the potential drop between the Grafoil and the specimen. However, it was found that non-uniform current distributions could provide high values. This was evidenced by the fact that in some cases the measured value of resistivity increased as the load on the specimen was increased. The ball joint connection was important in providing a uniform current distribution.

The nominal sample dimensions used was 1.905 cm diameter by 0.508 cm thick. The thickness varied from sample to sample.

The measurements were made at 300 K under a dead-weight load of 18.14 kgm. This was sufficient to cause the sample to indent the Grafoil uniformly.

Electrical resistivity was calculated from the equation.

$$\rho = \left(\frac{\Delta V}{I}\right) \frac{A}{L} \tag{7}$$

where

ρ = electrical resistivity
ΔV = voltage drop across sample
A = cross-section area of sample
I = direct current
L = sample thickness

All measurements were made with a current of 1 amp.

The uncertainty in the measurements was checked with some test runs. One test involved using a porous char specimen which was about 1.905 cm long. First, measurements were made on this sample with voltage probes inserted in the sample 0.790 cm apart. This provided a value without an interface problem. The value measured at 22.68 kgm load was 33 100 μΩ-cm. The char was then sanded to a thickness of 0.627 cm and the surface technique of measuring voltage was used. The value measured on the thin char at 22.68 K gm load was 33 300 μΩ-cm. Assuming isotropy, agreement was good.

A further test involved measurements on one of the chars prepared in this program (Specimen 11-122) which had been exposed to 3100 K. Measurements were made on this sample at a thickness of 0.503 cm and then it was sanded to 0.254 cm and the measurements repeated. At 18.14 kgm load, a value of 7900 μΩ-cm was measured with the sample 0.254 cm thick and a value of 8200 μΩ-cm was measured with the sample 0.254 cm thick. The fact that the measured value did not increase significantly when the sample thickness was halved indicates that the interface voltage drop was a small portion of the total. However, the overall value for the char may have changed due to the sanding since the char probably had somewhat of a variation in property through the thickness due to the degradation process.

Further experimental measurements on a low-resistivity graphite ($\rho \simeq 900$ μΩ-cm) indicated that the total interface voltage drop should at worst be 0.5 mv at 1 amp current for a 1.905 cm diameter specimen. This would indicate a 30 percent error for the lowest resistivity char evaluated ($\rho = 6000$μΩ-cm).

To summarize, the uncertainty in the electrical resistivity measurements is estimated to be a maximum of 30 percent for the lowest resistivity chars. More realistically, we expect that for most chars the uncertainty was on the order of 10 percent when good uniform contact was achieved as evidenced by a uniform impression of the char on the Grafoil.

Sonic Velocity

The basic apparatuses used in the measurement of ultrasonic velocity were a Sperry UM721 Reflectoscope and a Tektronix 564 Oscilloscope. Velocity is evaluated using the through-transmission, elapsed-time technique. The Sperry UM721 is used as the pulser, and the Tektronix 564 complete with a 3B3 time base (precision of 1 percent) and a 3A3 vertical amplifier is used as the signal measuring device.

In using the through-transmission, elapsed-time technique for measuring acoustic velocity, a short pulse of longitudinal-mode sound is transmitted through the specimen. An electrical pulse originates in a pulse generator and is applied to a ceramic piezoelectric crystal (SFZ). The pulse generated by this crystal is transmitted through a short delay line and inserted into the specimen. The time of insertion of the leading edge of this sound beam is the reference point on the time base of the oscilloscope which is used as a high-speed stopwatch. When the leading edge of this pulse of energy reaches the other end of the specimen, it is displayed on the oscilloscope. The difference between the entrance and exit times is used with the specimen length in calculating ultrasonic velocity. A short lucite delay line is used to allow time isolation of the sound wave from electrostatic coupling and to facilitate clear presentation of the leading edge of the entrant wave resulting in a more accurate "zero" for time.

Using 0.5/1.0 MHz transducers coupled with alcohol, the precision for this velocity measurement technique has been established for polygraphites such as ATJ-S to be ±0.005 cm per microsecond for a 10.16 cm long by 1.27 cm diameter specimen, to be ±0.025 cm per microsecond for a 0.635 cm long by 0.635 cm diameter specimen.

For the measurements in this program, a solid coupling media was used between the specimen and transducer to provide a clear signal. Sheets of silicone gum rubber about 0.318 cm thick were used at each interface. The transducers were loaded against the gum rubber with a loading fixture which works like the spindle on a drill press. Generally, this technique provided a reasonably clean signal for the measurements.

Using the gum rubber technique, the repeatability of the measurements was about 0.0127 cm per microsecond was obtained. In many cases, the specimen was destroyed when unloading after the test.

Thermal Expansion

Thermal expansion was measured with the quartz dilatometer described in Appendix II. Normally, a 7.62 cm specimen is used. Since the chars in this program were so thin, several squares of material about 0.508 cm long were stacked to provide a longer specimen.

A schematic of the method used to measure the thermal expansion of the thin char samples in the charring direction is given in

Figure 13. Squares of charred material about 0.635 cm x 0.635 cm x 0.508 cm thick were stacked inside a holder with a square section to provide either a 2.54 cm or a 5.08 cm sample, depending upon the amount of material available. Since the apparatus was calibrated for a 7.62 cm long specimen quartz extension rods were placed on either end of the sample. These rods were flat on the end which contacted the sample and had a 7.62 cm spherical radius on the other end.

The holder which contained the sample and extension rods was inserted in the dilatometer tube. Then the push rod was placed in the tube and the remainder of the buildup and evaluation was by standard techniques.

In some cases, the chars were impregnated with Amoco resin 18-210 prior to being machined into the squares. For those runs, the impregnated sample was built up as described and the impregnant was baked out by heating to about 672 K for one hour. After the bakeout, the apparatus was cooled to 300 K, initial dial gage readings were obtained and the measurement was made.

The calculation of the unit thermal expansion of the specimens was not as straight forward as it normally is because allowance had to be made for the extension rods since the specimen was less than 7.62 cm long. The unit thermal expansion was determined from the following equation:

$$\left(\frac{\Delta L}{L}\right)_S = \frac{L_T}{L_S}\left[\left(\frac{\Delta L}{L}\right)_T + \left(\frac{\Delta L}{L}\right)_{QC}\right] - \frac{L_E}{L_S}\left(\frac{\Delta L}{L}\right)_E \qquad (8)$$

where

$\left(\frac{\Delta L}{L}\right)_S$ = unit thermal expansion of specimen

$\left(\frac{\Delta L}{L}\right)_E$ = observed total thermal expansion divided by length of specimen and extension rod

$\left(\frac{\Delta L}{L}\right)_{QC}$ = correction for dilatometer tube based on 7.62 cm 3 inches long specimen

$\left(\frac{\Delta L}{L}\right)_E$ = unit thermal expansion of quartz extension rod

L_S = specimen length

L_E = length of quartz extension rod

$L_T = L_E + L_S$

In using equation (8), $(\frac{\Delta L}{L})_E$ was obtained from the NBS curve for fused silica. The correction for the dilatometer tube was obtained from calibration runs on a fused silica standard.

The uncertainty of these measurements with the quartz dilatometer is estimated to be $\pm 0.2 \times 10^{-3}$ cm/cm.

Lattice Spacing and Crystallite Size

The d_{002} lattice spacing and the L_{002} crystallite size were measured by x-ray diffraction techniques. The equipment for these measurements consisted of a Siemens Crystallaflex IV generator having a horizontal diffractometer. A copper x-ray tube and a scintillation counter along with a counting and recording console were used in conjunction with the generator and diffractometer.

The instrumental conditions for the measurements were as follows:

Diffractometer		Console	
Voltage	- 30kV	Dector voltage	- 625V
Amperage	- 20ma	Pulse height analyzer	
Entrance Slit	- 1.0mm	Baseline	- 17.8V
Exit Slit	- 0.1mm	Window	- 20.0V
Tube	- copper	Statistical Error	- 3%
Filter	- nickel	Chart Speed	- 1cm/min
Scan Speed	- 1/8°/min	Range	- variable

In preparing the samples, the entire char sample was ground to pass a 325 mesh screen. The sample was weighed, and -325 mesh reagent grade KCl equal to 10 percent of the char weight was added for an internal standard. This mixture was blended with sufficient silicone vacuum grease to make a workable mass. Depending on the character of the char, grease equivalent to 0.5 to 1.0 times the char weight was required. This plastic mass was pressed into a luecite holder having a cavity 2.5cm in diameter and 1mm deep. The specimen surface was made flat and parallel to the holder surface by scraping off the excess using a straight edge with sawing action.

Having determined the approximate intensity of the (002) graphite reflection, the appropriate range was selected for the recording console. The specimen was then scanned at 1/8°/min through the 2θ range of 22° to 30°. Within this range, the (002) graphite line and the (200) KCl line occur at approximately 26° and 28° 2θ respectively.

From this scan the angular line breadth at 1/2 peak height in degrees and the exact angular position of the peaks were determined graphically. The angular position was determined as the mid-point at 1/2 height.

The d_{002} value in Å was calculated from the Bragg equation, $\eta\lambda = 2 d_{002} \sin\theta$; where η = order of diffraction (1 in this case), λ = wavelength of X-radiation (1.5418, Kα cooper), θ = 1/2 of angular position of the peak in degrees.

This calculated value was corrected using the (200) reflection from KCl. The d_{200} value for the (200) reflection for KCl is 3.146 Å, ASTM card 40587. For each specimen a correction factor was established using the experimentally determined d_{200} and the ASTM value. This correction was applied to the calculated d_{002} value for the char specimen.

The L_{002} value was calculated from the Scherrer expression, $L_{002} = \frac{0.89 \times \lambda}{\beta \times \cos\theta}$; where L_{002} is the crystallite size in Å in the "c" direction and β is the corrected breadth of the (002) peak at 1/2 height in radians. Corrections for instrument broadening and Kα doublet were applied to the measured line breadth, B_0, to obtain β.

Some measurements were made of the lattice parameters as a function of position in the char sample. For those cases, the char was shaved to various measured depths and a sample was prepared as discussed above. In this way, the samples could be correlated with the average distance from the surface.

Porosity by Liquid Absorption

Porosity and bulk density were evaluated using a liquid absorption technique. Using this technique, mineral spirits (s.g. ∿0.76) is vacuum impregnated into samples of material. From measurements of dry weight, suspended weight and saturated weight, evaluations of absorption, density (bulk and apparent), and open porosity can be calculated directly. If the true density of the material sample is known, the total porosity and thus, the closed porosity of the material sample can be calculated.

The normal procedure used in making liquid absorption measurements involves first a thorough drying and then precise weighing of specimens to determine dry, suspended and saturated weights (recorded to nearest 0.0001 gram). First, the specimens are oven

dried at temperature above 373 K for two hours to drive out absorbed moisture and then weighed to determined dry weight. Individual specimens are then placed in small beakers which are placed on their sides in a desiccator. After the desiccator is sealed off, the pressure is reduced to 6.65 N/M^2 (50 microns of Hg) and held for two hours to remove entrapped air from the specimens. The desiccator is then purged with mineral spirits until the beakers containing the specimens are submerged. The desiccator is then vented, and the specimens are left in the desiccator for 20 minutes to allow vapor inside the specimens to condense.

The suspended weight is obtained by weighing the saturated specimen while suspended in the mineral spirits. The specimens are kept submerged by righting the beakers in the desiccator to maintain the mineral spirits level above the specimen. As shown in Figure 14, a basket is suspended from a balanced beam such that the level of mineral spirits in the individual beakers cover the specimen and basket at all times during the weighing operation. The tare weight of the basket, which is subtracted from the total suspended weight to determine the suspended weight of the specimen, is determined by weighing the suspended basket submerged in mineral spirits to the same depth that the specimen is weighed. Care is used to ensure that no air bubbles cling to the basket and that a clearance between the basket and sides of the beaker is maintained.

For determining saturated weight, the specimens are removed from the mineral spirits and wiped carefully to remove excessive surface mineral spirits. The specimens are then weighed immediately to determine the saturated weight.

From the three weights taken for each specimen (dry weight, suspended weight and saturated weight) percent water absorption, open porosity, bulk density and apparent density are determined. The total porosity can be determined also when the true density of the material is known. The equations used for these calculations are:

$$W_a = \left(\frac{W_{sa} - W_d}{W_d} \right) \frac{\rho_w}{\rho_m} \times 100 \text{ percent} \qquad (9)$$

$$P_o = \left(\frac{W_{sa} - W_d}{W_{sa} - W_{su}} \right) \times 100 \text{ percent} \qquad (10)$$

$$\rho_b = \left(\frac{W_d}{W_{sa} - W_{su}} \right) \times \rho_m \qquad (11)$$

$$\rho_a = \left(\frac{W_d}{W_d - W_{su}} \right) \times \rho_m \qquad (12)$$

$$P_t = \left(\frac{\frac{W_{sa} - W_{su}}{\rho_m} - \frac{W_d}{\rho_t}}{\frac{W_{sa} - W_{su}}{\rho_m}} \right) \times 100 \text{ percent} \qquad (13)$$

where

W_a = Water absorption
W_{sa} = Weight of sample when saturated with liquid m
W_d = Dry weight of sample
W_{su} = Weight of sample when suspended in liquid m
ρ_m = Density of liquid m (about 0.76 gm/cm^3 for mineral spirits - s.g. checked after each run)
ρ_w = Density of liquid water
ρ_t = True density of sample
ρ_b = Bulk density of sample
ρ_a = Apparent density of sample
P_o = Open porosity
P_t = Total porosity

Weights for this evaluation are determined using an analytical balance sensitive to 0.0001 gram. Instrument precision for measuring absorption is ±0.10, bulk density is ±0.002 gm/cm^3, open porosity is ±0.15 and total porosity is ±0.05.

Total porosity was calculated from equation (13). True density values obtained by liquid pycnometry on pulverized samples were used in the equation.

Weight Loss

Weight loss was determined from measurements of weight made before and after the samples were charred. The weight was measured on an analytical balance sensitive to 0.0001 gram. In some cases, the specimens fell apart during the char process and fell in the furnace and final weights could not be accurately obtained. Generally, this occurred at furnace preheat temperature of 1366 K and below.

Shrinkage

Shrinkage was obtained from measurements of the specimen thickness before and after charring. The measurements were made with micrometers.

The specimens did not shrink uniformly and the back surface of the char was somewhat unlike the heated surface. The final thickness was measured in the center of the char blank over the full thickness. Since the back portion of the chars was unlike that at the front (probably due to some two-dimensional heating near the back) the shrinkage measured was somewhat of an average over the full thickness and not related strictly to the front portion of the char which was used for subsequent physical property measurements. Nevertheless, the measured values are representative of the specimens cut from the blanks since the back face zone of the char which was removed was less than 1/4 of the overall thickness.

Bulk Density

Bulk density was calculated from measurements of weight and dimensions on char specimens. Reasonably good disc geometries were obtained from the chars prepared at furnace preheat temperatures of 2500 K and above. However, chars prepared at preheat temperatures of 2000 K and below generally could not be made into a good geometry because portions of the specimen fell off.

In the tables two bulk density values are given, the char bulk density was a crude value obtained from measurements on the entire char blank which generally had an irregular shape. The coupon density was obtained on the sample prepared from the blank.

For the chars prepared at furnace preheat temperatures of 2000 K and below, the blanks were impregnated before machining to a known geometry. After the specimens were machined the dimensions were measured with micrometers. Then, the impregnant was baked out at 672 K for one hour and the specimen was weighed.

Measurements of weight were made with an analytic balance with a sensitivity of 0.0001 gm. Measurements of dimensions were made with micrometers which were read to the nearest 0.0013 cm.

True Density

The true density was measured with a pycnometer, using the procedure outlined in ASTM C 135-66. Prior to making the measurements the samples were pulverized to as fine a particle size as

was possible. Normally, the particles were passed through a U. S. Standard 325 mesh screen which has an opening of 44×10^{-6}m. This is the smallest opening size available in the standard series. However, most of the particles were probably smaller than 44×10^{-6}m. This same procedure has been used in the past on arc-jet chars and measurements of the particle sizes after pulverization showed that nearly all of the particles were less than 12×10^{-6}m in size and that 75 percent were less than 2×10^{-6}m in size.

Only that portion of the char blanks ranging from 1/2 to 3/4 of the thickness from the front surface was used for these measurements because of the loose unstructured char on the back surface and to alleviate edge effects. Hence, the amount of material used for the measurements was less than the 1 gram weight recommended by ASTM C 135-66. For this reason, a pycnometer with a volume of only 10 cm^3 was used. The small sample size made the measurements difficult.

Both water and ethanol were used as fluids for the pycnometer. A wetting agent, Tergitol TNN, a nonionic detergent, which is a product of Union Carbide, was used for the measurements with water to reduce surface tension effects. We estimate that the true density measurements themselves had an uncertainty of about ±5 percent. The major uncertainty in the measurements, however, is that some entrained porosity may be retained after pulverization.

Micrography

Some micrographic work was performed on the chars as an aid in defining the structure. The samples for micrographic analysis were first impregnated with a plastic under atmospheric pressure and then after sectioning were reimpregnated under vacuum. The samples were resectioned and polished for photomicrographs.

Photomicrographs of the samples were made with a Vickers M-55 metallograph with a Polaroid camera attachment. Photomicrographs were made at magnifications of about 100 x and 500 x.

DATA AND RESULTS

Definition of Char Histories

Temperature measurements were made on chars prepared from the 0.577 gm/cm^3 phenolic-nylon at the different furnace preheat conditions to define the thermal responses. Temperatures were measured on the heated surface and at a depth of 0.714 cm below the heated surface. The overall blank thickness was 0.953 cm. Table 1

gives the relation between furnace preheat temperature and radiant cold wall heat flux.

Figures 15 through 22 give the results of the temperature measurements for the various conditions. These chars are called the chars prepared by rapid degradation. These curves define the time required for the material to fully char such that temperature uniformity is achieved between the front surface and a depth of 0.714 cm. This time decreases as the furnace preheat temperature is increased (cold wall heat flux increased).

The NASA Langley Research Center performed some calculations for two different conditions to analytically define the time required for thermal equilibrium. The results of these calculations are presented in Figures 18 and 22. Note in Figure 18 that at a furnace preheat temperature of 2000 K, about 150 seconds were required for thermal equilibrium over a 0.714 cm depth. As shown in Figure 22, 60 seconds were required to reach thermal equilibrium at a furnace preheat temperature of 3100 K. Observe in Figures 18 and 22 that the measured and calculated values are in reasonable agreement.

All of the char histories for the different preheat conditions are summarized in Figure 23. Cooling curves for cooling in the furnace are presented in the figure along with the heating curves. In general, about 100 seconds were required for the specimens to cool 500 K below the maximum temperature, this time was not counted.

Figure 24 gives the time required to reach thermal equilibrium versus furnace preheat temperature. This curve was used in defining the time-at-temperature. At any given furnace preheat condition, the time given in Figure 24 was subtracted from the total time in the powered-furnace to define the time-at-temperature.

Figure 25 gives the approximate temperature rise rate through the degradation zone (about 800 K) at the surface and at 0.714 cm below the surface. These curves were developed from the slopes of the temperature-time curves in Figures 18 through 22. These curves box the temperature rise rates through the char.

Figure 26 gives the char thickness as a function of time for furnace preheat temperatures of 2000 and 3000 K. These curves were obtained from the analytical results supplied by the NASA Langley Research Center.

In addition to the chars prepared by rapid degradation, chars were also prepared at slow heating rates. In general, these chars

were heated at a low temperature rise rate to the desired maximum temperature. The degradation condition for these chars was specified by the temperature rise rate. A typical curve is shown in Figure 27.

A specimen of the phenolic was charred at a very slow heating condition in the last attempt to develop a highly dense char. The temperature-time history of Specimen HMP is given in Figure 28. Note that the char cycle took 60 hours to reach 920 K. At that point in the cycle it was found that the specimen contained cracks and voids. However, since it was the best that was achieved it was further heat treated to 3033 K and used for measurements. Many other char cycles were attempted, none of which provided the desired crack-free specimen.

An estimate was made of the final temperature distribution through the arc-jet chars prepared by the NASA Langley Research Center. These chars were prepared in a nitrogen stream at a cold wall heat flux of 227 x 10^4 W/m^2 for 400 to 500 seconds. The enthalpy of the stream was 23 258 J/gm. The surface temperature was estimated from a radiation heat balance with an estimated hot wall heat flux of 204 x 10^4 W/m^2. Assuming that 6.8 x 10^4 W/m^2 was conducted in and a surface emittance of 0.8, the surface temperature was calculated to be 2561 K. Since the arc-jet specimen had been fully charred, it was assumed that the back face temperature reached 1000 K. Then, using our best estimate of the thermal conductivity a maximum temperature distribution was obtained.

The results of the calculation for the final temperature distribution in the arc-jet chars are presented in Figure 29. The X's on the figure give the approximate median locations from which specimens were removed. The O's give the median locations for samples removed for x-ray diffraction measurements as a function of position. The values of temperature shown were used for all correlations of the arc-jet data.

Char Structures Obtained

Pictures of the chars prepared from the 0.577 gm/cm^3 phenolic-nylon at the different conditions are presented in Figure 30 through 33. As shown in Figure 30, a very dense homogeneous char was obtained at the lowest heating rate of 0.09k/sec. Note in Figures 30 and 31 that the char fragmented at heating rates of 1.7 k/sec and 17 x 10^4 W/m^2 (1400 K furnace preheat). Specimens prepared at these conditions were unusable. At heat fluxes of 72.5 x 10^4 W/m^2 (2000 K furnace preheat) and above the chars had sufficient structural integrity to be used. However, the chars

prepared at 72.5 x 10^4 W/m^2 were marginal and all could not be used.

Observe in Figures 30, 31 and 33 that the cold face of the char had a much coarser structure than the heated face. It is believed that this resulted from a low heating rate at that surface coupled with some two-dimensional heating. The coarse surface was removed from the specimen when making specimens from the char blanks. A typical char structure with the coarse skin removed is shown in Figure 33. Generally, the removal of the skin on the cold face left a specimen thickness of about 0.508 cm. Hence, the specimens were taken from inside the region for which the thermal response had been defined.

Section views of chars made from the 0.577 gm/cm^3 phenolic-nylon are presented in Figures 34 and 35. These chars have a similar columnar structure to the arc-jet chars shown in Figure 1. The dark regions at the cold side of the chars are the coarse skin which was removed in subsequent sample preparation.

Specimen 1-22 and 1-24 shown in Figure 34 were prepared at a cold wall heat flux of 72.5 x 10^4 W/cm^2 (2000 K preheat). Specimen 1-87 shown in Figure 35 was prepared at 177 x 10^4 W/m^2 (2500 K preheat). Note the lack of curvature in Specimen 1-87 which was prepared at 177 x 10^4 W/m^2 as compared to Specimens 1-22 and 1-24. Further, the column were smaller and more aligned for Specimen 1-87 than for Specimens 1-22 and 1-24. Refer back to Figure 1 and note that a similar change in structure is noted between the hot and cold surfaces which had different heating rates. Thus, the laboratory chars correlate rather well visually with the arc-jet chars.

Pictures of the phenolic which was charred by rapid degradation are shown in Figure 36. These chars are similar in structure to those prepared from the phenolic-nylon. Again, the structure was tighter and had more integrity as the heating rate was increased.

The high-density phenolic-nylon had a char structure similar to the 0.577 gm/cm^3 phenolic-nylon.

Overlay photomicrographs at about 50 to 70 x of the chars prepared at the different heating rates are given in Figures 37 through 43. The photomicrographs were made such that the structure is viewed perpendicular to the exposed face. The impregnant used was very clear and because of this it is hard to discern the detailed char structure.

The chars shown in Figures 37 through 42 are ordered by heating rate. As shown in Figures 37 and 38, the char structure is uniformly porous for heating rates of 0.1 and 1.5 K/sec. The char structure contains more crack-type porosity at heating rates of 17 x 10^4 and 72.5 x 10^4 W/m^2 as shown in Figures 39 and 40. As the heating rate is further increased (see Figures 41 and 42) the structure again becomes more uniform and the cracks parallel to the direction of heat flow are evident.

In the photomicrographs shown in Figures 37 through 42, the white areas are the solid walls of the porous char structure. The gray areas are the impregnant. The dark areas are the voids in the char structure which may or may not contain impregnant. Note in Figure 42 that most of porous area is filled with impregnant.

An overlay photomicrograph of phenolic charred at 418 x 10^4 W/m^2 is given in Figure 43. The view given is perpendicular to the direction of heat flow. The structure of this char is peculiar in that there are numerous small cracks which are oriented perpendicular to the heat flow and then some large cracks parallel to the heat flow. The structure gives one the impression that outgassing may have occurred laterally.

Photomicrographs of chars prepared at various heating rates from the 0.577 gm/cm^3 phenolic-nylon are presented in Figures 44 through 47. Polarized light was used to best detect carbon vapor deposition. Little deposition is noted in Figure 44 for the range of low heating rates of 0.1 to 1.5° K/sec. However, as shown in Figures 45 through 47, there is some evidence of deposition for the chars prepared at heat fluxes of 17.5 x 10^4 W/m^2 and above. The deposition occurred predominately at the front face which was the face exposed to the heater. Photomicrographs at about 500 x and 1000 x of phenolic charred at 48 x 10^4 W/m^2 are given in Figure 48. Inside the pores, the chars appears somewhat graphite-like but there is little evidence of deposition.

Pictures of Specimen HMP which was prepared from phenolic at a very low and interrupted heating rate are shown in Figure 49. Even though the specimen had a bulk density above 1 gm/cm^3 the porosity is evident. This large porosity could not be removed even though the specimen was very slowly charred. The pores shown in Figure 49 were oriented parallel to the thickness direction of the virgin phenolic and hence may relate to the structure of the virgin material.

Effect of Cold Wall Heat Flux on Monitors. - This section deals with the results of measurements of the physical monitors of chars prepared from the low density phenolic-nylon at various heat fluxes. All of the data presented in this section are for chars which were exposed for short times at the maximum temperature. All monitor measurements were made at 300 K. The zero heat flux condition represents chars prepared at 0.1 and 1.5°K/sec.

The experimental data are presented in Tables 2 through 9 and in Figures 50 through 64.

Shown in Figures 50 and 51 are the effects of cold wall heat flux on the electrical resistivity of chars prepared to temperatures of 2000 and 3100 K, respectively. At 2000 K there was an increase in electrical resistivity from about 0.037 Ω-cm at the slow heating condition to 0.048 Ω-cm at a heat flux of 72.5×10^4 W/m^2. The effects of heat flux on chars prepared to 3100 K are presented in Figure 51. The electrical resistivity decreased with heat flux to a minimum at about 177×10^4 W/m^2 and then exhibited an increase up to a heat flux of 418×10^4 W/m^2. There does seem to be a minimum at 177×10^4 W/m^2; however, because of the range of values at 418×10^4 W/m^2 it appears that the electrical resistivity is not strongly influenced by heat flux above 72.5×10^4 W/m^2. There is very definitely a decrease in resistivity up to a heat flux of 72.5×10^4 W/m^2 for chars prepared to 3100 K.

The effects of heat flux on sonic velocity are presented in Figures 52 and 53 for chars prepared to temperatures of 2000 and 3000 K respectively. For chars prepared to 2000 K there was a decrease in sonic velocity from a very low heating rate to a heating rate of 72.5×10^4 W/m^2. For chars prepared to 3100 K, the sonic velocity exhibited a decrease to a heat flux of about 72.5×10^4 W/m^2 and appeared reasonably constant above this value.

The effects of heat flux on lattice spacing and crystallite size are presented in Figures 54 and 55 for chars prepared to 2000 and 3100 K, respectively. For chars prepared to 2000 K, there was a dramatic decrease in lattice spacing from the very low heating rate to a cold wall heat flux of 17×10^4 W/m^2. Above 17×10^4 W/m^2 the lattice spacing was constant. The crystallite size increased to a heat flux of 17×10^4 W/m^2 and then remained constant above that value.

For chars prepared to 3100 K, there was a decrease in lattice spacing up to a heat flux of about 17×10^4 W/m^2 and then the spacing remained reasonably constant out to a heat flux of 418×10^4 W/m^2. There appears to be a minimum at a heat flux of about

177 x 10^4 W/m^2. The crystallite size increased from a very low heat flux to a value of about 17 x 10^4 W/m^2 and then remained constant out to a heat flux of 177 x 10^4 W/m^2. There was a decrease in crystallite size as the heat flux increased from 177 x 10^4 W/m^2 to 418 x 10^4 W/m^2.

The effects of heat flux on weight loss are presented in Figures 56 and 57 for chars prepared to 2000 and 3100 K, respectively. For chars prepared to 2000 K, there was a continual decrease in weight loss as the heat flux was increased. For chars prepared to 3100 K (see Figure 57), the weight loss decreased until a heat flux of about 177 x 10^4 W/m^2 was reached and then remained relatively constant.

Data for bulk density as a function of heat flux for chars prepared to 2000 and 3100 K are presented in Figures 58 and 59, respectively. For chars prepared to 2000 K, there was a decrease in bulk density from a value of about 0.33 gm/cm^3 at a very low heating rate to a value of about 0.27 gm/cm^3 at a heat flux of 72.5 x 10^4 W/m^2. For chars prepared to 3100 K, the bulk density ranged from about 0.29 to 0.305 gm/cm^3. It is expected that the bulk density of the chars prepared to 2000 K at a heating rate of 72.5 x 10^4 W/m^2 would have retained the low bulk density had they been heated to 3100 K and hence the average value for those chars was presented in Figure 59.

The shrinkages in the charring direction as a function of heat flux for chars prepared to 2000 and 3100 K are presented in Figures 60 and 61, respectively. For chars prepared to 2000 K, the shrinkage was a maximum of 25 percent at a very low heating rate and decreased to a constant value of about 17.5 percent at a heat flux of 17 x 10^4 W/m^2. For chars prepared to 3100 K, the shrinkage was a maximum of about 22.5 percent at a very low heating rate and decreased to the range of 13 to 14.5 percent for heat fluxes above about 17 x 10^4 W/m^2.

The results of liquid absorption measurements on chars prepared at various heating rates are presented in Figure 62. The absorption increased from about 100 percent at a very low heating rate to a maximum of about 550 percent. Then, the absorption decreased to values of about 200 percent for heating rates from 72.5 x 10^4 W/m^2 to 418 x 10^4 W/m^2. Note that the absorption was always above 100 percent meaning that the weight of water absorbed was greater than the dry weight of the specimen.

The results of true density measurements on chars prepared from low-density phenolic-nylon to 3100 K at various heat fluxes are presented in Figure 63. The true density decreased from a

value of 1.41 gm/cm^3 at a very low heating rate to a minimum of 1.26 gm/cm^3 for char prepared at 17 x 10^4 W/m^2. For heat fluxes above 72.5 x 10^4 W/m^2 the true density was constant at about 1.44 gm/cm^3.

The porosities of chars prepared at various heat fluxes are presented in Figure 64. The values were obtained from the liquid absorption measurements and the true density values shown in Figure 63 were used to calculate the total porosity. The open porosity increased as the heat flux increased from a value of 37 percent at a low heating rate to a maximum of 80 percent at 17 x 10^4 W/m^2. For heat fluxes between 72.5 x 10^4 and 418 x 10^4, the open porosity ranged from 62 to 67 percent.

As shown in Figure 64, the closed porosity decreased from a value of about 39 percent at a low heating rate to a minimum of 8 percent at a heat flux 17 x 10^4 W/m^2. For heat fluxes above 72.5 x 10^4 W/m^2 the closed porosity ranged from 10 to 15 percent.

The total porosity of the chars reached a maximum of 88 percent at a heat flux of 17 x 10^4 W/m^2. At other heat fluxes the total porosity ranged from about 74 to 80 percent.

Note in Figure 64 that the char prepared at the lowest heat flux contained the most closed porosity and the open and closed porosities were about equal. In heat fluxes above about 72.5 x 10^4 W/m^2 the closed porosity was about 14 percent and the open porosity was about 64 percent for a total porosity of about 78 percent.

Effect of Time-at-Temperature on Monitors. - This section describes the results for the effects of time-at-temperature on the physical monitors for chars prepared from the low-density (0.577 gm/cm^3) phenolic-nylon. The chars were prepared at heat fluxes of 72.5 x 10^4, 177 x 10^4 and 418 x 10^4 W/m^2 to maximum temperatures of 2000, 2500 and 3100 K, respectively. The hold times at temperature were varied. The monitor properties were measured at 300 K. The experimental data for the effects of time-at-temperature are presented in Tables 1 through 8 and in Figures 65 through 78.

Figures 65, 66 and 67 give the results for the effects of time-at-temperature on the electrical resistivity for chars prepared to 2000, 2500 and 3100 K, respectively. The data scatter was quite severe at all temperatures. Nevertheless, the results indicate a decrease in electrical resistivity as a function of residence time at the various temperatures.

The electrical resistivity versus residence time for chars prepared to 3100 K is presented in Figure 67. The +'s on the figure represent values which have been normalized for sample thickness. These results are replotted on a semi-log scale in Figure 68. The correlation of electrical resistivity versus

thickness which was used for the normalization is given in Figure 69. The values were normalized to a thickness of 0.381 cm. Hence, results which at first glance appear to be scattered are found to be real variations due to sample thickness. Note that the effect of sample thickness decreases as the time-at-temperature increases. Thickness correlations were attempted at temperatures of 2000 and 2500 K and no strong correlations could be drawn.

The variation of electrical resistivity with sample thickness is probably related to the temperature gradients in the char when it was being prepared. Thus, different parts of the overall thickness of the char had different times at temperature and/or different amounts of vapor deposition. Since the thicknesses were different primarily because of differences in the amount of material removed from the cold side, the average distance from the heated surface changed with sample thickness. Hence, one would expect the short time chars to exhibit the strongest effect of sample thickness since changes occur most rapidly early in the char cycle.

That property gradients exist in the chars is further borne out with x-ray diffraction results. The results of x-ray diffraction measurements made as a function of position from the heated surface are presented in Table 10 and in Figure 70. The lattice spacing decreases as the distance from the heated surface increases; the crystallite size increases as the distance from the heated surface increases. Both effects indicate that the ordering of the char increases as the distance from the surface increases. Since more ordering usually results in a lower electrical resistivity, the electrical resistivity would be higher near the heated surface.

There are at least two reasons why the char could be more ordered as the distance from the heated surface increases. First, the time-at-temperature may be longer inside the char since the surface begins to cool immediately after the power is turned off. Hence, the inside will cool more slowly. Second, there may have been selective vapor deposition since the temperature inside was colder than the surface as the pyrolysis gases flowed out. Recall that these were 3100 K chars.

A composite plot of the effects of time-at-temperature on the electrical resistivity of the chars prepared at 2000, 2500 and 3100 K is presented in Figure 71. The slope of the curve is slightly greater for the chars prepared at 3100 K. Note that the curves do not overlap.

The effects of residence time on the sonic velocity for chars prepared to 2000, 2500 and 3100 K are presented in Figures 72, 73 and 74, respectively. Within the range of the data scatter there seems to be little effect of time-at-temperature on sonic velocity.

Lattice spacing and crystallite size versus residence time-at-temperature are presented in Figures 75, 76 and 77 for maximum char temperatures of 2000, 2500 and 3100 K. For the char prepared at 2000 K (see Figure 75), the lattice spacing decreased and the crystallite size increased as the time-at-temperature was increased. The lattice spacing reached a minimum of 3.44 Å which is not considered very well ordered.

Lattice spacing and crystallite size versus residence time-at-temperature for chars prepared to 2500 K are presented in Figure 76. The lattice spacing and crystallite size remained relatively constant to 1000 seconds and then the lattice spacing decreased and the crystallite size increased. Note that the values indicate very little order (3.44 Å disordered) except past 1000 seconds.

The effects of residence time on lattice spacing and crystallite size for chars prepared to 3100 K are presented in Figure 77. Lattice spacing decreased and crystallite size increased with increased time. The lattice spacing reached a minimum of 3.368 Å at 14 400 seconds.

A composite plot of the lattice spacings versus time-at-temperature for chars prepared by rapid heating to 2000, 2500 and 3100 K is presented in Figure 78. Note that the behavior of char prepared at 2500 K was somewhat different than that of the chars prepared at 2000 and 3100 K. There was no overlapping of the ranges of values which indicates a separation dependent upon maximum temperature.

Effect of Maximum Temperature on Monitors. - This section is concerned with the effects of maximum char temperature on the physical properties used as monitors of changes in the material. The experimental data are presented in Table 2 through 9 and in Figures 79 through 87. The data presented in the figures were for chars with short time exposures (less than about 200 seconds) and generally for which rapid cooling by radiation was employed. All monitor measurements were made at 300 K. The heat fluxes used in preparing the chars are given in the figures.

Shown in Figure 79 are the electrical resistivity values for chars prepared to different maximum temperatures. The x's shown in the figure are average values. For the chars prepared by rapid

degradation, the electrical resistivity exhibited a significant decrease with maximum char temperature. Note that the chars prepared at the different heating rates did not exhibit consistently different behaviors. The electrical resistivity decreased from a value of about 0.069 Ω-cm at 2060 K to a value of about 0.013 Ω-cm at 3070 K.

The chars prepared at very low heating rates exhibited a different behavior than the chars prepared by rapid degradation. As shown in Figure 79, the electrical resistivity of the slow chars was lower than that of the rapid chars at 2000 K but was higher at 3100 K. The electrical resistivity of the chars prepared at low heating rates decreased from about 0.043 Ω-cm at 1400 K to 0.031 Ω-cm at 3100 K.

The effect of maximum exposure temperature on sonic velocity is given in Figure 80. The results were rather scattered but the average values indicate a slight decrease in sonic velocity from a value of 0.195 cm/μsec at 1500 K to 0.182 cm/μsec at 3100 K.

There appears to be quite a bit of scatter in the results presented in Figures 79 and 80 for the effects of maximum temperature. In an effort to see if the scatter might be in the charred material rather than in the measurements a correlation was made between sonic velocity and electrical resistivity. The correlation is shown in Figure 81. Note in the figure that there is an apparent correlation between electrical resistivity and sonic velocity at the various maximum temperature levels. This is an indication that the samples for the different measurements, which were supposed to be the same, but gave different experimental values, might in reality be different.

The effect of maximum exposure temperature on lattice spacing is given in Figure 82. The chars prepared by rapid degradation exhibited a decrease in lattice spacing from a value of 4.1 Å at 1630 K to 3.49 Å at 1950 K and then decreased more slowly to a value of 3.394 Å at 3100 K. The chars prepared at slow heating rates exhibited a decrease in lattice spacing with temperature but never reached the ordering of the chars prepared by rapid degradation.

The effects of maximum exposure temperature on crystallite size are presented in Figure 83. The crystallite size increased uniformly with the maximum temperature to maximum values ranging from 122 to 337 Å at 3100 K.

Weight loss as a function of maximum exposure temperature for the low-density phenolic-nylon chars prepared in the laboratory

is presented in Figure 84. At slow heating rates, the weight loss increased from 72 percent at 1400 K to 77.5 percent at 3100 K. The weight loss was much lower for the chars prepared by rapid degradation. The weight loss for the rapid degradation condition ranged was 67.5 percent at 2000 K and decreased to a range of 62 to 64.5 percent at 3100 K. The chars prepared at heat fluxes of 177 x 10^4 to 418 x 10^4 W/m^2 had the least weight loss at 3000 K.

The effects of maximum exposure temperature on bulk density for the chars made in the laboratory from low-density phenolic-nylon are presented in Figure 85. At a very slow heating rate the bulk density decreased from 0.355 gm/cm^3 at 1400 K to 0.305 gm/cm^3 at 3100 K. For the chars prepared at higher heating rates the average value of bulk density was 0.273 gm/cm^3 at 2050 K and increased to average values of 0.325 and 0.305 gm/cm^3 at 2500 and 3000 K, respectively. The range of values was quite large at 2000 K.

The shrinkage of the low-density phenolic-nylon charred in the laboratory is presented in Figure 86 as a function of maximum exposure temperature. At a very slow heating rate the shrinkage decreased from 25 percent at 2000 K to 22.5 percent at 3100 K. The chars prepared by rapid degradation exhibited shrinkages of 18 percent at 2000 and 2500 K and 14.5 percent at 3100 K.

Thermal Conductivity. - Several thermal conductivity evaluations were made on the chars prepared in the laboratory from the low-density phenolic-nylon. The results of these measurements are presented in Table 11 and in Figures 87 through 89.

Shown in Figure 87 are the results of thermal conductivity measurements made on chars prepared to a maximum temperature of 1380 to 2000 K. Specimen 7-17 which was prepared at 0.1 K/sec to 1380 K had the lowest thermal conductivity. The highest value of thermal conductivity was measured on Specimen 1-111 which was charred by rapid degradation and held at 2000 K for 4 hours. The thermal conductivity of Specimen 11-88 which was charred at 0.1 K/sec to 1989 K was only slightly lower than that of Specimen 1-111. Note that the typical carbon-like behavior is exhibited by these specimens and the thermal conductivity is very low ranging from 0.62 to 0.81 W/m-K at 1000 K for chars prepared to 2000 K.

The results of thermal conductivity measurements on chars prepared from the low-density phenolic-nylon by rapid degradation to 2500 K are presented in Figure 88. Specimen 1-45 which was held at temperature for one second had a much lower thermal conductivity than Specimen 1-50 which was held at temperature for 4 hours. Specimen 1-45 exhibited a carbon-like character but

Specimen 1-50 showed evidence of some graphite-like behavior by a maximum in thermal conductivity at low temperatures. Note that it appears that the thermal conductivity curves for the two specimens are coverging somewhat at the higher temperatures.

The results of thermal conductivity measurements on chars prepared to 3100 K from the low-density phenolic-nylon are presented in Figure 89. Specimen 11-123 which was prepared by rapid degradation and held at 3100 K for 4 hours had the highest thermal conductivity. Specimens 1-86 and 1-92 which were prepared under the same conditions but held at temperature only 20 to 50 seconds had significantly lower values of thermal conductivity. However, all chars prepared by rapid heating exhibited a graphite-like character in thermal conductivity. Specimen 7-17 which was prepared at 0.1°K/sec to 3100 K exhibited a very low thermal conductivity as compared to the rapid chars and behaved in a carbon-like manner.

Thermal Expansion. - The results of thermal expansion measurements on the low-density phenolic-nylon chars prepared in the laboratory are presented in Figures 90 through 92. A composite plot of the thermal expansion curves is presented in Figure 93. Specimens 7-18 and 11-78 which were prepared at 0.1°K/sec to 1380 K and 3100 K had unit expansions of about 2.8×10^{-3} cm/cm at 1100 K. Specimen 11-123 which was prepared at a heat flux of 417×10^{4} W/m^2 and held at temperature for 4 hours had a unit expansion of 3.2×10^{-3} cm/cm at 1100 K. Observe in Figure 93 that these expansion values are within the range of ATJ-S graphite and are in reasonable agreement with values obtained from the literature [3] for glassy carbon. The order of expansion with thermal history seems confusing and might result from the anisotropy of the structures.

Low-Density Phenolic-Nylon Charred in the Arc-Jet

This section presents the results of measurements made on char which was prepared in the arc-jet from low-density phenolic-nylon. Specimens were cut from the arc-jet chars as shown in Figures 2 and 3 and the maximum temperature histories of the various specimen are shown in Figure 29.

Effect of Maximum Exposure Temperature. - The experimental results for monitor measurements on arc-jet chars which were cut from zones which had been at various maximum temperatures are presented in Table 12 and in Figures 94 through 98.

The effect of maximum exposure temperature on electrical resistivity is presented in Figure 94. The electrical resistivity of the arc-jet chars decreased with increasing exposure temperature. The values for the arc-jet chars fell within the range of the values plotted on the figure for the rapidly formed laboratory chars.

The effect of maximum exposure on the sonic velocity is presented in Figure 95. In general, the values for arc-jet-1 fell within the range of values for the laboratory chars while the values for arc-jet-2 were higher.

The lattice spacing and crystallite size of the arc-jet char as a function of position from the heated surface are presented in Table 13 and in Figure 96. The lattice spacings shown in Figure 96 are plotted as a function of maximum char temperature in Figure 97. The lattice spacings of the arc-jet chars are slightly lower than those of the laboratory chars prepared by rapid degradation to the same temperature. The values for the laboratory chars were obtained from Figure 78.

The bulk density of the arc-jet char as a function of maximum exposure temperature is given in Figure 98. The bulk density of the arc-jet char increased from 0.138 gm/cm^3 at a char temperature of 1800 K to 0.281 gm/cm^3 at a char temperature of 2500 K. The arc-jet chars had lower bulk densities than the rapidly formed laboratory chars.

Thermal Conductivity. - The results of thermal conductivity measurements on the arc-jet chars are presented on Table 11 and in Figure 99. The thermal conductivities of both samples evaluated were carbon-like in character. Specimen 2-2 which had been exposed to about 2500 K had a much higher thermal conductivity than Specimen 2-8 which had been to only about 1800 K. The values of thermal conductivity for Specimens 2-2 and 2-8 at 1000 K were 2 W/m-K and 0.37 W/m-K, respectively.

Thermal Expansion. - The results of thermal expansion measurements on the arc-jet chars are presented in Figure 100. All three samples evaluated had the same thermal expansion even though the maximum exposure temperature ranged from 1800 to 2500 K. These results are included in the composite plot of expansion shown in Figure 93. The arc-jet chars had lower values of expansion than the rapidly formed laboratory chars and close to the value for slowly formed chars.

High-Density Phenolic-Nylon Chars Made in Laboratory

A few high-density phenolic-nylon chars were made in the laboratory to see how they behaved relative to the low-density phenolic-nylon chars. Chars were prepared at heat fluxes of 72.5×10^4, 177×10^4 and 418×10^4 W/m^2 to maximum temperatures of 2000, 2500 and 3100 K, respectively. All chars had a short time exposure. The experimental results for these rapidly formed chars are presented in Table 14 and in Figures 101 through 105.

Effect of Maximum Exposure Temperature. - The results for the effect of maximum exposure temperature on the electrical resistivity of the char from the high-density phenolic-nylon are presented in Figure 101. The electrical resistivity decreased from a value of 0.067 Ω-cm at 2000 K to a value of 0.0065 Ω-cm at 3100 K.

The effect of maximum exposure temperature on sonic velocity is shown in Figure 102. The results on the few samples evaluated are scattered and an effect can not be correlated. However, the sonic velocity was about 0.175 cm/μsec.

The weight loss of the chars from the high-density phenolic-nylon is presented in Figure 103 as a function of maximum exposure temperature. The weight loss of the chars prepared by rapid degradation decreased from 75 percent at 2000 K to 67 percent at 3100 K. Chars prepared by slow heating to 3100 K exhibited a weight loss of about 79.5 percent.

The shrinkage in the charring direction of the high-density phenolic-nylon char is presented as a function of maximum exposure temperature in Figure 104. The shrinkage was very high, ranging from 22.5 percent at 2000 K to 26.5 percent at 3100 K.

The bulk density of the high-density phenolic-nylon char as a function of maximum exposure temperature is shown in Figure 105. The bulk density was 0.37 gm/cm^3 for a prechar temperature of 2000 K, increased to 0.74 gm/cm^3 for a 2600 K prechar temperature and then decreased to about 0.68 gm/cm^3 at a prechar temperature of 3100 K.

Thermal Conductivity. - The results of a thermal conductivity measurement on high-density phenolic-nylon charred in the laboratory are presented in Tables 11 and 14 and in Figure 106.

The results of the thermal conductivity measurement are plotted in Figure 106 for Specimen HD-5. This sample was prepared by rapid charring to a maximum temperature of 2600 K. The thermal

conductivity increased to a maximum of about 8.35 W/m-K at about 610 K and then decreased. The character of the thermal conductivity curve is graphite-like which indicates some degree of crystalline ordering for this specimen. The lattice spacing of the companion-specimen (HD-6) which was charred with Specimen HD-5 was 3.414 Å with a crystallite size of 220 Å. This represents low-level ordering.

Phenolic Char Made in Laboratory

Phenolic was charred in this program in an effort to develop a dense void-free char which could be used later to resolve uncertainties in the thermal modeling of radiant heat transport at high temperatures. Toward this end, chars were prepared at several extremely slow and interrupted heating rates in an attempt to obtain a very dense and structurally sound char. The desired void-free structure was not obtained but a char with a density of over 1 gm/cm^3 was obtained.

In addition to the work at slow heating rates, chars were prepared by rapid degradation at heat fluxes of 72.5 x 10^4, 177 x 10^4 and 418 x 10^4 W/m^2 to maximum exposure temperature of 2000, 2500 and 3100 K, respectively. The results of monitor measurements made at 300 K will be discussed first and then the results of thermal conductivity measurements will be covered. The results of the measurements of the monitors are presented in Table 15 and in Figures 107 through 111.

Effect of Maximum Exposure Temperature. - The results for the effect of maximum exposure temperature on the electrical resistivity of the phenolic char are presented in Figure 107. The electrical resistivity decreased from a value of 0.037 Ω-cm at a prechar temperature of 2000 K to 0.0145 Ω-cm at a prechar temperature of 3100 K.

The effect of maximum exposure temperature on the sonic velocity of the phenolic-char is given in Figure 108. The sonic velocity was constant at 0.12 cm/μsec to a prechar temperature of 2500 K and then decreased to a value of 0.105 cm/μsec at a prechar temperature of 3000 K.

The weight loss of the phenolic as a function of exposure temperature is plotted in Figure 109. For chars prepared by rapid degradation, the weight loss was about 45.5 percent at a prechar temperature of 2000 K and decreased to about 43 percent at a prechar temperature of 3000 K. The chars prepared at slow heating rates to 3000 K exhibited weight losses ranging from about 41 percent to 53 percent.

The shrinkage in the charring direction of the phenolic for various maximum exposure temperatures is given in Figure 110. The shrinkage was about 10 percent up to a prechar temperature of 2500 K and decreased to a value of about 2.5 percent at a prechar temperature of 3000 K. The shrinkage of a char prepared to 3000 K at a slow heating rate was about 7 percent. Note that the shrinkage of the phenolic was lower than that of either the low-density or high-density phenolic-nylon.

The bulk density of the phenolic char is presented in Figure 111 as a function of maximum exposure temperature. The bulk density of the chars prepared by rapid degradation increased from a value of 0.59 gm/cm^3 at a prechar temperature of 2000 K to 0.65 gm/cm^3 at a prechar temperature of 3000 K. The bulk density of phenolic which was charred at a very low heating rate to 3000 K was 1.12 gm/cm^3.

Thermal Conductivity. - The results of thermal conductivity measurements on the charred phenolic are presented in Tables 11 and 15 and in Figure 112. Shown in Figure 112 are the results of thermal conductivity measurements on phenolic char Specimens HMP and P-6 which were prepared to about 3100 K by slow heating and rapid degradation, respectively. A picture of Specimen HMP is given in Figure 49. Specimen HMP had the highest bulk density and also the highest thermal conductivity, reaching a value of 8.3 W/m-K at 1100 K. Further, Specimen HMP exhibited a carbon-like behavior in that there was no maximum in the thermal conductivity curve. On the other hand, Specimen P-6 exhibited a maximum in the thermal conductivity curve at 460 K and decreased above this temperature in a graphite-like manner. Specimen P-6 had a much lower bulk density than that of Specimen HMP and a lower thermal conductivity. Specimen P-5 which was the companion to Specimen P-6 during charring had a lattice spacing of 3.373 Å and a crystallite size of 270 Å. Specimen HMP exhibited no peak in the x-ray diffraction curves and hence was poorly order. Thus, Specimen P-6 was a much more highly ordered char than Specimen HMP. From this evidence one would expect higher thermal conductivity values for Specimen P-6. The thermal conductivity of this specimen was significantly lower than that of low-density phenolic-char Specimen 11-123 (see Figure 89) which had about the same lattice parameters and a much lower bulk density. The low thermal conductivity values for Specimen P-6 may be related to the char structure. Note in Figure 43 that the specimen contained numerous cracks perpendicular (in series) to the heat flow. This structure might provide a conductivity which is graphite-like in behavior but at a lower level.

Also shown in Figure 112 is a thermal conductivity curve for glassy carbon prepared from polyvinyl chloride. The material had been heat treated to 3033 K. The experimental results for the glassy carbon are presented in Figure 113. Note that the glassy carbon had a carbon-like character for thermal conductivity and a higher thermal conductivity than the slow charred phenolic. The lattice spacing of the glassy carbon was 3.49 Å which indicates poor ordering.

Thermal Expansion. - The results of thermal expansion measurements on Specimen P-5 which was prepared by rapid degradation to 3066 K are given in Figure 114. The expansion curve is also presented in the composite plot shown in Figure 93. The charred phenolic had a much higher thermal expansion than either the phenolic-nylon chars or the glassy carbon. The expansion reached a value of 5×10^{-3} cm/cm at 1100 K. The order of thermal expansion with thermal history seems confusing and might result from the anisotropy of the structures.

Correlations of Thermal Conductivity of Different Chars

A composite plot of the thermal conductivities of chars prepared from the low-density phenolic-nylon is given in Figure 115. All measurements were made in a nitrogen environment. The dotted lines shown on the curves are extrapolations of the data back to zero degrees. The character of the extrapolated curves may not be precisely correct but the general behavior is appropriate for carbonaceous materials. The characterization data on the specimens are presented in Tables 2-10 and the thermal conductivity data are presented in Table 11. The data from which the composite plot was developed are given in Figures 87 through 89 and in Figure 99.

A study of Figure 115 reveals that the thermal conductivity increases with maximum exposure temperature and with residence time at a given temperature. The higher the thermal conductivity the more ordered is the crystallite structure of the char. Note that the maximum in the thermal conductivity curves shift to higher temperatures as the thermal conductivity decreases (ordering decreases). The characters of the curves for various degrees of crystalline order is the same as that presented by Castle [4] which was postulated by Mrozowski for polycrystalline carbons.

Observe in Figure 115 that the arc-jet chars had thermal conductivity values which were consistent with those of the chars prepared in the laboratory at similar conditions. Further, the chars prepared to temperatures of 2000 K and below had very low levels of thermal conductivity which indicates a highly amorphous

and/or turbostratic structure. This is consistent with the comment by Fair [5] that very little three-dimensional ordering takes place in graphitizable carbons below about 2270 K.

Values for the thermal conductivity of the char solid (matrix) were calculated from the experimental results for the effective thermal conductivities. The equation which used to calculate the solid thermal conductivity was

$$K_m = \frac{K_{eff}}{1-P} \tag{14}$$

where

K_m = thermal conductivity of solid (matrix)

K_{eff} = measured thermal conductivity in nitrogen

$P = 1 - \frac{\rho_b}{\rho_t}$ = porosity

ρ_b = bulk density

ρ_t = true density

Radiation and gas conduction were neglected in the analysis. Radiation is small up to 1100 K and the conductivity of nitrogen is only 0.063 W/m-K at 1000 K. Hence, neglecting these components should not introduce a significant error. These calculations were made only to provide estimates of the solid conductivity and not to rigorously model the material. (Rigorous modeling of the geometry of the structure is required first).

The values calculated for the solid thermal conductivities of the various chars are presented in Figure 116. It is obvious from the figure that the thermal conductivities of the porous chars are a strong function of maximum temperature because the thermal conductivity of the char solid is a strong function of maximum exposure temperature. The chars prepared at temperatures of 2000 K and below had very low values of solid thermal conductivity which indicates very low-level ordering. Jamieson [6] gives a thermal conductivity value of about 7 W/m-K at 400 K for Kendall coke heat treated to 1471 K. This value is above the values calculated for the chars prepared to 2000 K. The chars prepared by rapid heating exhibit an orderly trend to higher values of solid thermal conductivity as the maximum exposure temperature and the residence time at temperature increase.

The glassy carbon and the phenolic charred at a very low heating rate exhibited carbon-like behavior even after heat treatment to a temperature above 3000 K. The char which was prepared from the low-density phenolic-nylon by rapid heating to 3100 K and then held at temperature four hours exhibited a strong graphite-like behavior and approached the thermal conductivity values for ATJ graphite, with grain, which are presented in Figure 116.

The real anomalous behavior in the solid thermal conductivity values presented in Figure 116 was for the phenolic charred at a high heating rate to 3100 K. The character of the curve was graphitic and lattice spacing measurements indicated a reasonably ordered structure, yet the solid thermal conductivity was lower than that of the more carbon-like glassy carbon. One reasonable explanation for this is that the structure had numerous cracks perpendicular to the heat flow (see Figure 43) and hence the thermal model used is extremely inaccurate for obtaining the solid thermal conductivity of that char.

A correlation is shown in Figure 117 between the effective thermal conductivity and electrical resistivity. There is a reasonable correlation between thermal conductivity and electrical resistivity to a value of electrical resistivity of 0.04 Ω-cm with the thermal conductivity decreasing as electrical resistivity increases. The thermal conductivity is independent of electrical resistivity for electrical resistivities greater than 0.04 Ω-cm. Observe that all of the phenolic-nylon chars fit the correlation reasonably well whatever the density or degradation conditions. The dotted line shown in Figure 117 is the curve which correlates most data for graphites [7]; however, graphites usually have electrical resistivity values less than 0.005 Ω-cm.

Figure 118 gives a correlation between the thermal conductivity of the solid as calculated from equation (14) and the electrical resistivity of the solid. The electrical resistivity of the solid was calculated from

$$\rho_s = (1-P)\ \rho_{eff} \tag{15}$$

where

ρ_s = electrical resistivity of solid

ρ_{eff} = measured electrical resistivity

P = porosity

There was a reasonably good correlation at up to an electrical resistivity of 0.009 Ω-cm with the thermal conductivity decreasing as the electrical resistivity increased. The correlation for these data falls below the correlation curve for artificial graphites.

A correlation between the effective thermal conductivity at 300 K and the lattice spacing is plotted in Figure 119. There was a reasonably strong correlation to a lattice spacing of about 3.44 Å with the thermal conductivity exhibiting a decrease as lattice spacing increased. The value for the high density char fell above the correlation, probably because of the higher conductivity as a result of its higher density. The value for the arc-jet char correlated rather well.

A correlation between the thermal conductivity of the solid and the lattice spacing is given in Figures 120 and 121. The chars prepared by rapid heating correlate well to a lattice spacing of 3.44 Å, even for the high-density phenolic-nylon and arc-jet chars. Chars prepared at slow heating rates seem to follow a different correlation and thermal conductivity is rather independent of lattice spacing for spacings greater than 3.44 Å.

A correlation between effective thermal conductivity and crystallite size is given in Figure 122. There is a reasonable strong correlation for crystallite sizes greater than 100 Å and a weak correlation for smaller crystallite sizes. The thermal conductivity increases as the crystallite size increases.

A plot of the thermal conductivity of the solid at 300 K versus crystallite size is given in Figure 123. Again there is a reasonably strong correlation for crystallite sizes above 100 Å and a weak correlation for sizes below 100 Å.

The effective thermal conductivities at 300 K for the chars prepared from low-density phenolic-nylon are plotted versus sonic velocity in Figure 124. Surprisingly, a reasonably good correlation is achieved to a sonic velocity of 0.22 cm/μsec. The thermal conductivity decreases as the sonic velocity increases. For sonic velocities above 0.22 cm/μsec little correlation was found.

A correlation of lattice spacing and crystallite size is given in Figure 125. The correlation between the two was fair. Lattice spacing decreased as crystallite size increased.

The effective thermal conductivity of the chars prepared in the laboratory from low-density phenolic-nylon is presented in Figures 126 and 127 as a function of time-at-temperature at temperatures of 2500 K and 3100 K. The curves shown in Figure 126

were established by first using the correlation shown in Figure 71 for electrical resistivity versus time-at-temperature. Then thermal conductivity was obtained from the resistivity values with the aid of Figure 117. Note that the experimental values fit the correlation reasonably well.

The effective thermal conductivity of the chars prepared in the laboratory from the low-density phenolic-nylon versus time-at-temperature is shown in Figure 127 for chars prepared at 2500 and 3100 K. One set of curves was established from the electrical resistivity data as described above. The second set of curves was established by the use of lattice spacing. First, the correlation between lattice spacing and time-at-temperature which is presented in Figure 78 was used. Then thermal conductivity was obtained from lattice spacing with the use of Figure 119. Observe that the experimental thermal conductivity values agree better with the correlations based on lattice spacing.

The effect of maximum exposure temperature on the effective thermal conductivity of the chars prepared in the laboratory from the low-density phenolic-nylon is shown in Figure 128. All of the values shown for rapid degradation are for chars with a short time exposure of less than about 200 seconds. The thermal conductivity of the chars prepared by rapid degradation increases slowly with temperature to about 2000 K, then there is a rapid rise in thermal conductivity with temperature to 3100 K. Observe that thermal conductivity values for the arc-jet chars are in reasonable agreement with those of the rapid chars prepared in the laboratory.

Of special interest in Figure 128 is the effect of maximum exposure temperature on the thermal conductivity of the char prepared by slow heating. At low temperatures, the thermal conductivity of the slowly heated chars is about the same as that of the chars prepared by rapid degradation. However, at a prechar temperature of 3100 K, the thermal conductivity of the chars prepared by slow heating is far below that of the char prepared by rapid degradation. The slowly heated char obviously does not reach the ordered crystalline state of the rapidly heated char and can not be altered as much by final temperature.

DISCUSSION

General

The properties of the chars prepared from the low-density phenolic-nylon were controlled by the heating rate, the residence time-at-temperature and the maximum exposure temperature. These effects will now be discussed.

Heating rate affected the properties of the low-density phenolic-nylon char in the following manner. At very low heating rates the char which was formed was found to be carbon-like or non-graphitic.. The properties such as electrical resistivity, lattice spacing and thermal conductivity all retained values typical of amosphous carbon even after heat treatment to 3100 K. This trend continued up to a cold wall heat flux of about 17×10^4 W/m^2. For chars prepared at heat fluxes of 72.5×10^4 W/m^2 and above and taken to 3100 K the monitors of electrical resistivity and lattice spacing indicated that the char was graphite-like. The properties for these chars were within the graphite range or graphitic in character. The electrical resistivity of the char solid reached values as low as 1200 to 1500 μΩ-cm which is within the graphite range. The lattice spacings of these chars reached values well below the generally recognized limit for non-graphitizing carbons of 3.44 Å. Hence, there seems to be a critical heat flux in the range of 17×10^4 W/m^2. Below the critical heat flux (or temperature rise rate) a non-graphitizing carbon is formed and above the critical heat flux a graphitizing carbon is formed.

The shrinkage of the chars prepared at heating rates below the critical values were on the order of 25 percent. Above the critical heating rate, shrinkage ranged from 13 to 18 percent. The weight loss of the chars decreased as a function of heating rate with values of about 78 percent at low heating rates and 61 to 65 percent at heating rates above the critical value.

Below the critical heat flux the closed porosity was about equal to the open porosity at a value of 40 percent. The open and total porosities reached maximums of 81 and 88 percent, respectively, at a heat flux of 17×10^4 W/m^2. At heat fluxes of 72.5×10^4 W/m^2 and above the total porosity remainded nearly constant at about 76 percent and the closed porosity was about 12 percent.

One anomalous behavior noted was that the true density reached a value of only 1.44 gm/cm^3 at heat fluxes above 72.5×10^4 W/m^2 after exposure to 3100 K. With the ordering noted

for other properties one might expect a higher value for true density. (Microporosity is suspected in this measurement of true density).

The reasons that heat fluxes above some critical value resulted in a more graphitizable structure may be due to deposition of a graphitizable carbon from the pyrolysis gases and/or a change in the degradation mechanisms of the virgin material which destroys the cross-linking and results in a more graphitizable carbon. Deposition is definitely a consideration since the pyrolysis gases flow through a char structure with a temperature profile. At very low heating rates the pyrolysis gases are released where the char is at a relatively low temperature and very little deposition occurs. A deposit on the chars is noted at heating rates of 177×10^4 W/m^2 and 418×10^4 W/m^2 which provide surface temperature of 2500 and 3100 K, respectively. Little deposit if any is noted for chars prepared at heat fluxes of 72.5×10^4 W/m^2 for which the char surface temperature is 2000 K. The weight loss is significantly lower for chars prepared at heat fluxes above the critical value by an amount which could result in perhaps 40 percent of the char mass being deposited carbon. However, differences in the degradation kinetics of the virgin material might also result in some lowering of the weight loss. A hard conclusion can not be drawn. Deposition surely seems to be a major part of the mechanism and degradation kinetics may also play a role. In any event, it is established that chars prepared at heating rates of 72.5×10^4 W/m^2 and above behave in a manner similar to graphitizable carbons.

Being graphitizable in nature, the properties of the chars prepared by rapid degradation should be dependent on the residence time-at-temperature. This effect was demonstrated by lattice spacing, crystallite size, electrical resistivity and thermal conductivity. The time dependency increased as the maximum exposure temperature increased. At 2000 K, the properties were somewhat sensitive to residence time but changes occurred slowly and the ordering of the crystalline structure was low. However, at temperatures of 2500 and 3000 K noticeable changes occurred in the properties as the residence time was increased. Generally, the changes occurred most rapidly for short times and the rate of change decreased as the residence time increased. There were significant changes in the thermal conductivity which occurred with residence time at 2500 and 3100 K (see Figure 127).

Maximum exposure temperature had a pronounced effect on electrical resistivity, lattice spacing, crystallite size and thermal conductivity for chars prepared by rapid degradation and with short residence times. All of these monitors indicated that

the ordering of the structure increased strongly as a function of maximum temperature above 2000 K. Very little work was done below 2000 K because rapid heating rates could not be employed while maintaining a low char temperature. However, the char is very poorly ordered at temperatures of 2000 K and below regardless of the heating rate and the effect at temperature will probably not significantly influence the degree of crystalline ordering.

The chars prepared in the laboratory at rapid heating rates were closely similar to chars prepared in the arc-jet. Comparisons of structure are given in Figures 1, 34 and 35. Note the similarity in structure even to the extent that the char prepared at 177 x 10^4 W/m^2 to 2500 K looks like the heated side of the arc-jet char (Figure 1) and the char prepared at 72.5 x 10^4 W/m^2 to 2000 K is similar to the cold side of the arc-jet char. Comparisons of the monitor properties of the chars prepared in the laboratory and in the arc-jet are presented in Figures 94 through 98. The electrical resistivity and lattice spacing of the arc-jet char agreed well with those properties of the laboratory chars. The bulk density of the arc-jet char was somewhat lower than that of the laboratory char (see Figure 98). However, at 2500 K the densities differed by only 14 percent. At 1800 K, the bulk density of the arc-jet char was only 0.138 gm/cm^3. The arc-jet char prepared to 1800 K may have had a considerably lower heating rate than the laboratory char prepared to 2000 K because of the large char thickness. The conduction heat flux near the cold surface was probably on the order of 6 to 8 x 10^4 W/m^2 near the end of the char cycle. These differences would have affected properties somewhat.

A comparison of the thermal conductivities of the arc-jet chars and laboratory chars is given in Figures 115 and 128. Note that the thermal conductivity values for the chars prepared by the two different methods were in good agreement where correlated with the maximum exposure temperature (heating rates "similar".)

The chars prepared from the high-density phenolic-nylon and the phenolic exhibited the same behavior of monitors with maximum exposure temperature as the chars from the low-density phenolic-nylon. Of course, monitor levels were different since these chars had much higher densities than the chars from the low-density phenolic-nylon. Of particular interest is the fact that a correlation between the thermal conductivity of the solid and lattice spacing for the char from the high-density phenolic-nylon fell on the correlation curve for the char from the low-density material (see Figure 120). Thus, the chars from the high and low-density materials seemed to undergo the same changes in

crystalline order and modeled similarly. Even though the phenolic appeared to undergo the same changes in crystalline order and seemed to relate to the monitors similarly, they did not model the same as the low-density phenolic-nylon chars probably because of geometric differences in the structures.

Sensitivity of Monitors to Charring Conditions

The monitors which were most sensitive to defining differences between chars prepared at different degradation conditions were electrical resistivity, lattice spacing, crystallite size and thermal conductivity. All of these monitors changed as the nature of the material changed due to heating rate, residence time-at-temperature and maximum exposure temperature. The changes in sonic velocity with a change in charring condition were so small that the data scatter masked the effects. Likewise, the thermal expansion was difficult to relate to the thermal history of the char.

Electrical resistivity and lattice spacing both decreased as the residence time and/or maximum temperature was increased and the char solid became more ordered, particularly for the higher heating rate chars. Thermal conductivity and crystallite size increased with residence time and maximum temperature as more ordering occurred, again particularly for the higher heating rate chars.

Sensitivity of Monitors to Thermal Conductivity

The same monitors which were sensitive to charring conditions were sensitive to changes in thermal conductivity. In fact, the correlations between these monitors and thermal conductivity were better than the correlations between the monitors and the charring conditions. The monitors correlated well until a high degree of disorder was reached. At very low levels of graphitization the monitors became insensitive to thermal conductivity. Or to put it another way, the thermal conductivity reached very low values and changed little for the highly disordered states.

The correlations of the monitors and thermal conductivity are presented in Figures 117 through 124. Observe in Figure 117 that little change in thermal conductivity was noted for electrical resistivity values above 0.04 Ω-cm. Likewise, the same effect was noted in Figure 120 when the lattice spacing reached the value for turbo-stratic carbon of 3.44 Å. It should be noted that there were other chars which had about the same level of thermal

conductivity as those for which data are presented in Figure 120 for which no peaks were observed in the x-ray diffraction patterns. These chars were highly disordered. Again, note in Figure 122 that the thermal conductivity changed little at crystallite size below 100 Å. A material with a crystallite size below 100 Å is considered highly disordered.

A most surprising result was that thermal conductivity correlated well with sonic velocity, as shown in Figure 124, since sonic velocity was not a good monitor for the effects of charring conditions. Observe in Figure 124 that the thermal conductivity changed little for sonic velocity above 0.22 cm/μsec.

The general view that one obtains from the correlations of the thermal conductivity and the monitors is that the monitor measurements must have fair precision. This leads to the summation that the scatter seen in the monitors as a function of charring condition might have been related to differences in the chars due to the variability of the charred material perhaps by subtle differences in charring conditions, sample preparation and/or virgin material variability. In any event, it is fortunate that numerous samples were prepared so that meaningful curves could be drawn through the scatter.

Anticipated Response of Thermal Conductivity to Charring Conditions

The results on the low-density phenolic-nylon permits an estimate of the response of the material to a "flight" heating rate. At heating rates during degradation above about 17×10^4 W/m^2 it is anticipated that the char will behave in the manner of a graphitizable carbon. Thus for chars prepared or generated at other than very low heating rates, the char can obtain more crystalline order and the thermal conductivity will increase as the maximum exposure temperature increases and the residence time increases.

The anticipated increases in ordering of the material as evidenced by increases in the thermal conductivity of the char at 300 K are presented in Figures 127 and 128 for the effects of residence time and maximum exposure temperature. Observe in Figure 127 that the thermal conductivity at 300 K can more than double after four hours at temperatures of 2500 K and 3100 K. Further, the rate of increase of thermal conductivity is greatest at very short times. The effect of maximum exposure temperature presented in Figure 128 indicates that the thermal conductivity of the char will change little up to about 2000 K and that

significant ordering will occur above 2000 K with a dramatic increase in thermal conductivity (high heating rate chars).

Changes in the thermal conductivity at 300 K discussed above indicate the effects of the high temperature exposures on the degree of ordering or graphitization of the char. The problem still remains of determining the "instantaneous" thermal conductivity of the char at high temperatures for a given degree of ordering achieved at that high temperature. The properties could shift with a small additional time exposure at elevated temperature. Extrapolation techniques based on a knowledge of the behavior of graphitic materials will have to be developed and some key measurements made to confirm the results. Some initial estimates of this behavior are made in a later section.

CONCLUSIONS

The changes in the properties of ablative chars which accompany the charring process can be observed in the laboratory and quantitized. Relations exist between the crystalline state of the charred material and physical properties which allow one to anticipate the response of a material to ablative conditions.

Chars prepared at very low heating rates are not the same as chars prepared near "use" heating rates. Rather these chars were found to be non-graphitizing in nature whereas the chars prepared at higher heating rates were found to be graphitizable. This difference in the crystalline nature of the chars has a profound influence on the properties for temperature excursions above 2000 K. Once the heating rate reaches a value of probably about 17×10^4 W/m^2 the ability of the char to graphitize even more readily is less influenced by the charring heat flux.

For "rapid" chars, residence time-at-temperature and maximum exposure temperature have a significant effect on the thermal conductivity of chars prepared above 2000 K. Below 2000 K the properties are carbon-like and not as sensitive to these variables. In fact, for chars prepared at temperatures from, say, 800 K to 2000 K the same properties (carbon-like) can probably be obtained on chars prepared by either slow heating or rapid heating. However, if slow heating is used one must be careful to correct the results to the bulk density value of the char prepared by rapid degradation.

Chars prepared in the laboratory by rapid degradation were found to exhibit the same behavior as chars prepared in the arc-jet other exposure conditions being equal. Hence, laboratory

studies made under controlled degradation conditions can be used to define the behavior of an ablative material. Sufficiently high heat fluxes can be obtained to provide the proper char structure.

Best Monitors

Several physical properties were used as monitors to relate the effects of degradation conditions and the resulting physical nature of the char. The monitors which were found to be most sensitive to the physical nature of the char were electrical resistivity, lattice spacing, crystallite size and thermal conductivity. Electrical resistivity, lattice spacing and crystallite size correlated well with both the degradation conditions and with the thermal conductivity at 300 K. Hence, the effect of degradation conditions on thermal conductivity can be studied with the aid of properties which correlate with thermal conductivity. Of the two best monitors, electrical resistivity, requires a structural sound specimen of some reasonable thickness and lattice spacing requires only a small sample of material from a zone of little thickness.

Transient Behavior of Thermal Conductivity

The purpose of this program was not to define the transient thermal conductivity curve of an ablating system but rather to study the relations of degradation conditions and monitor relationships. However, the results were sufficient to make some reasonable extrapolations of thermal conductivity and provide a first-order estimate of the transient behavior. This estimate may provide some useful information for parameteric studies with the NASA Langley Charring Ablators Program.

The current best estimate of the thermal conductivity of the 0.577 gm/cm^3 phenolic-nylon is presented as the solid line in Figure 129. Data were obtained to about 1100 K on chars prepared by rapid degradation to various temperatures for short time exposures. These data were extrapolated to elevated temperatures through a consideration of the character of the thermal conductivity curves as a function of temperature. The circles with the X's are the points of intersection of the extrapolated thermal conductivity curves with the formation temperature and represent the best estimate during actual ablation for a given temperature. The solid curve was drawn through these "boxed" values. The portion of the curve from 800 K to about 1200 K was established from data reductions of temperature measurements during quasi

steady-state ablation tests [see p. 176 of ref. 8]. The estimated values fall below the values presented in Reference 9 for 0.577 gm/cm^3 phenolic-nylon and above the values presented in Reference 10 for 0.208 gm/cm^3 phenolic-nylon. Further work will be required to refine these curves.

RECOMMENDATIONS

The success of the work with monitors in this program leads to the conclusion that the work should be carried to further stages. This section gives some recommendations as to the direction of future work that should result in the ability to define the transient thermal conductivity of charring ablators.

It has been demonstrated that thermal conductivity can be defined to about 1100 K by direct and essentially uncorrected measurement on chars which are structurally and physically like chars formed during short-time ablation at elevated temperatures. Further, direct thermal conductivity measurements on the laboratory chars prepared at various formation temperatures can probably be extended to 2000 K without serious problems arising from the effects of residence time-at-temperature. Thus, the thermal conductivity for an ablating char can now be established with confidence to 2000 K so long as geometry is reproduced. The additional curve character plus the reduced extrapolation range to the higher temperature will provide a sound basis for the definition of the transient thermal conductivity. With the use of the monitors, the conductivity can be extended to the higher temperatures by the continued correlation between laboratory and flight chars. For example, 3000 K chars would be made, their monitors checked with flight chars, conductivity measured to 2800 K and then monitors remeasured to determine the stability of the char during the measurement.

Basic thermal modeling of the geometry of the structure should continue on the chars. The porous nature of the chars allows heat transport by radiation and gas conduction. Both effects must be defined in order to extrapolate the thermal conductivity results on short time chars to elevated temperatures. The radiant heat transport will play an important part in extrapolations to elevated temperatures and must necessarily be understood. The fact that chars of similar crystalline nature and structure were prepared from both and high-density phenolic-nylon is important to modeling and provides a check. These chars can be fully graphitized such that properties will not change with residence time for subsequent exposures to near 3100 K and then thermal conductivity measured over nearly the full temperature range. These chars provide two significantly different levels of thermal conductivity because of differences in

in bulk density. Hence, a simultaneous analysis of the thermal conductivity values for these different density chars should allow a separation of the solid conduction and radiation.

Modeling is also required to understand the effects of environment on gas conduction and convection. The gas conditions change from the laboratory environment to "in-flight". Hence, to extrapolate the results one must be able to predict the effect of the environment.

It is recommended that the program continue on to the second phase as outlined in our original proposal for this work.

Last, it is recommended that some investigations should be begun of the effects of degradation conditions on the physical properties of ablators different than the phenolic-nylon. We fully expect that the same behaviors would be noted and a generalized procedure could be established.

Southern Research Institute
Birmingham, Alabama
July, 1972

APPENDIX I

A COMPARATIVE ROD APPARATUS FOR MEASURING THERMAL CONDUCTIVITY TO 2000°F

Southern Research Institute's comparative rod apparatus is used to measure thermal conductivities of a wide variety of materials from -300°F to 2000°F. This apparatus, shown schematically in Figure 1, consists basically of two cylindrical reference pieces of known thermal conductivity stacked in series with the cylindrical specimen. Heat is introduced to one end of the rod, composed of the references and specimen, by a small electrical heater. A cold sink or heater is employed at the opposite end of the rod as required to maintain the temperature drop through the specimen at the preferred level. Cylinders of zirconia may be inserted in the rod assembly to assist in controlling the temperature drop. Radial losses are minimized by means of radial guard heaters surrounding the rod and consisting of three separate coils of 16, 18 or 20-gage Kanthal wire wound on a 2 or 4-inch diameter alumina core. The annulus between the rod and the guard heaters is filled with diatomaceous earth, thermatomic carbon, bubbled alumina or zirconia powder. Surrounding the guard is an annulus of diatomaceous earth enclosed in an aluminum or transite shell.

The specimens and references (see Figure 2) are normally 1-inch diameter by 1-inch long. Thermocouples located 3/4 inch apart in radially drilled holes measure the axial temperature gradients. Thermocouples located at matching points in each guard heater are used to monitor guard temperatures, which are adjusted to match those at corresponding locations in the test section.

In operation, the apparatus is turned on and allowed to reach steady state. The guard and rod heaters are adjusted to minimize radial temperature gradients between the rod and guard sections consistent with maintaining equal heat flows in the references. Temperatures are measured on a Leeds and Northrup Type K-3 potentiometer, and the temperature gradients calculated. A typical temperature profile in the test section is shown in Figure 3.

The thermal conductivity of the specimen is calculated from the relation

$$K_s = \frac{\dfrac{K_1 \Delta T + K_2 \Delta T}{2\Delta T_s}}{\dfrac{\Delta X_s}{\Delta X_r}}$$

where K_1 and K_2 are the thermal conductivities of the upper and lower references; ΔT_1, ΔT_2 and ΔT_s are the temperature differences in the upper and lower references and specimen, respectively; ΔX_s and ΔX_r are the distances between thermocouples in the specimen and references.

Note that for purely axial heat flow, the products $K_1\Delta T_1$ and $K_2\Delta T_2$ should be equal. Due to imperfectly matched guarding and other factors, this condition is seldom attained in practice; therefore, the average of the two values is used in the calculations. Their difference is maintained as small as possible, usually within 5% of the smaller.

For identical specimens, the ratio $\Delta X_s/\Delta X_r$ should be unity but may vary due to the uncertainty in hole locations. To prevent introducing an additional error in calculations, ΔX is determined as follows: the depth of the hole is measured by inserting a snugly fitting drill rod in the hole, measuring the projecting length and subtracting it from the total length of the rod. The slope, or angle the hole makes with the perpendicular to the specimen axis, is determined by making measurements to the face of the hole and the outer end of the drill rod with respect to a datum plane, using a dial gage. From these measurements, the location of the bottom of the hole can be calculated.

Generally, measurements with the comparative rod apparatus are performed in an inert helium environment. The apparatus can also be operated in vacuum and at gas pressures of up to 100 psig. We have had experience operating under all conditions.

The primary reference materials which we use are Code 9606 Pyroceram and Armco iron for measurements on materials with low and high thermal conductivities, respectively. Primary standard reference sets are kept and are used to calibrate other references made from the same materials. The standards of Code 9606 Pyroceram were made from a batch of material which NBS purchased shortly after their measurements on a sample of Code 9606 Pyroceram. The curve which Flynn presented for the thermal conductivity of the Pyroceram is given in Figure 4.[1] Note that the curve is in good agreement

---

[1] Robinson, H.E. and Flynn, D. R., Proceedings of Third Conference on Thermal Conductivity, pages 308-321, 1963 (with author's permission)

with the recommended values from NSRDS-NBS 8[2]. The standards of Armco iron were made from the stock which was used in the round-robin investigations from which Powell[3] developed the most probable values for Armco iron. The curve used for the Armco iron standards is shown in Figure 5. Powell estimated the uncertainty to be within ±2 percent over the temperature range from 0° to 1000°C. Note in Figure 5 that numerous evaluations of Armco iron from other batches of material have agreed within ±3 percent (coefficient of variation about curve) with Powell's original data.

In addition to Code 9606 Pyroceram and Armco iron several other materials have been used as references. These include copper for high conductivity specimens, 316 stainless steel for specimens of intermediate thermal conductivity and Teflon or Pyrex for low conductivity materials.

Copper references have been calibrated against Armco iron and excellent agreement with literature data has been obtained. Thermal conductivity values obtained from calibrations of 316 stainless steel against Pyroceram, Armco iron and a set of 316 stainless steel standards are presented in Figure 6. Note the consistency of the data obtained with the three different sets of references. The coefficient of variation of the data shown in Figure 6, about the curve value, was ±3.3%. These data indicate the internal consistency of the stainless steel and the reference materials. Note that the thermal conductivity values for 316 stainless steel presented in Figure 6 lie between values reported by several steel manufacturers and Lucks and Deem.[4]

The calibrations indicate that for materials with moderate to high thermal conductivities the apparatus operates with a precision of about ±3 percent and a total uncertainty of about ±5 percent at temperatures above 0°F if temperatures between the guard and test section are closely matched. Below 0°F, the precision achieved to date has been about ±7 percent with a total uncertainty of about ±10 percent. We anticipate that the precision and uncertainty at cryogenic temperatures can be improved by additional calibrations.

---

[2] Powell, R. W., C. Y. Ho and P. E. Liley, Thermal Conductivity of Selected Materials, NSRDS-NBS 8, Department of Commerce, November 25, 1966

[3] Powell, R. W., Proceedings of Third Conference on Thermal Conductivity, pages 322-341, 1963

[4] WADC TR58-476, "The Thermophysical Properties of Solid Materials," Armour Research Foundation, November, 1960.

Some additional data obtained on the comparative rod apparatus are shown in Figure 7 and 8. Figure 7 shows thermal conductivity data for ATJ graphite, with grain, using Armco iron as the reference material. These data show excellent agreement with earlier data obtained here and by other sources[5] [7]. The maximum scatter of the comparative rod points was about 5 percent.

Figure 8 shows data for thermocouple grade constantan obtained on the comparative rod apparatus using Armco iron references, and on Southern Research Institute's high temperature radial inflow apparatus. Note the excellent agreement. These data also show close agreement with data obtained by Silverman[4] on an alloy of very similar composition.

---

[5] ASD-TDR-62-765, "The Thermal Properties of Twenty-Six Solid Materials to 5000°F or Their Destruction Temperatures," Southern Research Institute, August, 1962

[6] Pears, C. D., Proceedings of Third Conference on Thermal Conductivity, 453-479 (1963)

[7] NSRDS-NBS 16, "Thermal Conductivity of Selected Materials", Part 2, by C. Y. Ho, R. W. Powell and P. E. Liley, National Bureau of Standards, 1968.

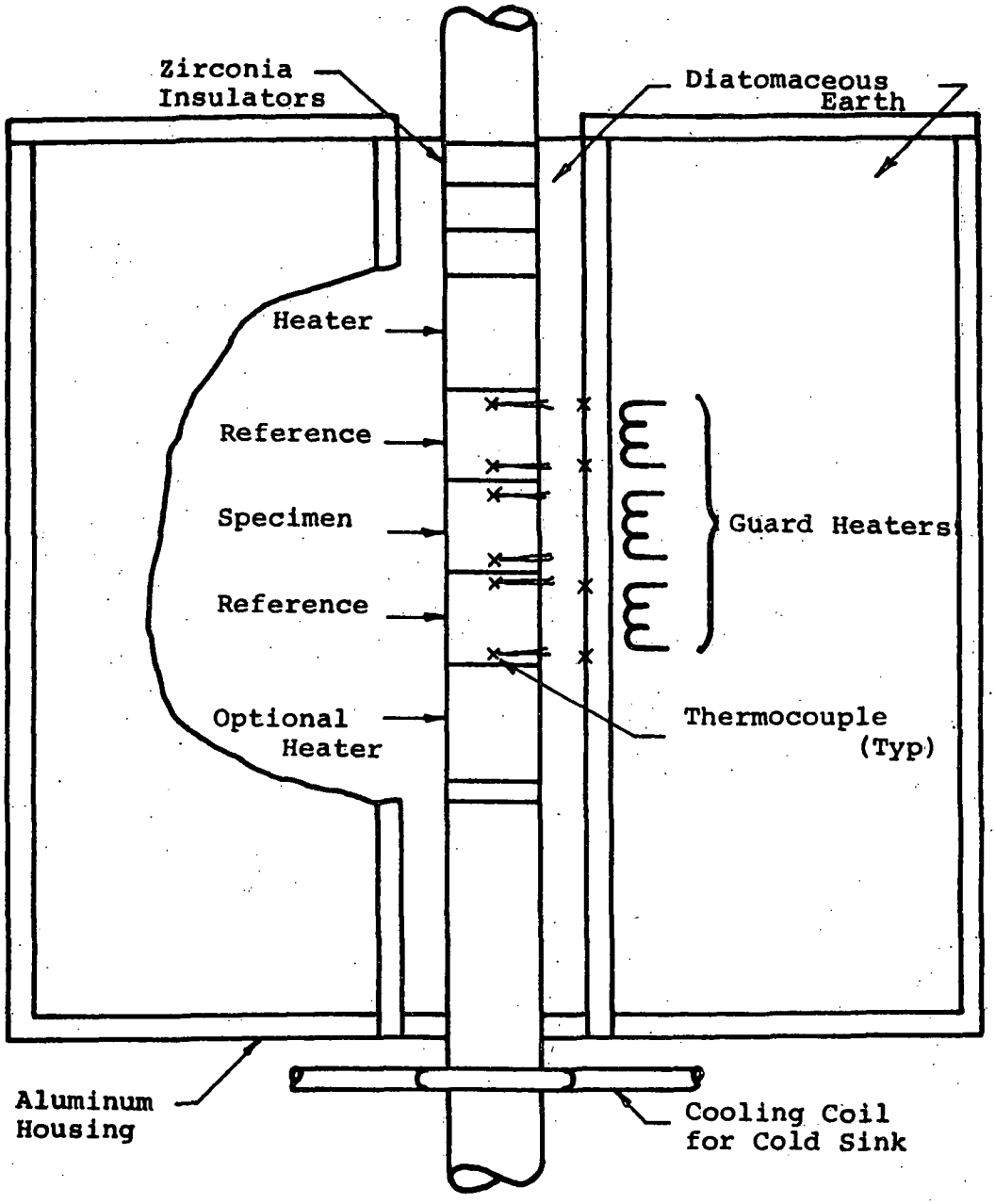

Figure A1. Schematic of Comparative Rod Thermal Conductivity Apparatus

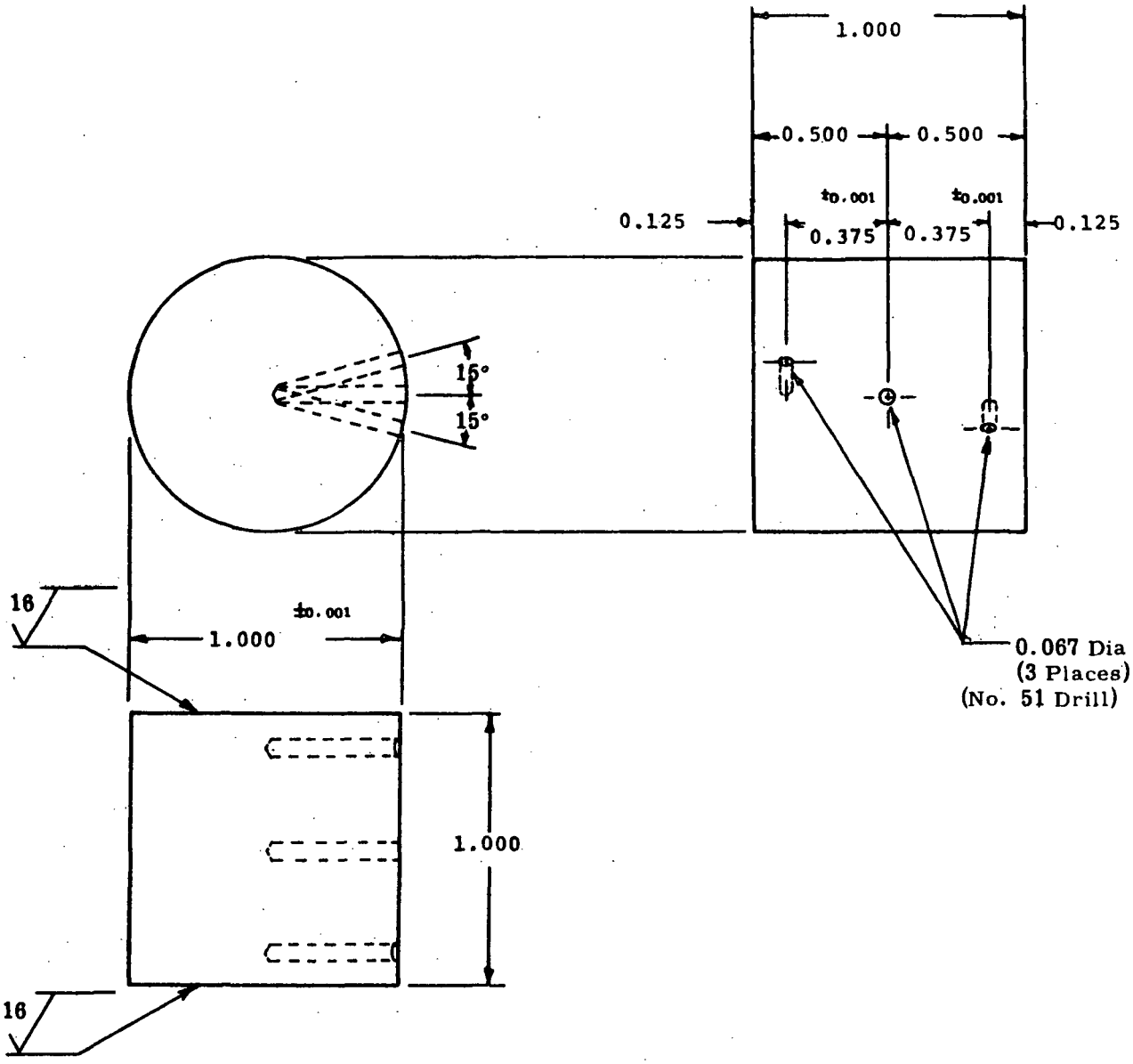

Note: All dimensions ±0.005 except where noted

Figure A2. Drawing of Specimen for Thermal Conductivity Measurements in Comparative Rod Apparatus to 1800°F

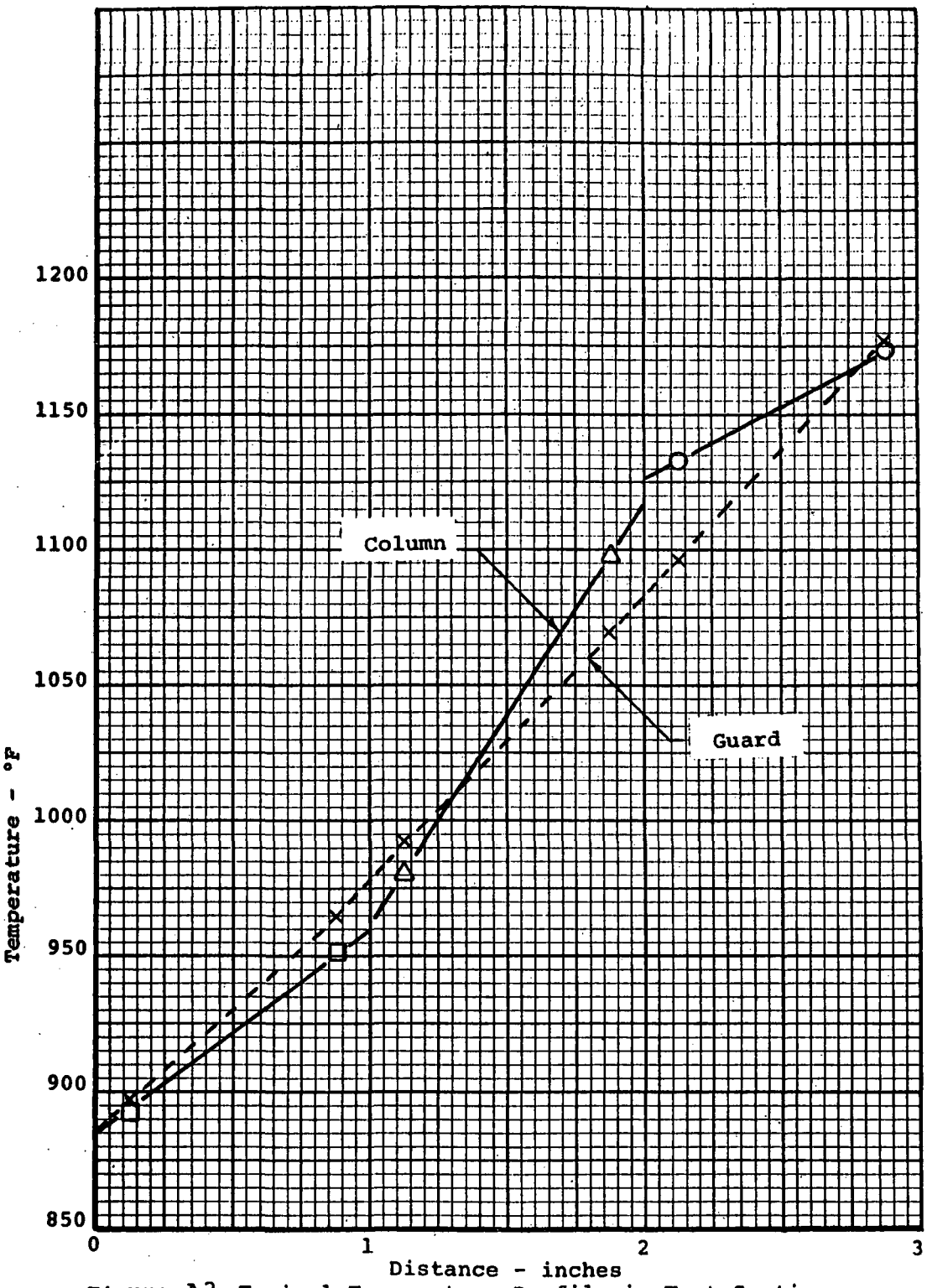

Figure A3. Typical Temperature Profile in Test Section

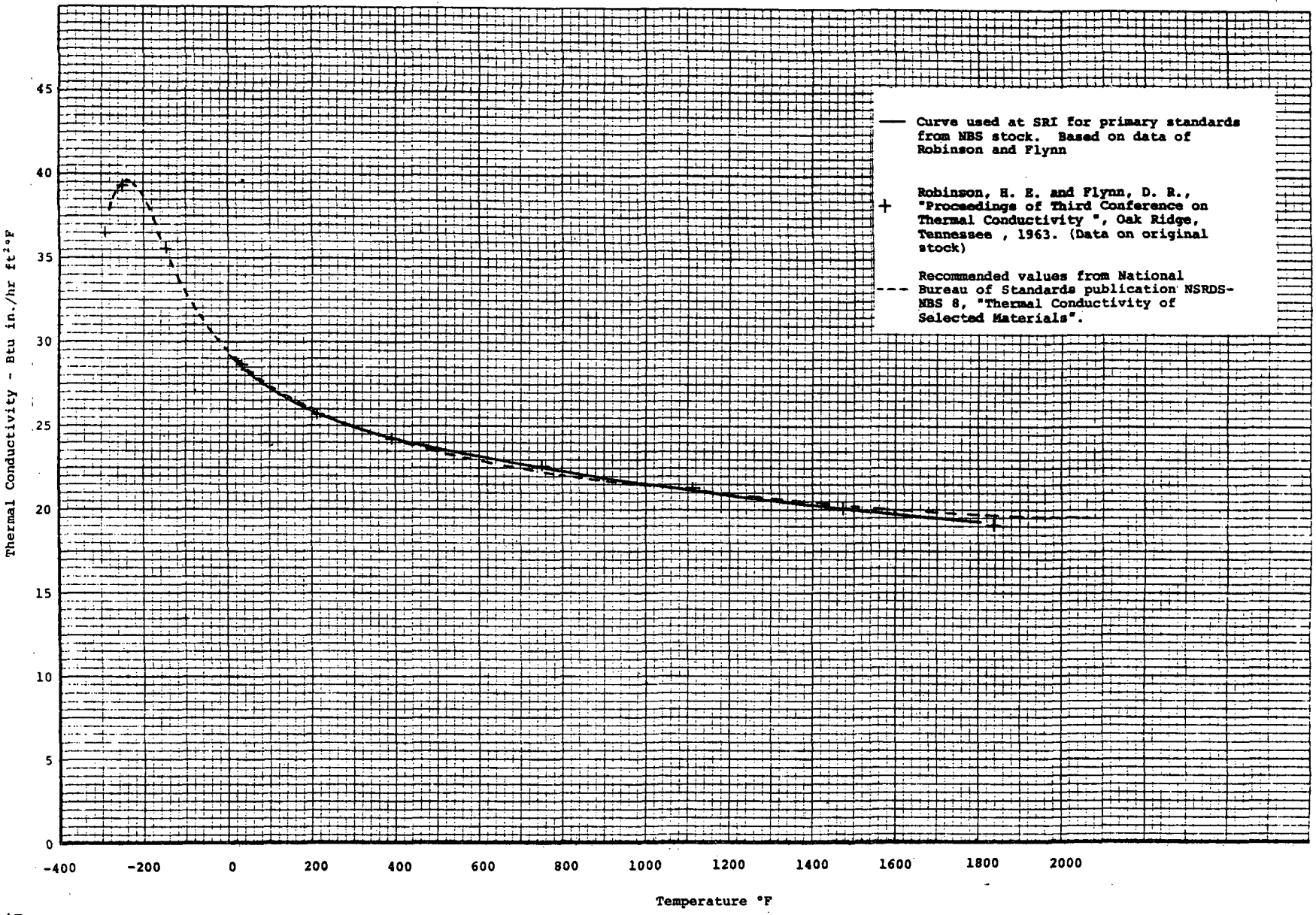

Figure A4. The Thermal Conductivity of Primary SRI Standards from NBS Stock of Code 9606 Pyroceram

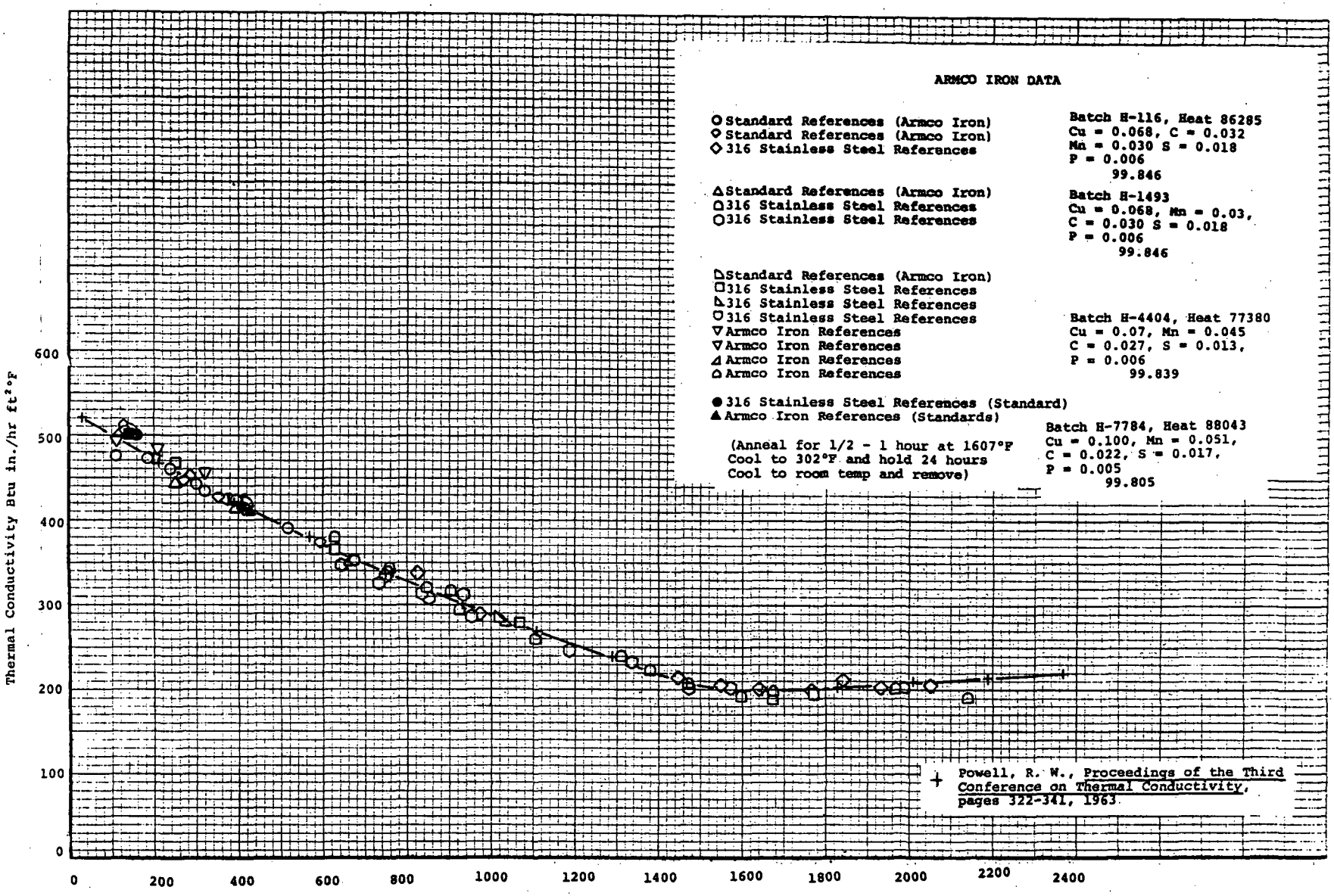

Figure A5. The Thermal Conductivity of Armco Iron

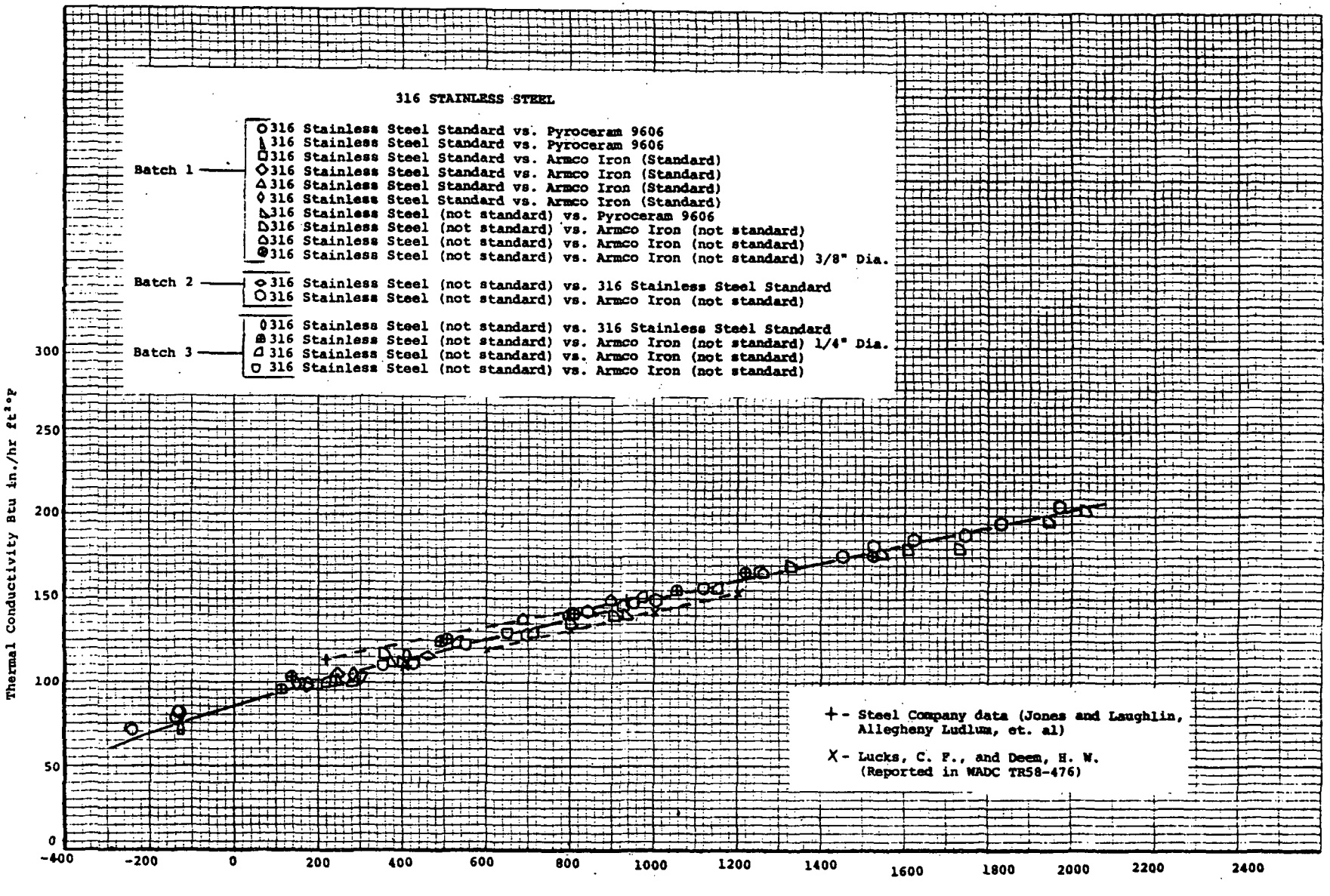

Figure A6. The Thermal Conductivity of 316 Stainless Steel

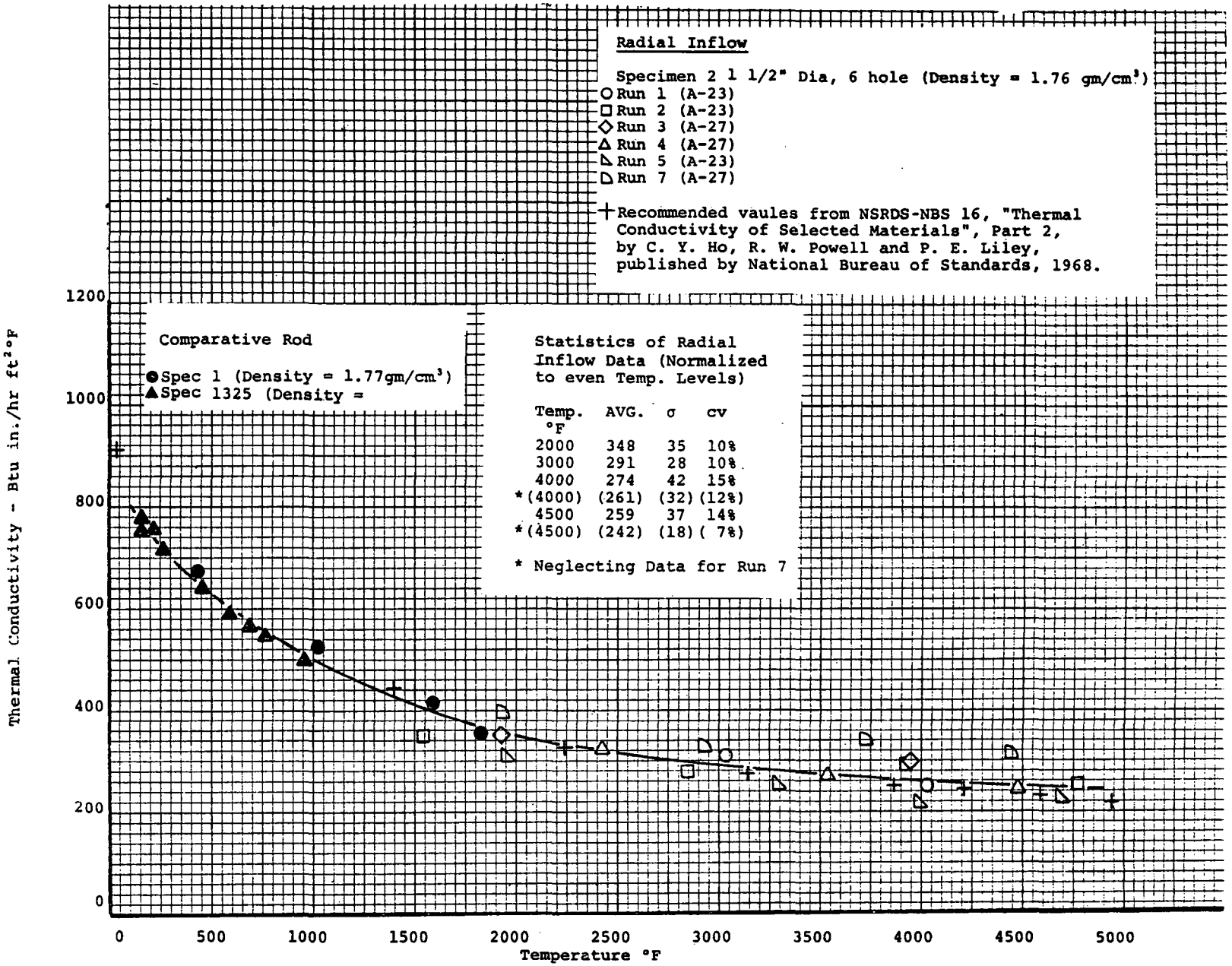

Figure A7. The Thermal Conductivity of ATJ Graphite, With Grain

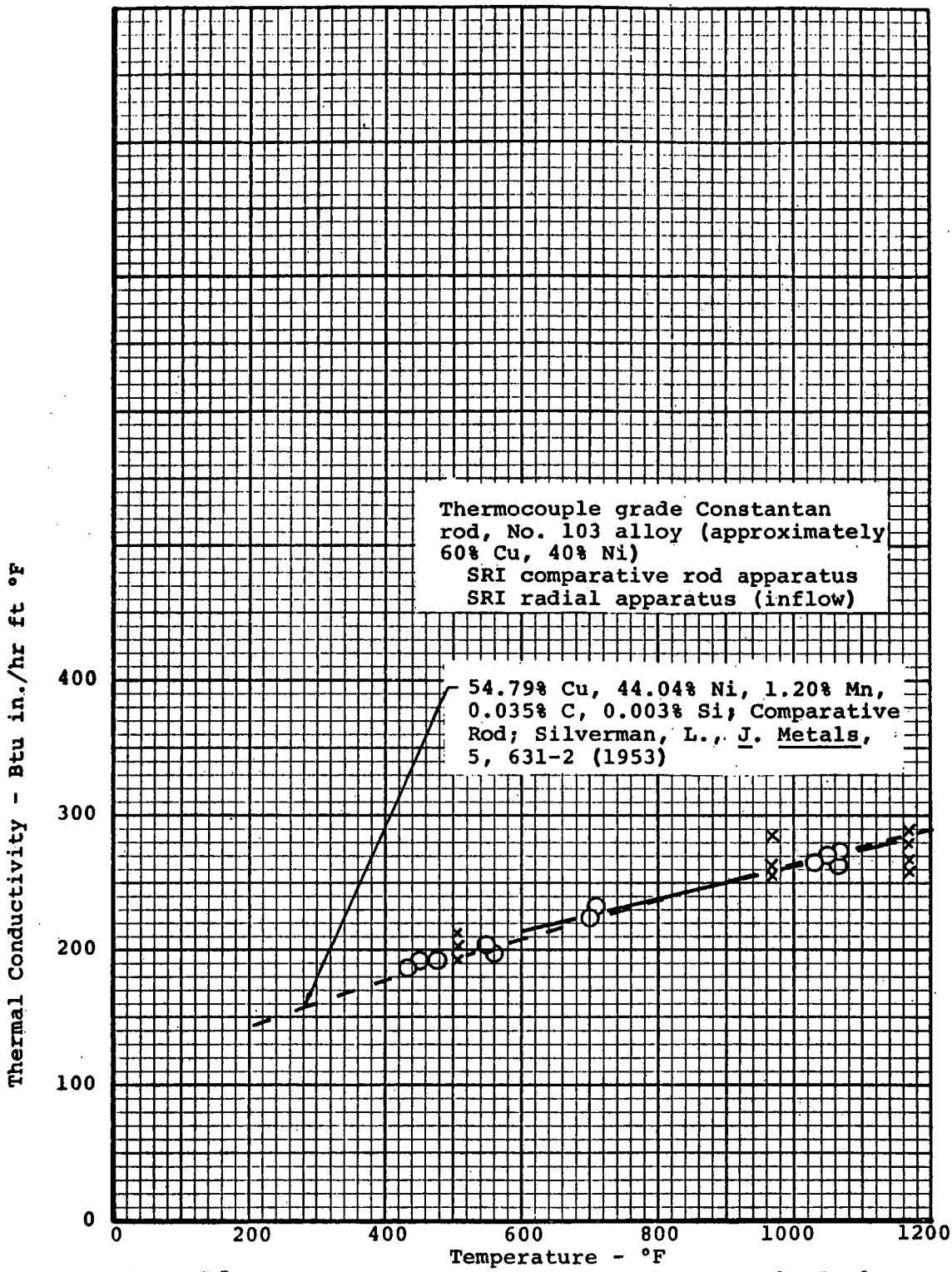

Figure A8. The Thermal Conductivity of Thermocouple Grade Constantan Rod

TABLE 1

SUMMARY OF DEGRADATION CONDITIONS

Furnace preheat temp K	Approximate cold wall heat flux (Btu/sec ft^2)	W/m^2	Measured temp rise rate through degradation zone (K/sec)	Remarks
----	----	----	0.17	Controlled temp response
----	----	----	1.5	
1400	15	17×10^4	16	
----	----	----	22	Turned power to max at time zero (cycled power)
2000	64	72.5×10^4	38	
2500	156	177×10^4	49	
3100	368	418×10^4	61	

TABLE 2

SUMMARY OF DATA OBTAINED ON CHARS PREPARED FROM LOW-DENSITY PHENOLIC-NYLON IN THE LABORATORY AT A HEATING RATE OF 0.1 K/SEC

CHARRING CONDITION: CONTROLLED TEMPERATURE RESPONSE
APPROXIMATE TEMPERATURE RISE RATE: 0.1 K/SEC COOLING IN FURNACE

Spec No	Max Temp K	Time at Uniform Max Temp (Sec)	Weight Loss (%)	Shrinkage (%)	Virgin Bulk Density (gm/cm^3)	Virgin Sonic Velocity (cm/μsec)	Char Bulk Density (gm/cm^3)	Coupon Bulk Density (gm/cm^3)	Char True Density (gm/cm^3)	Char Sonic Velocity (cm/μsec)	Char Elec Resis (Ω-cm)	d_{002} Lattice Spacing (A)	Crystallite Size L_c (A)	Water Absorption (%)	Open Porosity / Closed Porosity (%)	Thermal Conductivity at 300K ($\frac{W}{m\ K}$)	Spec Thickness (cm)
11-88	1989	27	74.2	24.6	0.573		0.331			0.219	0.0419			108.3	37/38.8	0.44	0.649
11-89	1989	27	74.5	25.1	0.569		0.325			0.252	0.321	4.0					0.631
11-77	3100	20	76.2	23.1	0.619		0.308		1.41	0.231	0.0300	3.5					0.554
11-78	3100	20	76.3	21.8	0.617		0.304			0.219	0.0313						0.557
7-17	1380	3600	71.6	24.5	0.577	0.184	0.358	0.358		0.237	0.042	No Peaks	No Peaks			0.26	0.656
7-18	1380	3600	72.6	24.8	0.584	0.184	0.355	0.356			0.043						0.635
7-17	3100	3600			0.577			0.313		0.207 0.242	0.0388					1.10	0.503

TABLE 3

SUMMARY OF DATA ON CHAR PREPARED FROM LOW-DENSITY PHENOLIC-NYLON IN THE LABORATORY AT A HEATING RATE OP 1.5 K/SEC

CHARRING CONDITION: CONTROLLED TEMPERATURE RESPONSE
APPROXIMATE TEMPERATURE RISE RATE: 1.5 K/SEC COOLING IN FURNACE

Spec No	Max Temp K	Time at Uniform Max Temp (Sec)	Weight Loss (%)	Shrinkage (%)	Virgin Bulk Density (gm/cm^3)	Virgin Sonic Velocity (cm/μsec)	Char Bulk Density (gm/cm^3)	Coupon Bulk Density (gm/cm^3)	Char True Density (gm/cm^3)	Char Sonic Velocity (cm/μsec)	Char Elec Resis (Ω-cm)	d_{002} Lattice Spacing (Å)	Crystallite Size L_c (Å)	Water Absorption (%)	Open Porosity / Closed Porosity (%)	Thermal Conductivity at 300K $(\frac{W}{m\ K})$	Spec Thickness (cm)	Remarks
11-94	2021	1	73.0	16.8	0.552		0.227										0.807	Spec fragmented
11-95	2021	1	72.2	19.3	0.528									177	52/25.5		0.782	" "
11-75	3150	1		18.2	0.621												0.779	" "
11-76	3150	1	79.3	19.7	0.623				1.30								0.765	" "

TABLE 4

SUMMARY OF DATA ON CHAR PREPARED FROM LOW-DENSITY PHENOLIC-NYLON IN LABORATORY AT A HEATING RATE OF 22 K/SEC

CHARRING CONDITION: CYCLED POWER
APPROXIMATE TEMPERATURE RISE RATE: 22 K/SEC COOLING IN FURNACE

Spec No	Max Temp K	Time at Uniform Max Temp (Sec)	Weight Loss (%)	Shrinkage (%)	Virgin Bulk Density (gm/cm^3)	Virgin Sonic Velocity (cm/μsec)	Char Bulk Density (gm/cm^3)	Coupon Bulk Density (gm/cm^3)	Char True Density (gm/cm^3)	Char Sonic Velocity (cm/μsec)	Char Elec Resis (Ω-cm)	d_{002} Lattice Spacing (Å)	Crystallite Size L_c (Å)	Water Absorption (%)	Open Porosity / Closed Porosity (%)	Thermal Conductivity at 300K ($\frac{W}{m\ K}$)	Spec Thickness (cm)
11-47	1770	1	70.1	15.0	0.592		0.224										0.810
11-85	1770	1	68.5	16.2	0.555		0.236										0.848
11-100	2044	1	69.3	17.9	0.615		0.238										0.723

TABLE 5

SUMMARY OF DATA ON CHAR PREPARED FROM LOW-DENSITY PHENOLIC-NYLON IN THE LABORATORY AT A HEATING RATE OF 16 K/SEC

CHARRING CONDITION: 1400K PREHEATED FURNACE
COLD WALL HEAT FLUX: 17×10^6 W/m^2
APPROXIMATE TEMPERATURE RISE RATE: 16 K/SEC COOLING IN FURNACE

Spec No	Max Temp K	Time at Uniform Max Temp (Sec)	Weight Loss (%)	Shrinkage (%)	Virgin Bulk Density (gm/cm^3)	Virgin Sonic Velocity (cm/μsec)	Char Bulk Density (gm/cm^3)	Coupon Bulk Density (gm/cm^3)	Char True Density (gm/cm^3)	Char Sonic Velocity (cm/μsec)	Char Elec Resis (Ω-cm)	d_{002} Lattice Spacing (Å)	Crystallite Size L_c (Å)	Water Absorption (%)	Open Porosity / Closed Porosity (%)	Thermal Conductivity at 300K ($\frac{W}{m\ K}$)	Spec Thickness (cm)
11-90	1957	20	70.4	21.4	0.535		0.229					3.491	56				0.780
11-91	1957	20	67.5	11.0	0.543		0.230							545	80.8/7.4		0.830
11-73	3100	270	68.8	13.2	0.621		0.216			0.197	0.025	3.381	338				0.603
11-74	3100	270	69.5	13.8	0.624		0.213		1.26	0.203							0.596

TABLE 6

SUMMARY OF DATA OBTAINED ON CHAR PREPARED FROM LOW-DENSITY PHENOLIC-NYLON IN THE LABORATORY AT A HEATING RATE OF 22 K/SEC

CHARRING CONDITION: 1500K PREHEATED FURNACE
APPROXIMATE TEMPERATURE RISE RATE: 22 K/SEC RAPID COOLING

Spec No	Max Temp K	Time at Uniform Max Temp (Sec)	Weight Loss (%)	Shrinkage (%)	Virgin Bulk Density (gm/cm^3)	Virgin Sonic Velocity (cm/μsec)	Char Bulk Density (gm/cm^3)	Coupon Bulk Density (gm/cm^3)	Char True Density (gm/cm^3)	Char Sonic Velocity (cm/μsec)	Char Elec Resis (Ω-cm)	d_{002} Lattice Spacing (Å)	Crystallite Size L_c (Å)	Water Absorption (%)	Open Porosity / Closed Porosity (%)	Thermal Conductivity at 300K $(\frac{W}{m\ K})$	Spec Thickness (cm)	Remarks
1-122	1500	1			0.590	0.163												Sample fell apart
1-123	1500	1			0.578	0.162												Sample fell apart

TABLE 7

SUMMARY OF DATA OBTAINED ON CHARS PREPARED FROM LOW-DENSITY PHENOLIC-NYLON IN THE LABORATORY AT A HEATING RATE OF 38 K/SEC

CHARRING CONDITION: 2000K PREHEATED FURNACE
COLD WALL HEAT FLUX: 72.5 x 10^4 W/m^2
APPROXIMATE TEMPERATURE RISE RATE: 38 K/SEC COOLING IN FURNACE

Spec No	Max Temp K	Time at Uniform Max Temp (Sec)	Weight Loss (%)	Shrinkage (%)	Virgin Bulk Density (gm/cm³)	Virgin Sonic Velocity (cm/μsec)	Char Bulk Density (gm/cm³)	Coupon Bulk Density (gm/cm³)	Char True Density (gm/cm³)	Char Sonic Velocity (cm/μsec)	Char Elec Resis (Ω-cm)	d_{002} Lattice Spacing (Å)	Crystallite Size L_c (Å)	Water Absorption (%)	Open Porosity / Closed Porosity (%)	Thermal Conductivity at 300K ($\frac{W}{m\,K}$)	Spec Thickness (cm)	Remarks
11-45	1971	-70	59.4	16.3	0.600		0.244			0.209	0.046						0.341	Specimen may have fallen
11-46	1971	-70	60.1	16.2	0.597		0.238			0.214	0.039						0.372	
11-92	2021	-39	64.9	16.0	0.561		0.244			0.212	0.069	3.5					0.504	
11-93	2021	-39	65.3	17.8	0.556		0.245			0.224	0.034	3.475	52				0.388	
11-61	1629		72.9	13.5	0.596		0.205		1.23			4.1						
11-62	1629		72.8	13.1	0.590		0.203										0.826	
11-67	3075	70	64.5	13.0	0.611		0.228		1.44	0.201	0.0085	3.385	241				0.462	
11-68	3075	70	64.4	12.4	0.604		0.225			0.175	0.015						0.442	
1-1	2027	60	68.3	22.6	0.513		0.225										0.740	
1-2	2027	60	67.8	20.8	0.528		0.231	0.220		0.165	0.124						0.500	
1-3	2010	60	69.4	18.9	0.549		0.226	0.351		0.161	0.067						0.508	
1-4	2010	60	68.8	19.6	0.557		0.232			0.182							0.509	
1-5	2044	60	68.3	18.2	0.558		0.230	0.236		0.187	0.116						0.500	
1-6	2044	60	67.1	19.0	0.565		0.233	0.256		0.184	0.228						0.510	
11-98	2033	37	66.4	17.9	0.612		0.262	0.349		0.252	0.066					0.35	0.447	
11-63	2516	60	65.7	16.9	0.586		0.242		1.42	0.173	0.027						0.381	
11-64	2516	60	65.4	17.1	0.576		0.237			0.194	0.0176	3.445	128				0.346	
11-65	2855	1	64.7	16.8	0.561		0.226		1.40	0.179	0.0071	3.425	127				0.351	
11-66	2855	1	65.7	18.6	0.559		0.227										0.250	
Added Bottom Purge																		
1-21	2016	-10	66.9	17.5	0.556		0.166	0.228									0.785	
1-22	2016	-10	67.6	17.8	0.562	0.168	0.225										0.783	
1-23	2021	-10	67.2	16.8	0.567	0.170	0.227										0.791	
1-24	2021	-10	67.8	18.0	0.575	0.171	0.226										0.784	
1-29	2055	50	67.4	16.8	0.572	0.170	0.227	0.289		0.209	0.062						0.467	
1-30	2055	50	68.0	18.2	0.570	0.170	0.226	0.252		0.196	0.109						0.503	
1-31	2055	50	67.8	16.7	0.578		0.227	0.319		0.196	0.161						0.499	
1-32	2055	50	67.8	17.0	0.576		0.226			0.207							0.502	Small part for velocity
1-33	2021	50	68.1	17.7	0.595	0.168	0.236			0.186	0.118						0.494	
1-34	2021	50	67.0	17.9	0.566	0.171	0.232			0.193	0.169						0.503	
1-35	2021	50	67.4	17.0	0.553	0.167	0.220			0.167	0.164						0.495	In three parts for velocity
1-36	2021	50	67.6	18.8	0.589	0.169	0.239			0.186	0.053						0.503	In four parts for velocity

TABLE 8

SUMMARY OF DATA OBTAINED ON CHARS PREPARED FROM LOW-DENSITY PHENOLIC-NYLON IN THE LABORATORY AT A HEATING RATE OF 40 K/SEC

CHARRING CONDITION: 2500 K PREHEATED FURNACE
COLD WALL HEAT FLUX: 177×10^4 W/m^2
APPROXIMATE TEMPERATURE RISE RATE: 49 K/SEC COOLING IN FURNACE

Spec No	Max Temp K	Time at Uniform Max Temp (Sec)	Weight Loss (%)	Shrinkage (%)	Virgin Bulk Density (gm/cm^3)	Virgin Sonic Velocity (cm/μsec)	Char Bulk Density (gm/cm^3)	Coupon Bulk Density (gm/cm^3)	Char True Density (gm/cm^3)	Char Sonic Velocity (cm/μsec)	Char Elec Resis (Ω-cm)	d_{002} Lattice Spacing (A)	Crystallite Size L_c (A)	Water Absorption (%)	Open Porosity / Closed Porosity (%)	Thermal Conductivity at 300K ($\frac{W}{m\ K}$)	Spec Thickness (cm)
11-43	2511	-30	57.0	15.5	0.601		0.258	0.341		0.205	0.024						0.434
11-44	2511	-30	59.4	16.3	0.604		0.264	0.350		0.192	0.013						0.398
11-55	2528	1	62.4	15.9	0.611		0.264	0.354		0.200	0.0138	3.444	97				0.433
11-56	2528	1	62.5	16.0	0.611		0.265	0.320		0.164	0.0259						0.554
11-57	2539	50	62.9	15.0	0.606		0.254	0.330		0.191	0.0189	3.446	95				0.473
11-58	2539	50	63.9	15.7	0.611		0.250	0.322		0.184	0.0161						0.431
11-59	2539	910	63.8	16.5	0.597		0.249	0.350		0.200	0.0114	3.437	110				0.383
11-60	2539	910	64.2	16.8	0.599		0.248	0.317		0.197	0.021						0.393
11-124	2539	14400	63.1	17.6	0.594		0.256	0.298		0.186	0.044						0.500
11-125	2539	14400	63.6	17.0	0.607		0.256	0.316		0.192	0.028						0.498
1-7	2516	10	63.9	18.1	0.553		0.238										0.779
1-8	2516	10	64.2	18.5	0.572		0.244										0.777
1-9	2505	10	61.7	19.4	0.544		0.255	0.312		0.198	0.031						0.529
1-10	2505	10	63.1	19.4	0.566		0.255	0.332		0.180	0.024						0.459
1-11	2550	10	62.6	19.5	0.541		0.244	0.358		0.175	0.028						0.350
1-12	2550	10	63.0	20.0	0.553		0.249	0.336		0.174	0.030						0.442
1-13	2550	14400	63.3	20.3	0.535	0.153	0.236	0.299		0.149	0.0256						0.470
1-14	2550	14400	63.6	20.6	0.546	0.159	0.242	0.303		0.154	0.0263						0.468
			Added Bottom Purge														
1-15	2516	10	64.5	20.8	0.526	0.152	0.230	0.326		0.153	0.0302						0.330
1-16	2516	10	63.8	19.4	0.532	0.156	0.234	0.334		0.174	0.0253						0.356
1-17	2516	10	64.0	22.2	0.500	0.137	0.225	0.337		0.146	0.0257						.311
1-18	2516	10	64.2	20.8	0.511	0.143	0.226	0.316		0.162	0.0323						0.329
1-41	2561	10	63.2	16.9	0.572	0.170	0.244	0.312		0.205	0.023						0.418
1-42	2561	10	62.9	17.5	0.552	0.166	0.240	0.310		0.211	0.0235						0.414
1-43	2522	10	63.7	18.6	0.561	0.165	0.243	0.315		0.198	0.0327						0.443
1-44	2522	10	62.9	19.9	0.536	0.159	0.240	0.317		0.167	0.0280						0.406
11-115	2438	10	63.8	17.1	0.592		0.252	0.315		0.178	0.0468						0.500

TABLE 8 (CONTINUED)

RAPID COOLING

Spec No	Max Temp K	Time at Uniform Max Temp (Sec)	Weight Loss (%)	Shrinkage (%)	Virgin Bulk Density (gm/cm^3)	Virgin Sonic Velocity (cm/μsec)	Char Bulk Density (gm/cm^3)	Coupon Bulk Density (gm/cm^3)	Char True Density (gm/cm^3)	Char Sonic Velocity (cm/μsec)	Char Elec Resis (Ω-cm)	d_{002} Lattice Spacing (Å)	Crystallite Size L_c (Å)	Water Absorption (%)	Open Porosity / Closed Porosity (%)	Thermal Conductivity at 300K ($\frac{W}{m\ K}$)	Spec Thickness (cm)	Remarks
1-45	2494	1	60.6	16.0	0.541	0.172	0.245	0.314		0.205	0.027					1.65	0.478	
1-46	2494	1	61.4	16.4	0.559	0.173	0.252		1.43	0.209	0.031	3.433	114				0.474	
1-49	2533	14400	63.4	18.2	0.580	0.172	0.245		1.43	0.209	0.0228	3.405	173				0.406	
1-50	2533	14400	63.5	16.8	0.570	0.173	0.239	0.314		0.202	0.020					4.2	0.383	
1-65	2579	1	61.9	16.7	0.582	0.162	0.262	0.339		0.195	0.0275						0.439	
1-66	2579	1	61.6	16.7	0.575	0.166	0.255										0.797	
1-76	2528	90	64.1	17.8	0.585	0.166	0.249	0.325			0.019						0.254	Broken
1-77	2528	90	64.1	17.3	0.579	0.168	0.246	0.327			0.027						0.405	
1-86	2649	100	61.8	17.0	0.563	0.154	0.246	0.313		0.188	0.019			181	61.8 / 14.4		0.498	
1-87	2649	100	60.9	16.7	0.577	0.162	0.256										0.792	
1-88	2776	60	61.4	15.8	0.582	0.158	0.251	0.314		0.179	0.014						0.524	
1-89	2776	60	62.1	16.1	0.581	0.161	0.261										0.799	
1-90	3030	60	62.4	13.4	0.585	0.158	0.224	0.287		0.192	0.0063	3.371	325				0.405	
1-91	3030	60	61.5	13.2	0.579	0.165	0.226										0.826	

TABLE 9

SUMMARY OF DATA OBTAINED ON CHAR PREPARED FROM LOW-DENSITY PHENOLIC-NYLON IN THE LABORATORY AT A HEATING RATE OF 61 K/SEC

CHARRING CONDITION: 3100 K PREHEATED FURNACE
COLD WALL HEAT FLUX: 418 x 10^4 W/m^2
APPROXIMATE TEMPERATURE RISE RATE: 61 K/SEC COOLING IN FURNACE

Spec No	Max Temp K	Time at Uniform Max Temp (Sec)	Weight Loss (%)	Shrinkage (%)	Virgin Bulk Density (gm/cm^3)	Virgin Sonic Velocity (cm/μsec)	Char Bulk Density (gm/cm^3)	Coupon Bulk Density (gm/cm^3)	Char True Density (gm/cm^3)	Char Sonic Velocity (cm/μsec)	Char Elec Resis (Ω-cm)	d_{002} Lattice Spacing (Å)	Crystallite Size L_c (Å)	Water Absorption (%)	Open Porosity / Closed Porosity (%)	Thermal Conductivity at 300 K (W/m K)	Spec Thickness (cm)
11-86	3080	20	62.2	24.6	0.513		0.241	0.313		0.180	0.029					5.9	0.400
11-87	3080	20	61.2	16.0	0.547		0.233	0.300		0.168	0.0094						0.460
11-71	3080	37	62.0	14.0	0.626		0.256	0.303		0.161	0.0245						0.577
11-72	3080	37	62.3	14.6	0.622		0.253		1.36	0.180	0.0172	3.410	122				0.444
11-120	3125	276	62.4	15.2	0.610		0.251										0.811
11-121	3125	276	62.5	13.9	0.608		0.244					3.398	162				0.823
11-122	3136	14400	62.4	17.0	0.610		0.251	0.356	1.65	0.174	0.008						(0.503) (0.254)
11-123	3136	14400	59.8	14.6	0.611		0.261	0.313		0.171	0.0119	3.368	300			13.2	0.561
11-101	3090	30	Bottom Purge Added							0.177	0.0081						0.402
1-25	3136	30	61.8	15.4	0.573	0.171	0.235	0.276		0.159	0.0205						0.503
1-26	3136	30	62.4	15.6	0.580	0.171	0.235	0.304		0.155	0.0164						0.434
1-27	3136	30	61.8	14.2	0.571	0.171	0.234	0.273		0.157	0.0194						0.585
1-28	3136	30	62.2	14.8	0.576	0.172	0.237	0.305		0.177	0.0188						0.523
1-37	3114	30	62.3	14.1	0.564	0.164	0.226	0.299		0.176	0.0179						0.420
1-38	3114	30	61.9	14.1	0.584	0.172	0.239			0.183	0.0159						0.458
1-39	3114	30	62.4	13.3	0.570	0.164	0.230		1.45	0.173	0.0188	3.394	139				0.450
1-40	3114	30	62.5	16.1	0.557	0.163	0.230	0.309	1.53	0.176	0.0191	3.394	152				0.451
1-67	3103	20	62.0	14.9	0.584	0.168	0.237					(3.392 HF) (3.374M)	(151) (294)				0.812
1-68	3103	20	61.3	14.5	0.573	0.167	0.233	0.301		0.173	0.015						0.416
1-92	3058	50	62.2	15.2	0.592	0.165	0.246	0.337		0.194	0.017	3.397	140			61	0.387
1-93	3058	50	60.7	13.6	0.575	0.169	0.241	0.285		0.185	0.022			238	67.1/13.6		0.319
1-94	3114	40	61.9	14.5	0.586	0.166	0.240	0.320		0.172	0.013						0.410
1-95	3114	40	61.3	13.8	0.579	0.163	0.234										0.821
1-96	3170	240	62.1	14.9	0.583	0.160	0.228	0.322		0.173	0.0134						0.268
1-97	3170	240	60.6	13.8	0.552	0.163	0.222	0.284		0.189	0.0077						0.455
1-98	3142	240	59.6	10.8	0.558	0.160	0.219	0.277		0.183	0.008						0.441
1-99	3142	240	59.4	13.1	0.546	0.159	0.224										0.827
1-100	3143	540	61.5	15.4	0.560	0.160	0.226	0.315		0.178	0.012						0.287
1-101	3143	540	61.7	14.1	0.580	0.165	0.235					(3.379 HF) (3.369M)	(232) (325)				0.820
1-102	3114	255	61.7	14.9	0.583	0.164	0.237										0.811
1-103	3114	255	61.8	13.8	0.584	0.165	0.233										0.826
1-108	3148	540	62.0	14.0	0.591	0.164	0.233	0.304		0.188	0.008						0.459
1-109	3148	540	61.7	14.3	0.577	0.165	0.232										0.818

TABLE 10

SUMMARY OF X-RAY DIFFRACTION MEASUREMENTS IN-DEPTH ON CHAR MADE IN LABORATORY FROM LOW-DENSITY PHENOLIC-NYLON

Specimen No.	Mean Distance from Heated Surface (cm)	d_{002} Lattice Spacing Å	L_{002} Crystallite Size Å
11-120-1	0.0368	3.4076	126
11-121-1			
11-121-2	0.112	3.4044	140
11-121-3	0.192	3.3964	156
11-121-4	0.281	3.3932	176
11-121-5	0.370	3.3900	212
	Average	3.3983	162

TABLE 11

SUMMARY OF THERMAL CONDUCTIVITY DATA ON CHARS

Specimen Number	Charring Condition	Time At Uniform Temp (Sec)	Mean Temperature (°F)	Mean Temperature (°K)	Thermal Conductivity BTU in/hr ft² °F Raw	Corrected For Heat Shunting	Corrected For Inter-Face Resis	Corrected $\left(\frac{W}{m\text{-}K}\right)$	Spec Thickness (cm)
	Low-Density Phenolic-Nylon								
7-17	0.1 K/sec to 1366K	3600	158	343	3.2	2.2	--	.32	.656
			365	458	3.65	2.6	--	.37	
			526	548	4.11	2.9	--	.42	
			1046	836	5.16	3.45	--	.50	
			1366	1014	5.25	3.3	--	.48	
7-17	0.1 K/sec to 1366K & then 1 K/sec to 3100K	3600	148	338	8.25	7.5	--	1.08	.503
			489	527	10.63	9.8	--	1.41	
			1014	819	11.60	10.6	--	1.53	
			1440	1055	10.99	9.7	--	1.40	
1-83	72.5 x 10^4 w/m² to 2000K	50	187	359	4.12	3.2	--	.46	.362
			572	573	5.47	4.3	--	.62	
			975	797	5.83	4.3	--	.62	
			1429	1049	5.75	3.8	--	.55	
1-111	72.5 x 10^4 w/m² to 2000K	14400	180	355	4.78	3.85	--	.55	.509
			485	525	6.00	4.95	--	.71	
			957	787	6.83	5.4	--	.78	
			1439	1055	7.38	5.6	--	.81	
11-88	.1 K/sec to 1989K	27	143	335	4.20	3.4	--	.49	.649
			465	514	5.46	4.4	--	.63	
			1031	826	6.73	5.2	--	.75	
			1441	1056	6.89	5.0	--	.72	
1-45	177 x 10^4 w/m² to 2500K	1	179	355	13.0	12.4	12.7	1.83	.478
			509	538	15.3	14.8	15.2	2.19	
			998	810	18.0	17.8	18.6	2.68	
11-98	72.5 x 10^4 w/m² to 2000K	37	517	543	4.84	3.7	--	.53	.446
			1040	833	5.99	4.45	--	.64	
			1486	1081	6.73	4.8	--	.69	

TABLE 11 (CONTINUED)

Specimen Number	Charring Condition	Time At Uniform Temp (Sec)	Mean Temperature (°F)	Mean Temperature (°K)	Thermal Conductivity BTU in/hr ft² °F Raw	Thermal Conductivity BTU in/hr ft² °F Corrected For Heat Shunting	Thermal Conductivity BTU in/hr ft² °F Corrected For Inter-Face Resis	Corrected $\frac{W}{m-k}$	Specimen Thickness (cm)
1-50	177 x 10^4 w/m² to 2500K	14400	243	390	28.4	28.4	31.3	4.51	
			513	540	28.5	28.7	31.9	4.60	.384
			1016	820	26.6	26.5	29	4.18	
11-86	418 x 10^4 w/m² to 3100K	20	404	480	34.8	35.1	39.9	5.75	
			976	798	30.5	30.8	34.4	4.95	.399
			1502	1090	28.7	29.7	33	4.75	
1-92	418 x 10^4 w/m² to 3100K	50	176	353	35.4	35.8	40.9	5.90	
			521	545	36.2	36.5	41.9	6.04	.387
			935	775	33.4	34.0	38.8	5.60	
			1404	1035	31.7	33.1	37.3	5.38	
11-123	418 x 10^4 w/m² to 3100K	14400	357	454	66.7	68.2	81	11.69	
			737	665	58.6	60.8	70	10.1	.560
			1374	1019	46.4	49.3	55.5	8.00	
	ARC-JET								
2-2	227 x 10^4 w/m² to ∿ 2170K	400	156	342	14.9	14.4	15	2.16	
			484	524	18.2	17.7	18.4	2.65	.509
			949	783	18.6	18.2	19.1	2.76	
			1499	1088	20.3	20.1	21.4	3.08	
2-8	227 x 10^4 w/m² to ∿ 1445K	400	145	336	2.32	1.35	--	.195	
			520	544	3.12	1.80	--	.26	.508
			980	800	3.76	2.10	--	.30	
			1392	1029	4.92	2.85	--	.41	
	High-Density Phenolic-Nylon								
HD-5			145	336	41.02	41.4	48.2	6.95	
			500	533	47.06	48.1	57.1	8.25	.298
			999	810	42.88	44.1	52	7.50	
			1494	1085	38.80	40.0	46.5	6.70	
			985	803	43.49	44.9	53	7.6	
			1496	1086	32.49	34.0	39	5.6	

TABLE 11 (CONTINUED)

Specimen Number	Charring Condition	Time At Uniform Temp (Sec)	Mean Temperature (°F)	Mean Temperature (°K)	Thermal Conductivity BTU in/hr ft²°F Raw	Thermal Conductivity BTU in/hr ft²°F Corrected For Heat Shunting	Thermal Conductivity BTU in/hr ft²°F Corrected For Inter-Face Resis	Corrected $(\frac{W}{m-k})$	Spec Thickness (cm)
	Phenolic Char								
HMP	slow temp rise to 3041		130	328	37.2	37.5	40.5	5.85	
			428	493	44.7	45.4	49.9	7.19	.663
			1034	830	50.4	52.3	58.3	8.40	
			1479	1077	47.9	51.5	57.3	8.25	
P-6	397 x 10^4 w/m² to 3013K	240	165	347	24.7	24.7	26.5	3.82	
			491	528	25.8	25.7	27.5	3.96	.530
			1001	811	21.9	21.8	23.3	3.36	
			1515	1097	17.9	17.5	18.3	2.64	

TABLE 12

SUMMARY OF DATA OBTAINED ON CHAR PREPARED FROM LOW-DENSITY PHENOLIC-NYLON
(CHAR PREPARED AND SUPPLIED BY NASA LANGLEY)

CHARRING CONDITION: ARC-JET AT h = 23 258 JOULES/gm - NITROGEN
COLD WALL HEAT FLUX: 227 x 10^4 W/m^2

Spec No	Max Temp K	Time at Uniform Max Temp (Sec)	Weight Loss (%)	Shrinkage (%)	Virgin Bulk Density (gm/cm³)	Virgin Sonic Velocity (cm/μsec)	Char Bulk Density (gm/cm³)	Coupon Bulk Density (gm/cm³)	Char True Density (gm/cm³)	Char Sonic Velocity (cm/μsec)	Char Elec Resis (Ω-cm)	d_{002} Lattice Spacing (A)	Crystallite Size L_c (A)	Water Absorption (%)	Open Porosity / Closed Porosity (%)	Thermal Conductivity at 300K $(\frac{W}{m\ K})$	Spec Thickness (cm)
1-1	2500	~400 sec						0.266		0.187	0.0218						0.508
1-2	2500							0.265		0.195	0.0234						0.510
1-3	2500							0.259		0.221	0.0182						0.510
1-4	2260							0.193		0.199	0.0237						0.509
1-5	2260																
1-6	2260							0.200		0.210	0.0269						0.510
1-7	1800							0.127		0.200	0.1050						0.509
1-8	1800																
1-9	1800							0.121		0.214	0.0756						
2-1	2500							0.295		0.244	0.0174						0.509
2-2	2500							0.332								2.01	0.508
2-3	2500							0.268		0.224	0.0223						0.509
2-4	2260							0.223		0.246	0.0329						0.509
2-5	2260																
2-6	2260							0.214		0.229	0.0296						0.508
2-7	1800							0.158		0.193	0.0865						0.510
2-8	1800															0.170	0.508
2-9	1800							0.158		0.205	0.0903						0.509

TABLE 13

SUMMARY OF X-RAY DIFFRACTION MEASUREMENTS IN-DEPTH ON LOW-DENSITY PHENOLIC-NYLON CHARRED IN ARC-JET AT 227 x 10^4 W/m^2

Specimen No.	Mean Distance from Heated Surface (cm)	d_{002} Lattice Spacing (Å)	L_{002} Crystallite Size (Å)
ARC-JET 1	0.0407	3.426	145
ARC-JET 2	0.241	3.428	125
ARC-JET 3	0.569	3.434	120
ARC-JET 4	0.876	3.436	105
ARC-JET 5	No Measurable Peaks		
ARC-JET 6	No Measurable Peaks		
Average =		3.431	124
Note: Lattice Spacing was potassium chloride corrected.			

TABLE 14

SUMMARY OF DATA OBTAINED ON CHAR PREPARED FROM HIGH-DENSITY PHENOLIC IN THE LABORATORY AT DIFFERENT HEATING RATES TO DIFFERENT TEMPERATURES

Spec No	Max Temp K	Time at Uniform Max Temp (Sec)	Weight Loss (%)	Shrinkage (%)	Virgin Bulk Density (gm/cm^3)	Virgin Sonic Velocity (cm/μsec)	Char Bulk Density (gm/cm^3)	Coupon Bulk Density (gm/cm^3)	Char True Density (gm/cm^3)	Char Sonic Velocity (cm/μsec)	Char Elec Resis (Ω-cm)	d_{002} Lattice Spacing (Å)	Crystallite Size L_c (Å)	Water Absorption (%)	Open Porosity / Closed Porosity (%)	Thermal Conductivity at 300K ($\frac{W}{m\ K}$)	Spec Thickness (cm)	Char Conditions	Remarks
HD-1	1539	135																1511 K Preheat	Fragmented
HD-2	1539	135																1511 K Preheat	Fragmented
HD-3	2066	210	74.9	19.0	1.204		0.373	0.364		0.122	0.0678						0.583	2010 K Preheat	Rapid cooling; Blank loose
HD-4	2066	210	74.7	25.9	1.204		0.409	0.370		0.199	0.0656						0.612	2010 K Preheat	Rapid cooling; Blank loose
HD-5	2651	110						0.755		0.170	0.0132					6.5	0.298	2606 K Preheat	Rapid cooling; Ok
HD-6	2651	110	69.5	25.3	1.204		0.477	0.731		0.178	0.0084	3.414	220				0.332	2606 K Preheat	Rapid cooling; Ok
HD-7	3136	140	67.5	26.8	1.204		0.493	0.709		0.188	0.0060						0.380	3103 K Preheat	Ok
HD-8	3136	140	67.1	26.2	1.205		0.488	0.656		0.166	0.0070	3.368	415				0.450	3103 K Preheat	Ok
HD-9	3114																	15K/sec to 3114K	Fragmented
HD-10	3114																	15K/Sec to 3114K	Fragmented
HD-11	3136																	slow char 3136K	Fragmented
HD-12	3136																	slow char 3136K	Fragmented
HD-13	3035		79.7	23.0	1.205		0.626	0.637			0.0715						0.524	slow char 3136K	Cracked
HD-14	3035		79.9	28.5	1.205		0.649	0.667			0.0459						0.526	slow char 3136K	Cracked

TABLE 15

SUMMARY OF DATA OBTAINED ON CHAR PREPARED FROM PHENOLIC
IN THE LABORATORY AT DIFFERENT HEATING RATES TO DIFFERENT TEMPERATURES

Spec No	Max Temp K	Time at Uniform Max Temp (Sec)	Weight Loss (%)	Shrinkage (%)	Virgin Bulk Density (gm/cm^3)	Virgin Sonic Velocity (cm/μsec)	Char Bulk Density (gm/cm^3)	Coupon Bulk Density (gm/cm^3)	Char True Density (gm/cm^3)	Char Sonic Velocity (cm/μsec)	Char Elec Resis (Ω-cm)	d_{002} Lattice Spacing (Å)	Crystallite Size L_c (Å)	Water Absorption (%)	Open Porosity / Closed Porosity (%)	Thermal Conductivity at 300K $(\frac{W}{m\ K})$	Spec Thickness (cm)	Char Conditions
P-1	3035		40.8	7.0	1.261		1.166										0.738	slow 0.043 K/sec first cycle
P-2	3035																	slow 0.127 K/sec
P-3	2022	90	44.9	5.8	1.266		0.587										0.834	2010 K preheat 38 K/sec
P-4	2022	90	45.8	11.7	1.255		0.523	0.590		0.120	0.0370						0.570	2010 K preheat 38 K/sec
P-5	3066	180	42.4	2.8	1.263		0.606	0.647		0.103	0.0174	3.373	270				0.501	3013 K preheat 61 K/sec
P-6	3066	180	43.6	1.8	1.258		0.605	0.655		0.107	0.0132					3.5	0.530	3013 K preheat 61 K/sec
P-7	2494	130	44.1	11.4	1.257		0.558	0.618		0.122	0.0285						0.530	2505 K preheat 49 K/sec
P-8	2494	130	43.8	9.3	1.263		0.565	0.625		0.118	0.0303						0.499	2505 K preheat 49 K/sec
P-9	399				1.259													slow heating - fragmented
P-10	928				1.256													slow heating - fragmented
P-11	726				1.264													slow heating - fragmented
HMP	3041		53.2	20.6	1.251		1.062	1.126				No Peak	No peak			5.5	0.663	slow See Figure 20

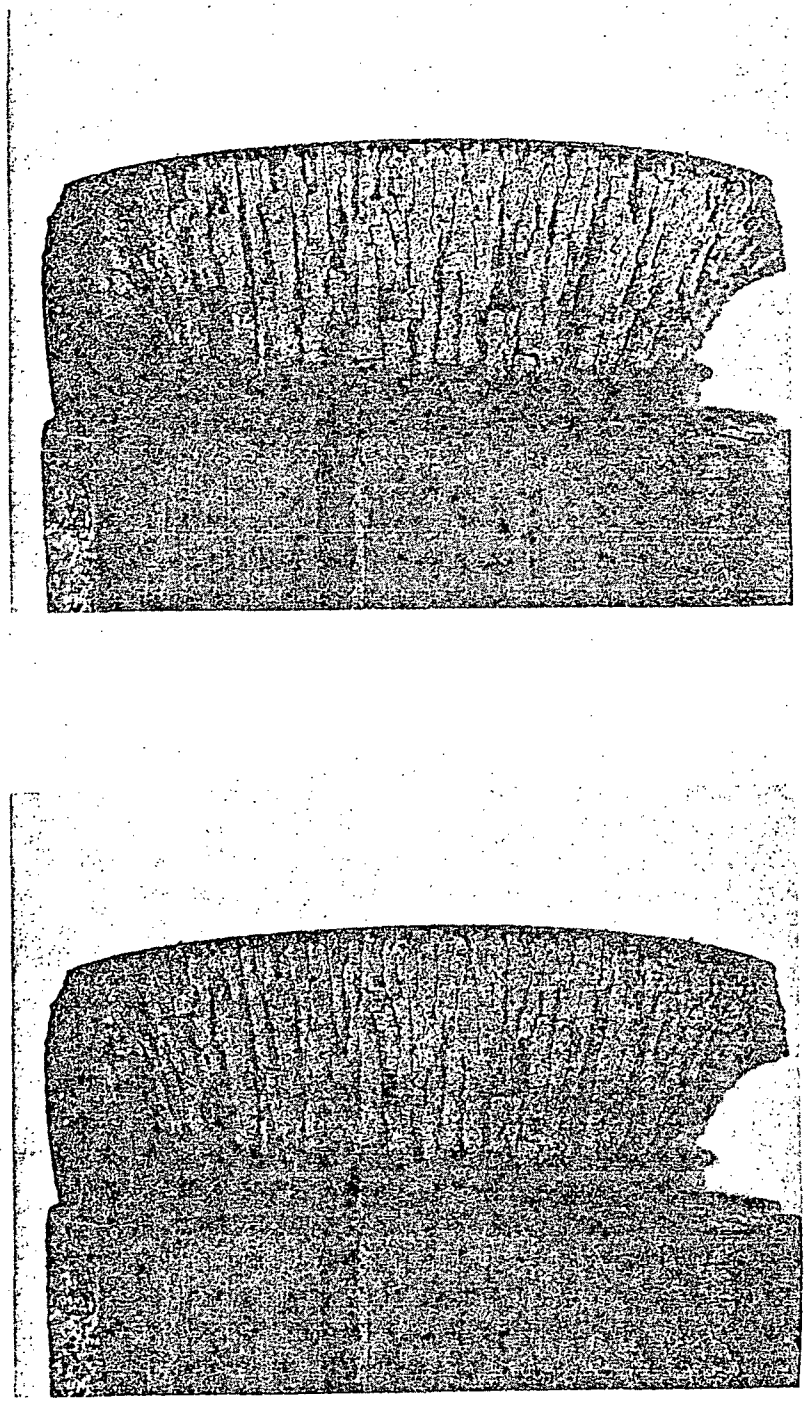

Figure 1. Pictures of chars prepared in the arc-jet in nitrogen at 226×10^4 W/m^2 for 400-500 seconds

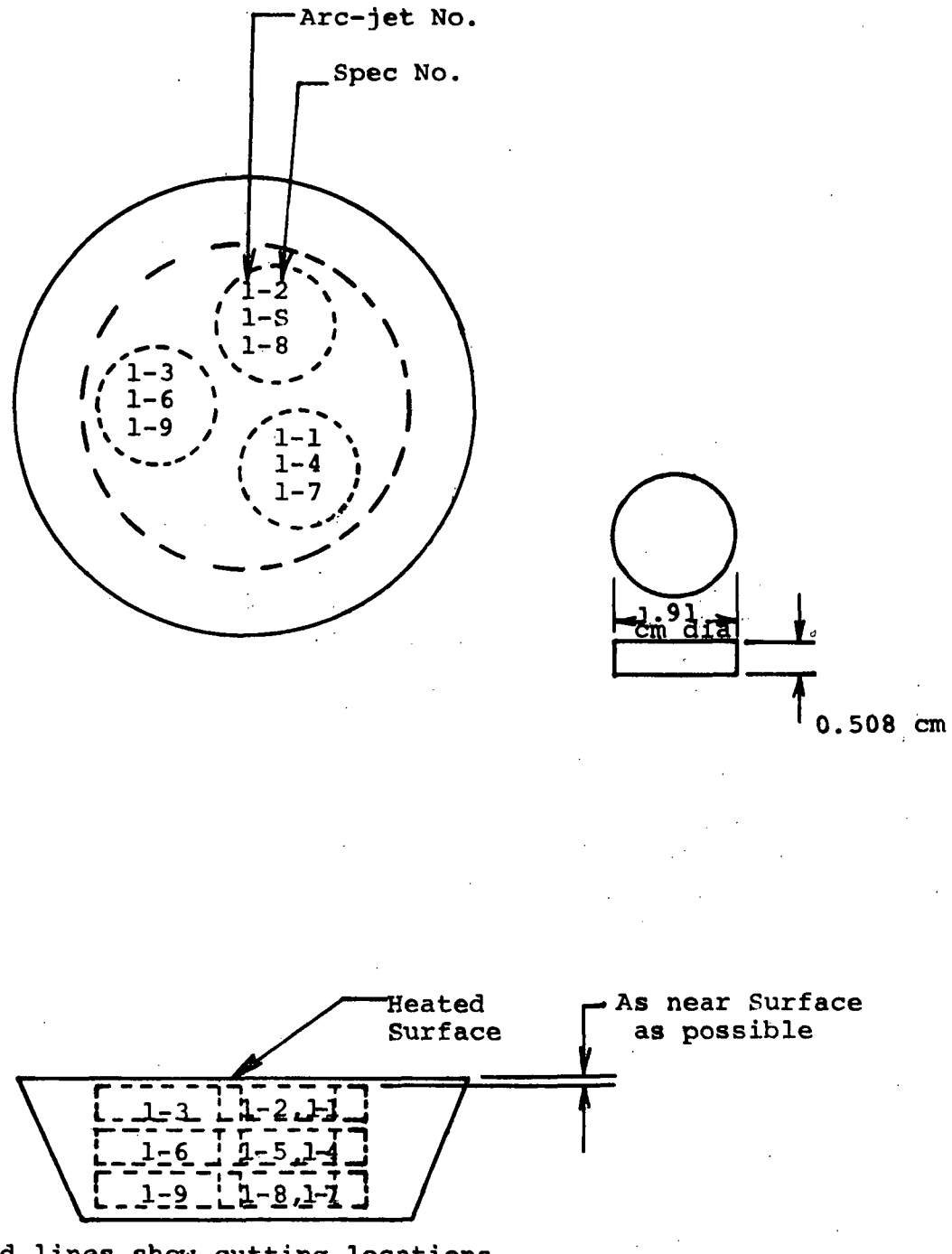

Figure 2. Cutting plan for arc-jet chars 1 and 2.

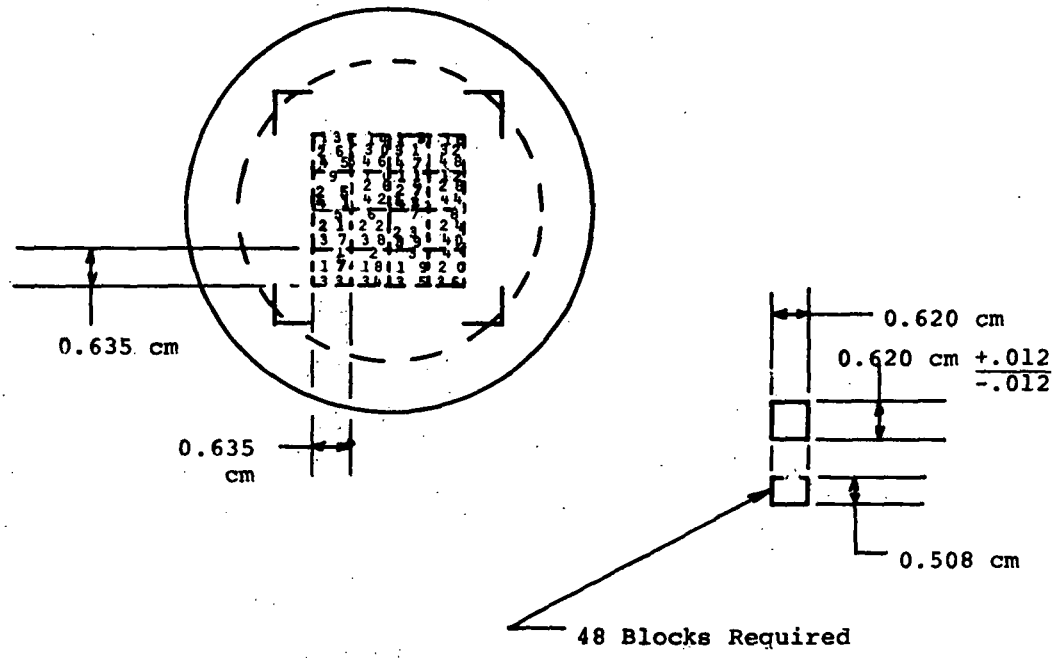

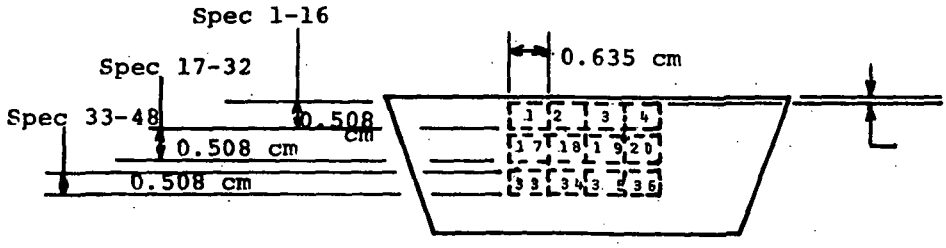

Dotted lines show cutting locations

Figure 3. Cutting plan for arc-jet char number 3

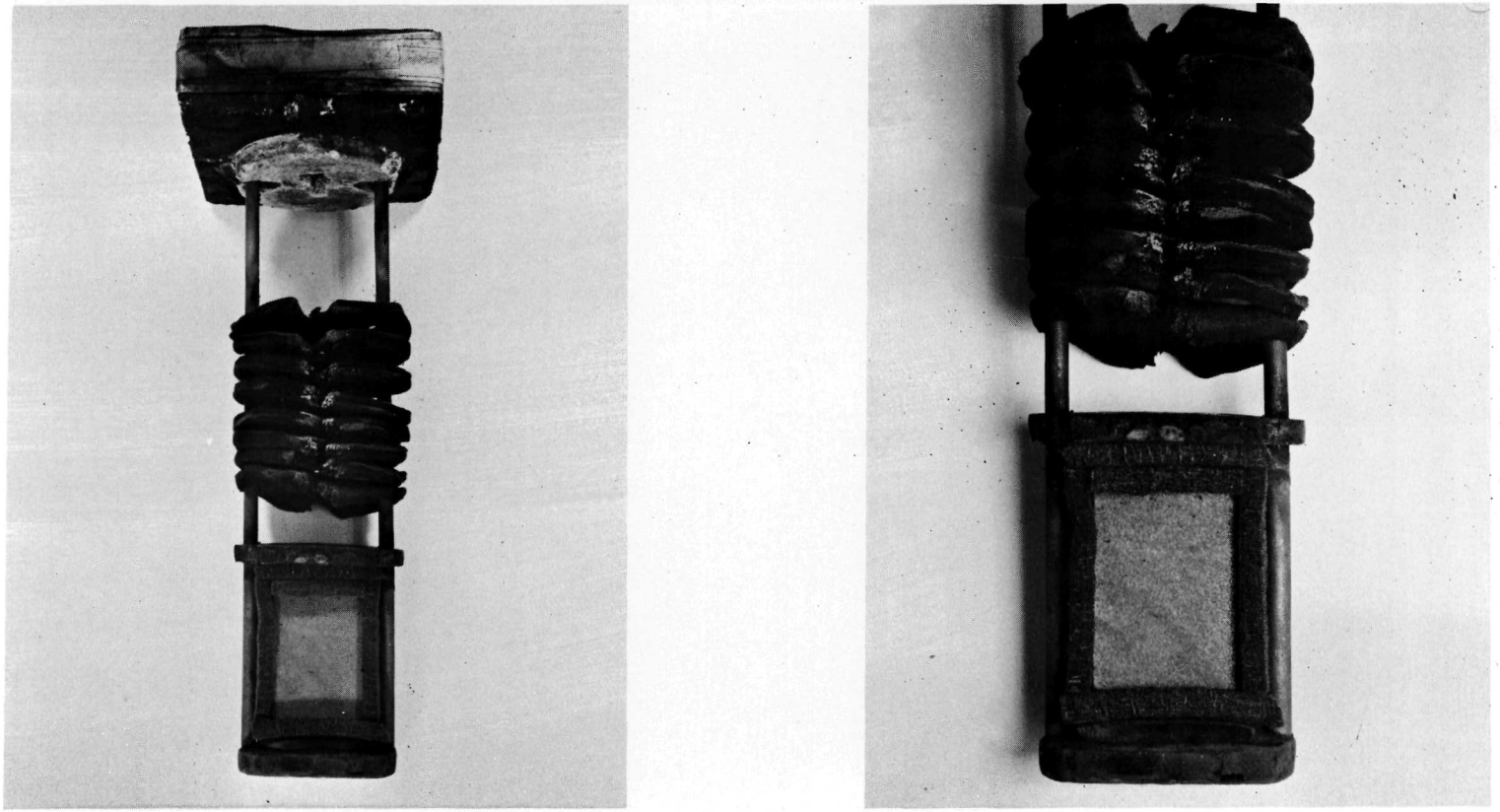

Notes:
1. Two specimens charred simultaneously back-to-back (Front specimen shown)
2. Specimen is inserted in heater tube with 7.5 cm diameter
3. Temperature measured through sight port in furnace by sighting at center of specimen
4. Typical specimen blank size 6.35 cm x 3.81 cm x 0.952 cm

Figure 4. Picture of specimen holder for preparing char samples shown with virgin specimen installed

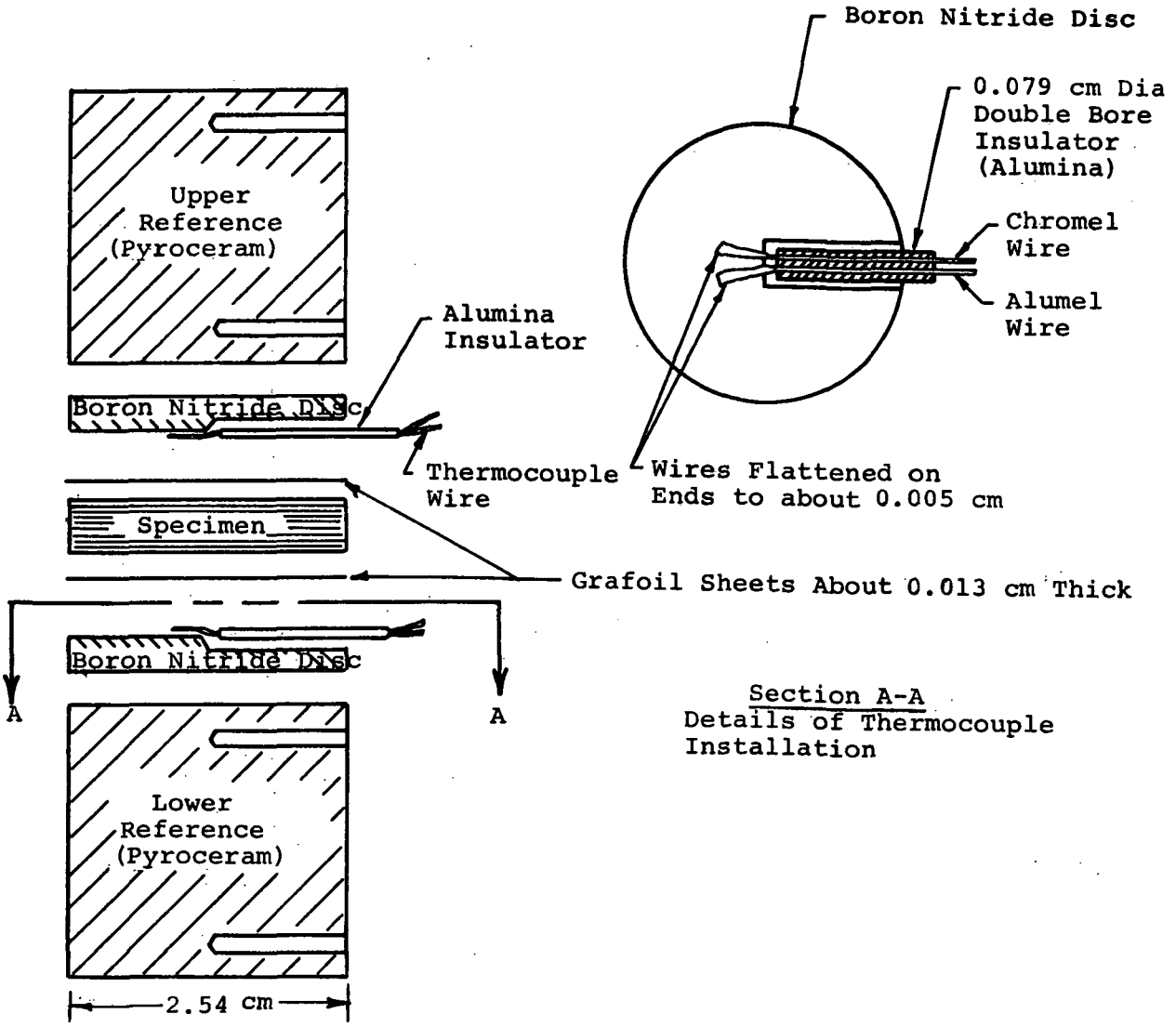

Figure 5. Expanded schematic of "bare-wire" technique for measurement of surface temperature in comparative rod apparatus

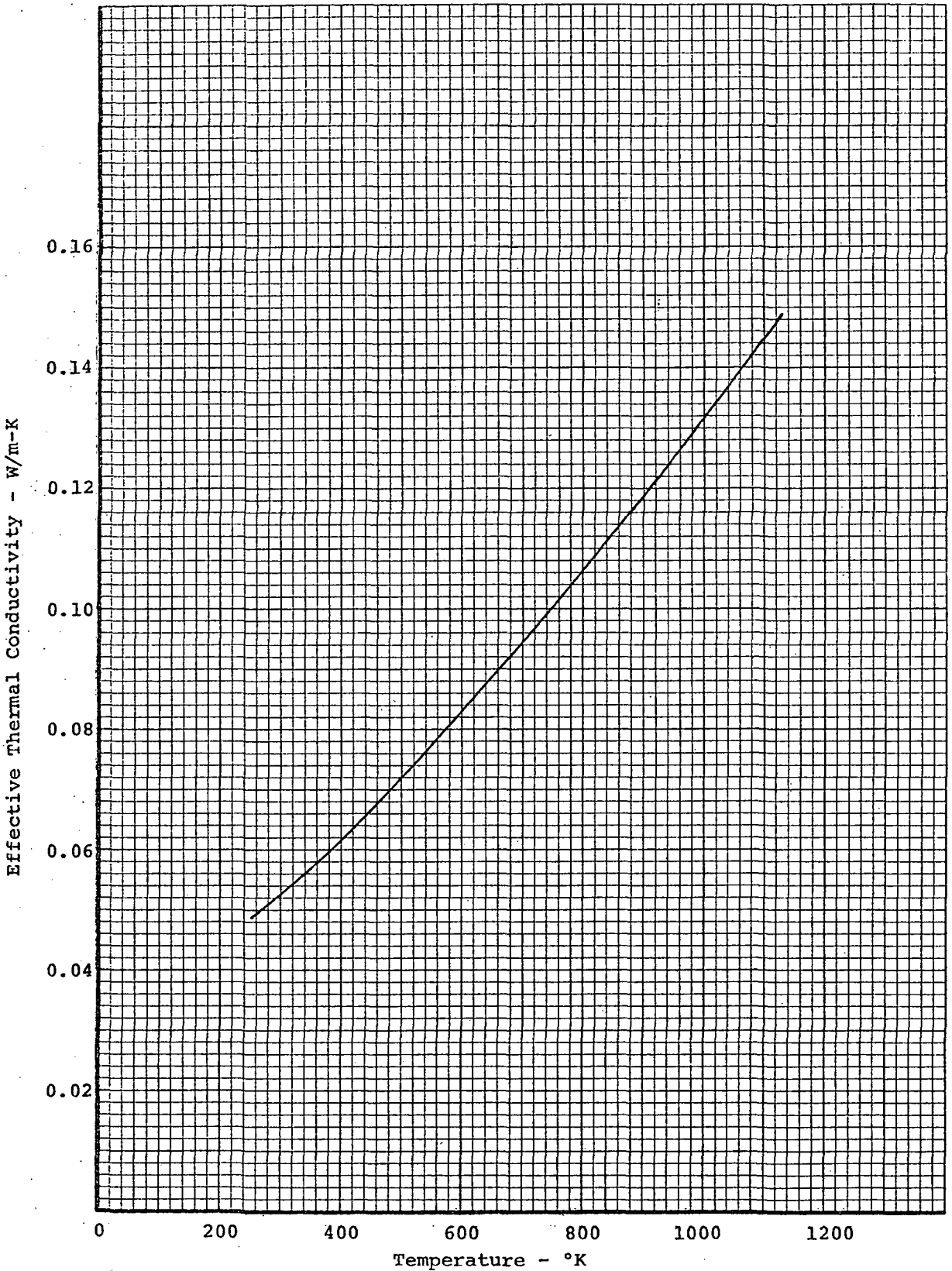

Figure 6. Effective thermal conductivity values used for thermatomic carbon in a nitrogen environment

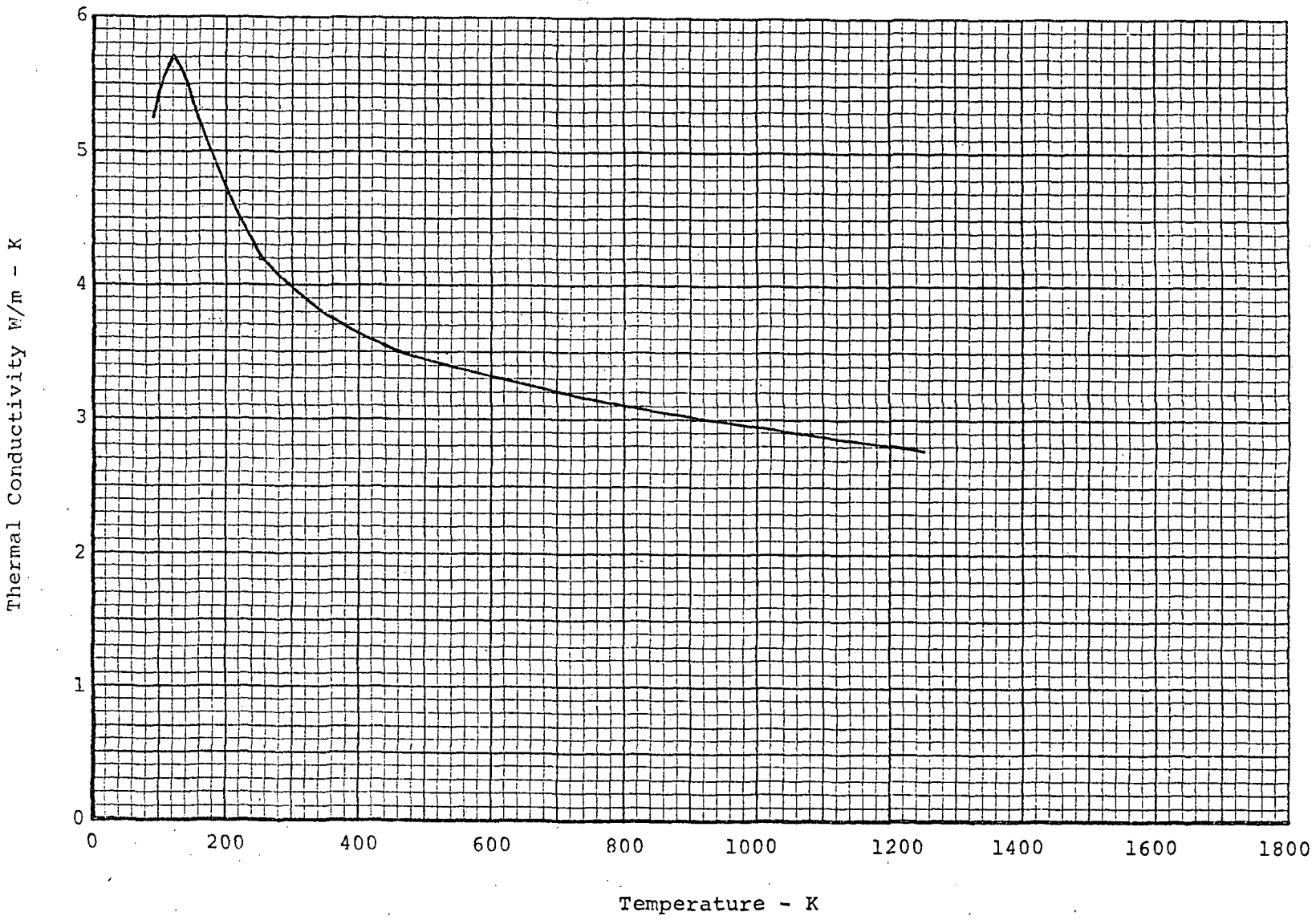

Figure 7. The thermal conductivity of primary SRI standards from NBS stock of Code 9606 Pyroceram

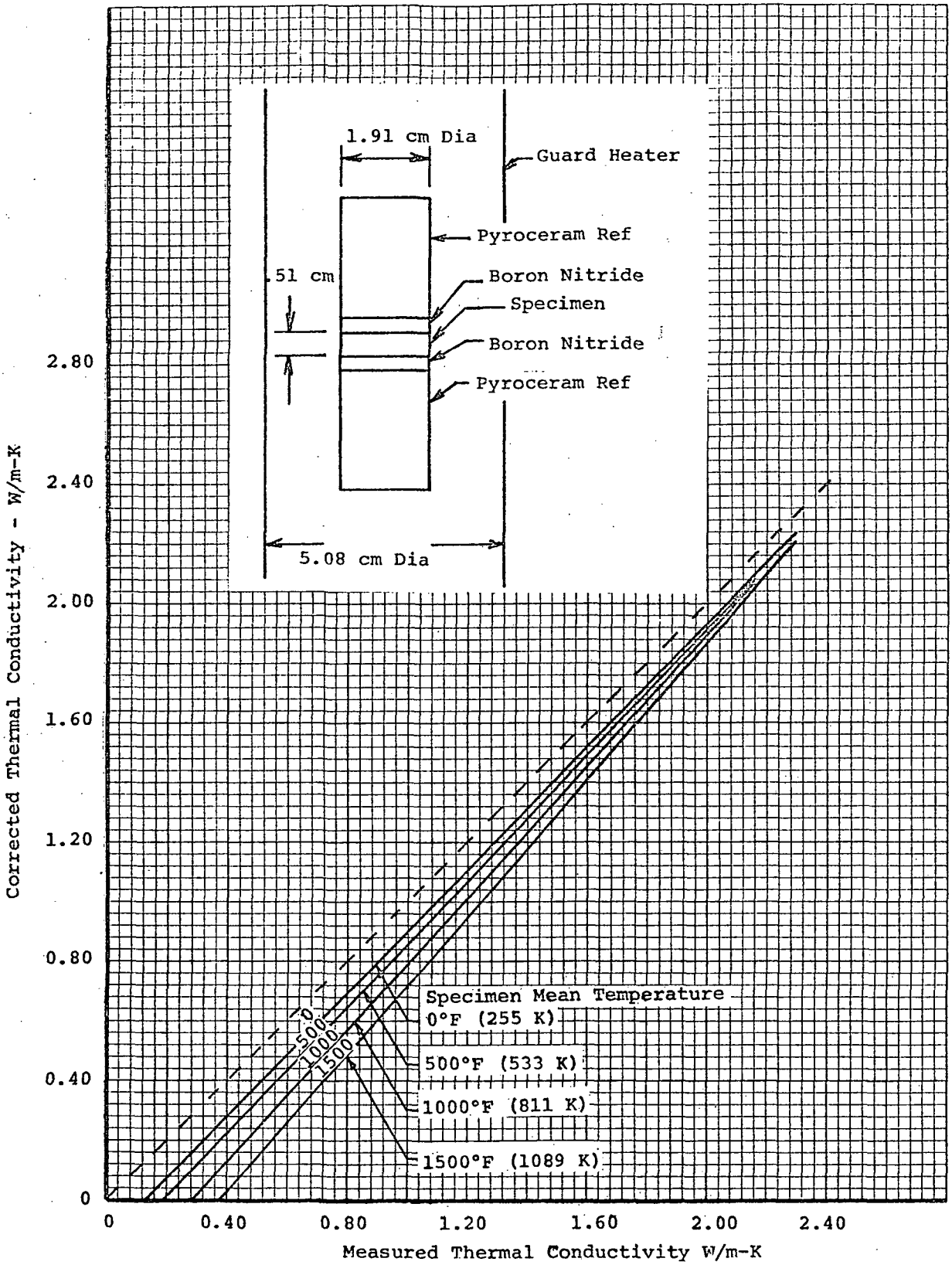

Figure 8. Correction to comparative rod thermal conductivity measurements for heat bypass

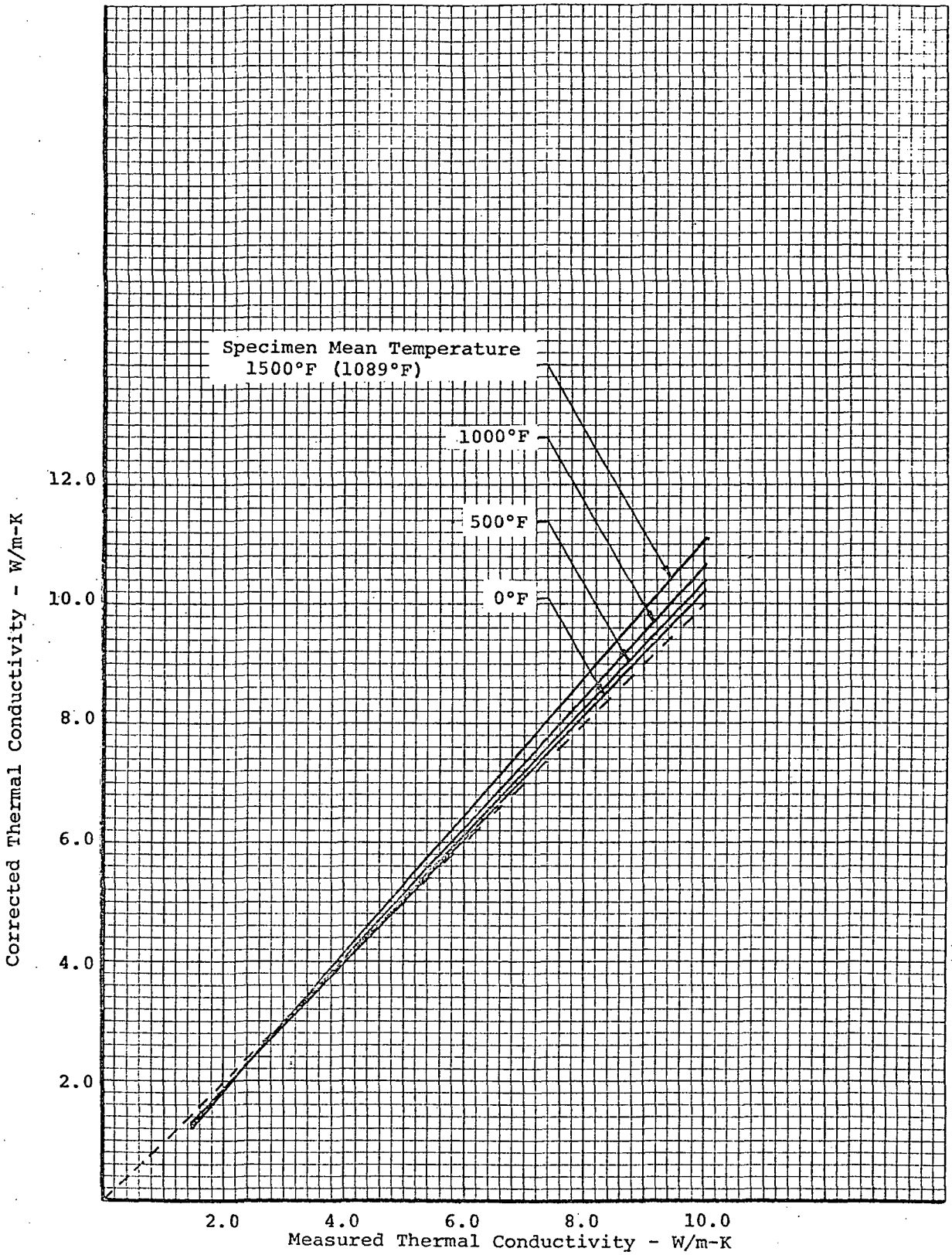

Figure 9. Correction to comparative rod thermal conductivity measurements for heat bypass

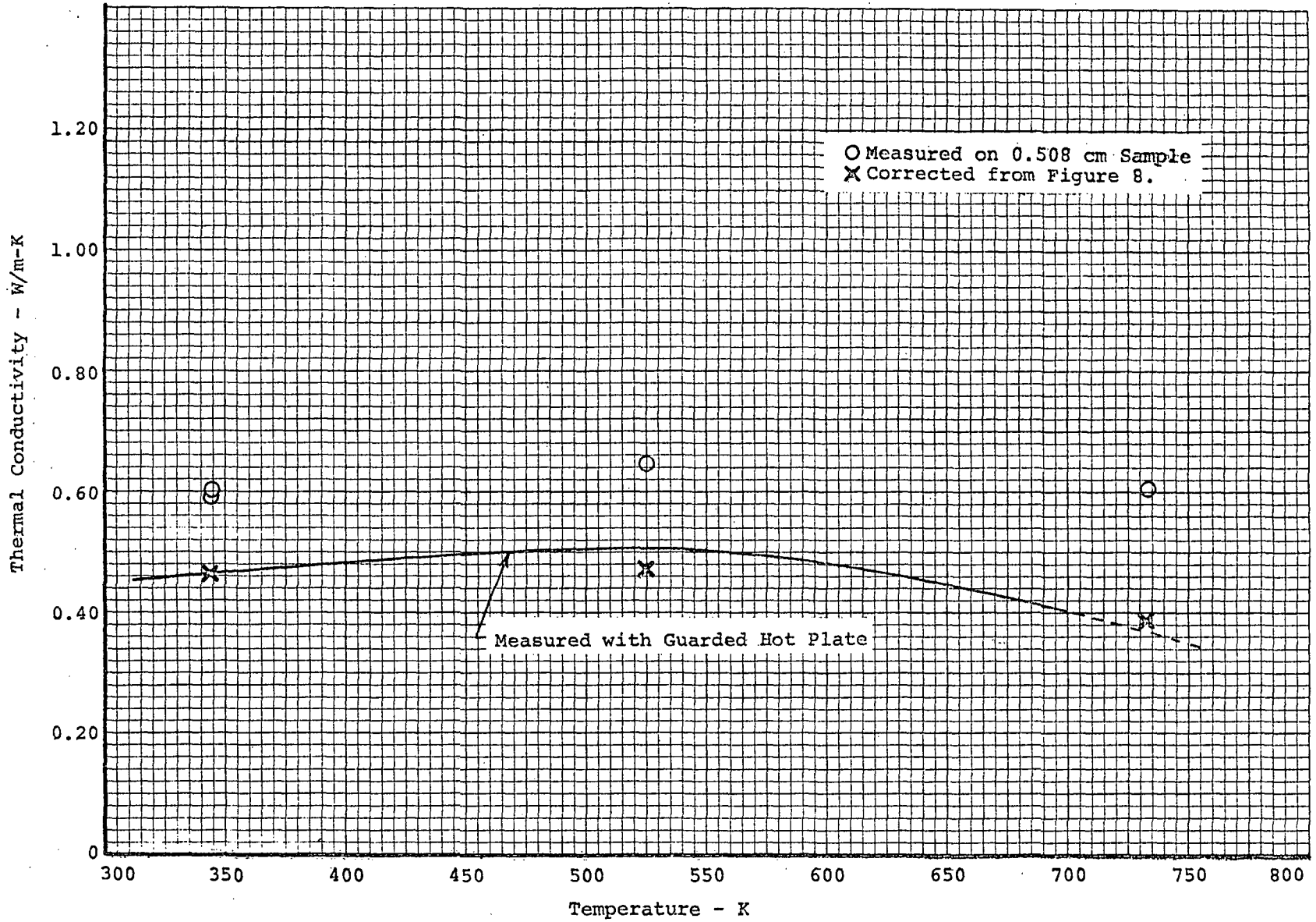

Figure 10. Thermal conductivity of FM 5131 in the thickness direction as measured with comparative rod apparatus

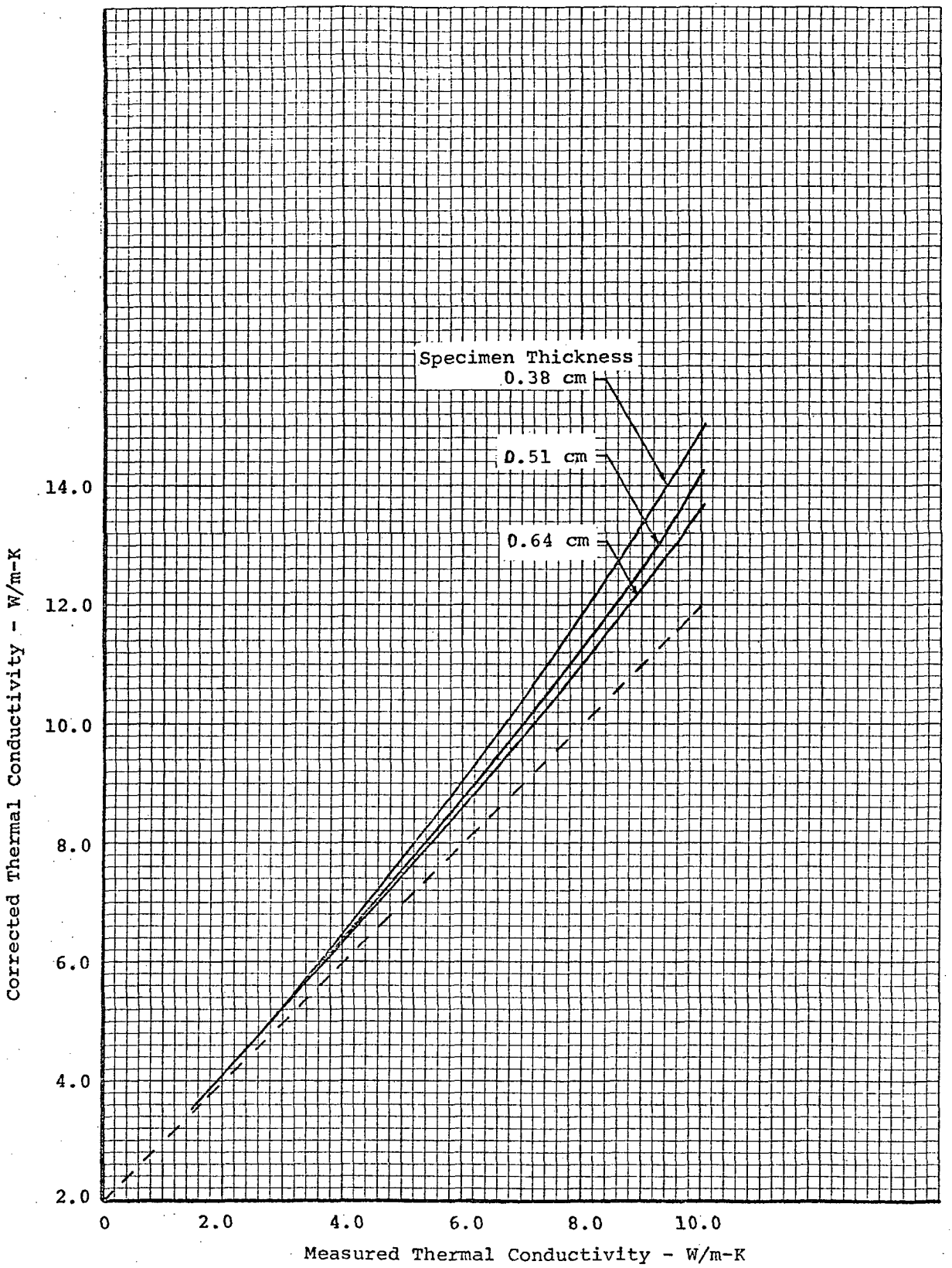

Figure 11. Correction to comparative rod thermal conductivity measurements for interface resistance

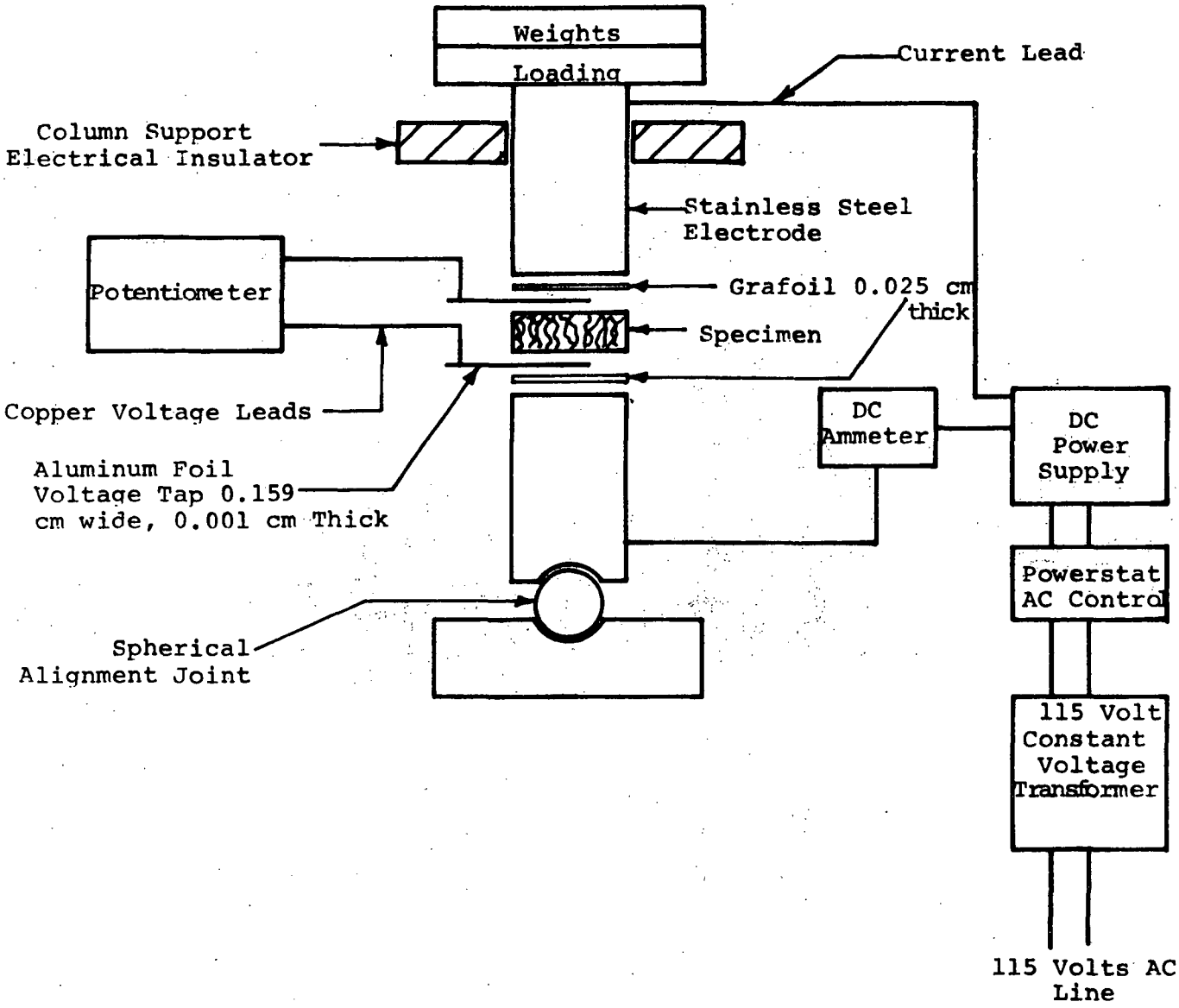

Figure 12. Schematic of apparatus used to measure electrical resistivity

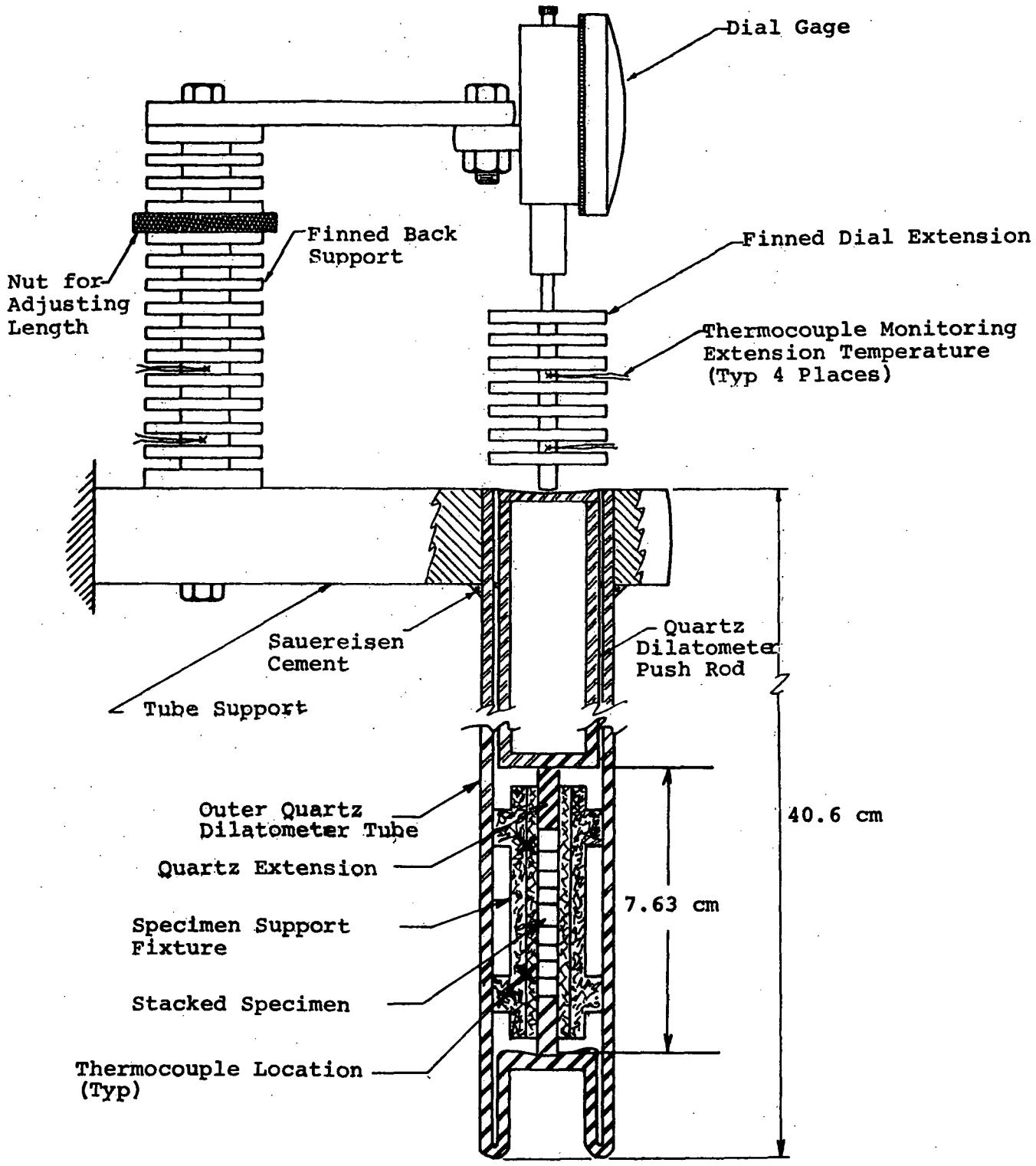

Figure 13. Assembly of quartz tube dilatometer for thermal expansion measurements

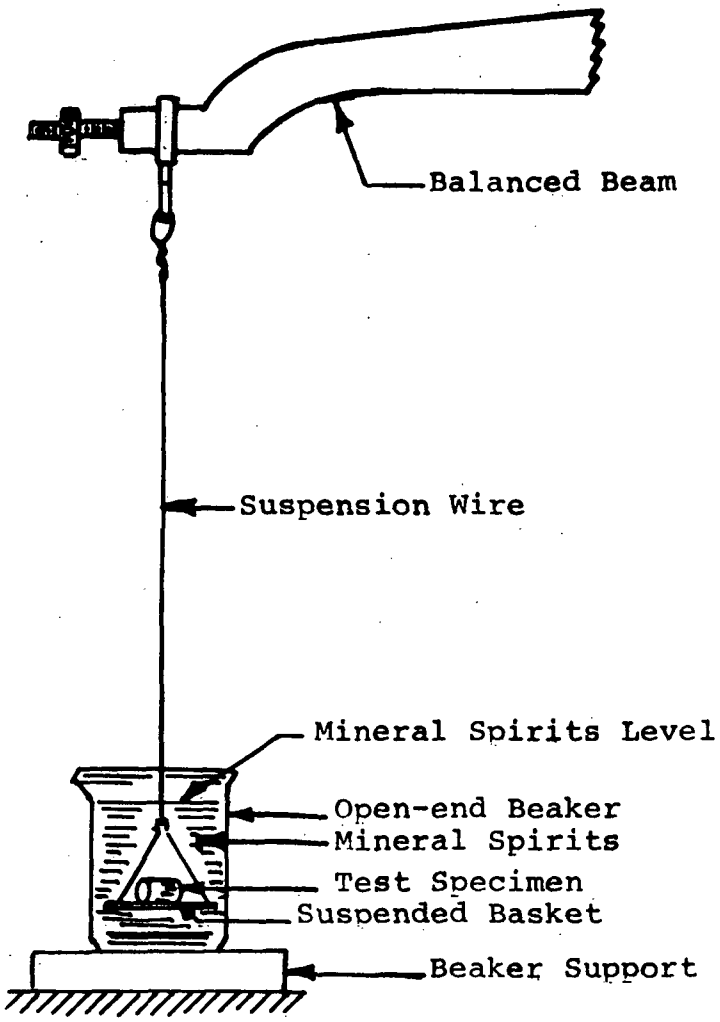

Figure 14. Setup for determining suspended weight of saturated specimen for liquid absorption evaluation

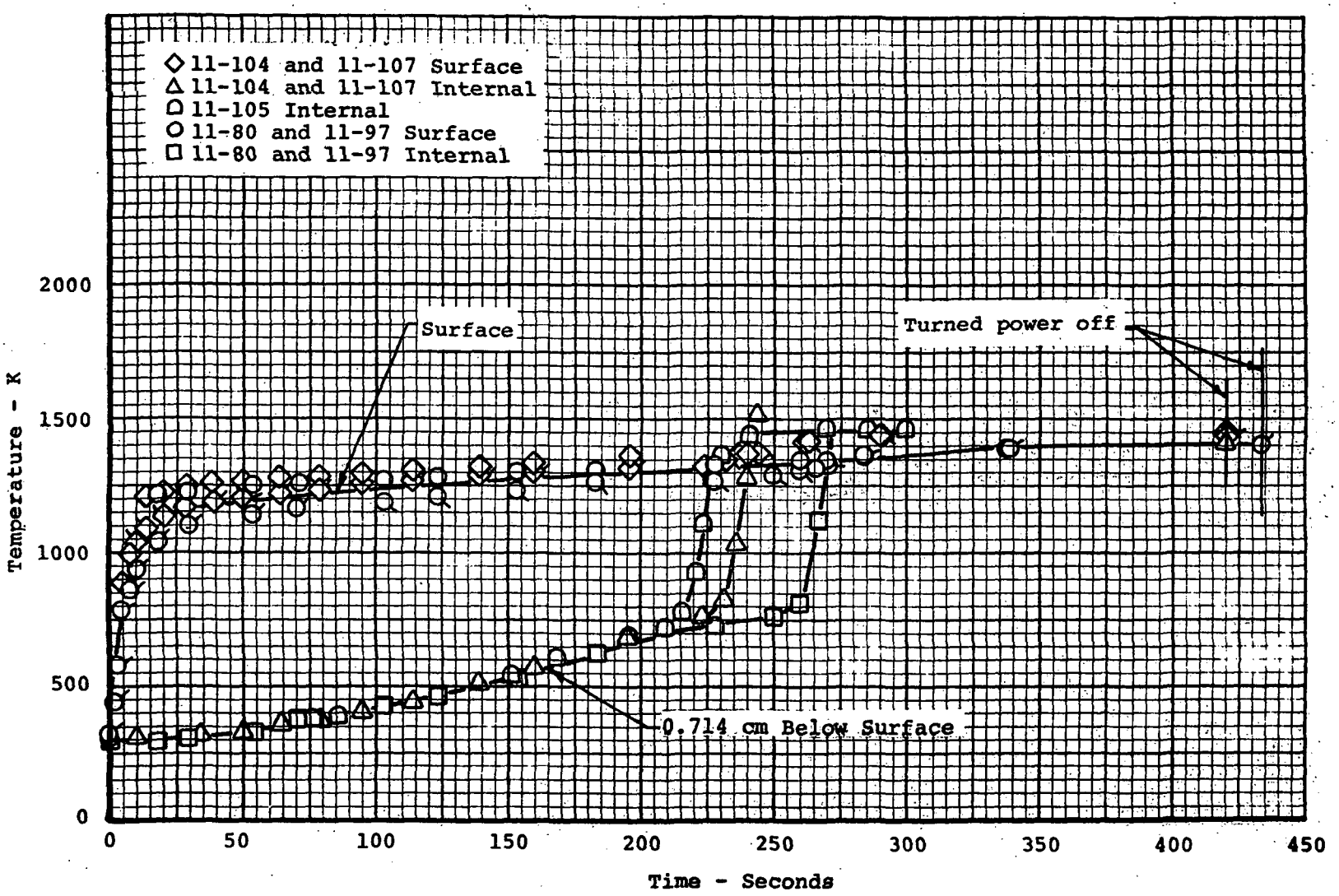

Figure 15. Temperature response for low-density phenolic-nylon specimen immersed in 1405 K preheated furnace

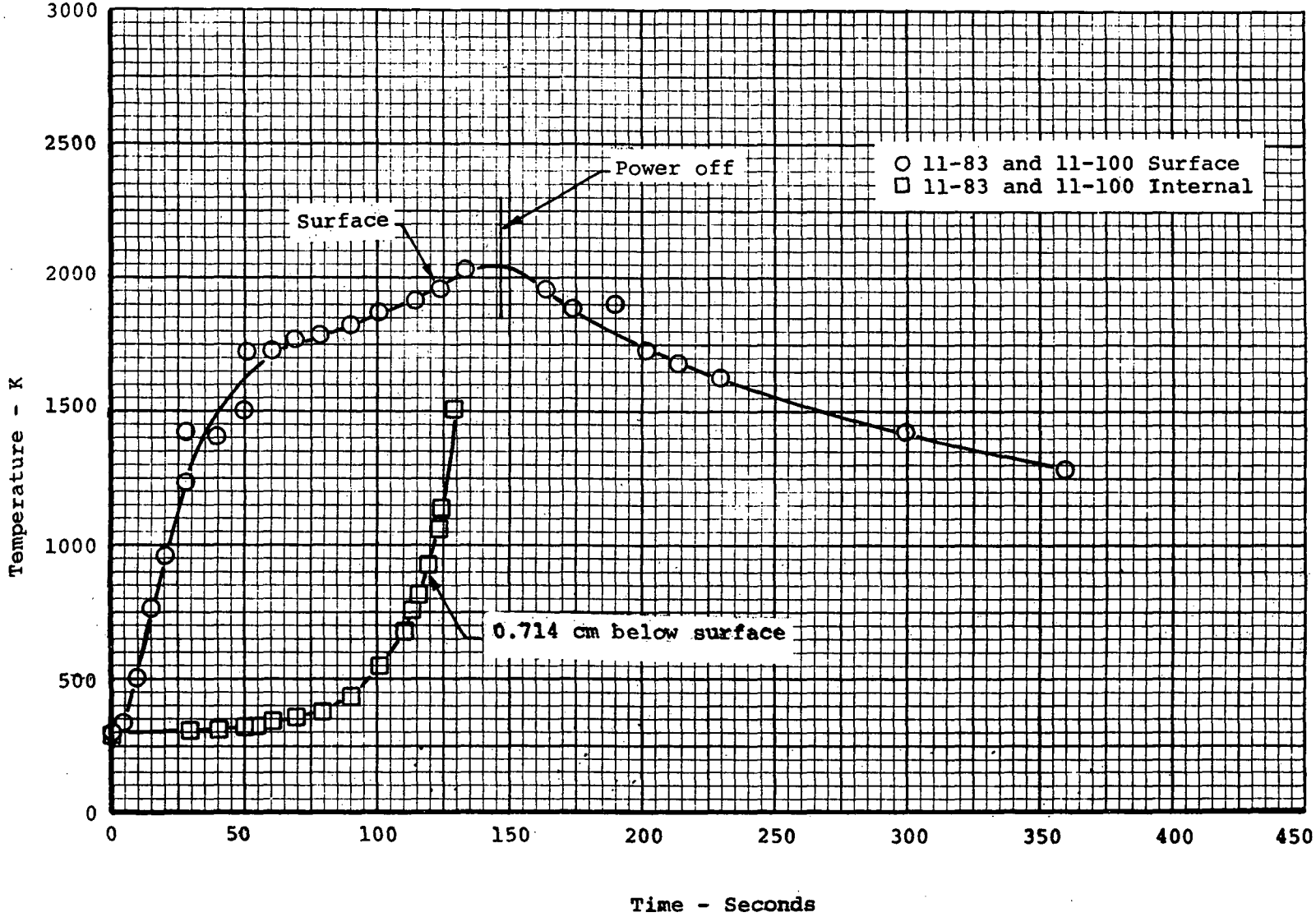

Figure 16. Temperature response for low-density phenolic-nylon specimen immersed in furnace in which power was cycled to maximum at time zero

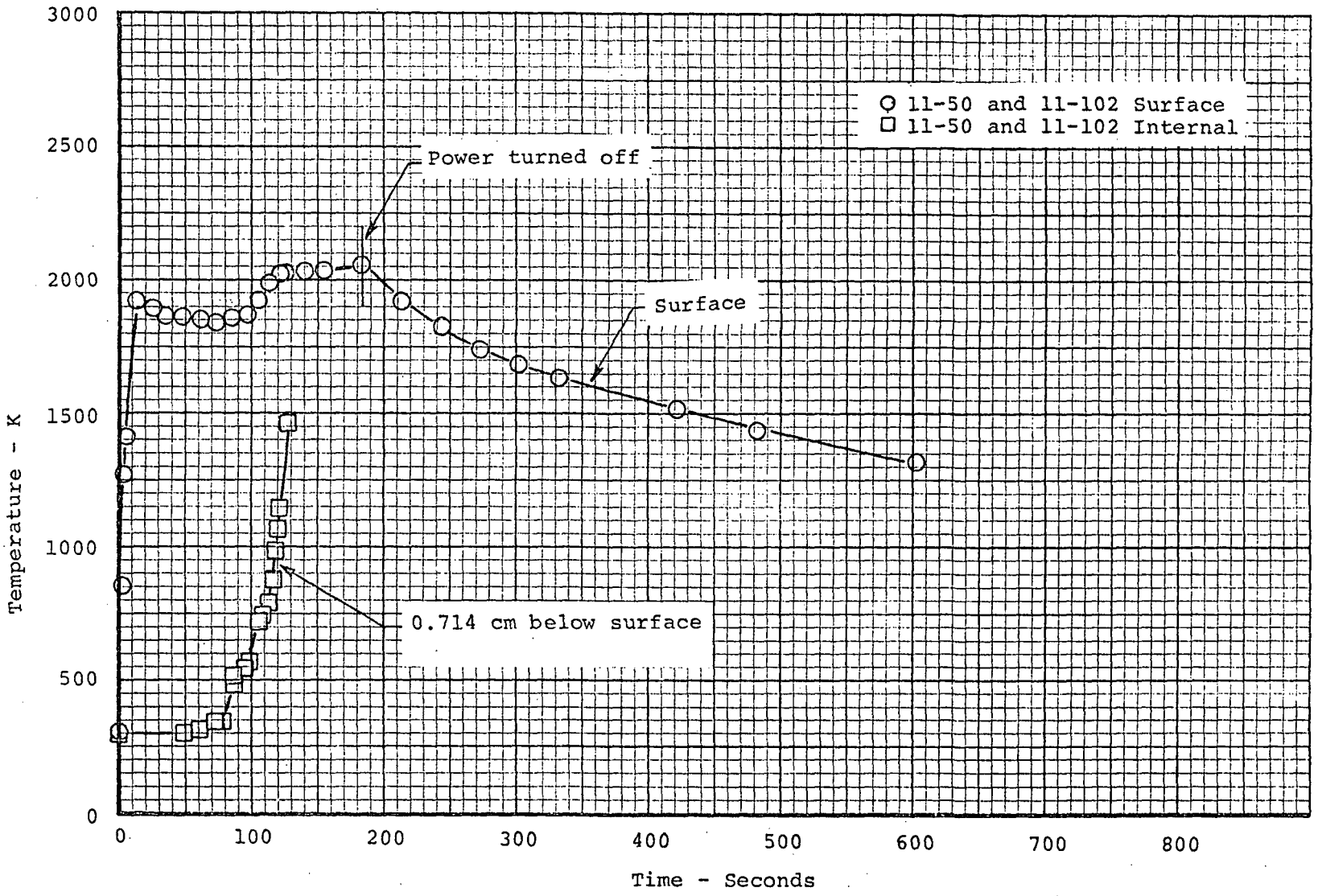

Figure 17. Temperature response for low-density phenolic-nylon specimen immersed in 2000 K preheated furnace

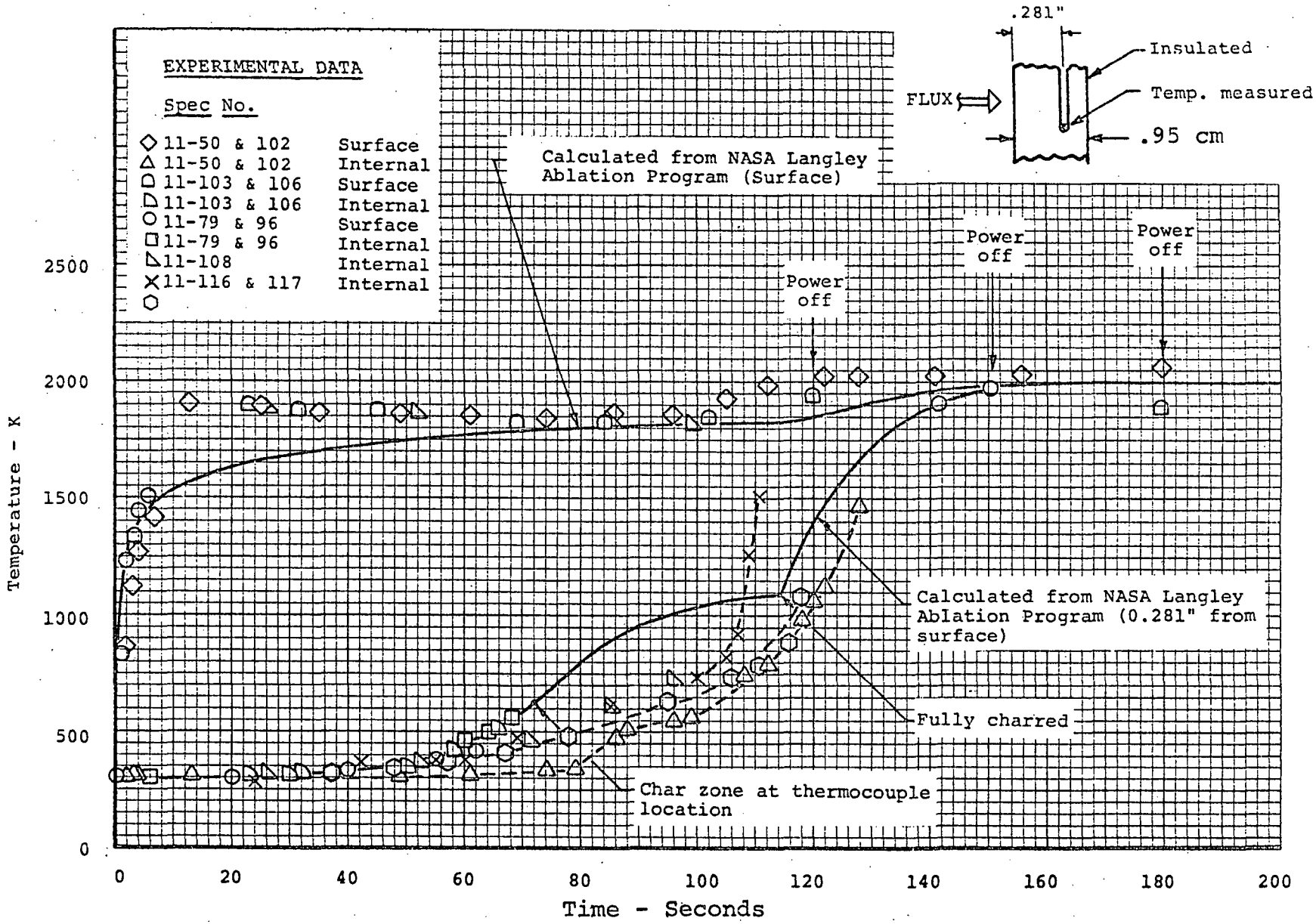

Figure 18. Temperature-time response for low-density phenolic-nylon specimen exposed to 2000 K preheated furnace

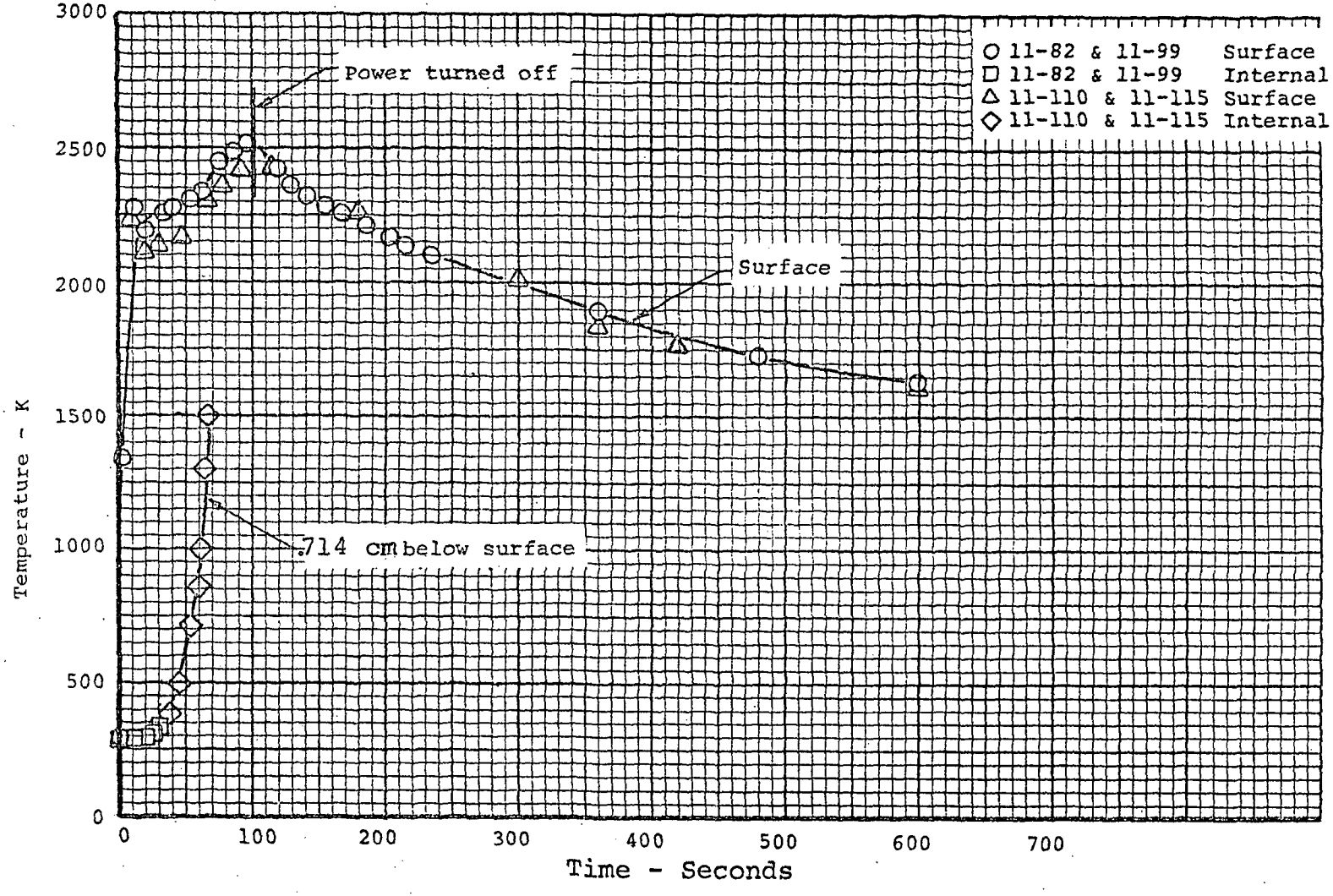

Figure 19. Temperature response for low-density phenolic-nylon specimen immersed in 2500 K preheated furnace

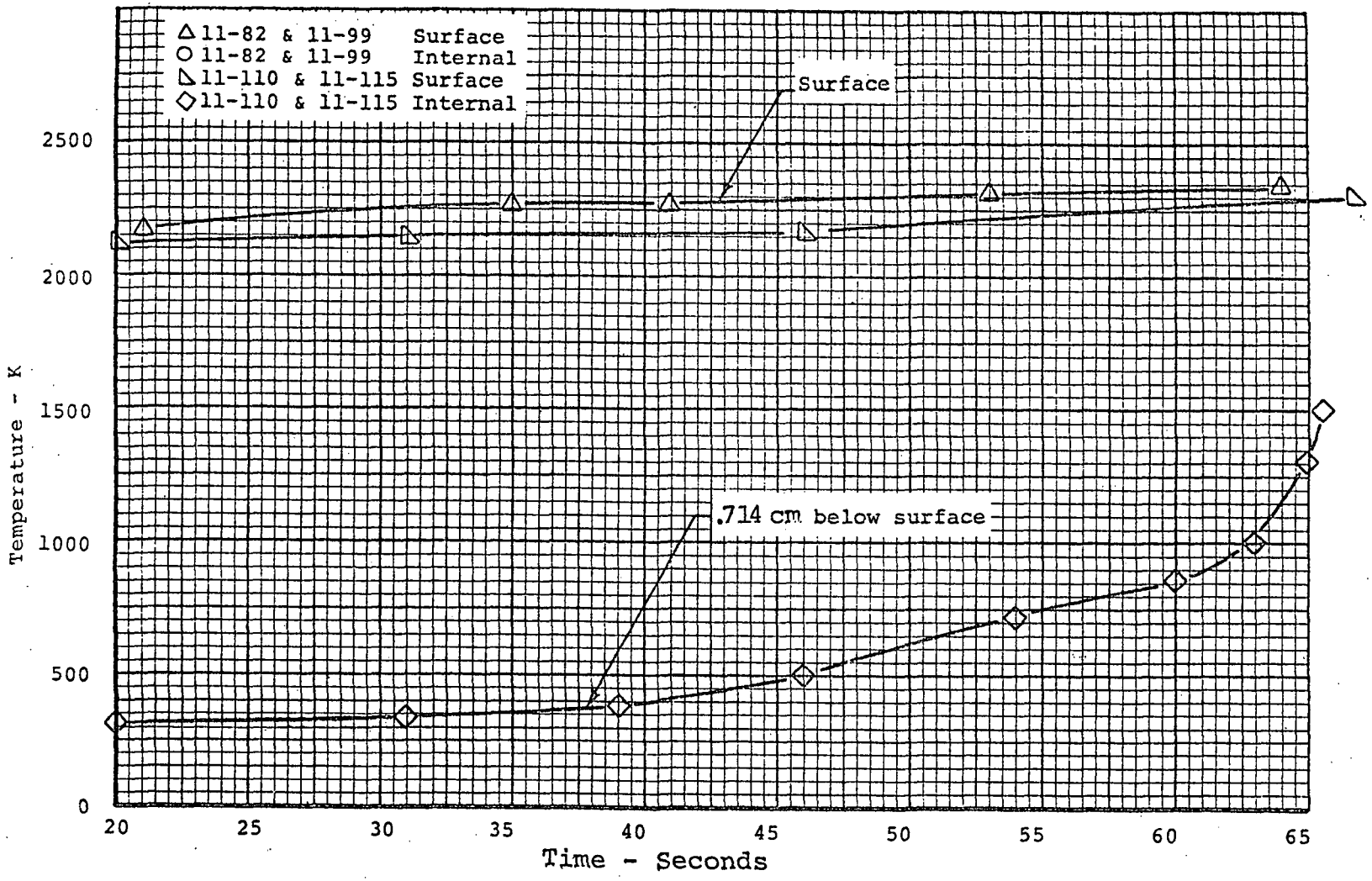

Figure 20. Temperature response for low-density phenolic-nylon specimen immersed in 2500 K preheated furnace

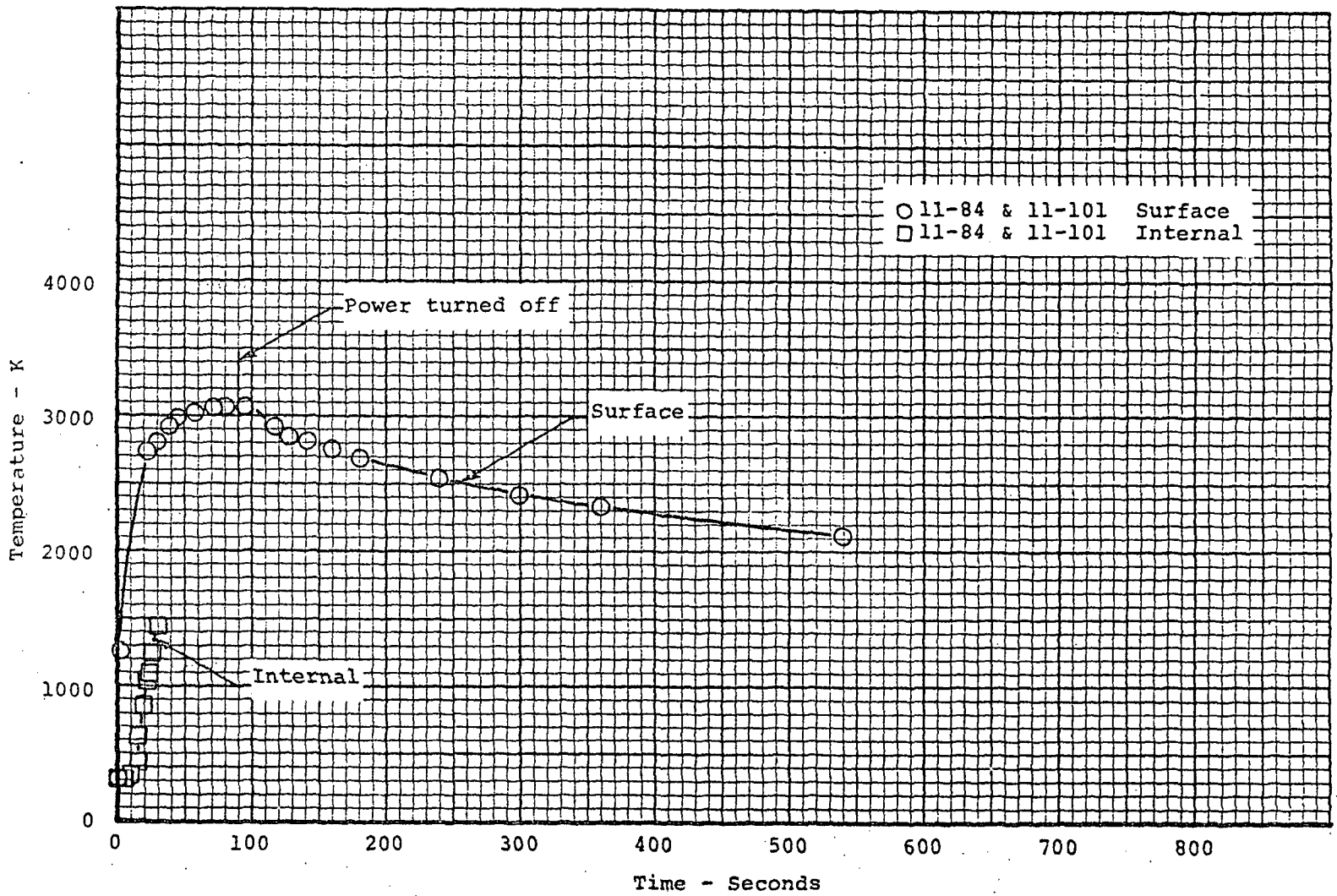

Figure 21. Temperature response for low-density phenolic-nylon for specimen immersed in 3100 K preheated furnace

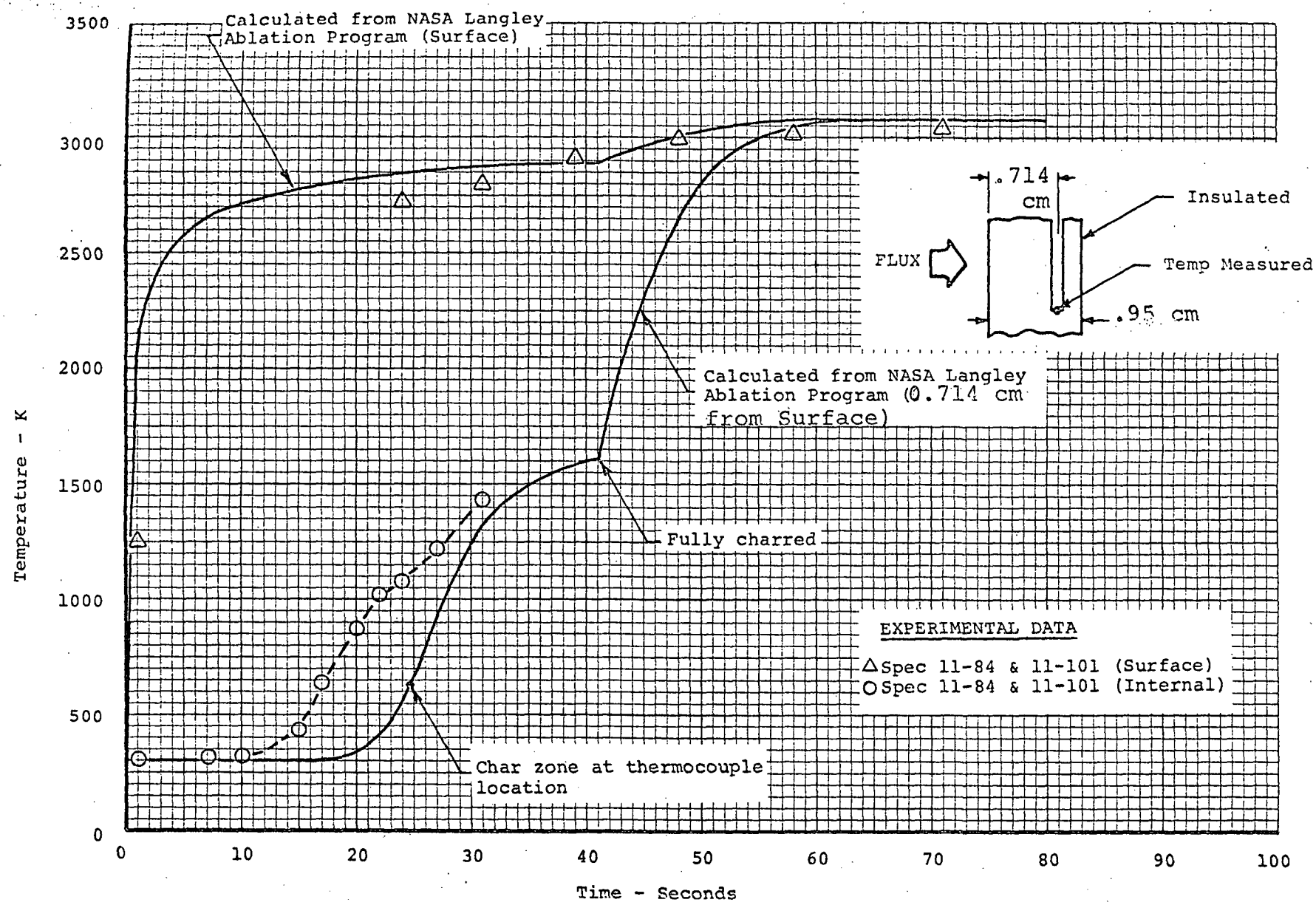

Figure 22. Temperature-time response for low-density phenolic-nylon specimen exposed to 3100 K preheated furnace

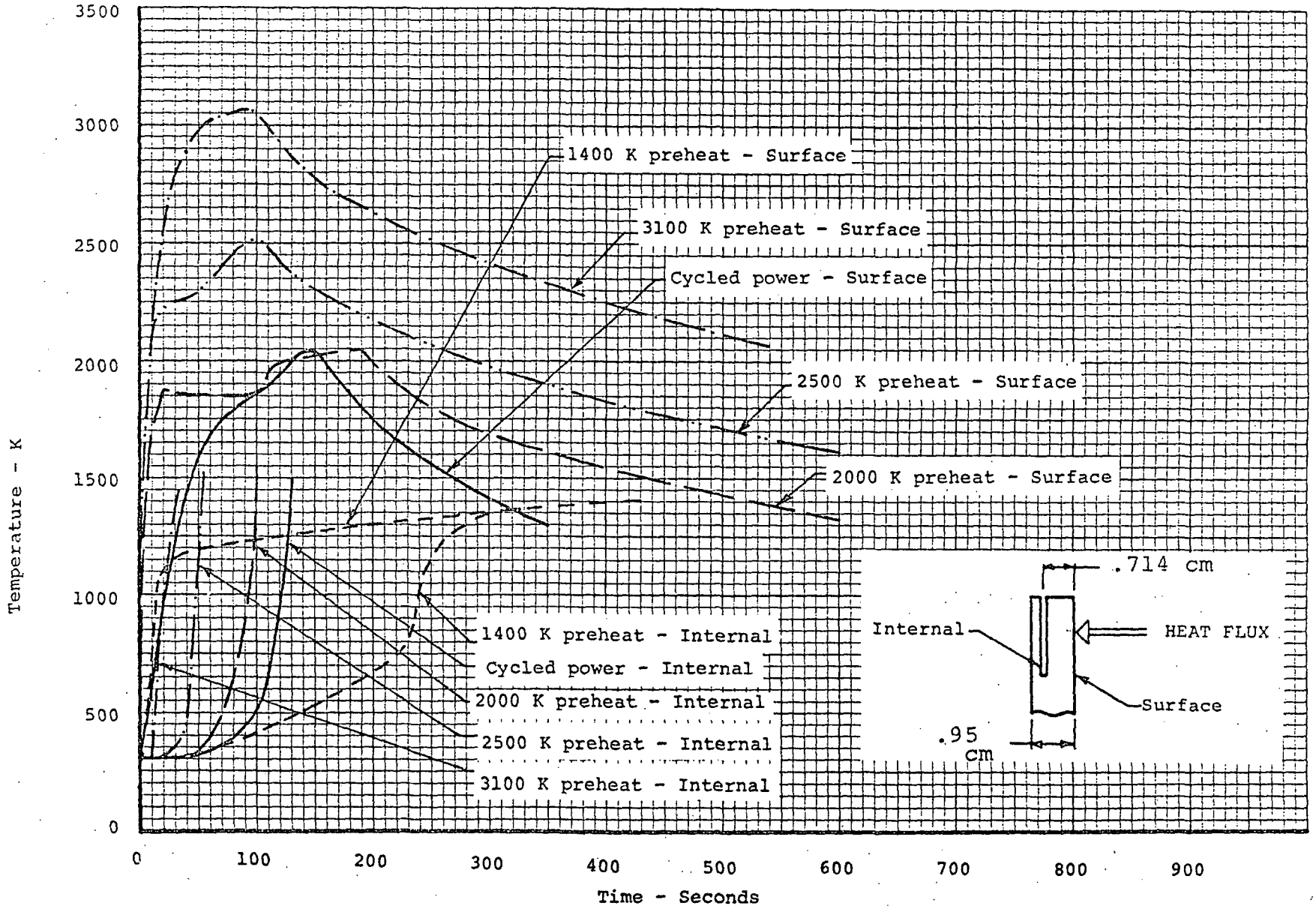

Figure 23. Measured temperature responses within low-density phenolic-nylon during degradation for various heating conditions

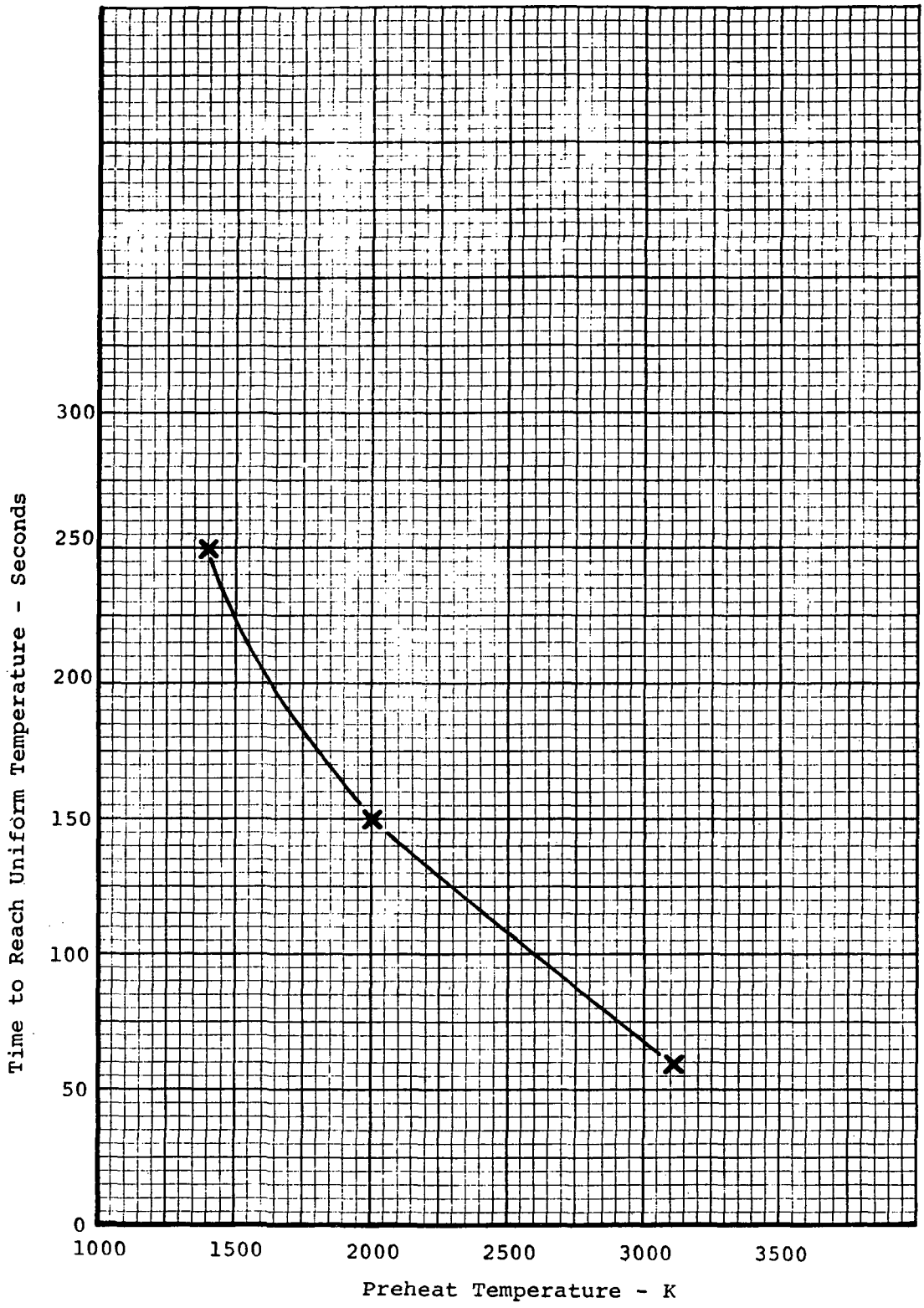

Figure 24. Time required to achieve thermal equilibrium versus furnace preheat temperature

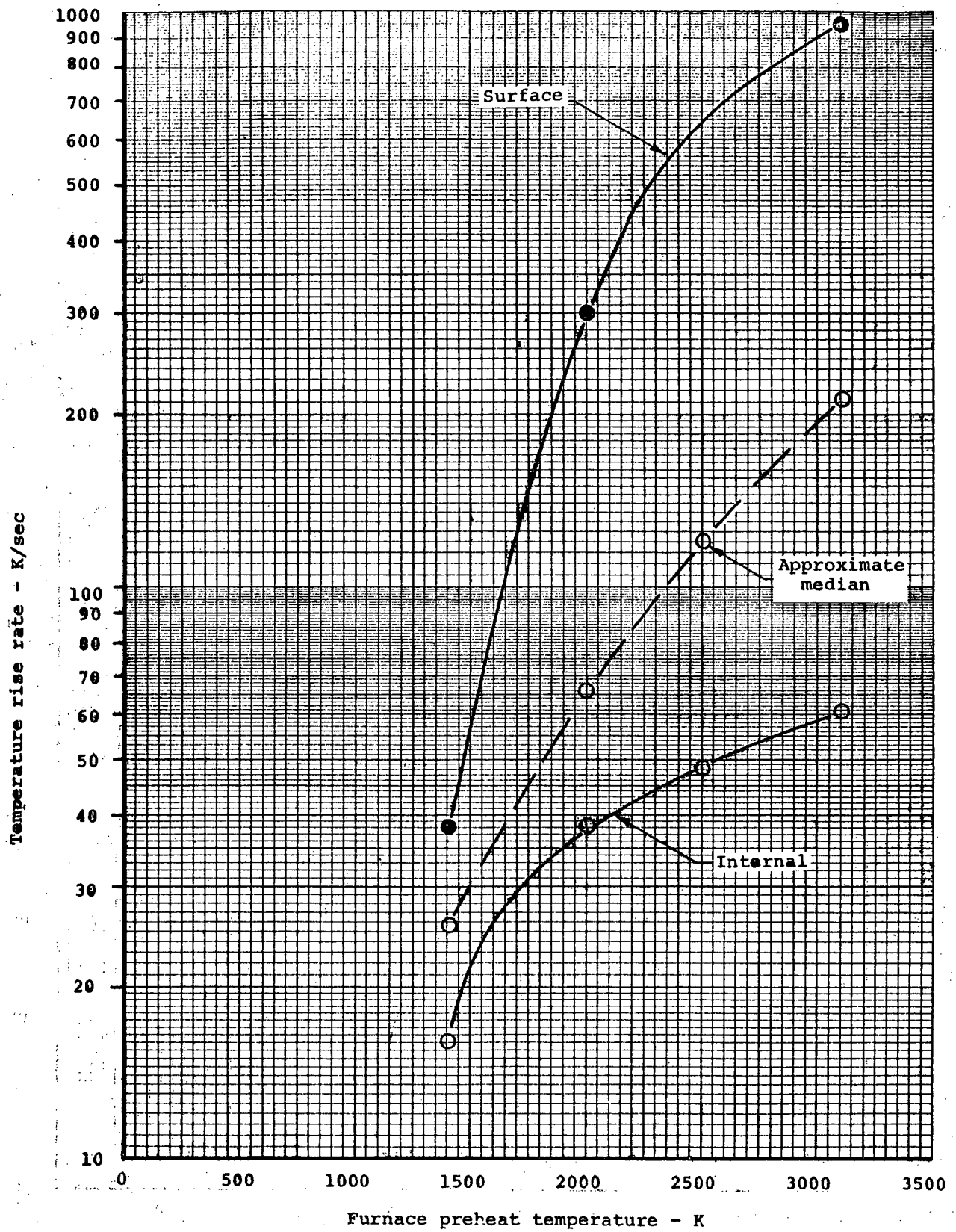

Figure 25. Temperature rise rate through degradation zone on low-density phenolic-nylon versus furnace preheat temperature

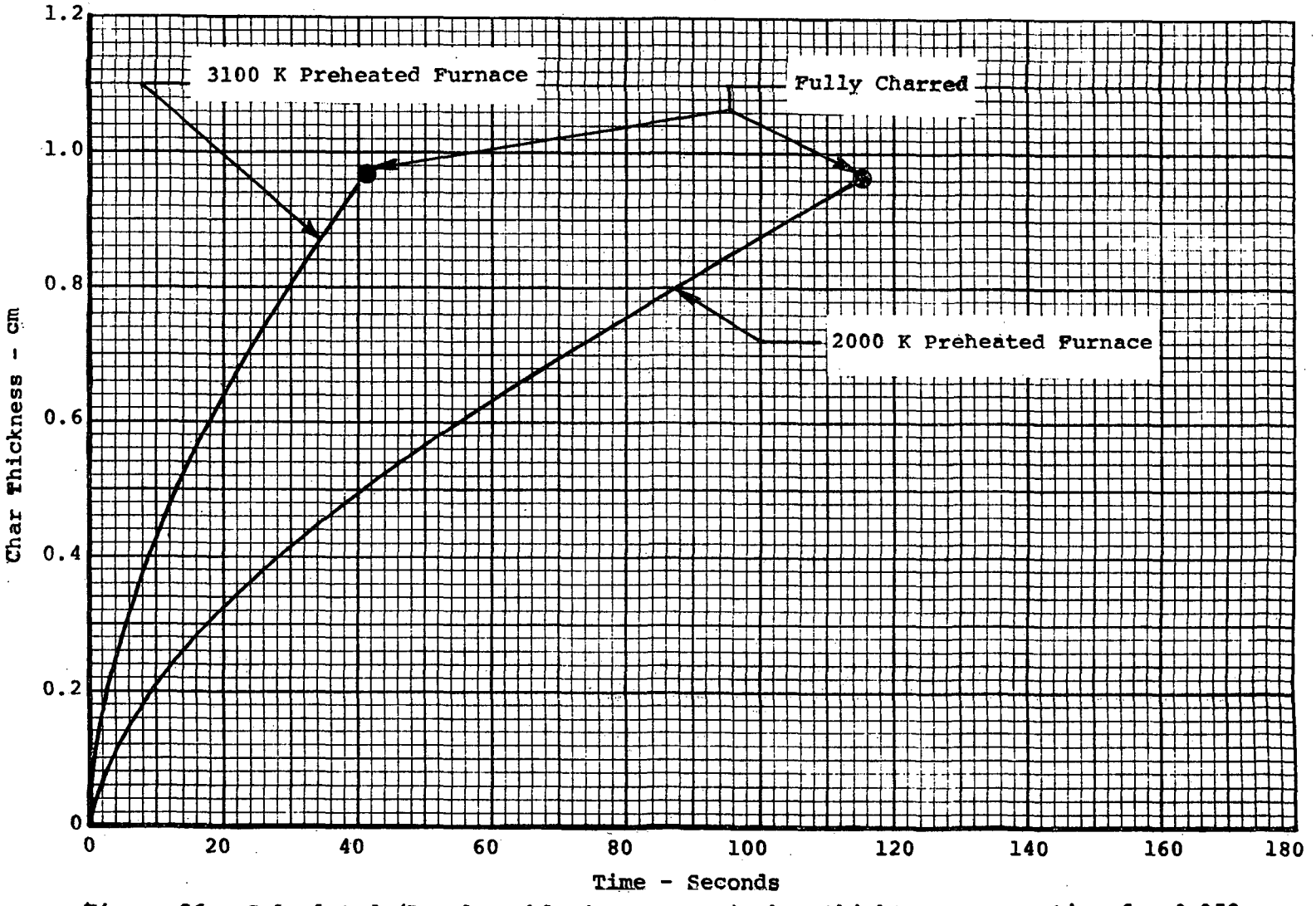

Figure 26. Calculated (Langley Ablation Program) char thickness versus time for 0.952 cm thick phenolic-nylon exposed to 2000 K and 3000 K preheat furnace temperatures

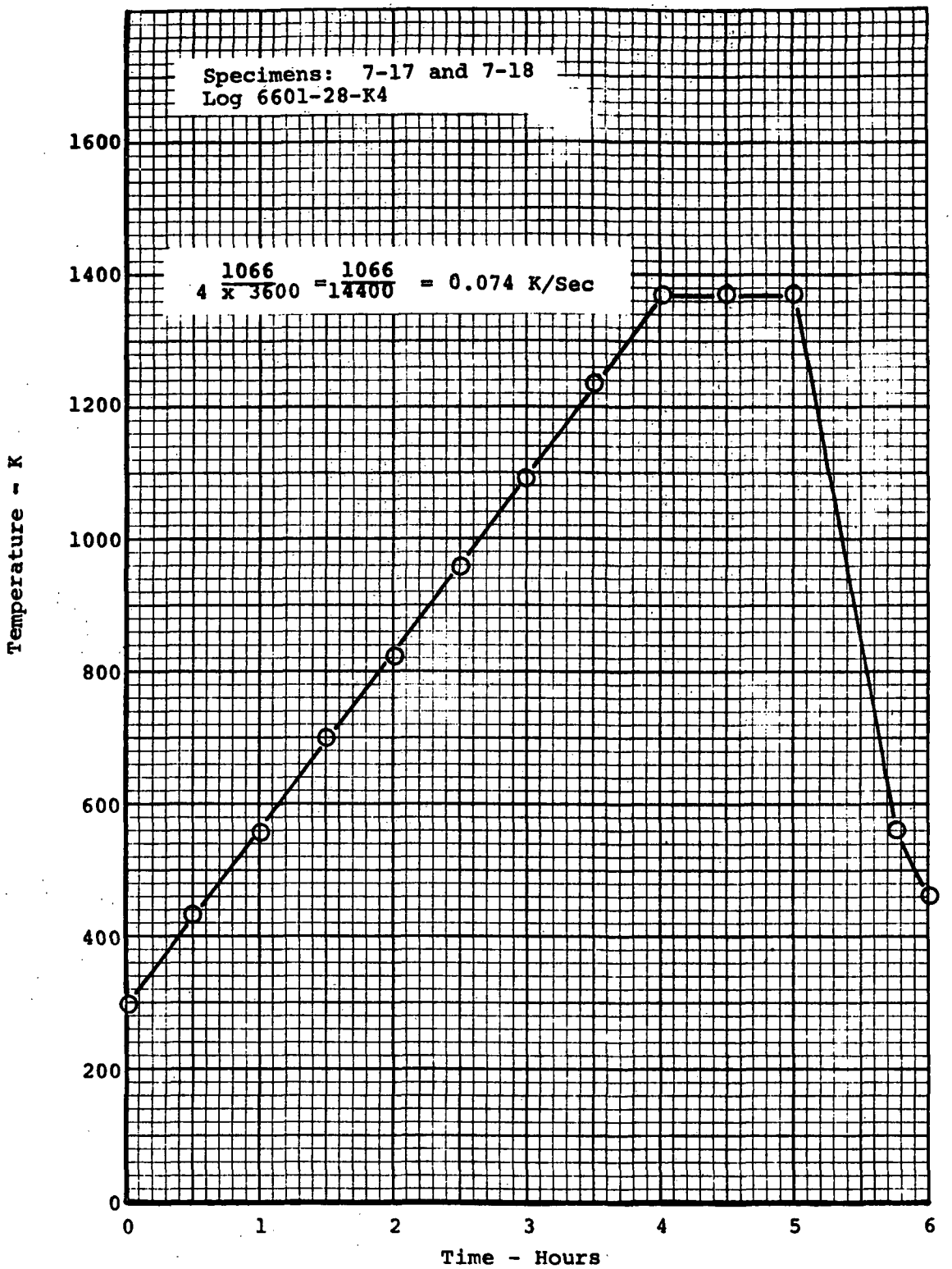

Figure 27. Typical temperature - time curve for low-density phenolic-nylon prepared in the laboratory at low heating rates

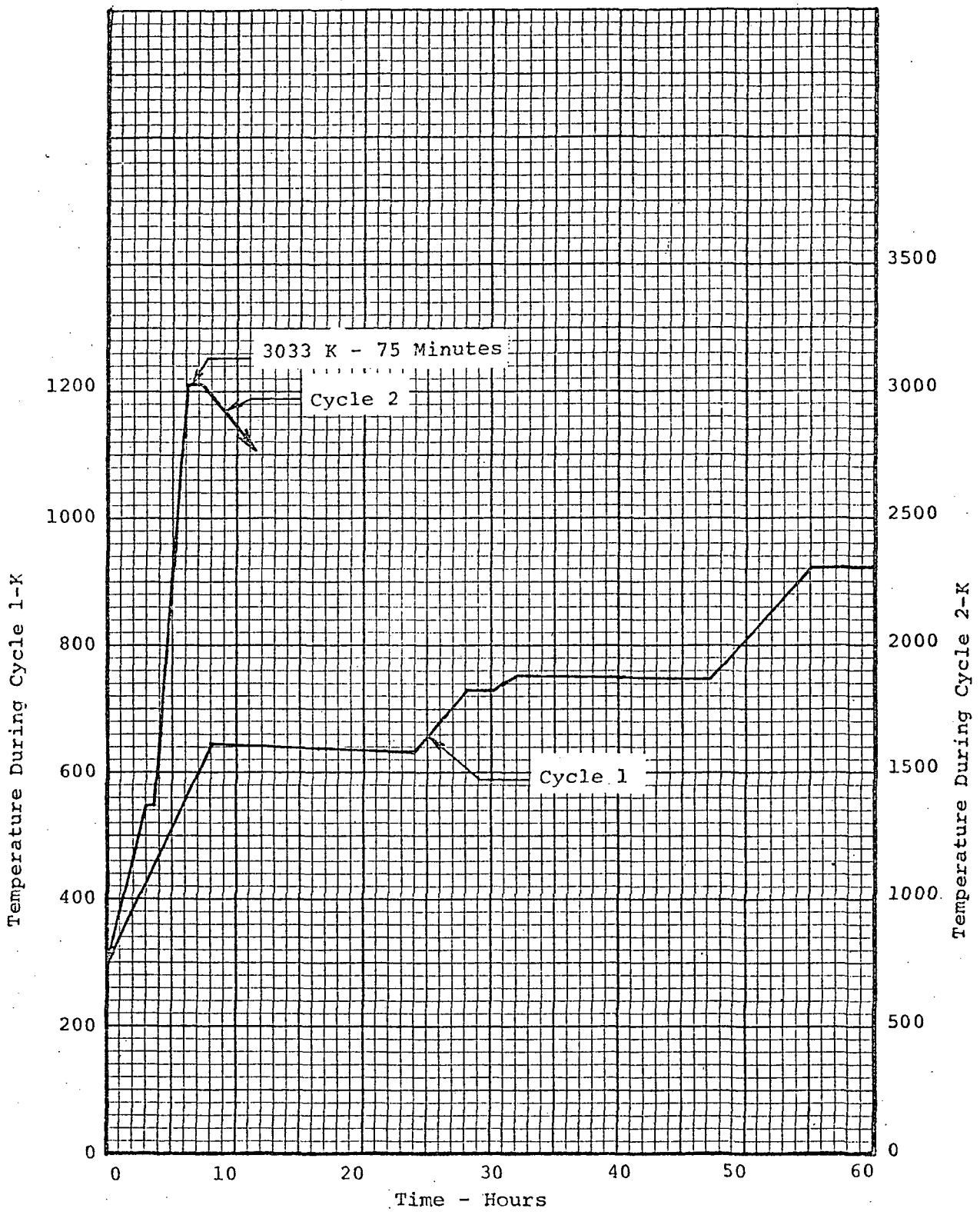

Figure 28. Temperature history for char specimen HMP prepared in the laboratory from phenolic at a very low heating rate

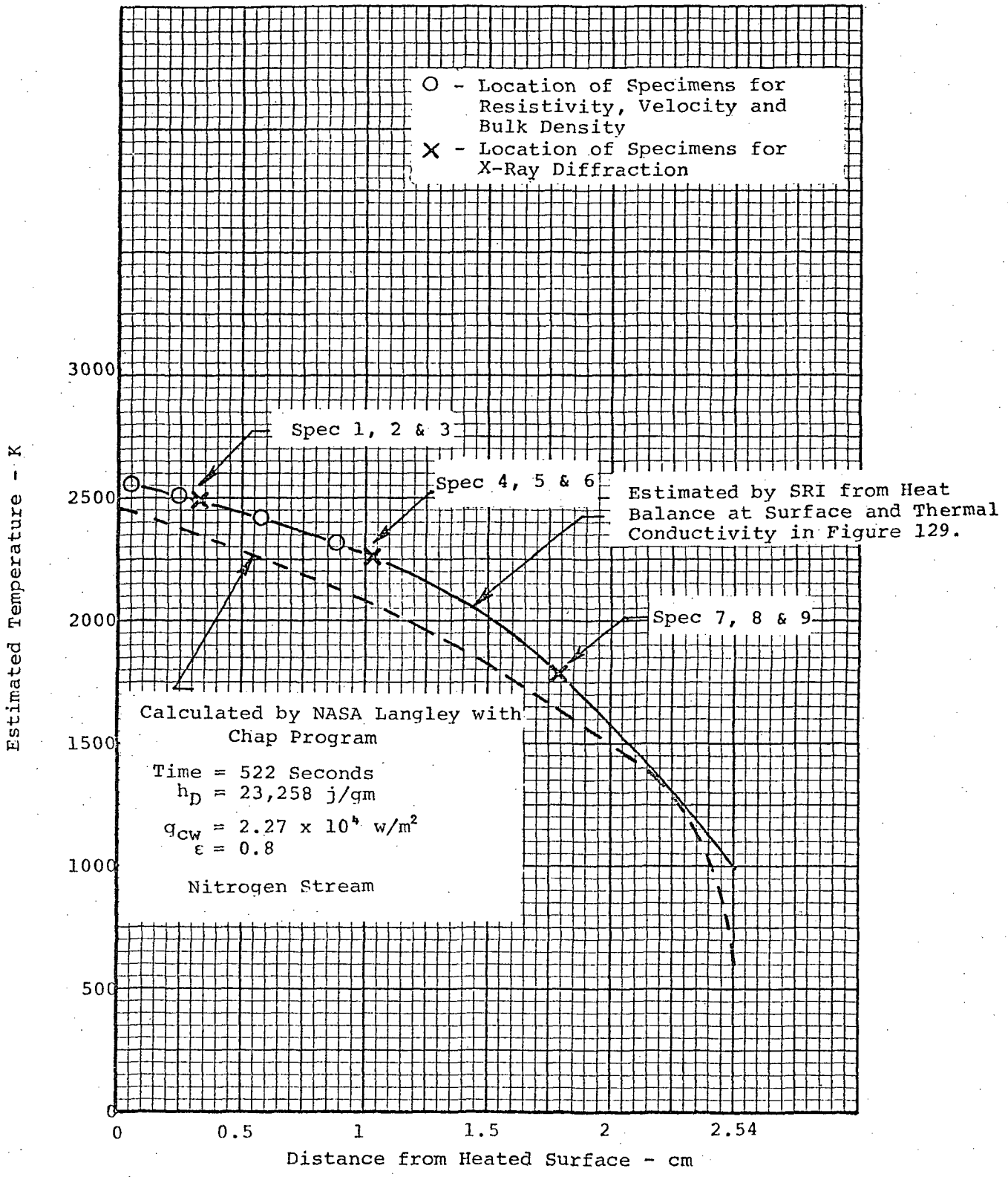

Figure 29. Estimated final temperature distribution through arc-jet char prepared in nitrogen at 226 x 10^4 W/m^2 cold wall heat flux

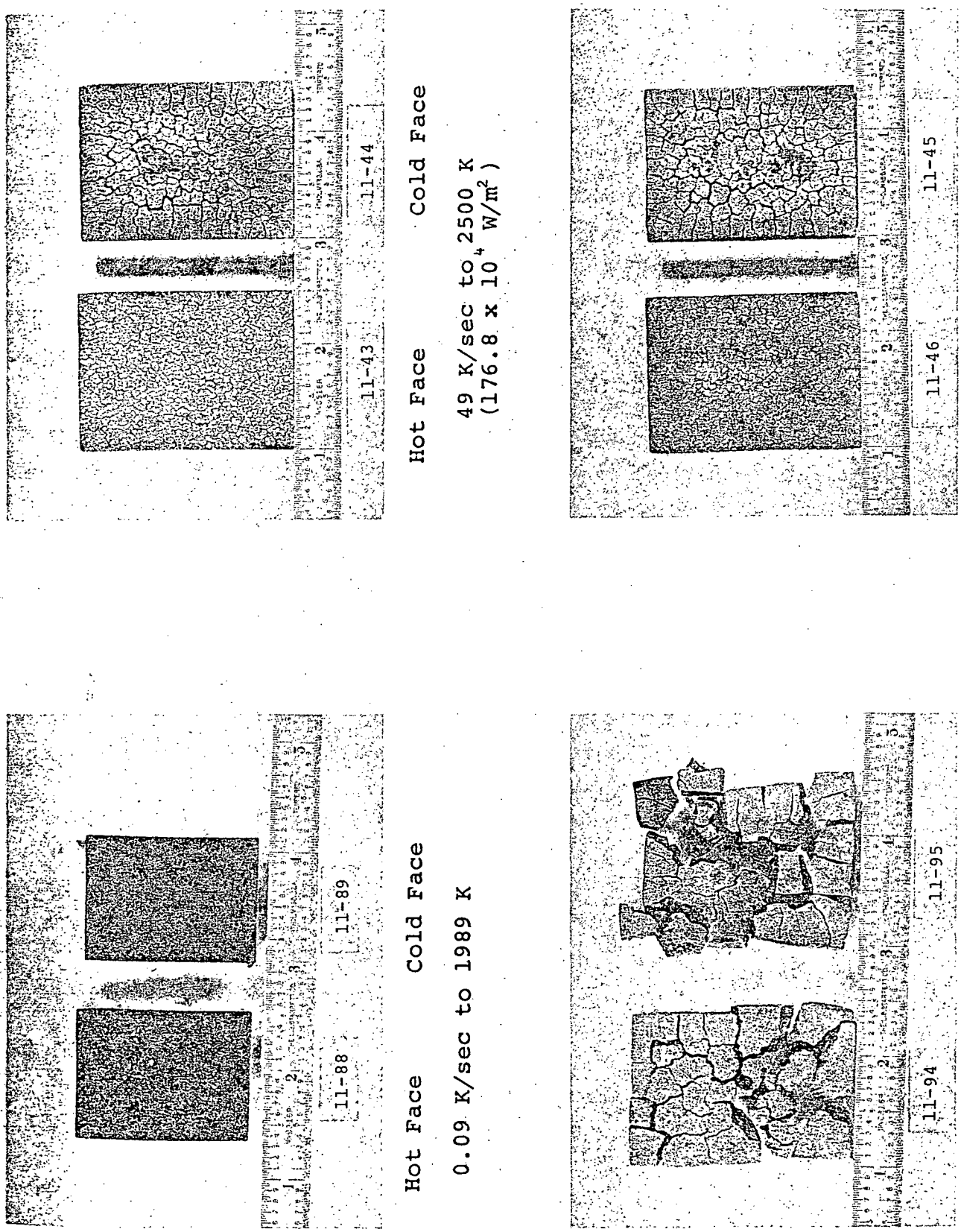

Figure 30. Pictures of low-density phenolic-nylon chars preapared in the laboratory at different heating rates to 2000 K

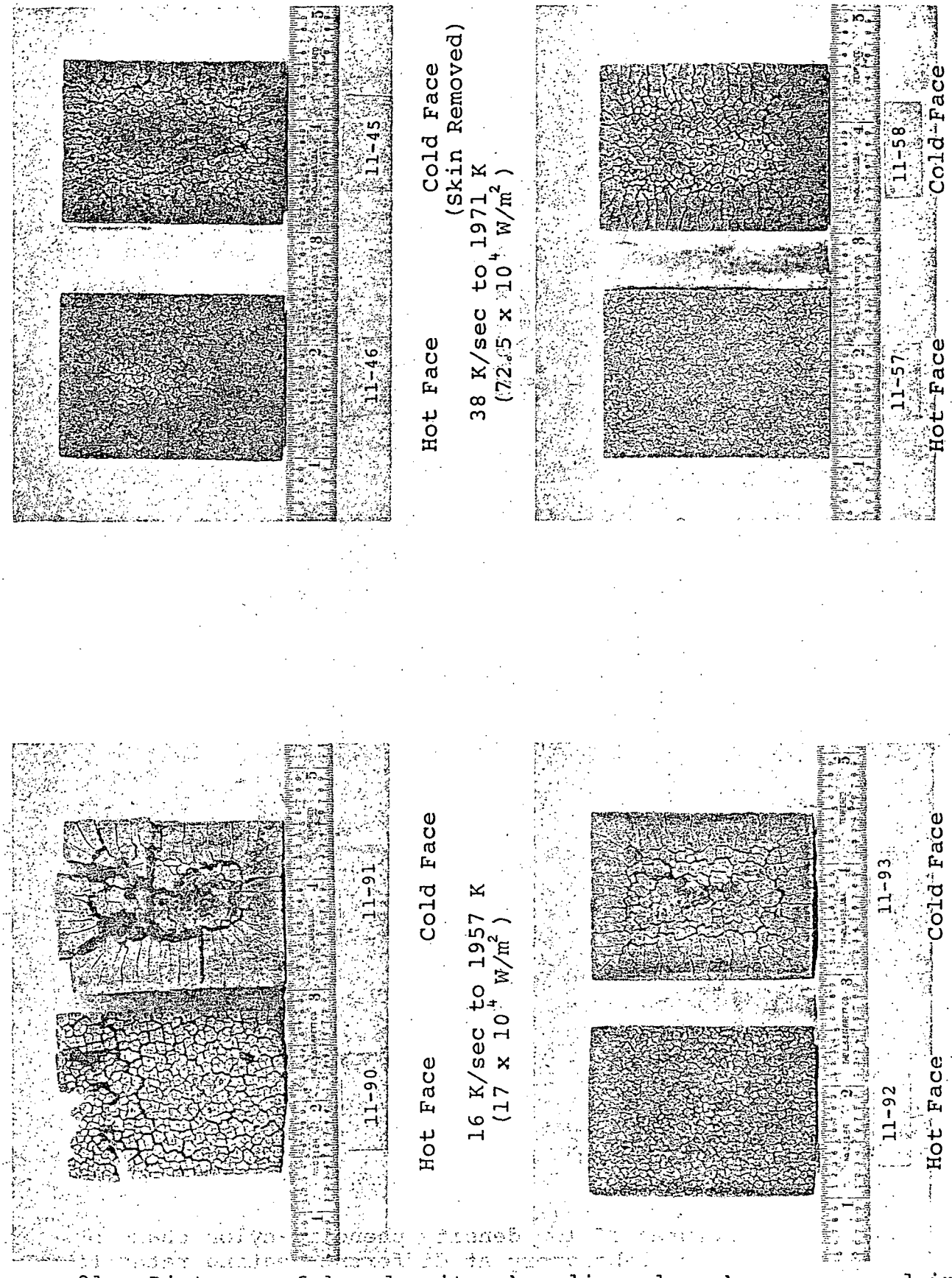

Figure 31. Pictures of low-density phenolic-nylon chars prepared in the laboratory at different heating rates to 2000 K

Figure 32. Pictures of low-density phenolic-nylon chars prepared in the laboratory at different heating rates to 3100 K

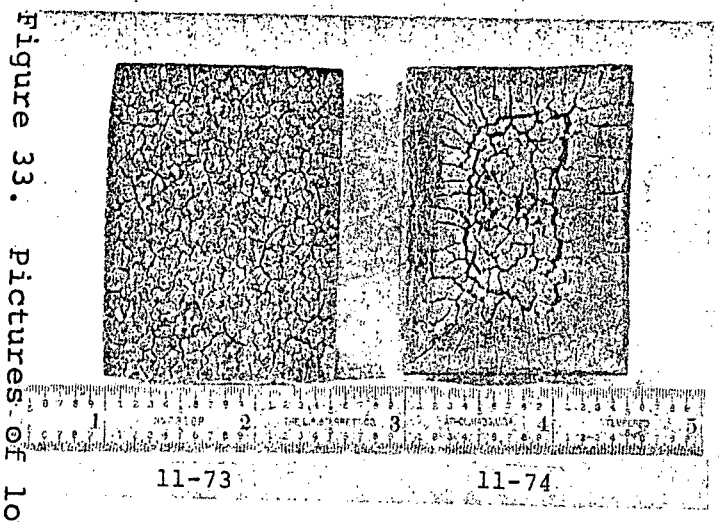

Hot Face Cold Face

16 K/sec to 3100 K
(17 x 10^4 W/m^2)

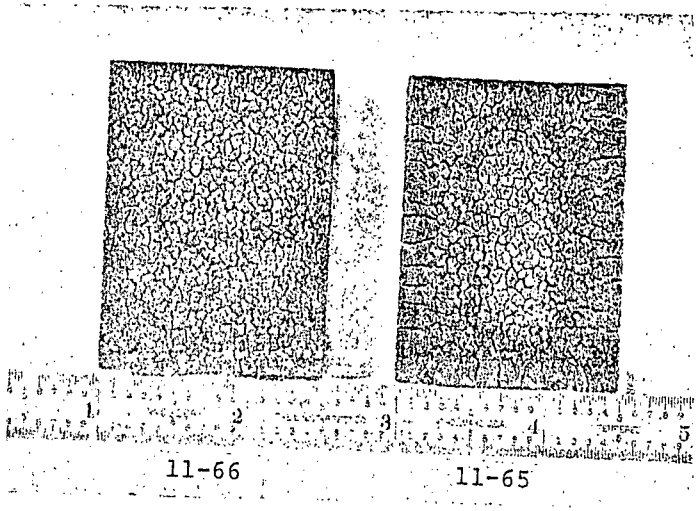

Hot Face Cold

38 K/sec to 2855 K
(72.5 x 10^4 W/m^2)

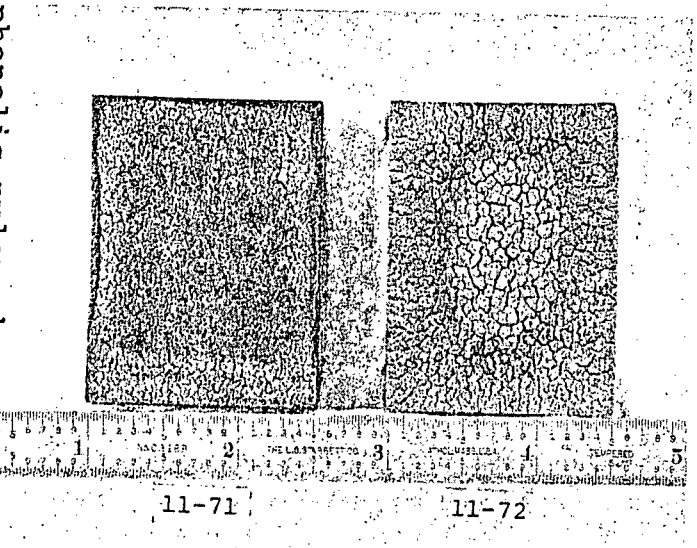

Hot Face Cold Face

61 K/sec to 3080 K
(417 x 10^4 W/m^2)

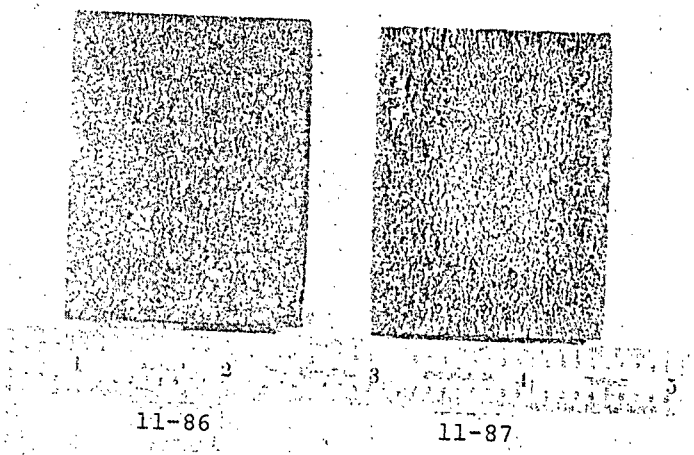

Hot Face Cold Face
(Skin Removed)

61 K/sec to 3080 K
(417 x 10^4 W/m^2)

Figure 33. Pictures of low-density phenolic-nylon chars prepared in the laboratory at different heating rates to 3100 K

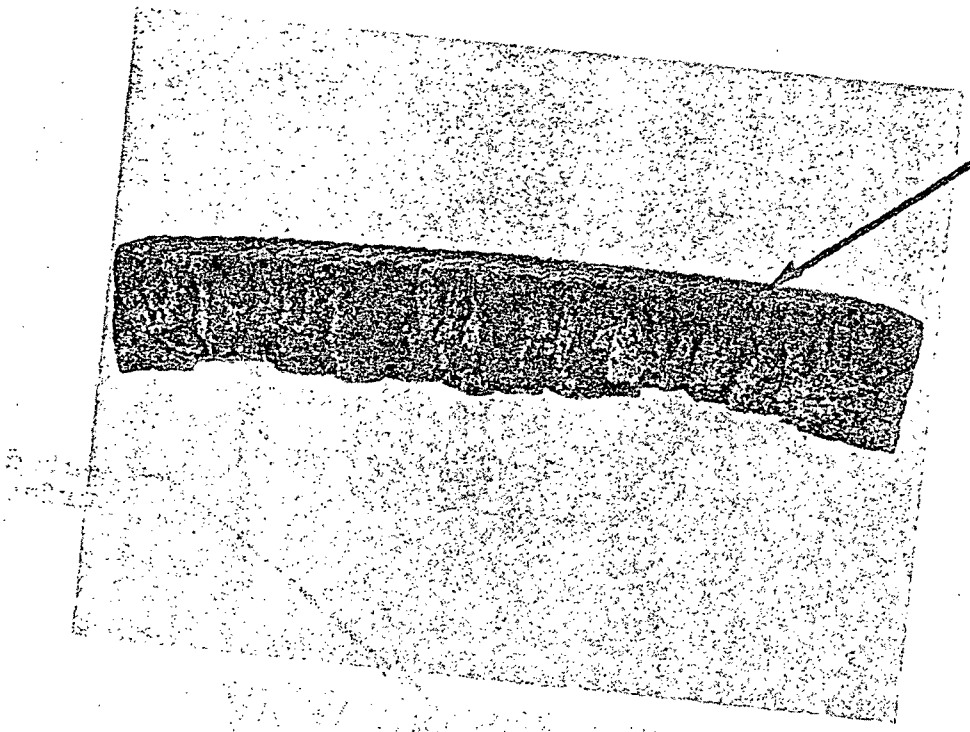

Specimen 1-24, 72.5 x 10^4 W/m^2

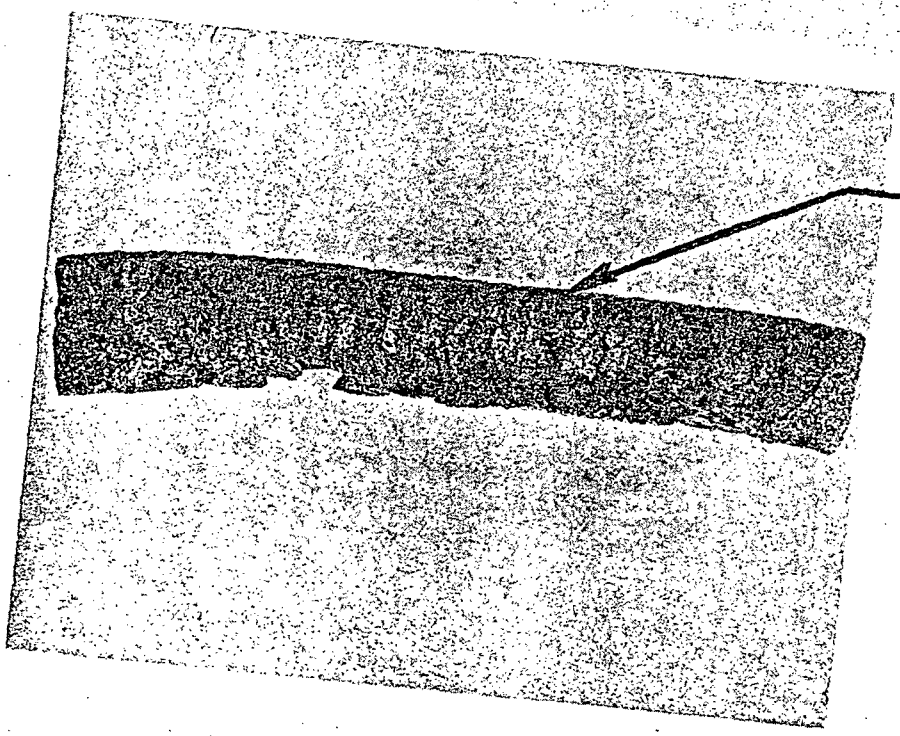

Specimen 1-22, 72.5 x 10^4 W/m^2

Figure 34. Section views of low-density phenolic-nylon rapid char specimen 1-22 and 1-24 prepared in the laboratory

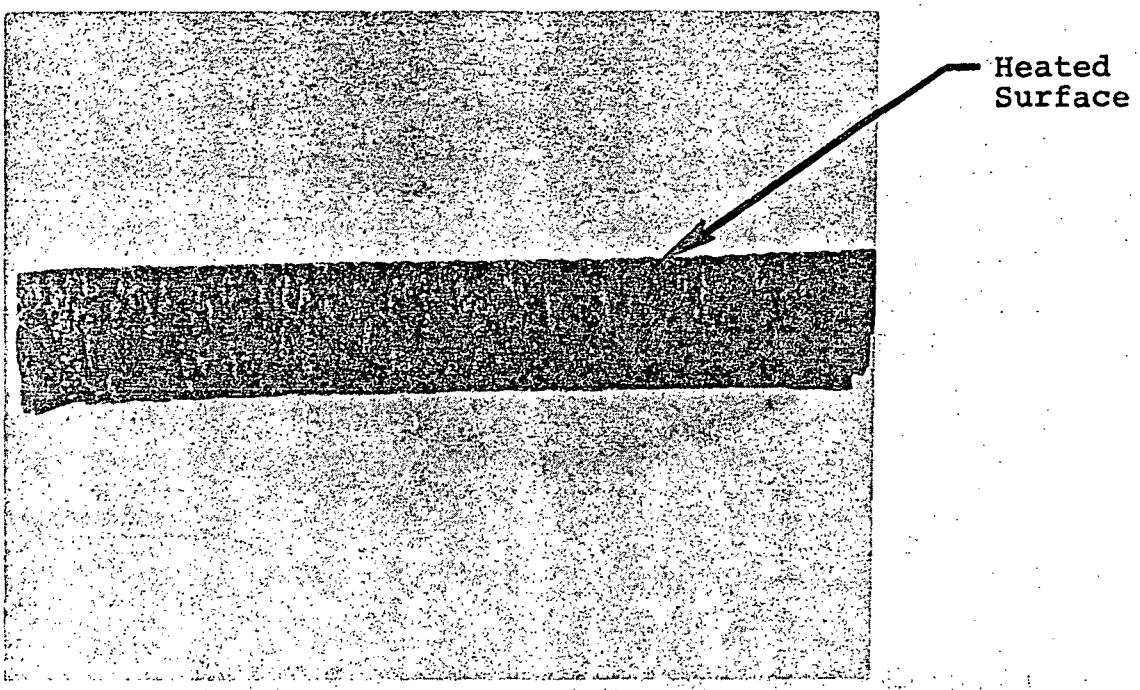

176.8×10^4 W/m^2

Figure 35. Section view of low-density phenolic-nylon rapid char specimen prepared in the laboratory

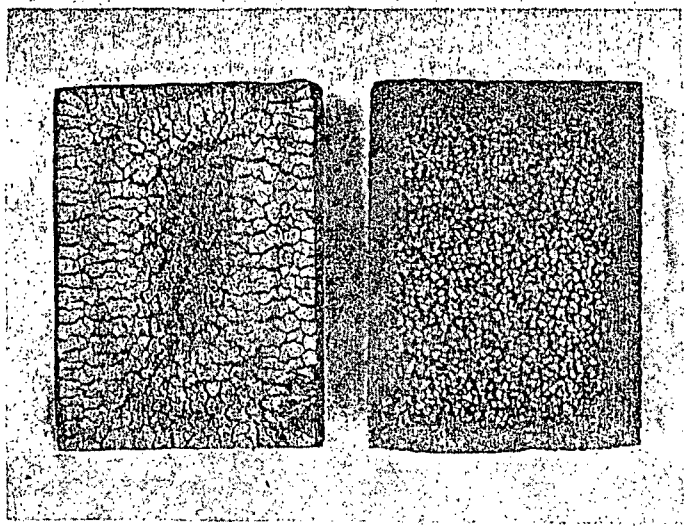

61K/sec to 3000 K
(413 x 10^4 W/m^2)

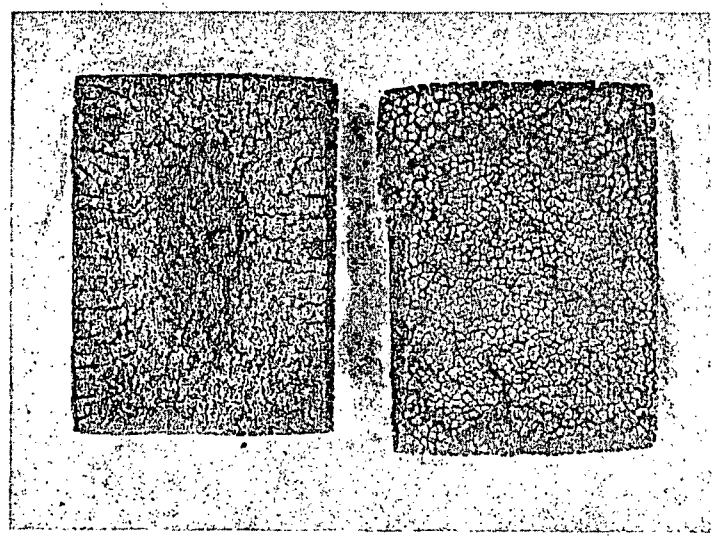

38K/sec to 2000 K
(72.5 x 10^4 W/m^2)

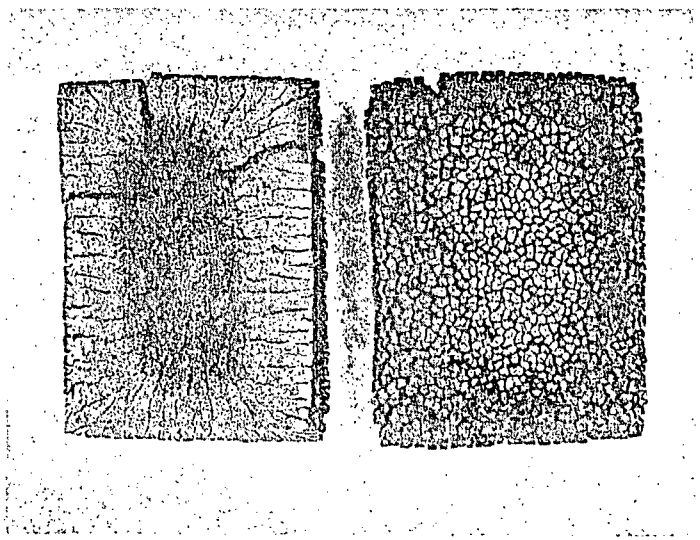

49K/sec to 2500 K
(177 x 10^4 W/m^2)

Figure 36. Pictures of char prepared in the laboratory from phenolic to different temperatures

Figure 37. Photomicrograph at 71 X of low-density phenolic-nylon char prepared in the laboratory at a heating rate of 0.1 K/sec to 1989 K

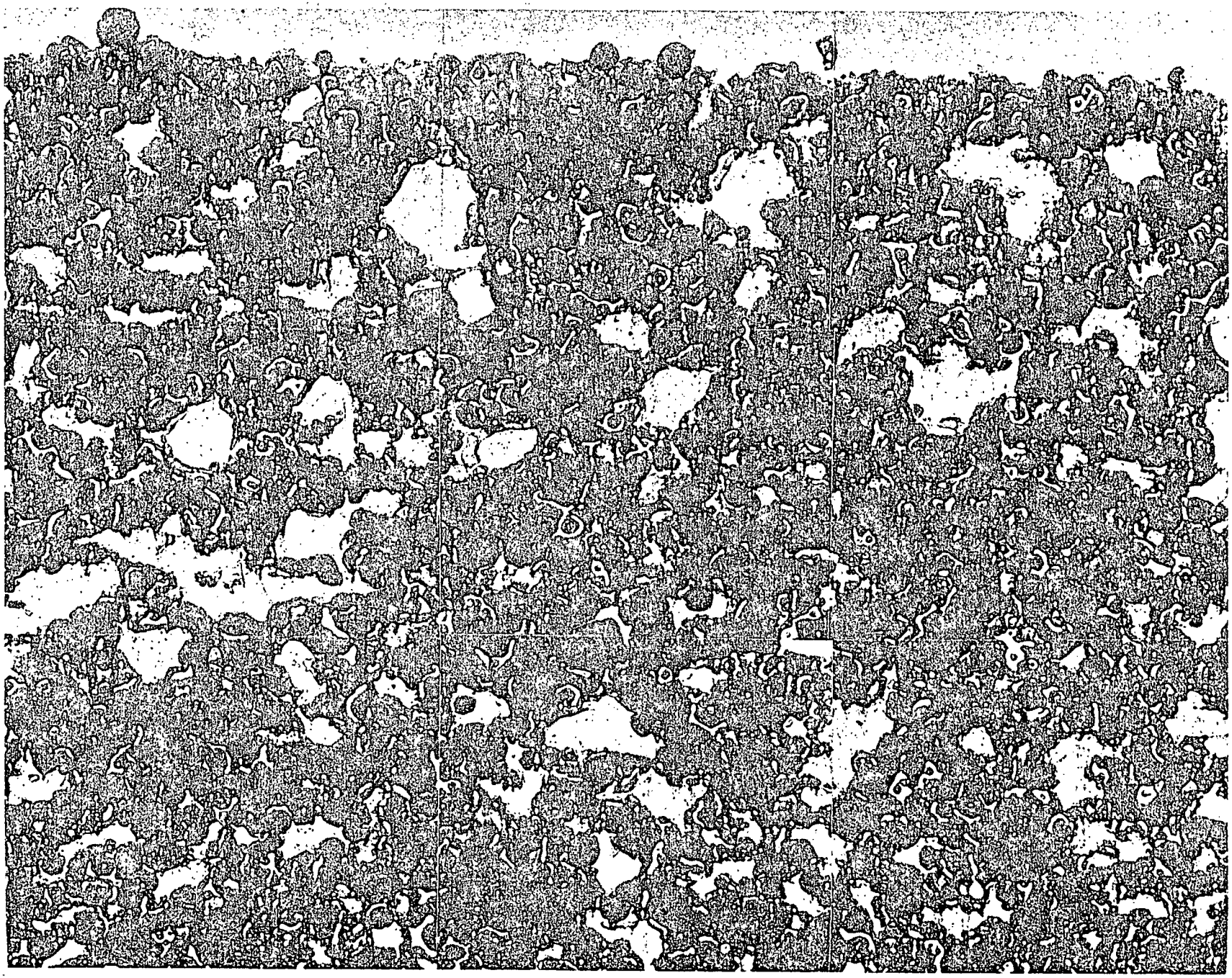

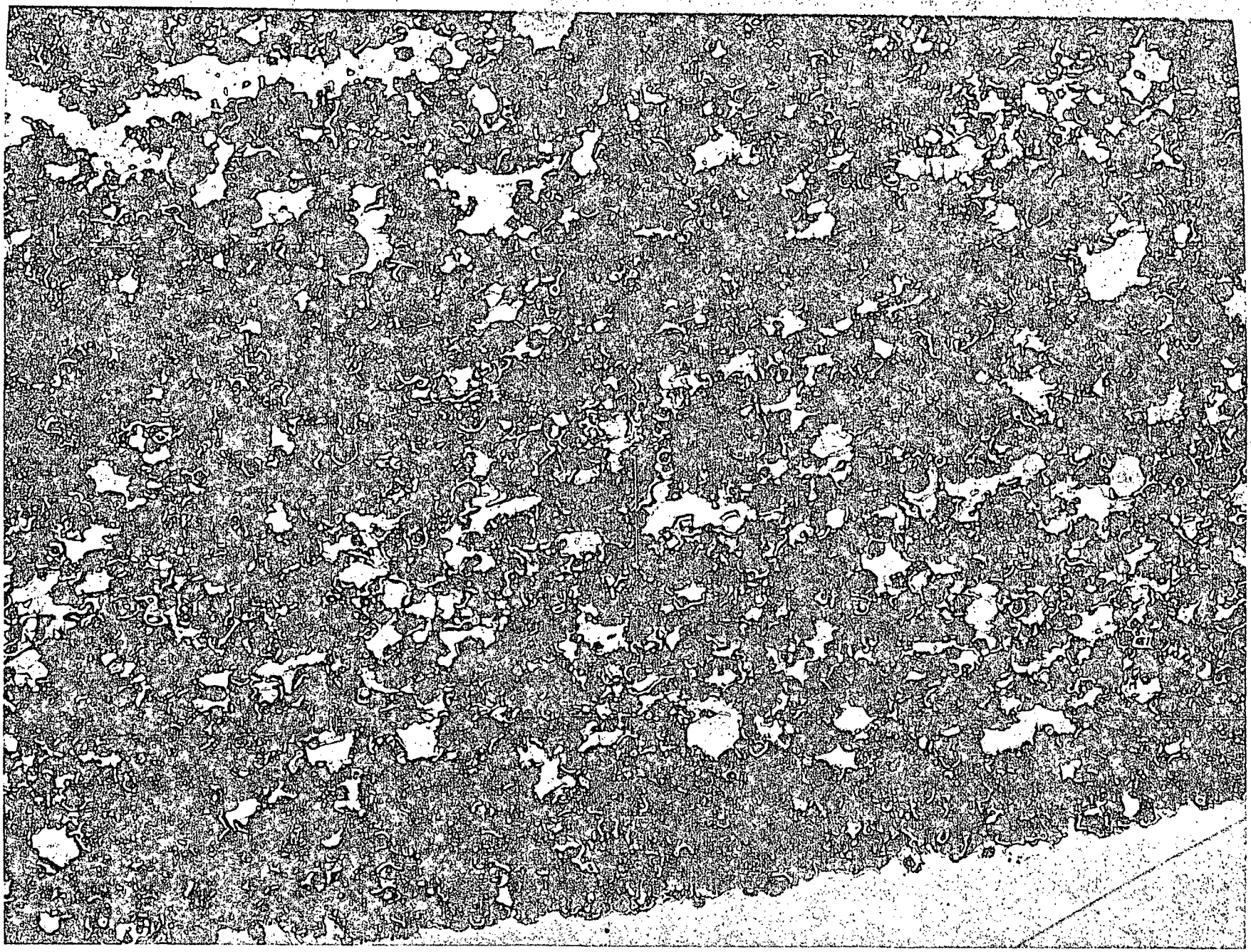

Figure 38. Photomicrograph at 54 X of low-density phenolic-nylon char specimen 11-95 prepared in the laboratory at a heating rate of 1.5 K/sec to 2021 K

Figure 39. Photomicrograph at 54 X of low-density phenolic-nylon char specimen 11-91 prepared in the laboratory at a temperature rise rate of 16 K/sec (cold wall heating rate of 17 x 10^4 W/m^2)

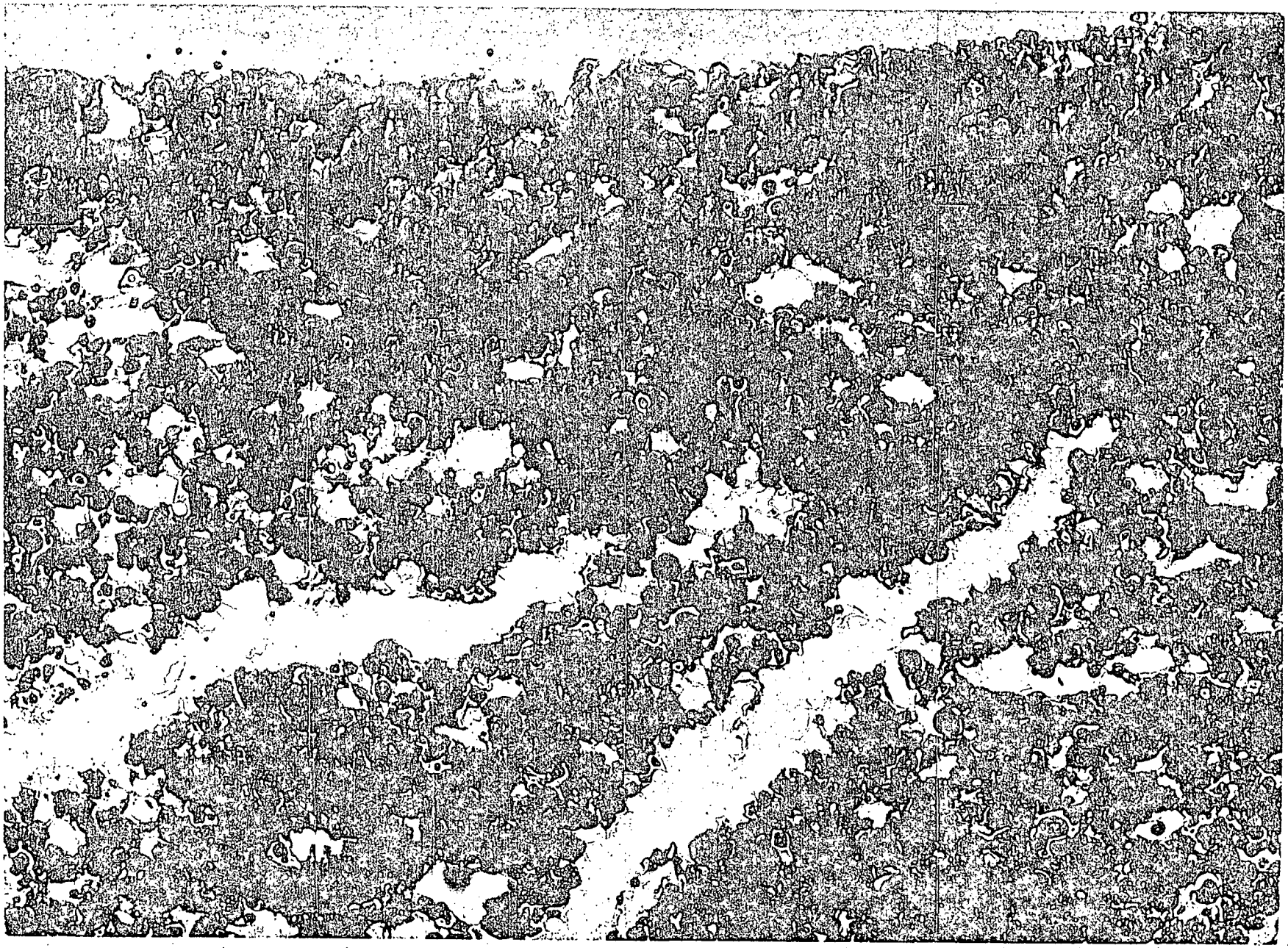

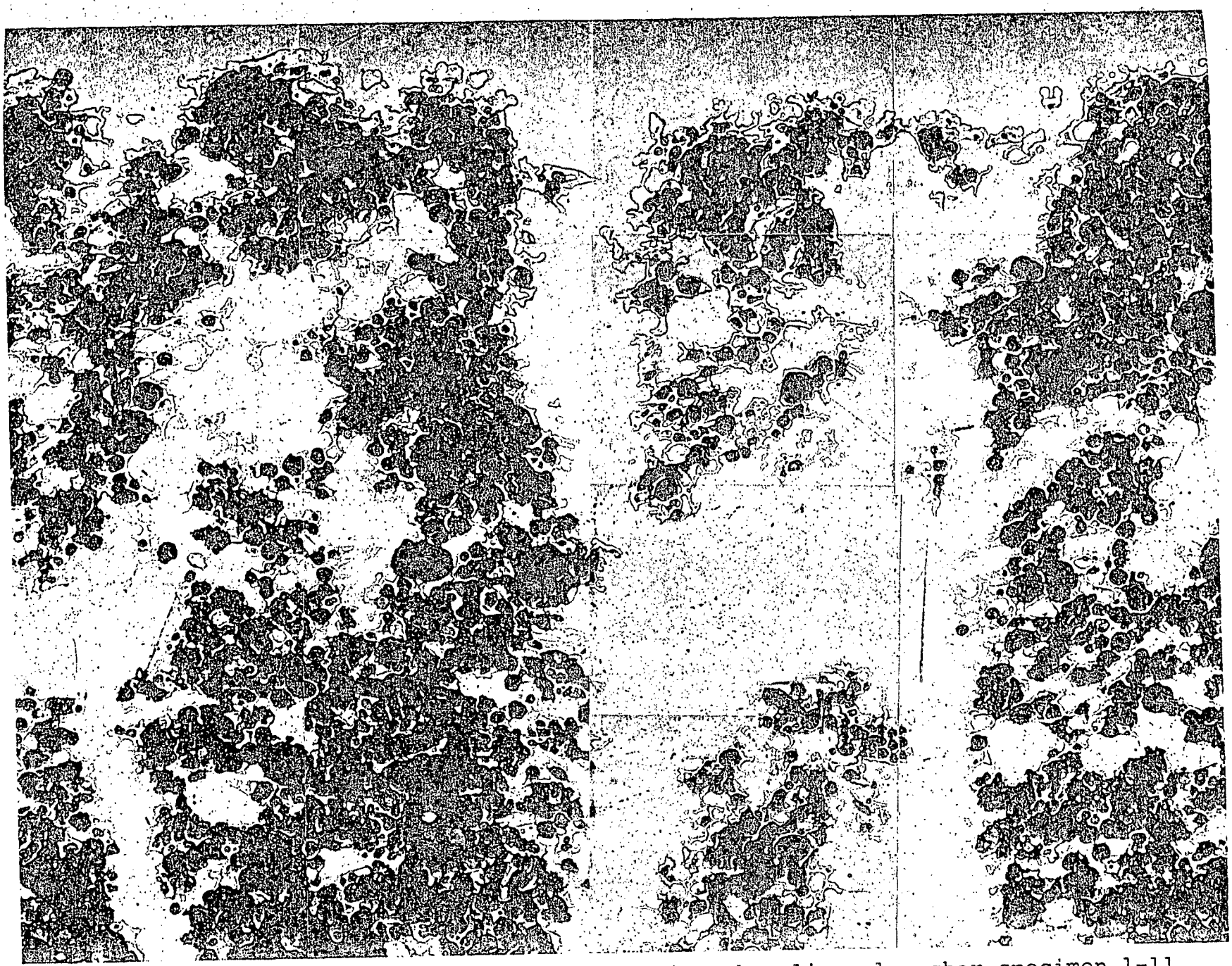

Figure 40. Photomicrograph at 55 X of low-density phenolic-nylon char specimen 1-11 prepared in the laboratory at a temperature rise rate of 38 K/sec (cold wall heating rate of 72.5×10^4 W/m^2 to 2033K)

Figure 41. Photomicrograph at 54 X of low-density phenolic-nylon char specimen 1-86 prepared in the laboratory at a temperature rise rate of 49 K/sec (cold wall heating rate of 177 x 10^4 W/m^2 to 2649 K)

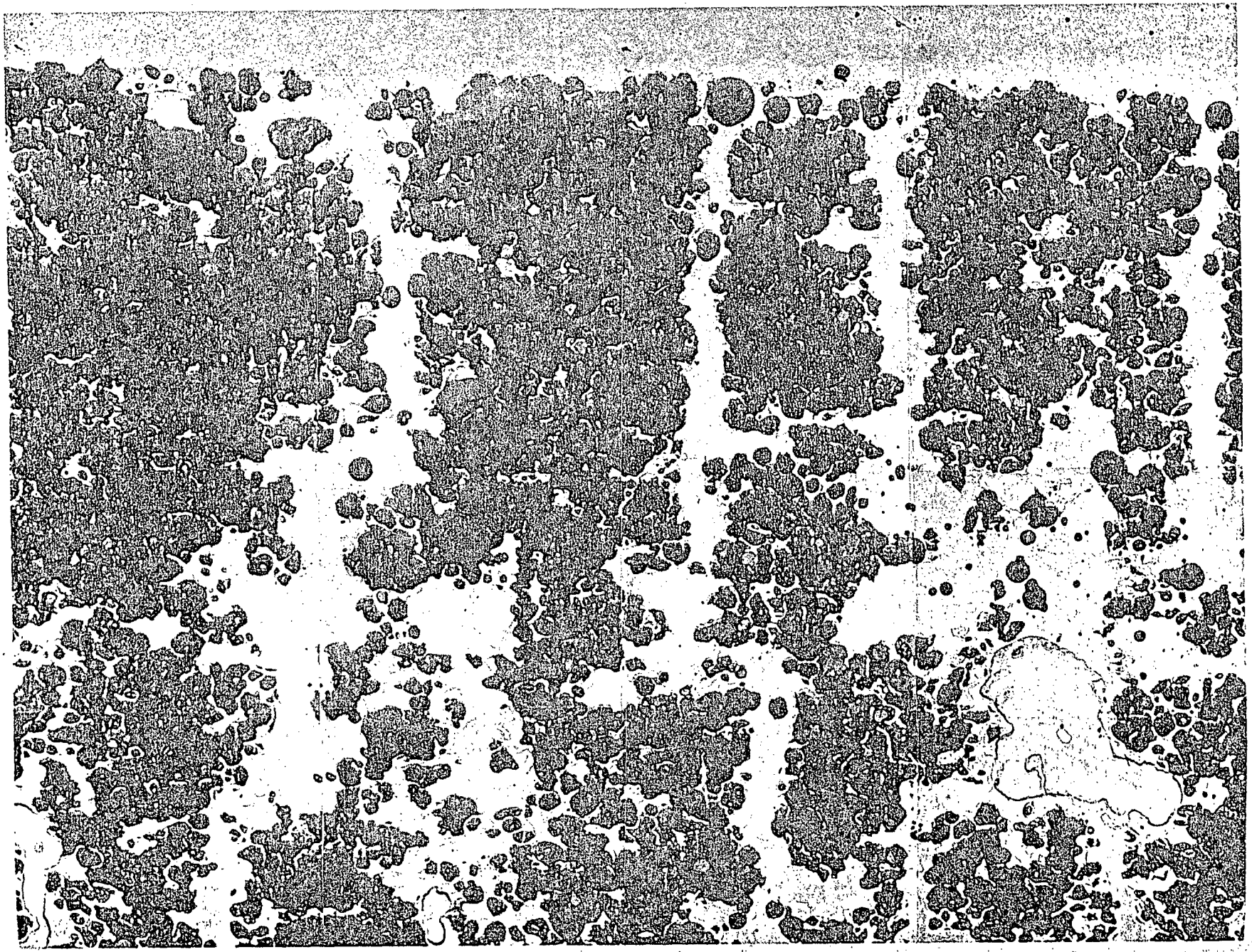

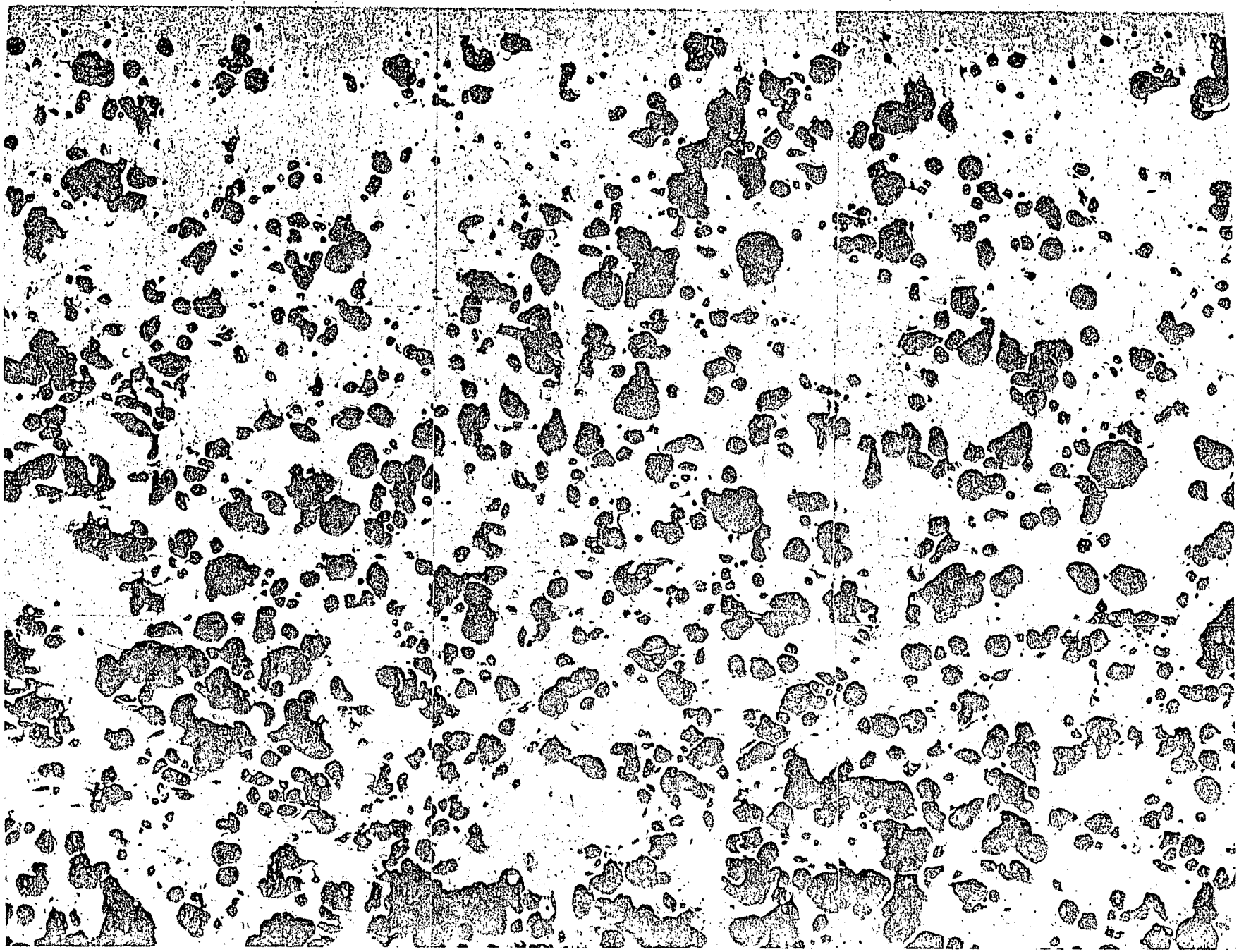

Figure 42. Photomicrograph at 71 X of low-density phenolic-nylon char specimen 11-87 prepared in the laboratory at a temperature rise rate of 61 K/sec (cold wall heating rate of 418 x 10^4 W/m^2 to 3080 K)

Figure 43. Photomicrograph at 55 X of phenolic char specimen P-6 prepared in the laboratory at a temperature rise rate of 61 K/sec (cold wall heating rate of 418 x 10^4 W/m^2 to 3066 K)

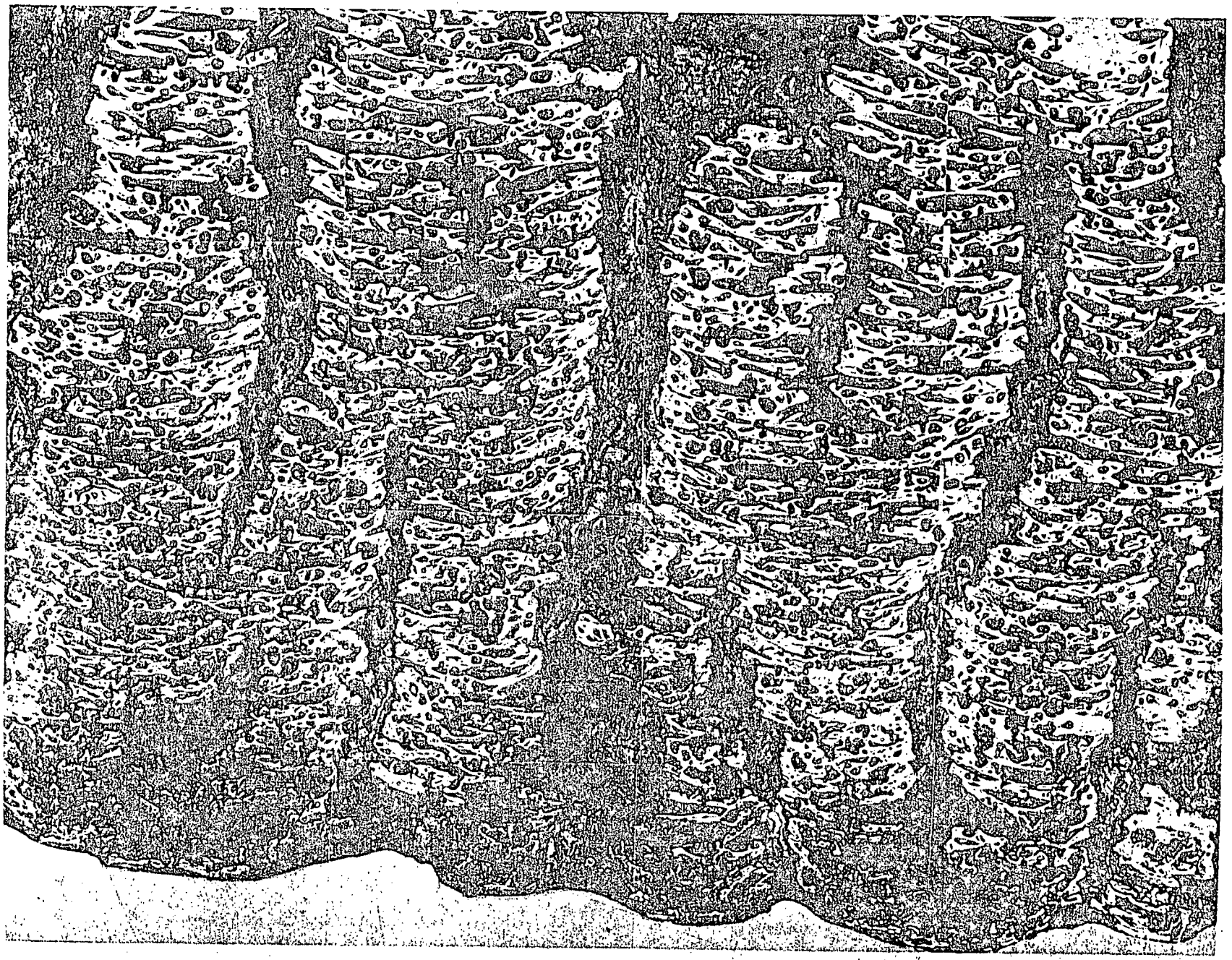

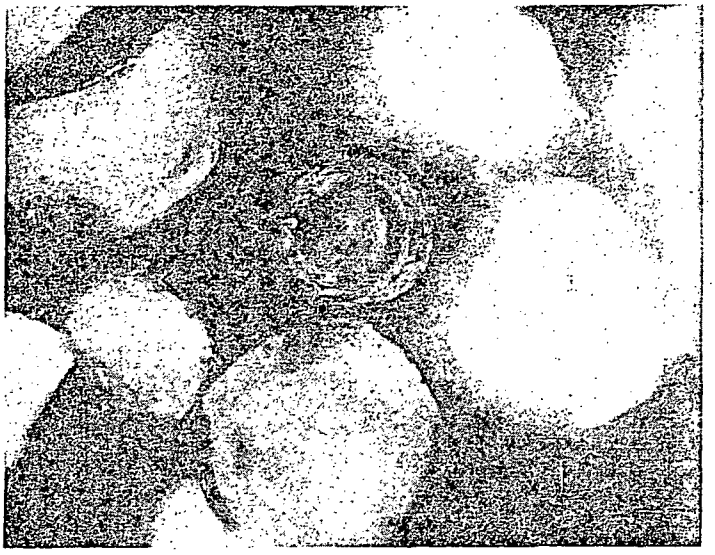

Specimen 11-88, 0.1°K/sec to 1989°K

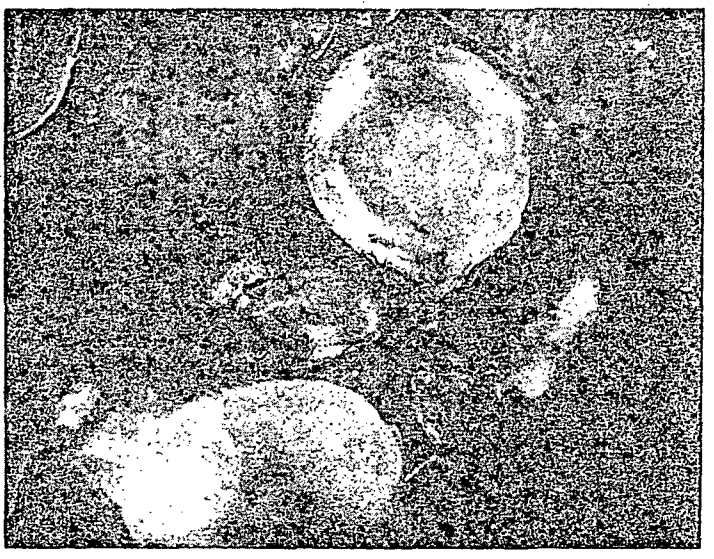

Specimen 11-95, 1.5°K/sec to 2021°K

Figure 44. Photomicrographs at 960 X under polarized light of low-density phenolic-nylon char prepared in the laboratory at low heating rates to 2000 K. (Photomicrographs courtesy of NASA Langley)

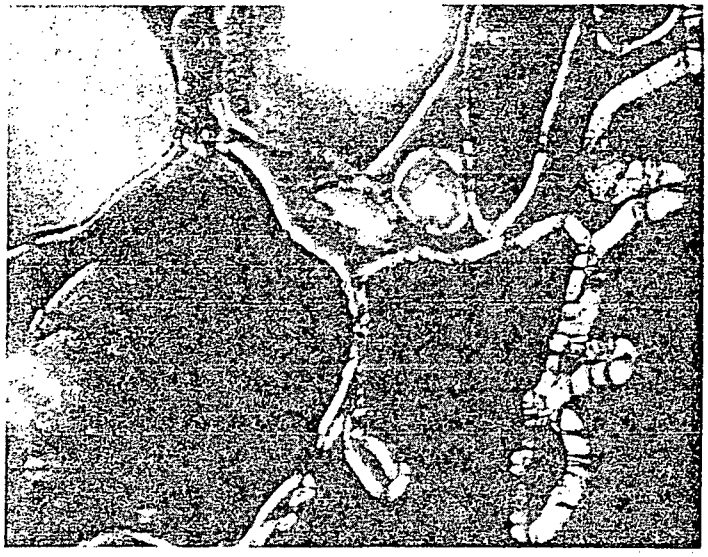

Front Face, Exposed to Heater

Back Face

Figure 45. Photomicrographs at 960 X under polarized light of low-density phenolic-nylon char specimen 11-91 prepared in the laboratory at a temperature rise rate of 16 K/sec (17×10^4 W/m^2 cold wall heat flux) to 1957 K. (Photomicrographs Courtesy of NASA Langley)

Front Face, Exposed to Heater

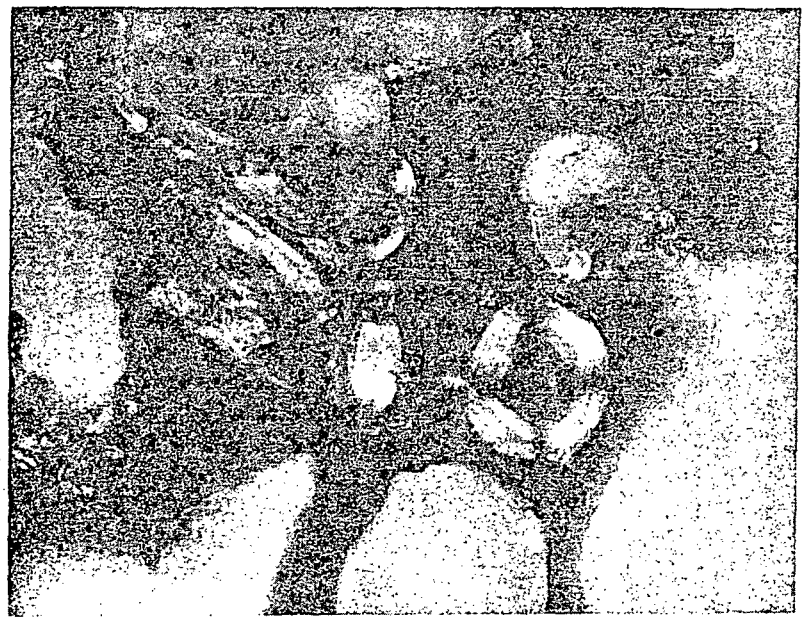

Back Face

Figure 46. Photomicrographs at 960 X under polarized light of low-density phenolic-nylon char specimen 1-112 prepared in the laboratory at a temperature rise rate of 38 K/sec (72.5×10^4 W/m^2 cold wall heat flux) to 2033 K. (Photomicrographs Courtesy of NASA Langley)

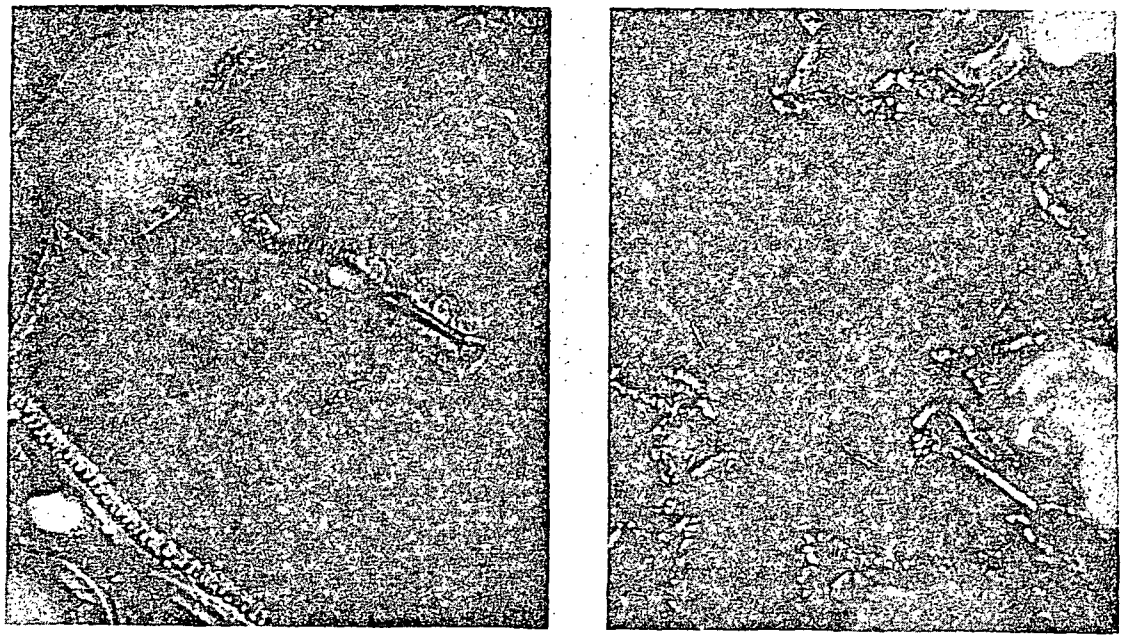

Front Face, Exposed to Heater Back Face

Specimen 1-86, 49°K/sec to 2649°K
177 x 10^4 W/m^2 Cold Wall Heat Flux

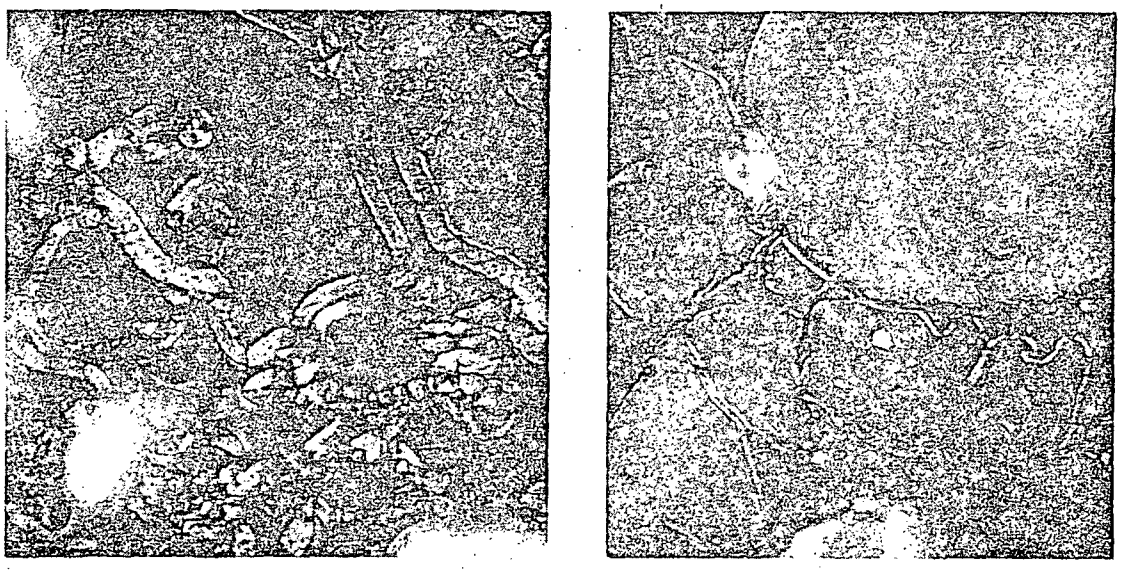

Front Face, Exposed to Heater Back Face

Specimen 11-87, 61°K/sec to 3080°K
418 x 10^4 W/m^2 Cold Wall Heat Flux

Figure 47. Photomicrographs at 960 X under polarized light of low-density char specimens prepared in the laboratory at different heating rates and to different temperatures. (Photomicrographs Courtesy of NASA Langley)

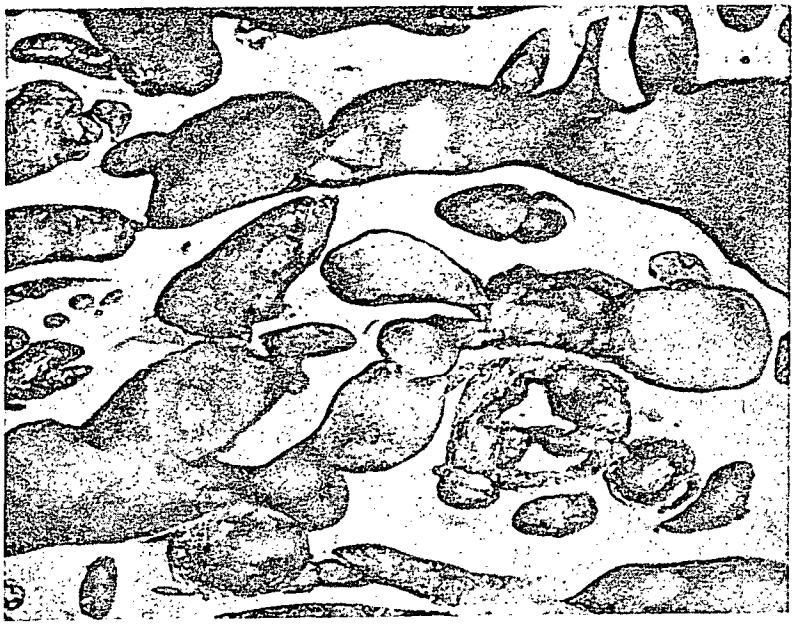

500X

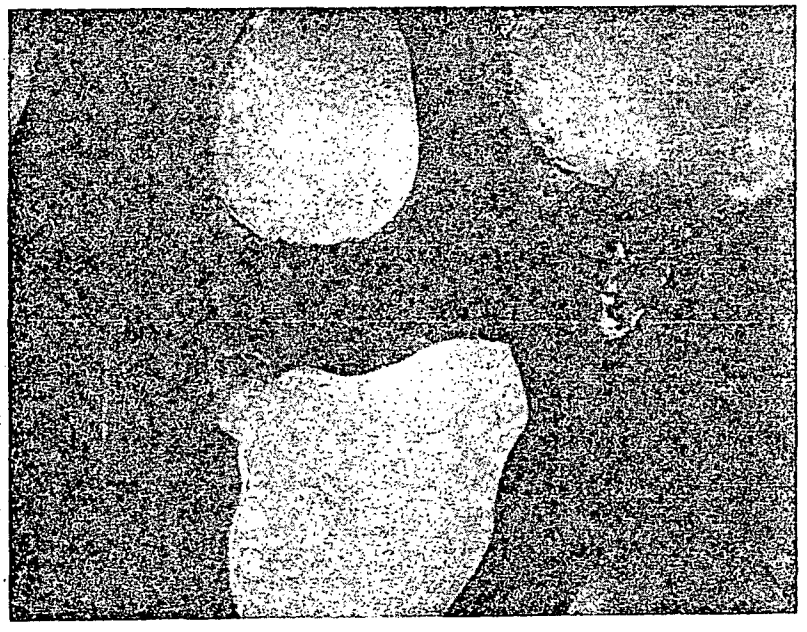

960X, Polarized Light
(Courtesy of NASA Langley)

Figure 48. Photomicrographs of phenolic char specimen P-6 prepared in the laboratory at a temperature rise rate of 61 K/sec (418 x 10^4 W/m^2 cold wall heat flux) to 3066

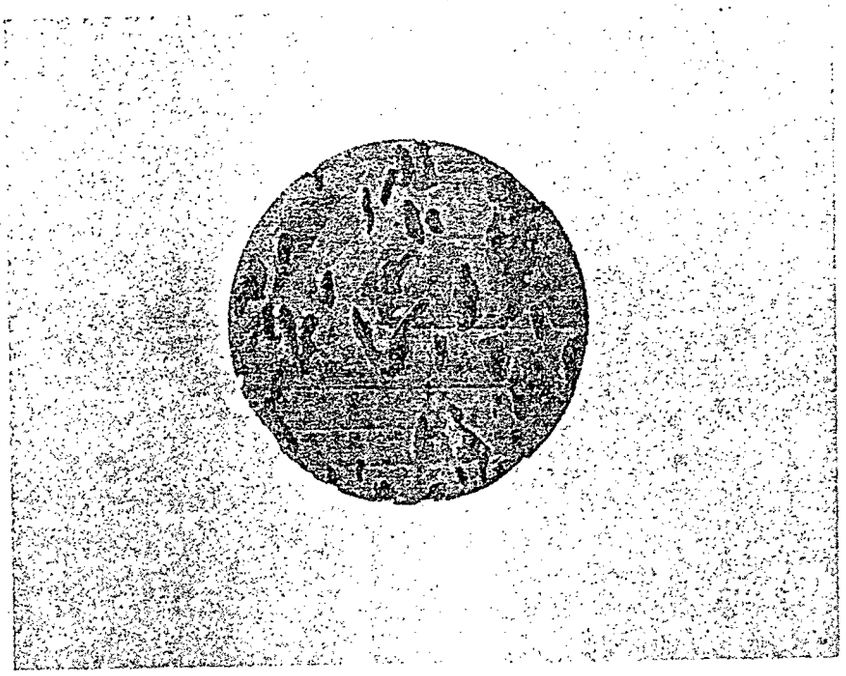

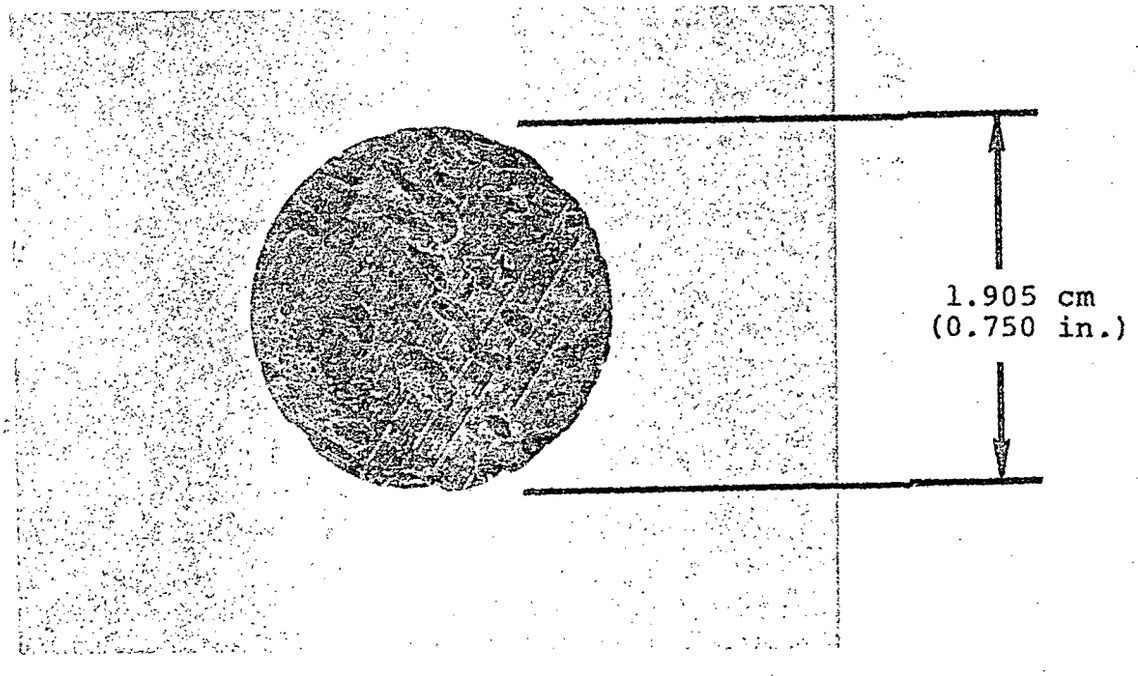

Figure 49. Pictures of phenolic specimen HMP prepared in the laboratory at a very low heating rate to 3033 K

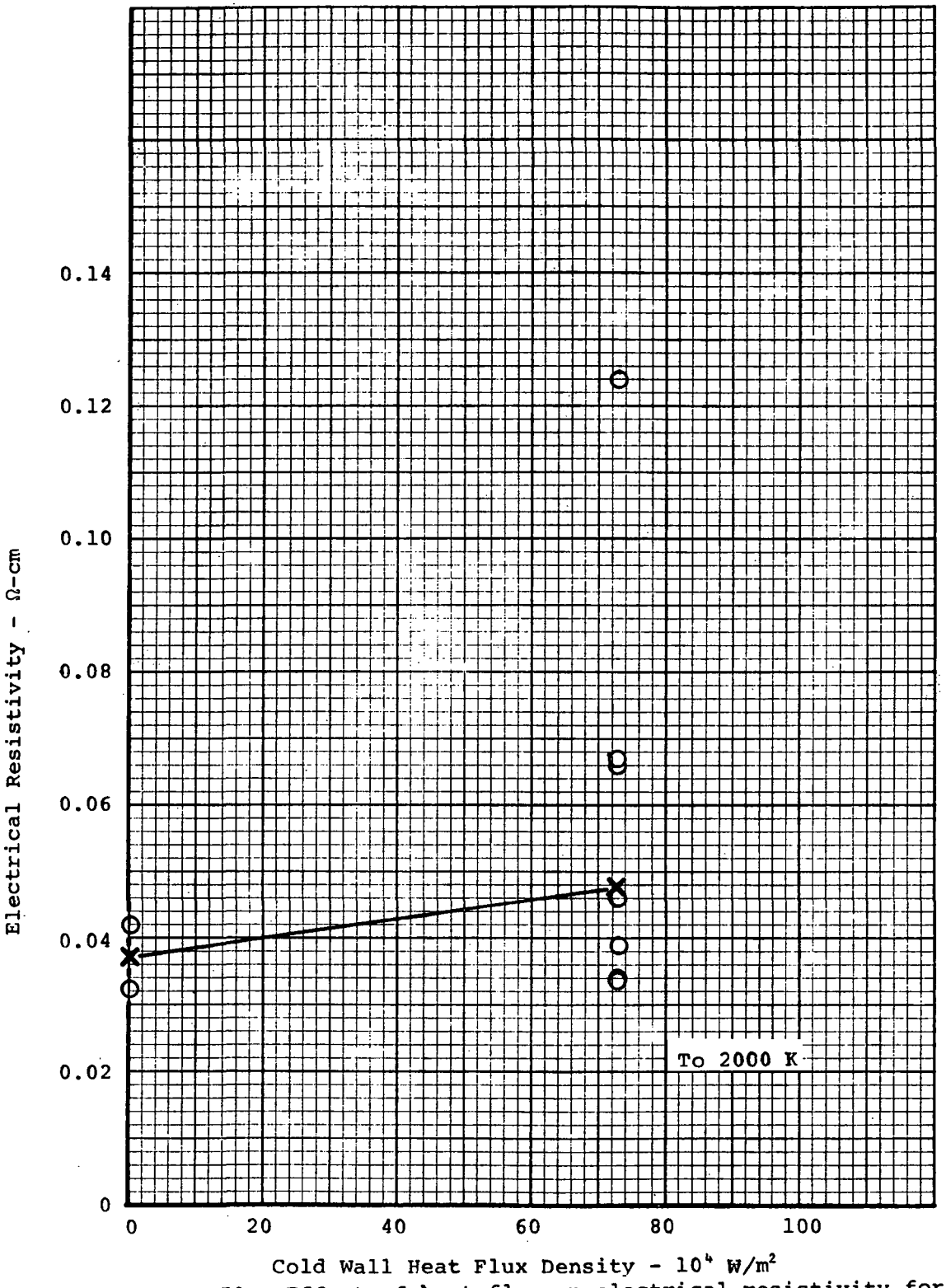

Figure 50. Effect of heat flux on electrical resistivity for chars prepared in the laboratory to 2000 K from low-density phenolic-nylon

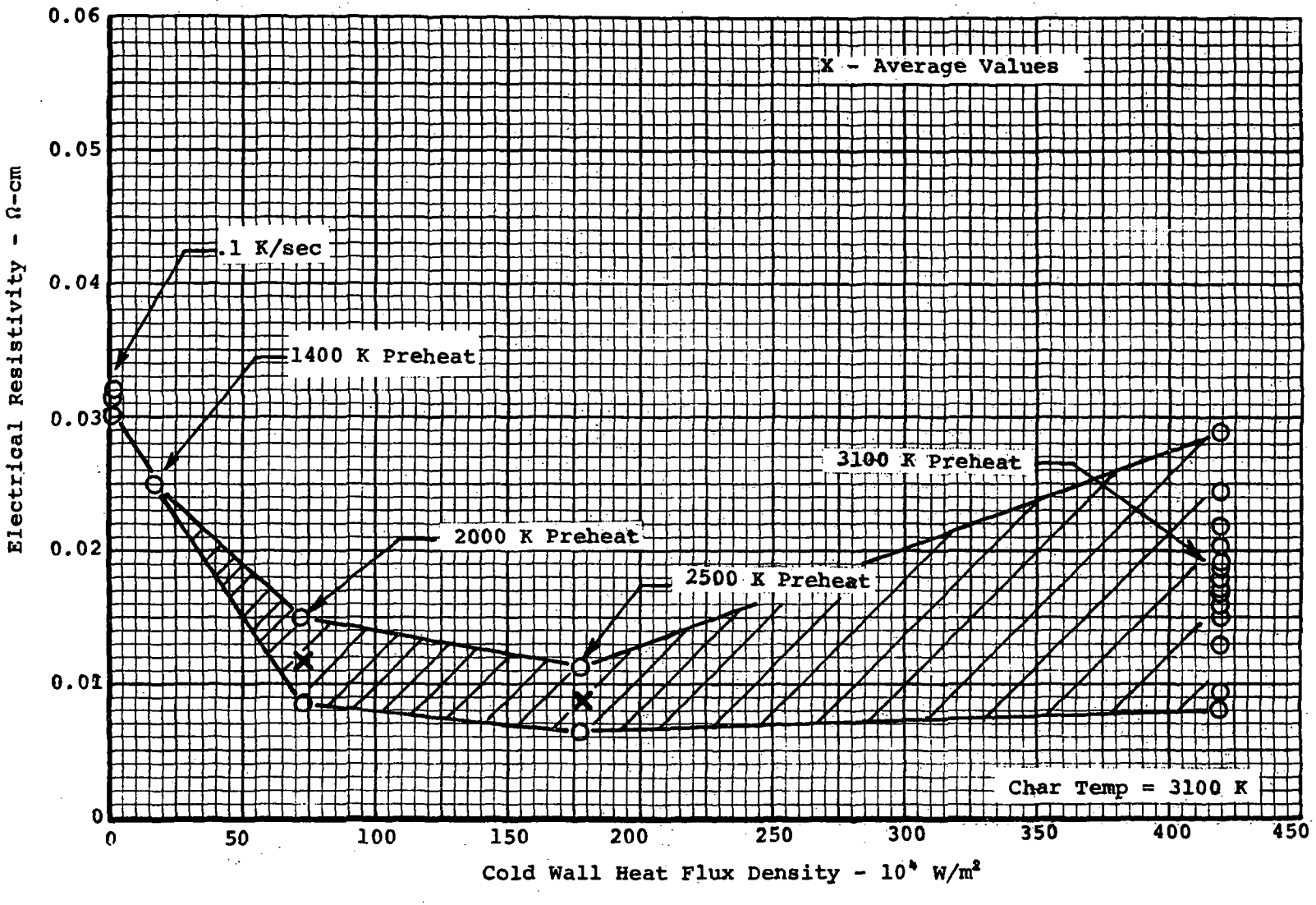

Figure 51. Effect of heat flux on electrical resistivity for chars prepared in the laboratory to 3100 K from low-density phenolic-nylon

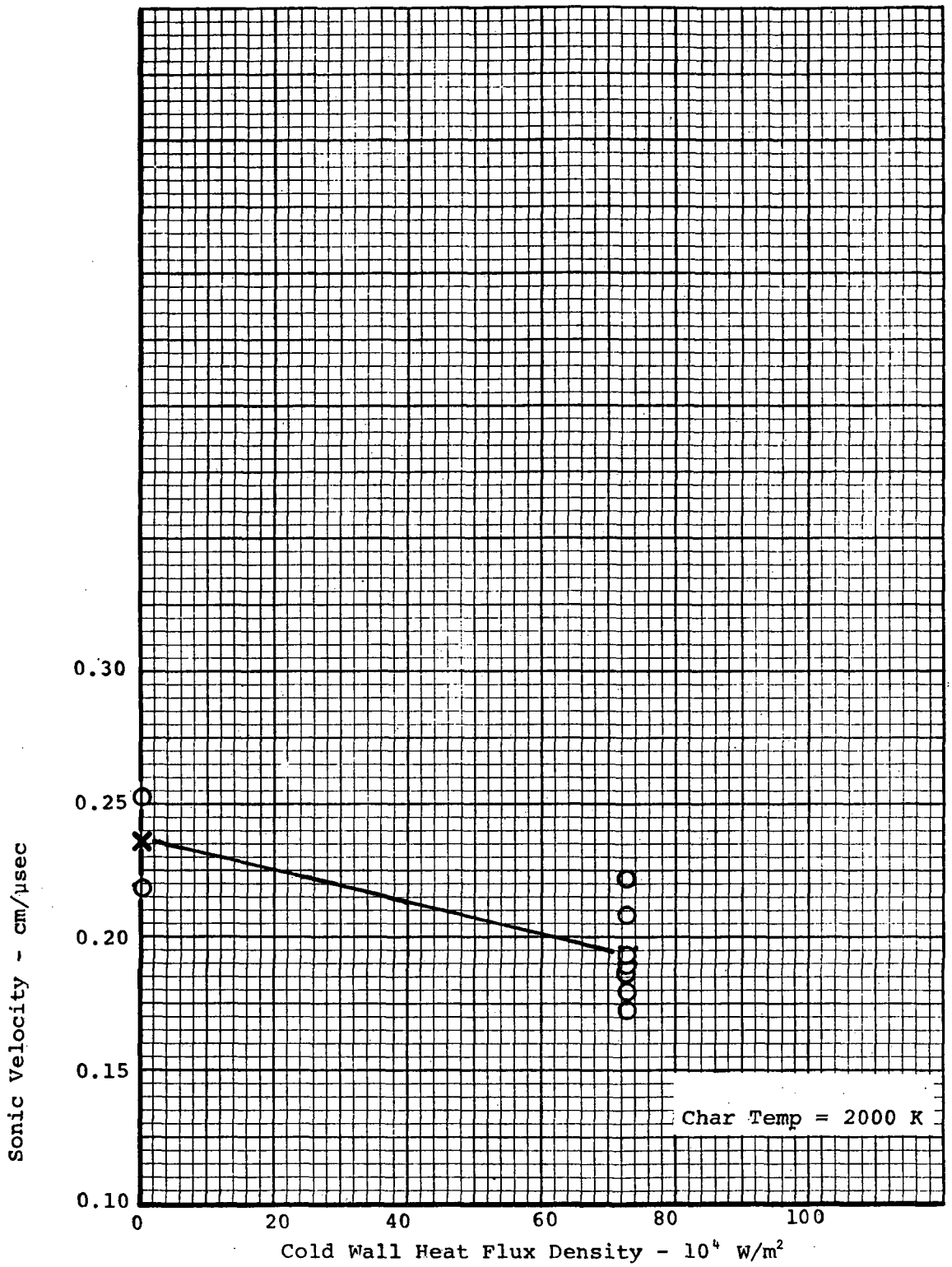

Figure 52. Effect of heat flux on sonic velocity for chars prepared in the laboratory to 2000K from low-density phenolic-nylon

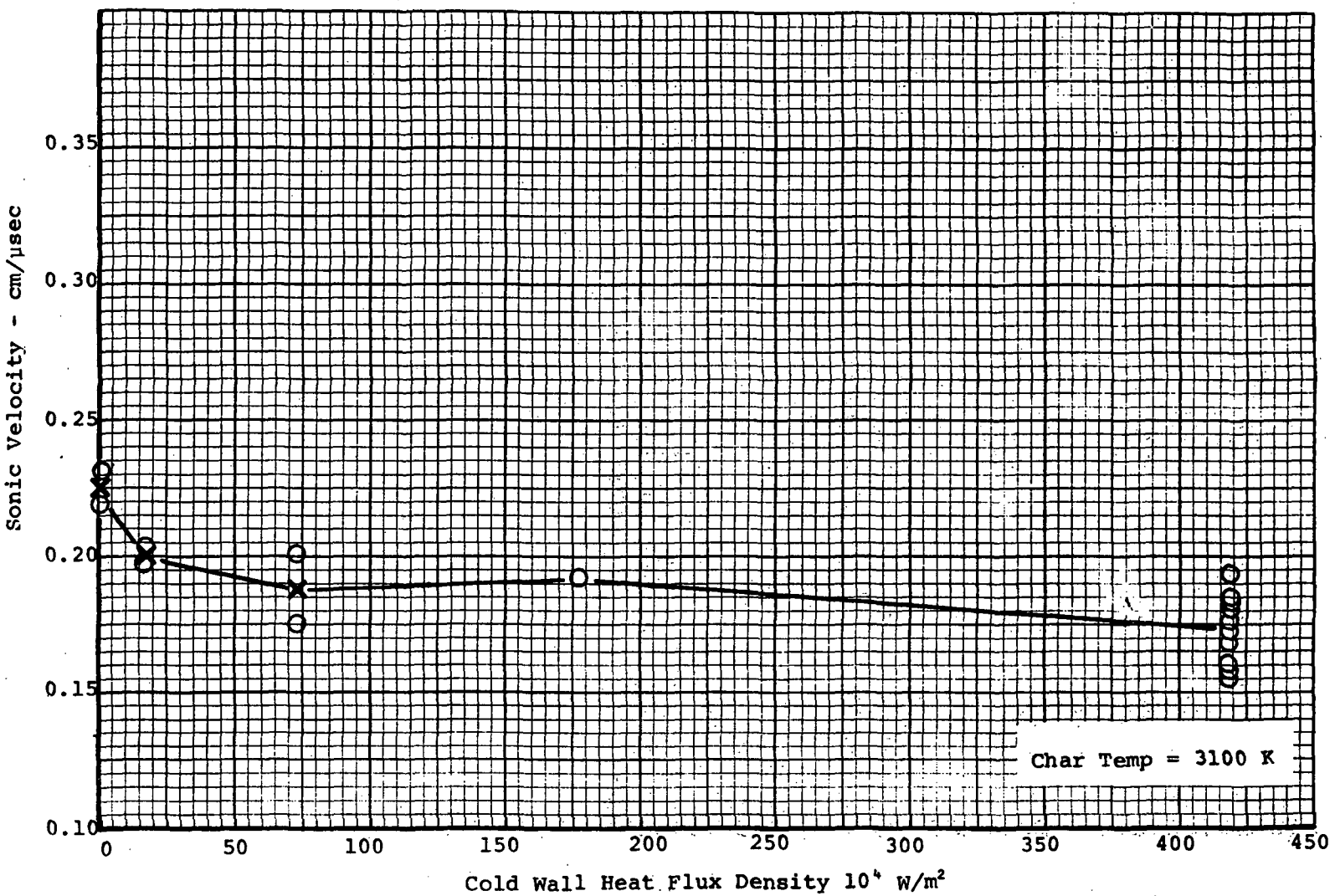

Figure 53. Effect of heat flux on sonic velocity for chars prepared in the laboratory to 3100 K from low-density phenolic-nylon

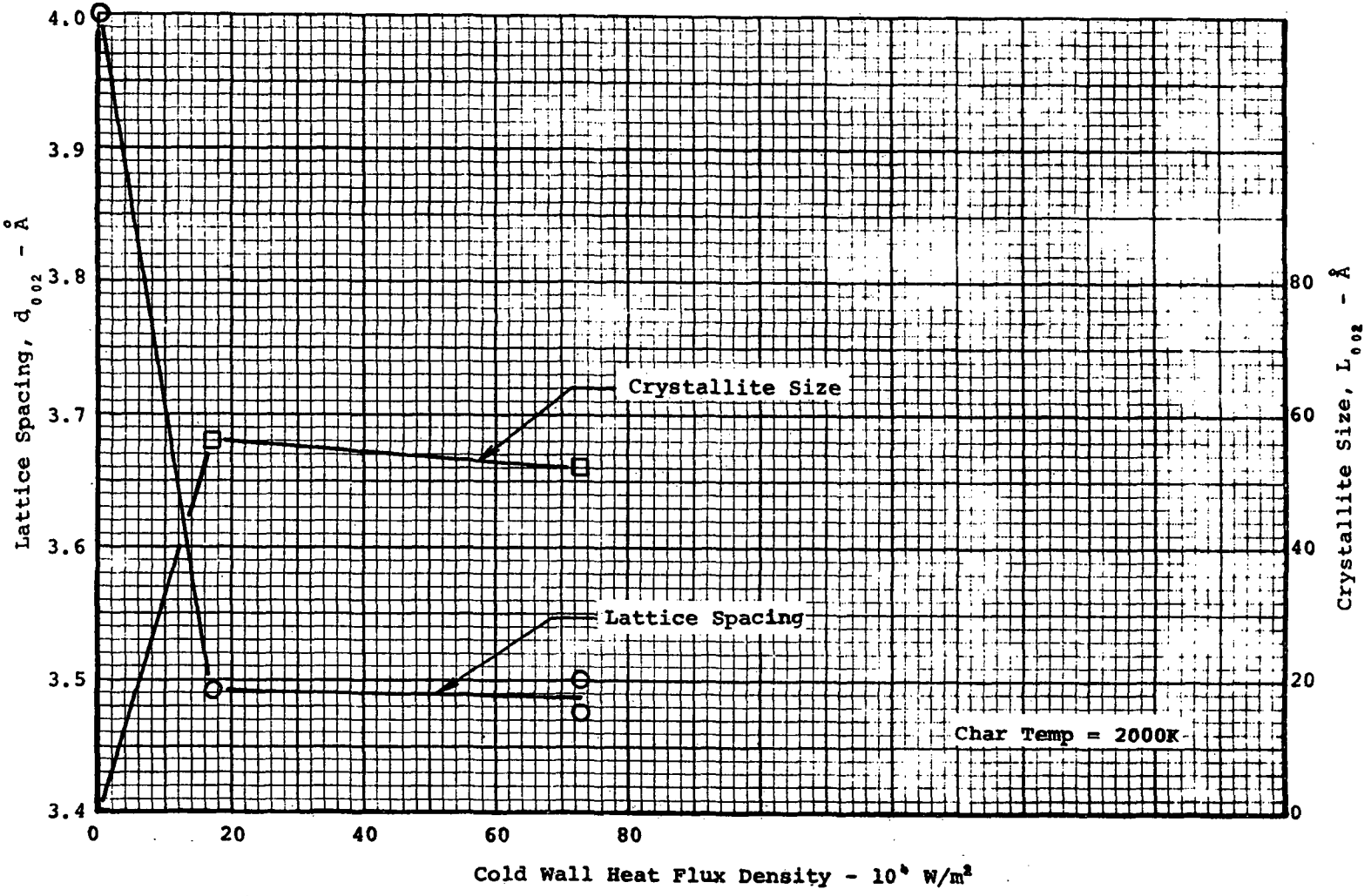

Figure 54. Effect of heat flux on d_{002} lattice spacing and L_{002} crystallite size for chars prepared in the laboratory to 2000 K from low density phenolic-nylon

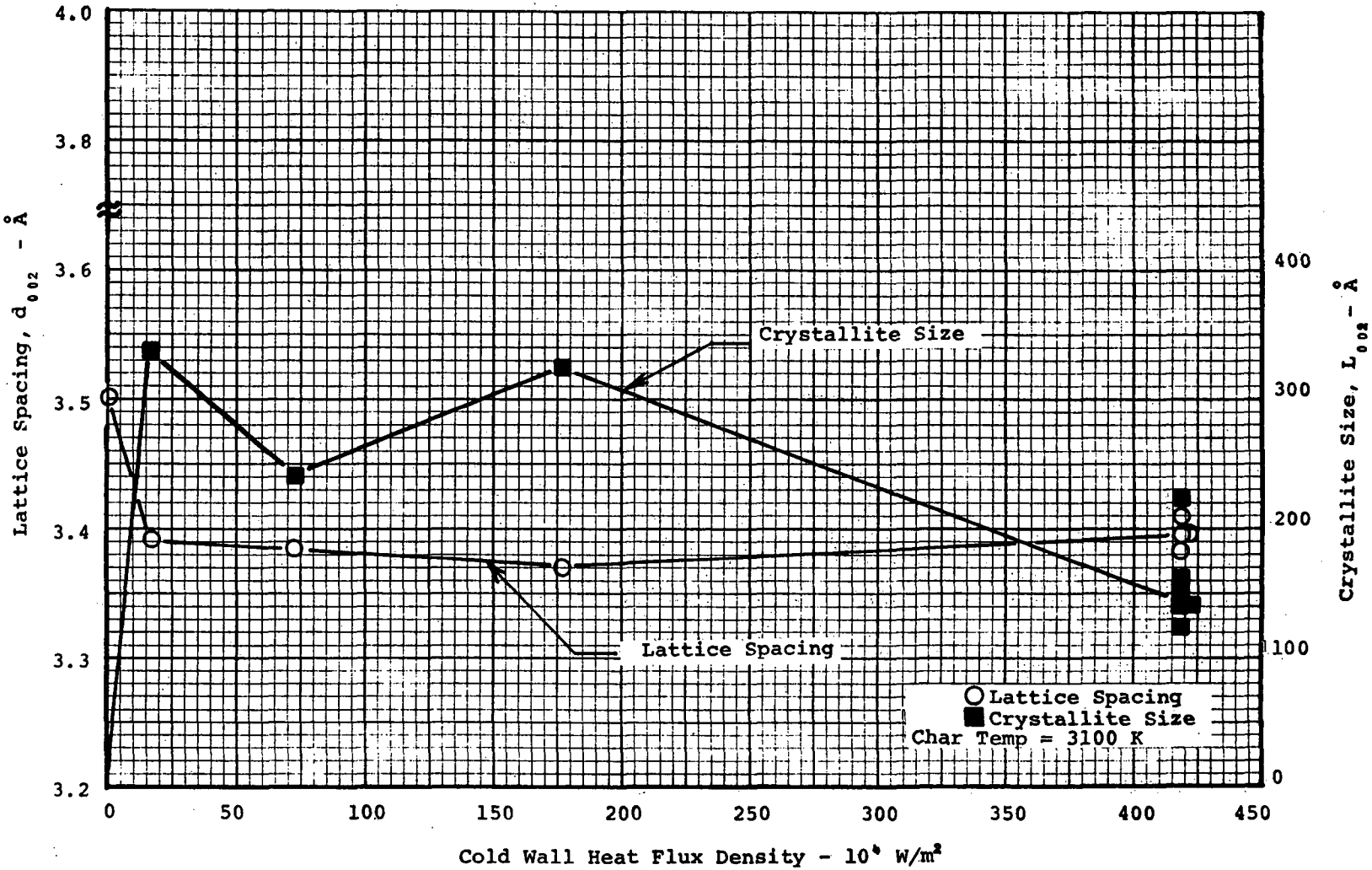

Figure 55. Effect of heat flux on d_{002} lattice spacing and L_{002} crystallite size for chars prepared in the laboratory to 3100 K from low-density phenolic-nylon

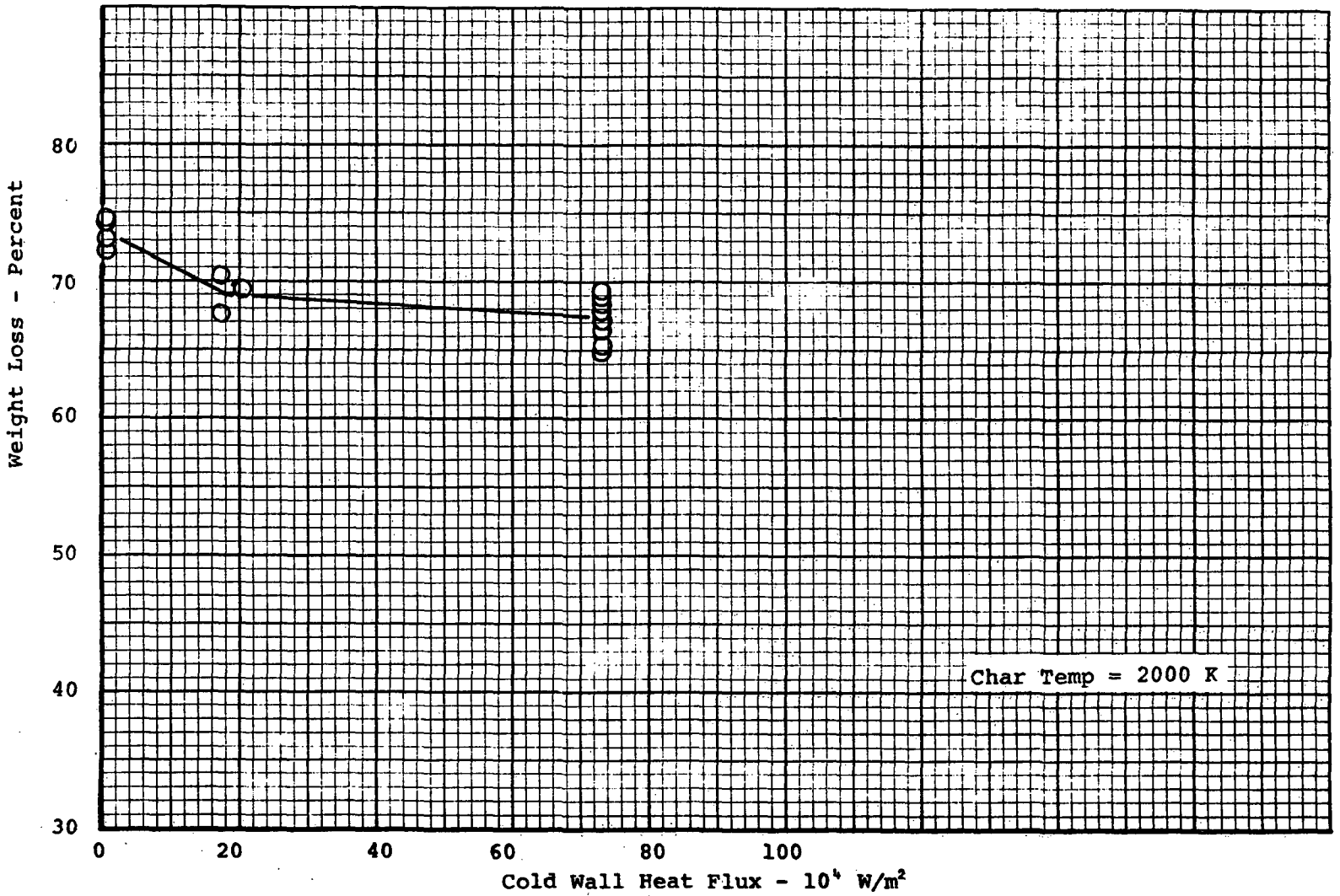

Figure 56. Effect of heat flux on weight loss for chars prepared in the laboratory to 2000 K from low-density phenolic-nylon

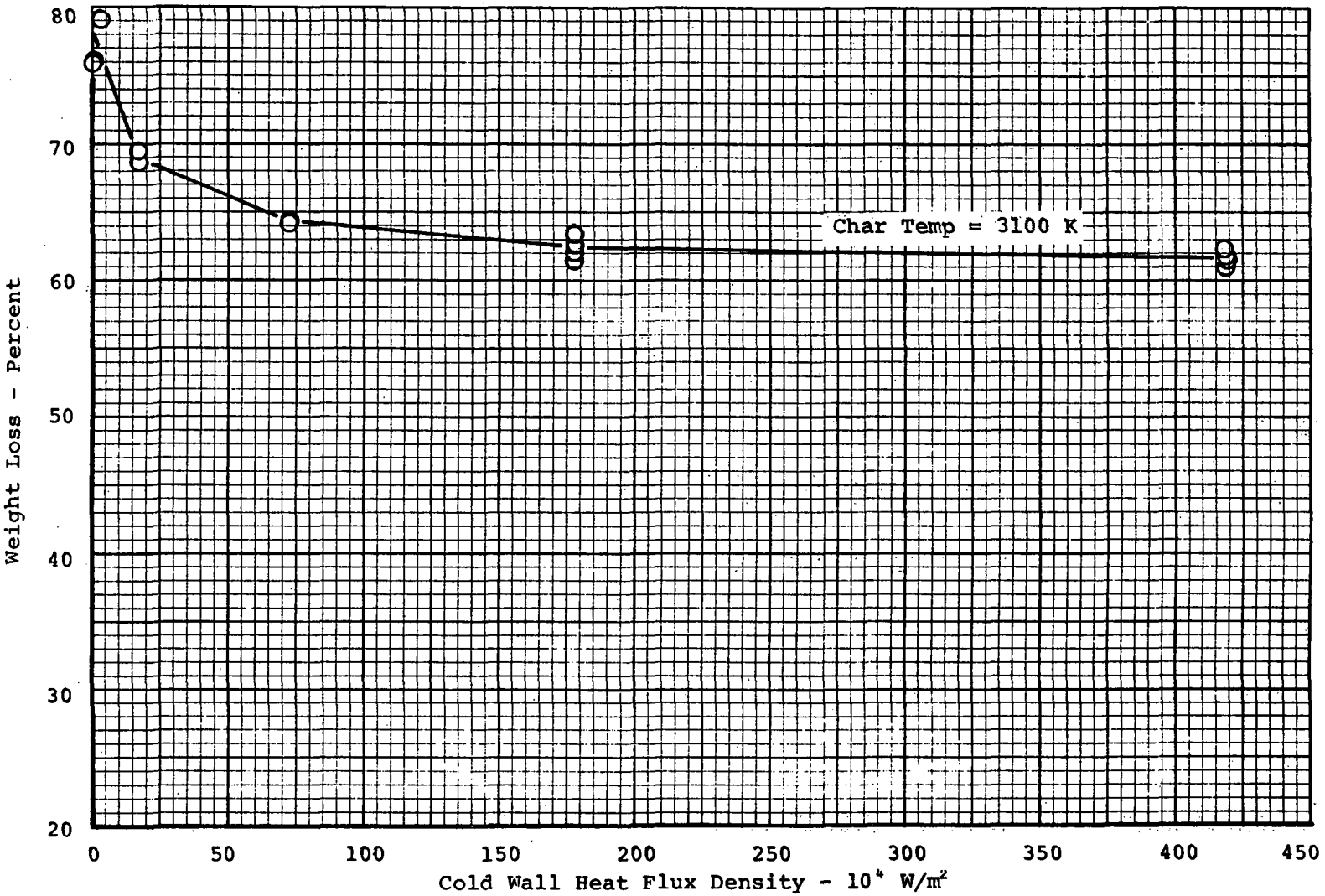

Figure 57. Effect of heat flux on weight loss for chars prepared in the laboratory to 3100 K from low-density phenolic-nylon

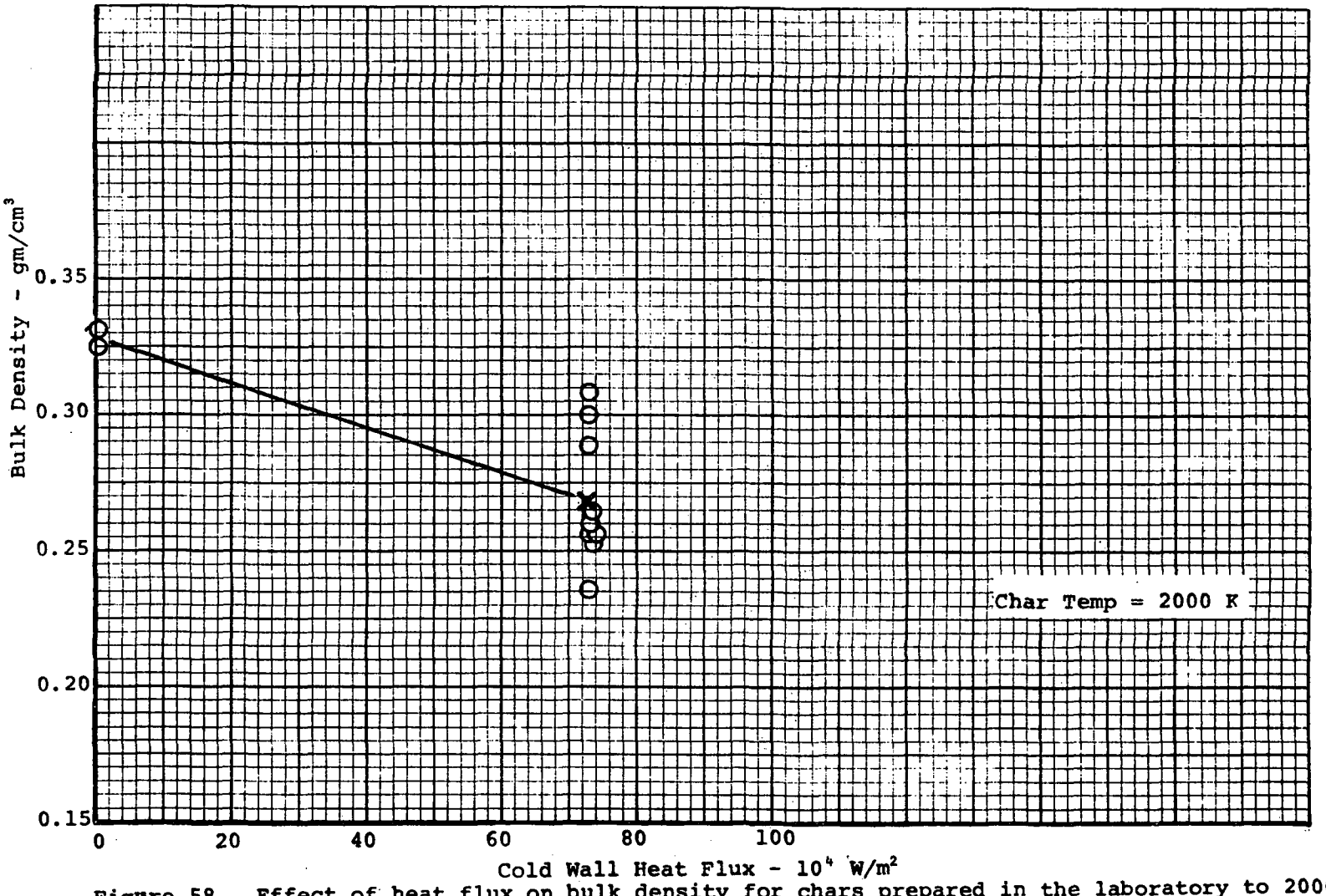

Figure 58. Effect of heat flux on bulk density for chars prepared in the laboratory to 2000 K from low-density phenolic-nylon

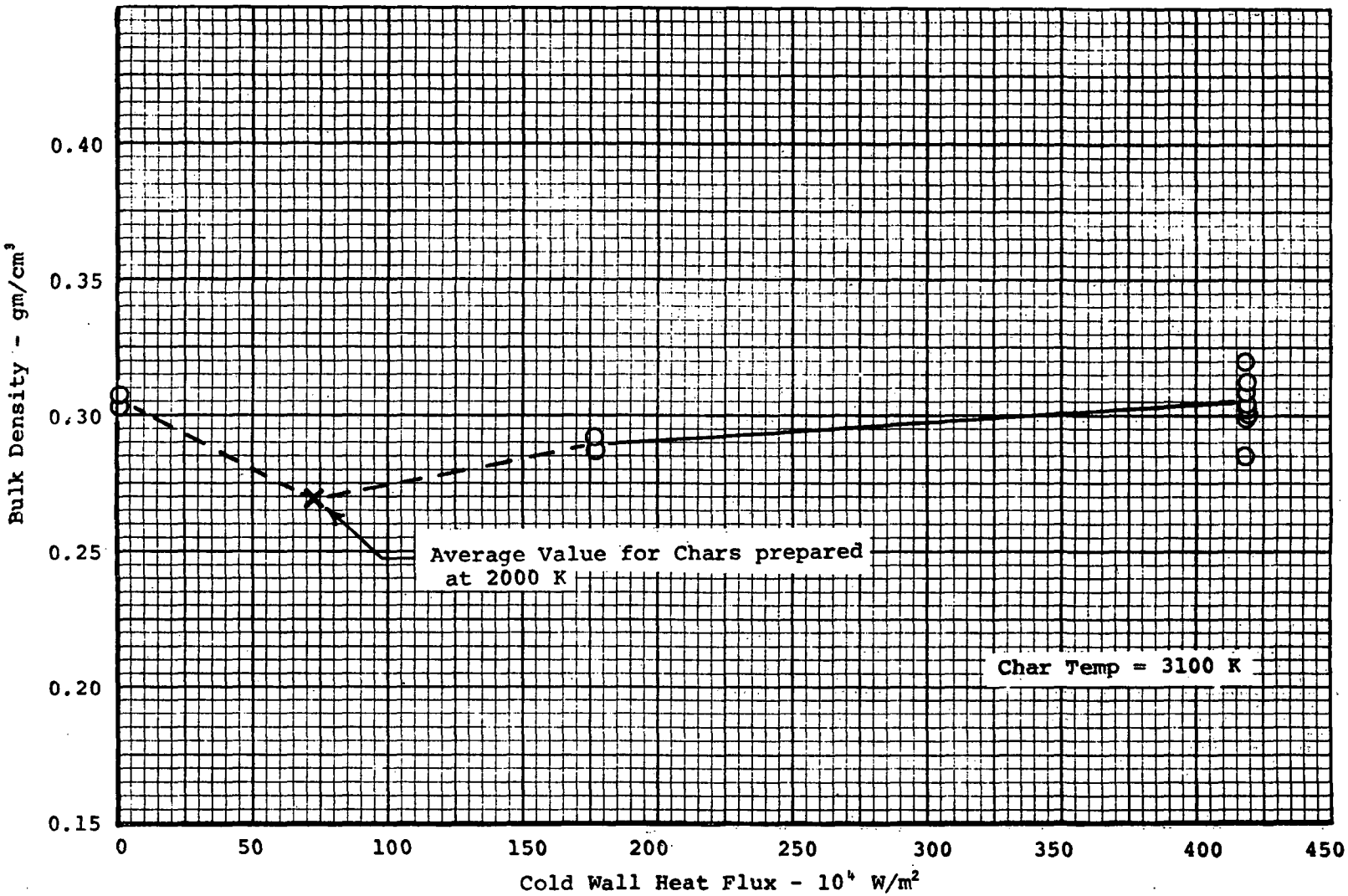

Figure 59. Effect of heat flux on bulk density for chars prepared in the laboratory to 3100 K from low-density phenolic-nylon

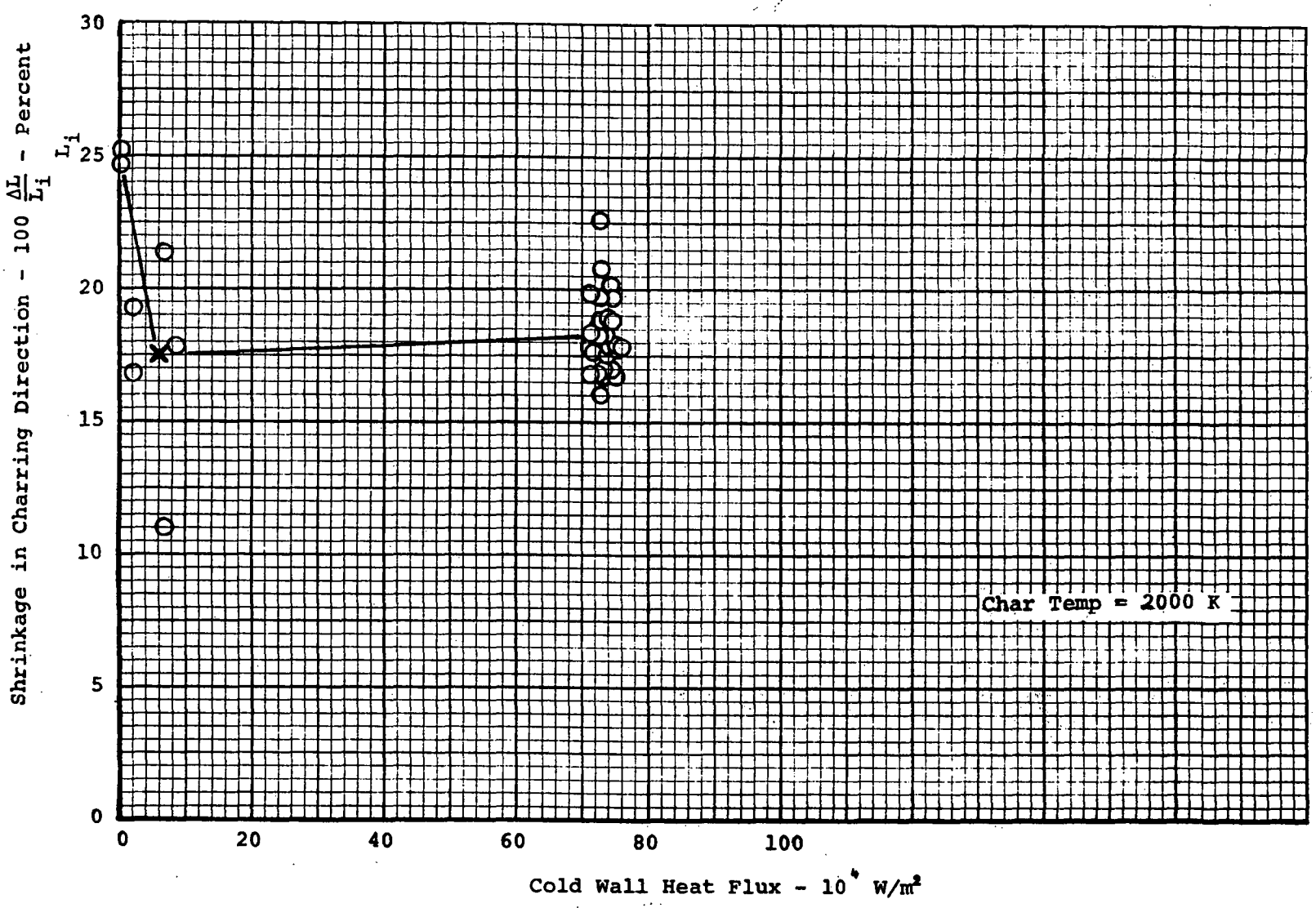

Figure 60. Effect of heat flux on shrinkage in the charring direction for chars prepared in the laboratory to 2000 K from low-density phenolic-nylon

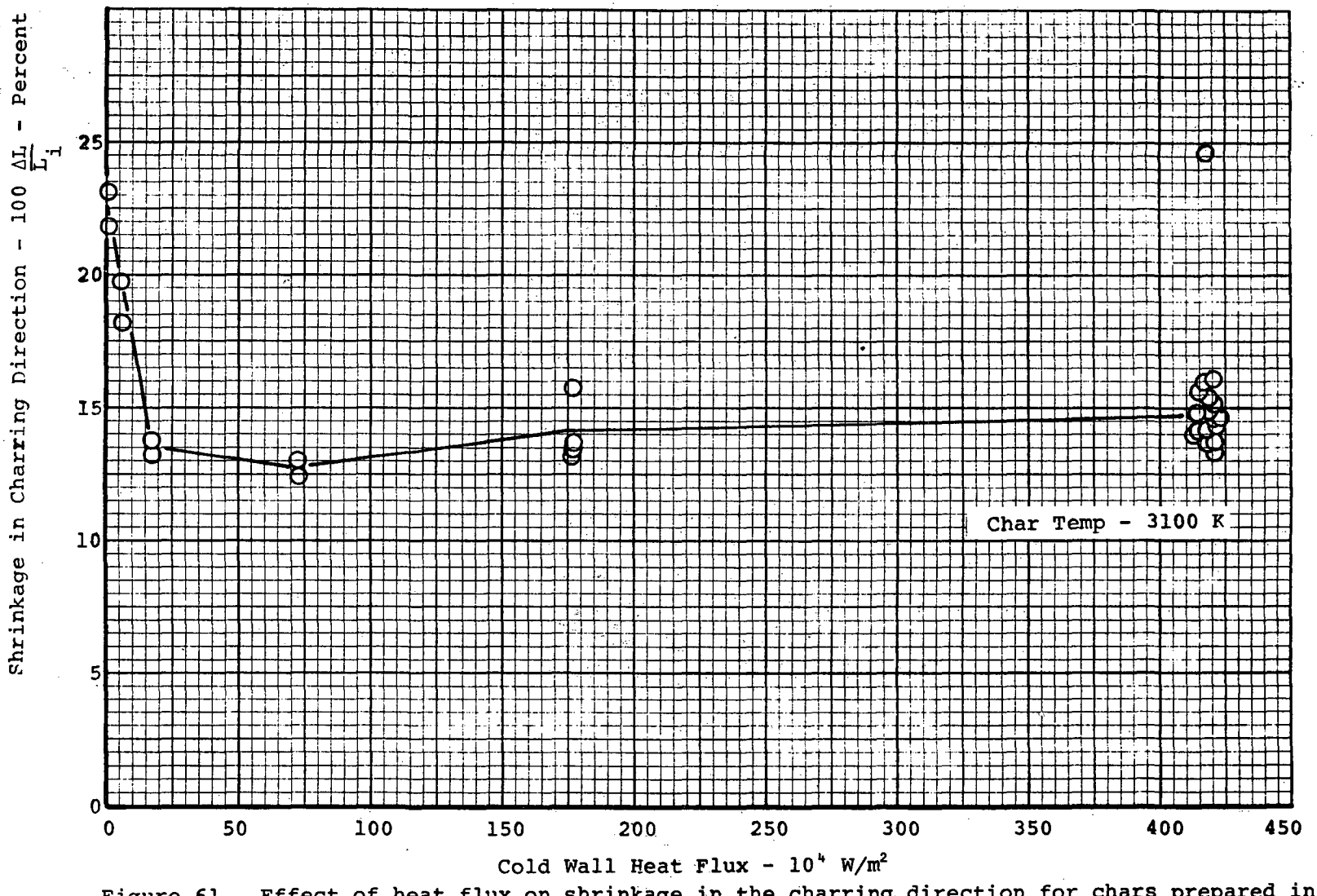

Figure 61. Effect of heat flux on shrinkage in the charring direction for chars prepared in the laboratory to 3100 K from low-density phenolic-nylon

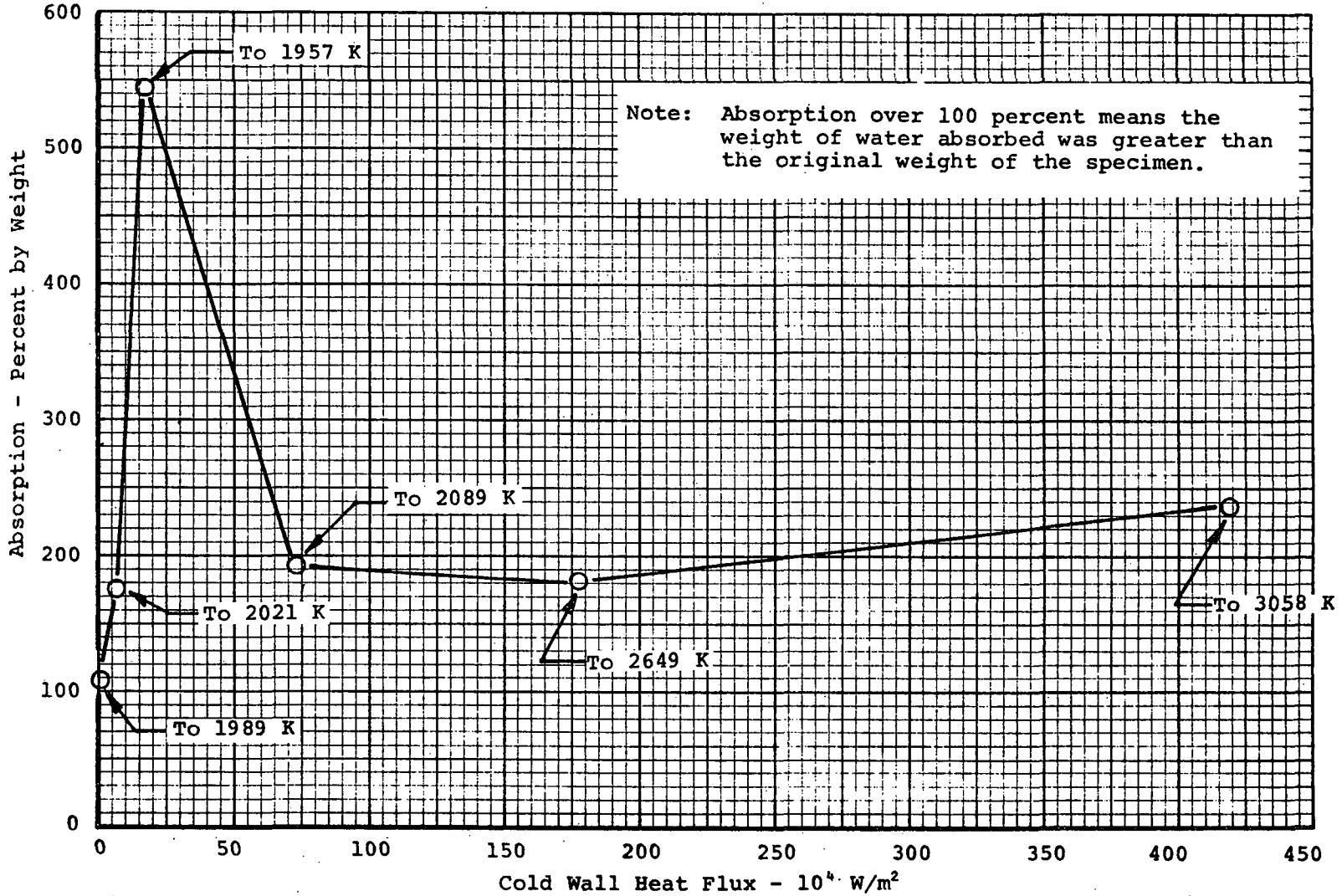

Figure 62. Effect of heat flux on liquid absorption for chars prepared in the laboratory to 2000 and 3000 K from low-density phenolic-nylon

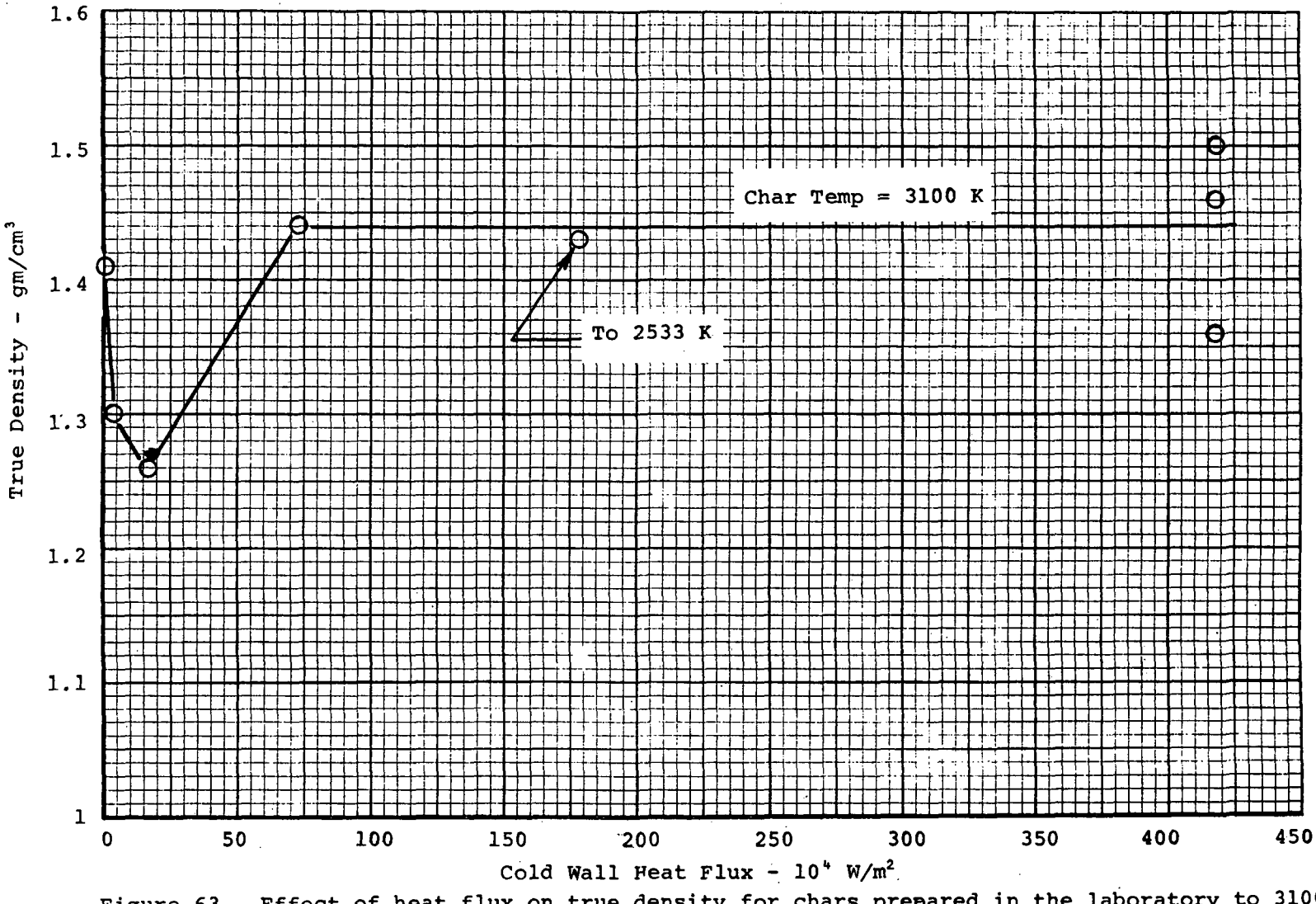

Figure 63. Effect of heat flux on true density for chars prepared in the laboratory to 3100 K from low-density phenolic-nylon

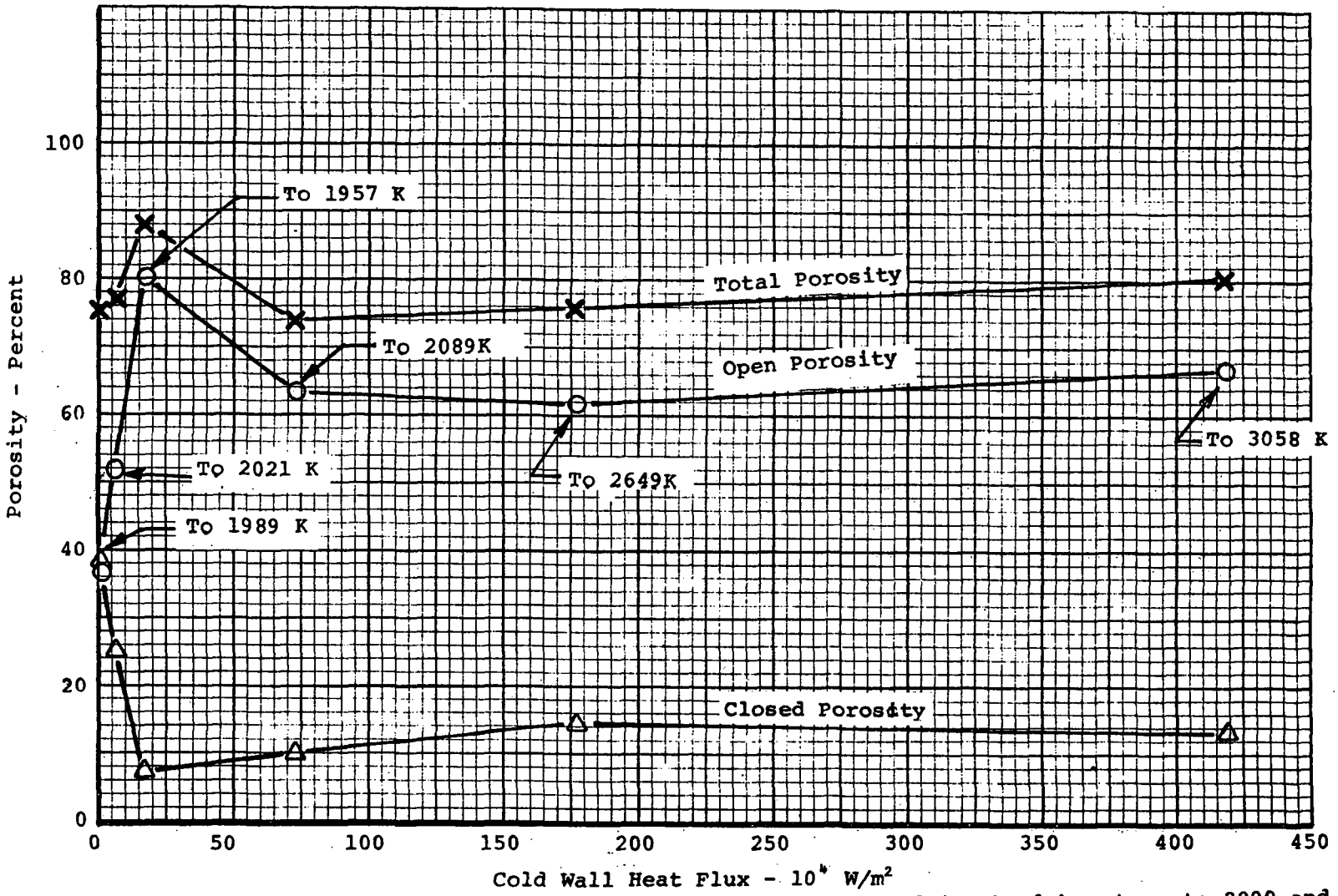

Figure 64. Effect of heat flux on porosity for chars prepared in the laboratory to 2000 and 3000K from low-density phenolic-nylon

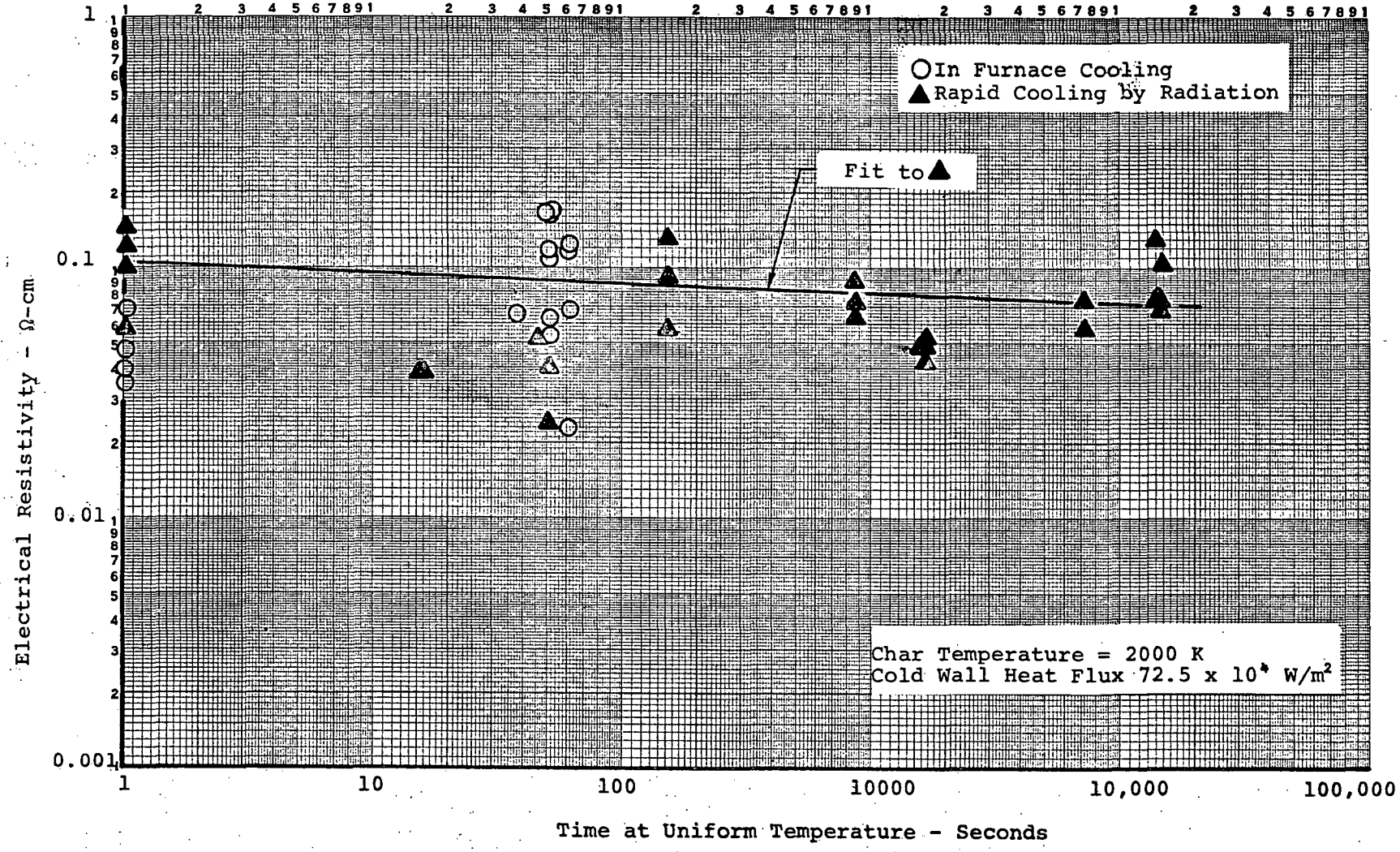

Figure 65. Effect of time-at-temperature on electrical resistivity for chars prepared in the laboratory to 2000 K from low-density phenolic-nylon

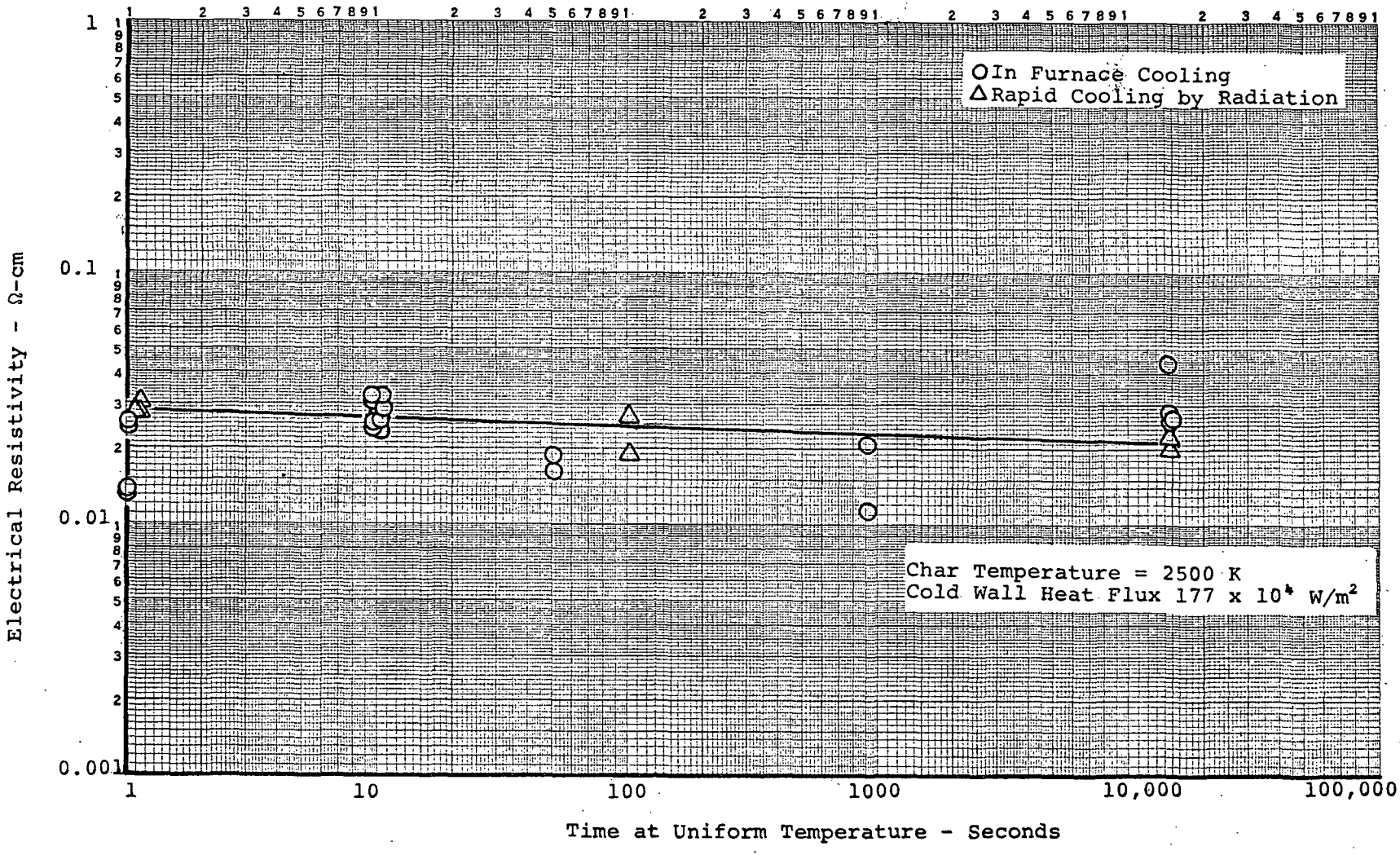

Figure 66. Effect of time-at-temperature on electrical resistivity for chars prepared in the laboratory to 2500 K from low-density phenolic-nylon

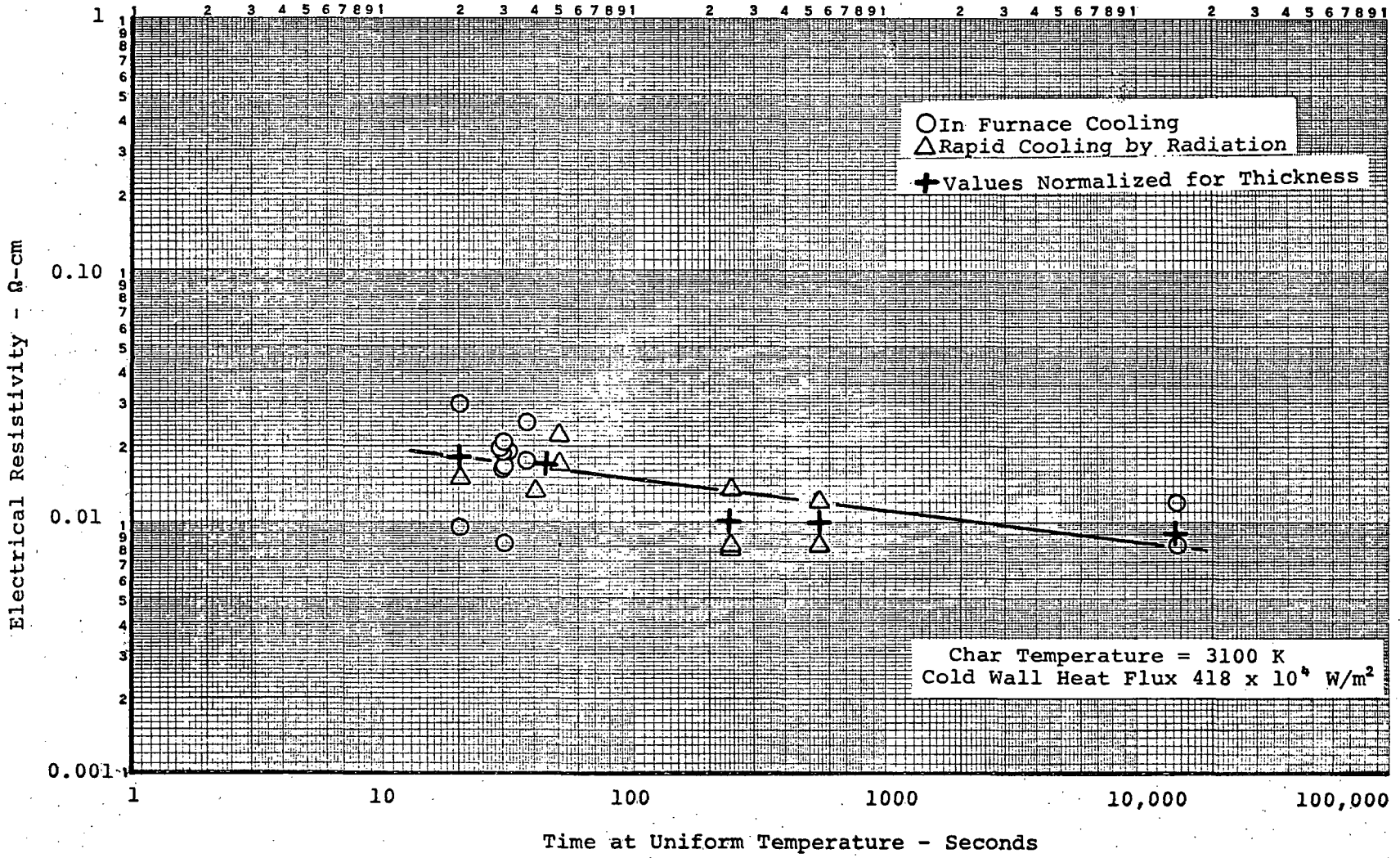

Figure 67. Log plot of effect of time-at-temperature on electrical resistivity for chars prepared in the laboratory to 3100 K from low-density phenolic-nylon

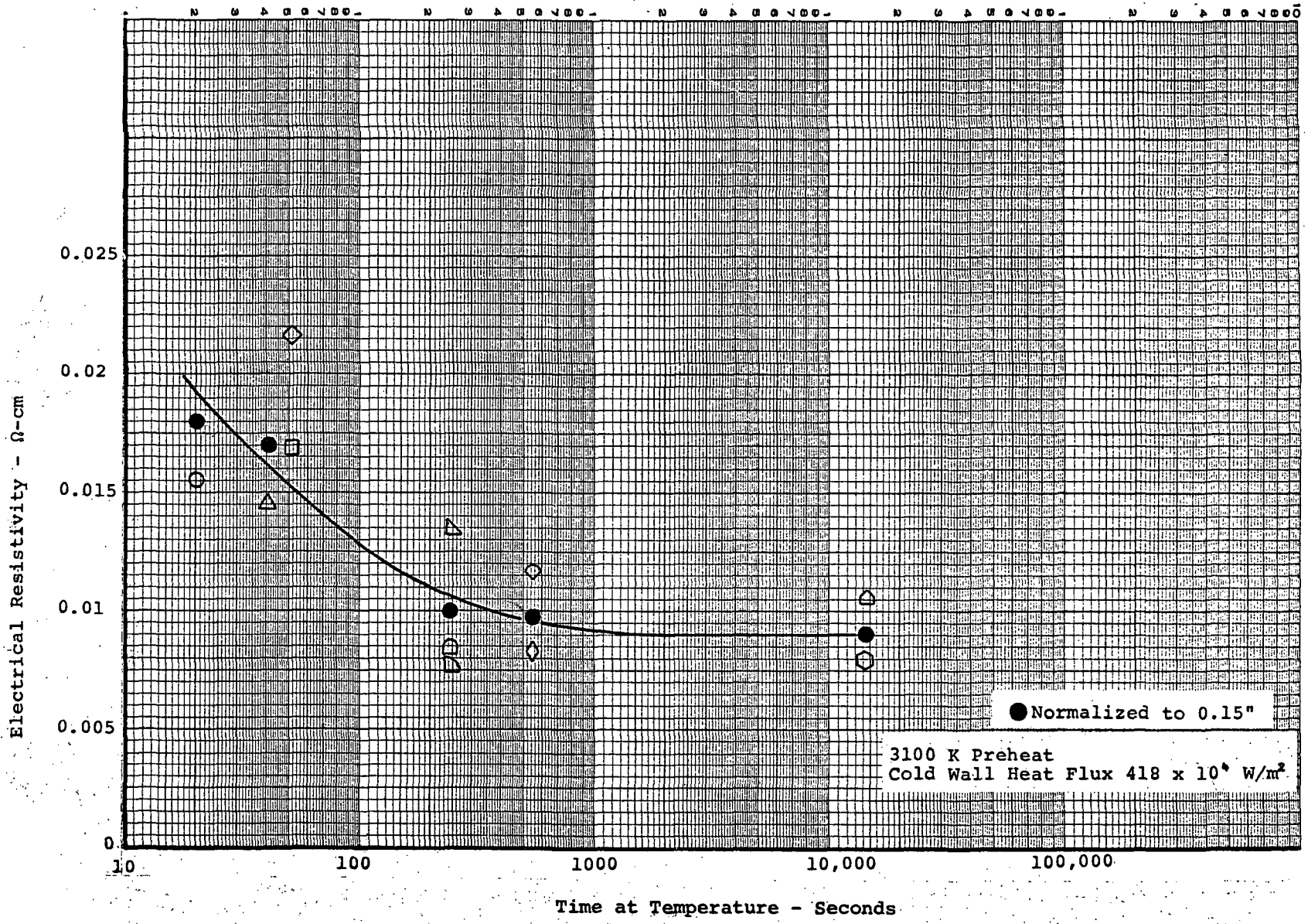

Figure 68. Semi log plot of effect of time-at-temperature on electrical resistivity of chars prepared in the laboratory to 3100 K from low-density phenolic-nylon

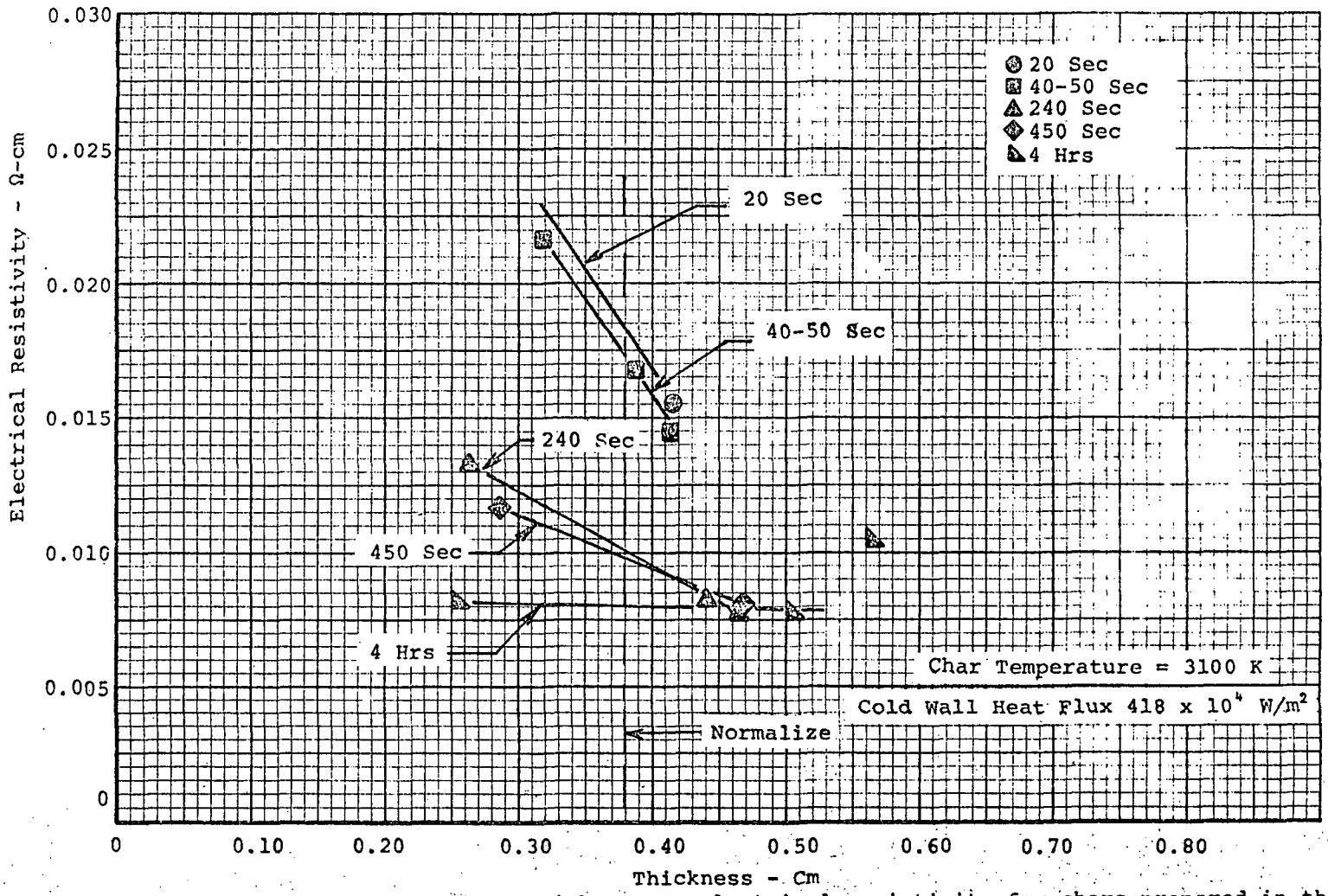

Figure 69. Effect of specimen thickness on electrical resistivity for chars prepared in the laboratory to 3100 K from low-density phenolic-nylon

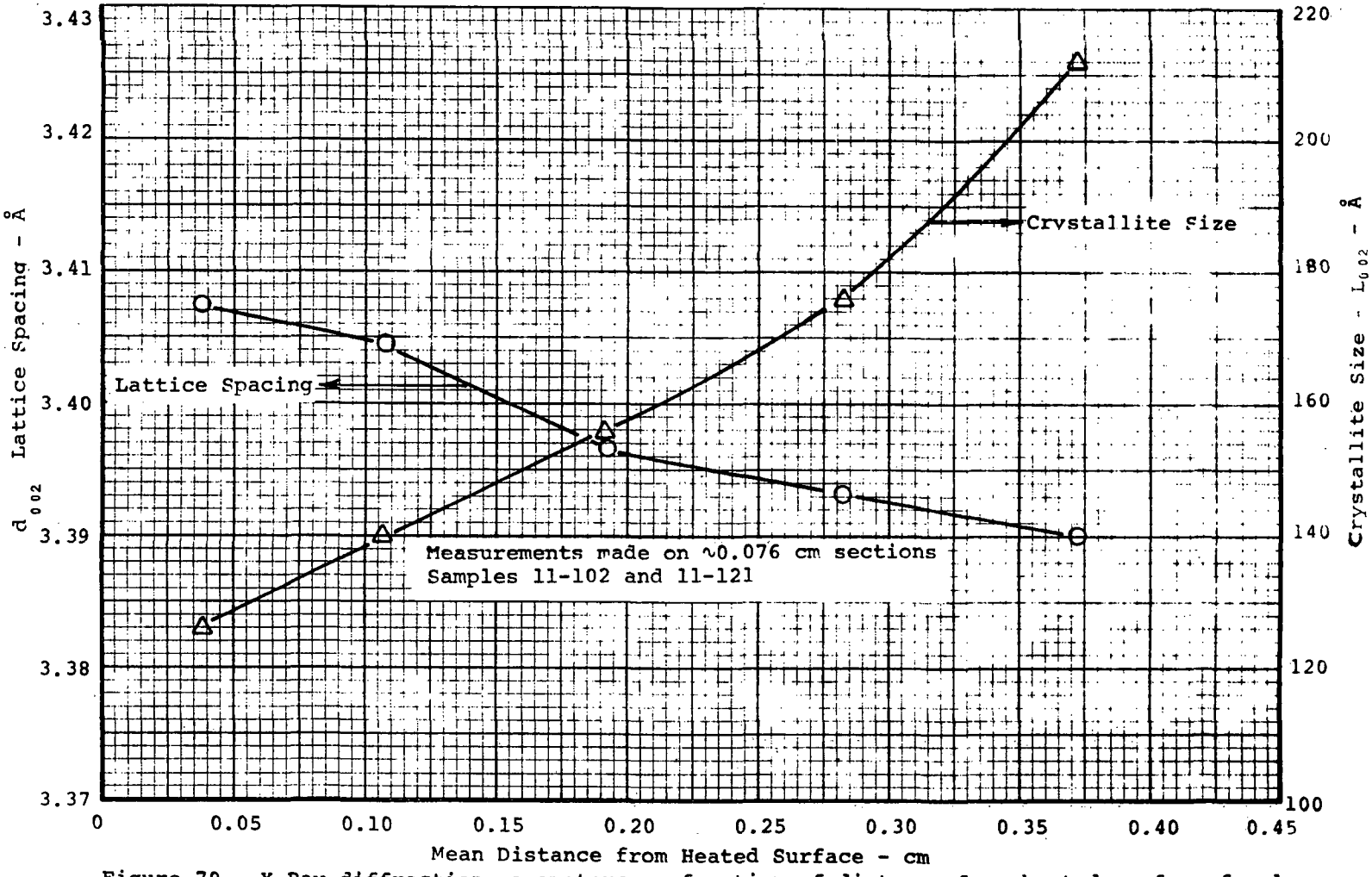

Figure 70. X-Ray diffraction parameters as function of distance from heated surface for low-density phenolic-nylon prepared in the laboratory at 418 x 10^4 W/m^2 cold wall heat flux (61 K/sec rise rate) to 3100 K

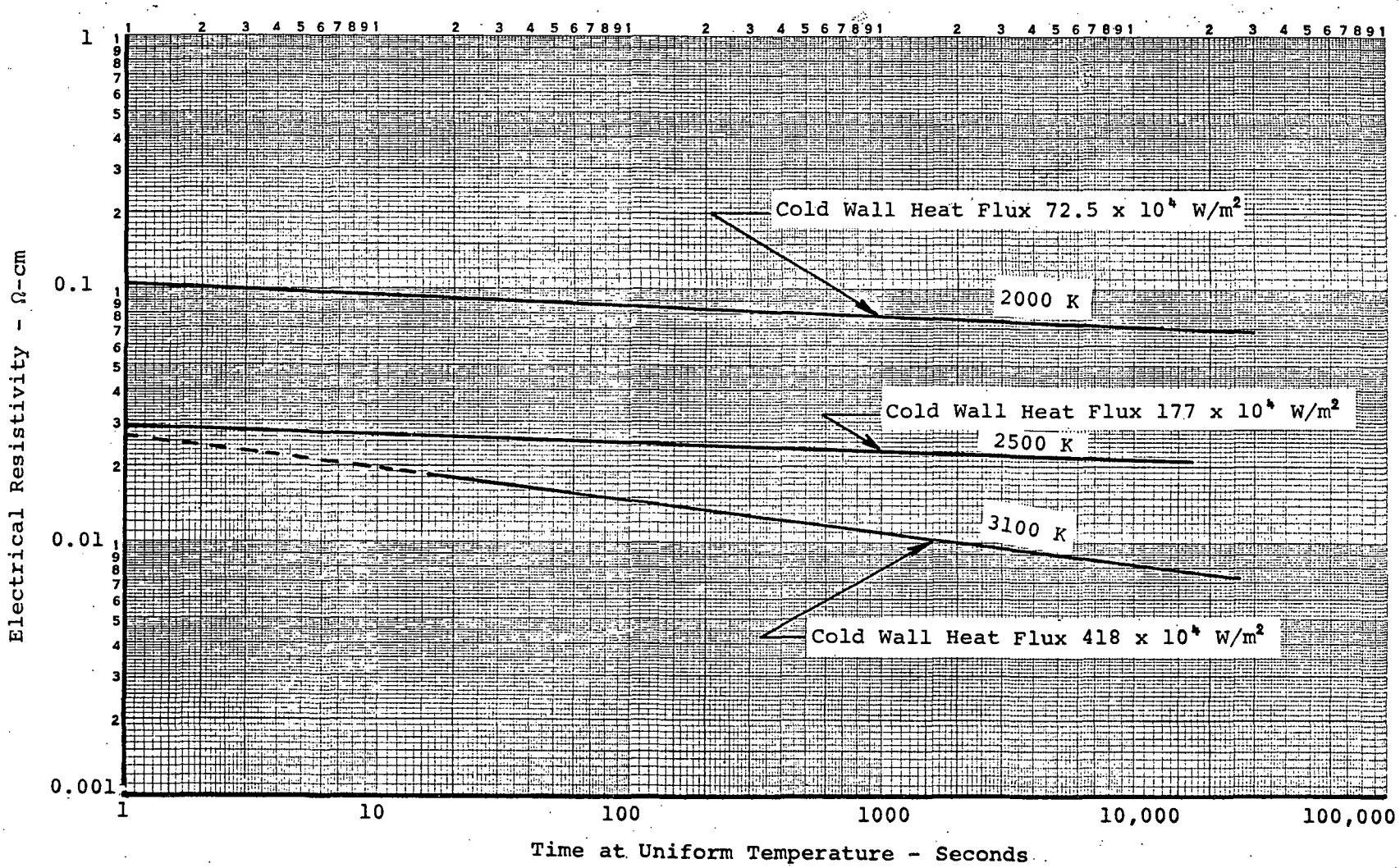

Figure 71. Composite plot of effects of time-at-temperature on electrical resistivity for chars prepared in the laboratory to 2000, 2500 and 3100 K from low-density phenolic-nylon

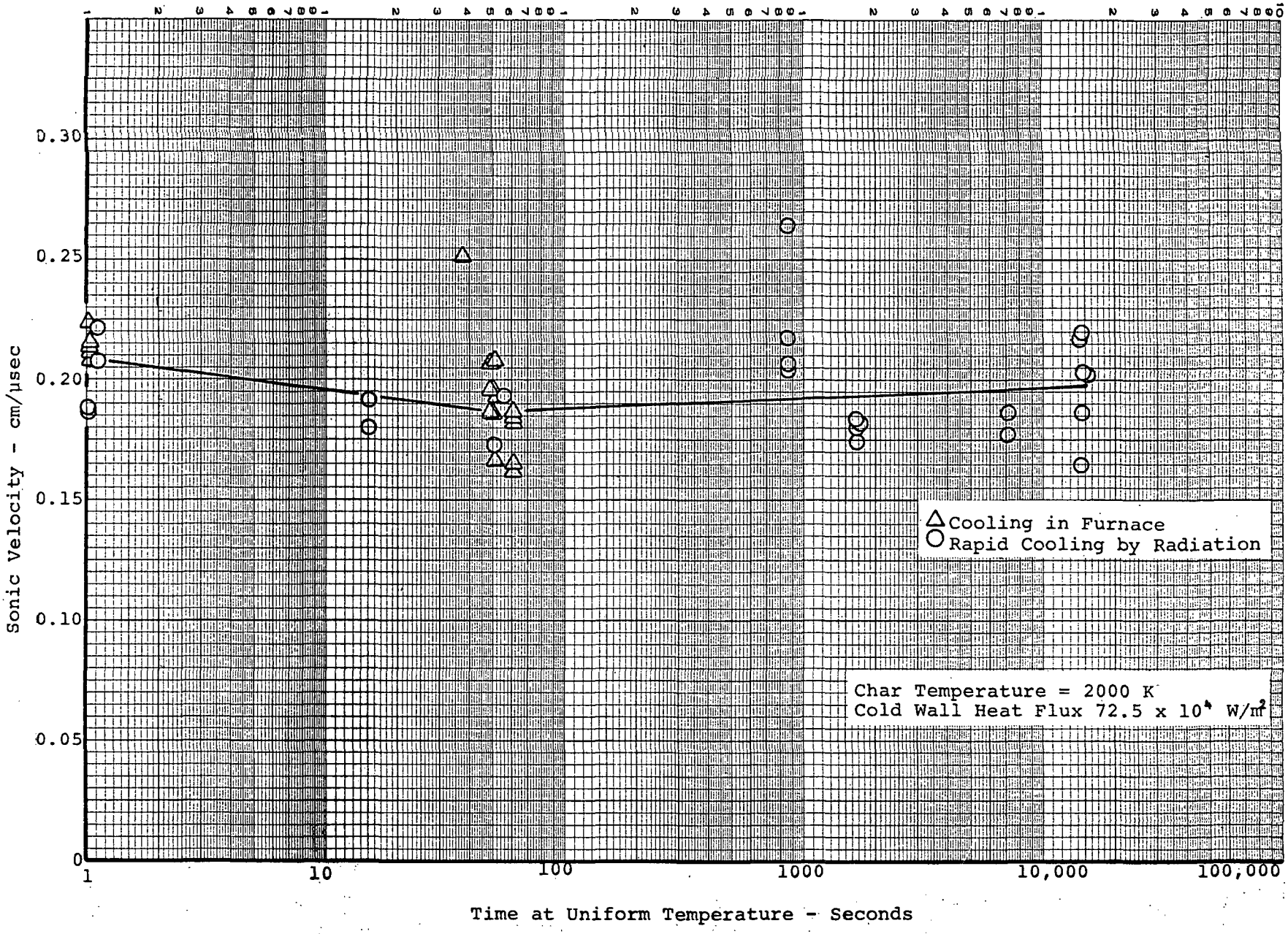

Figure 72. **Effect of time-at-temperature on sonic velocity for chars prepared in the laboratory to 2000 K from low-density phenolic-nylon**

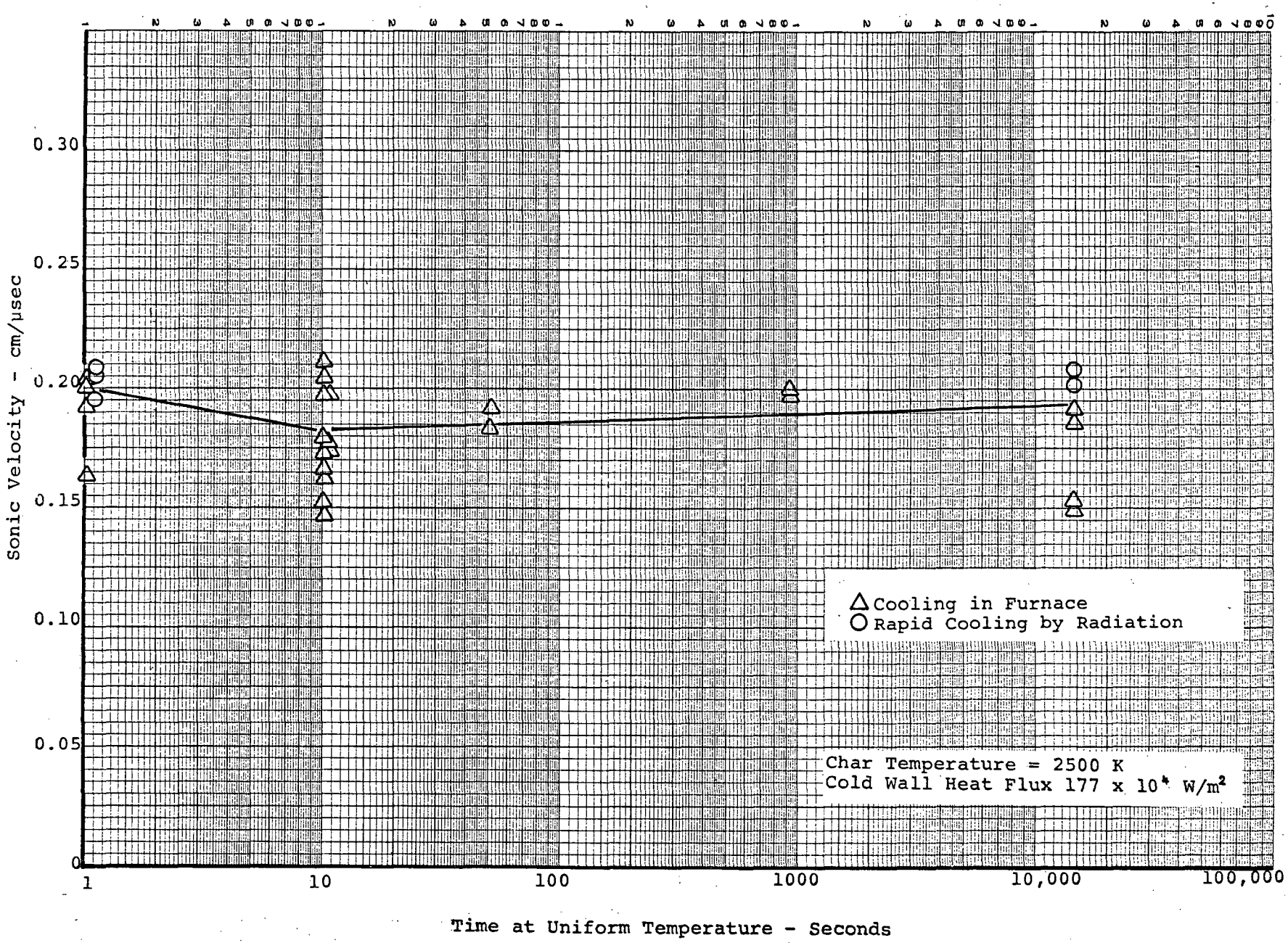

Figure 73. Effect of time-at-temperature on sonic velocity for chars prepared in the laboratory to 2500 K from low-density phenolic-nylon

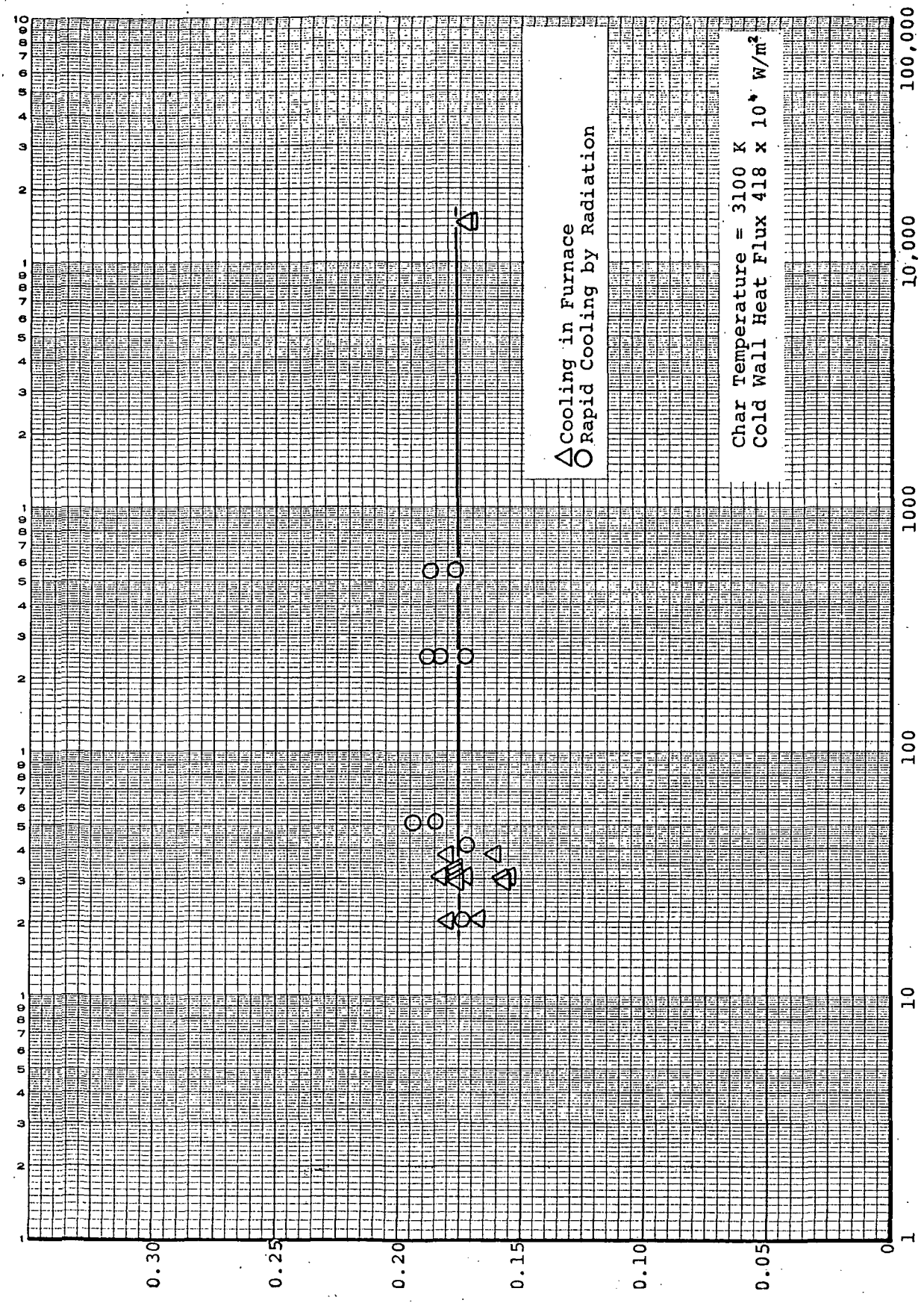

Figure 74. Effect of time-at-temperature on sonic velocity for chars prepared in the laboratory to 3100 K from low-density phenolic-nylon

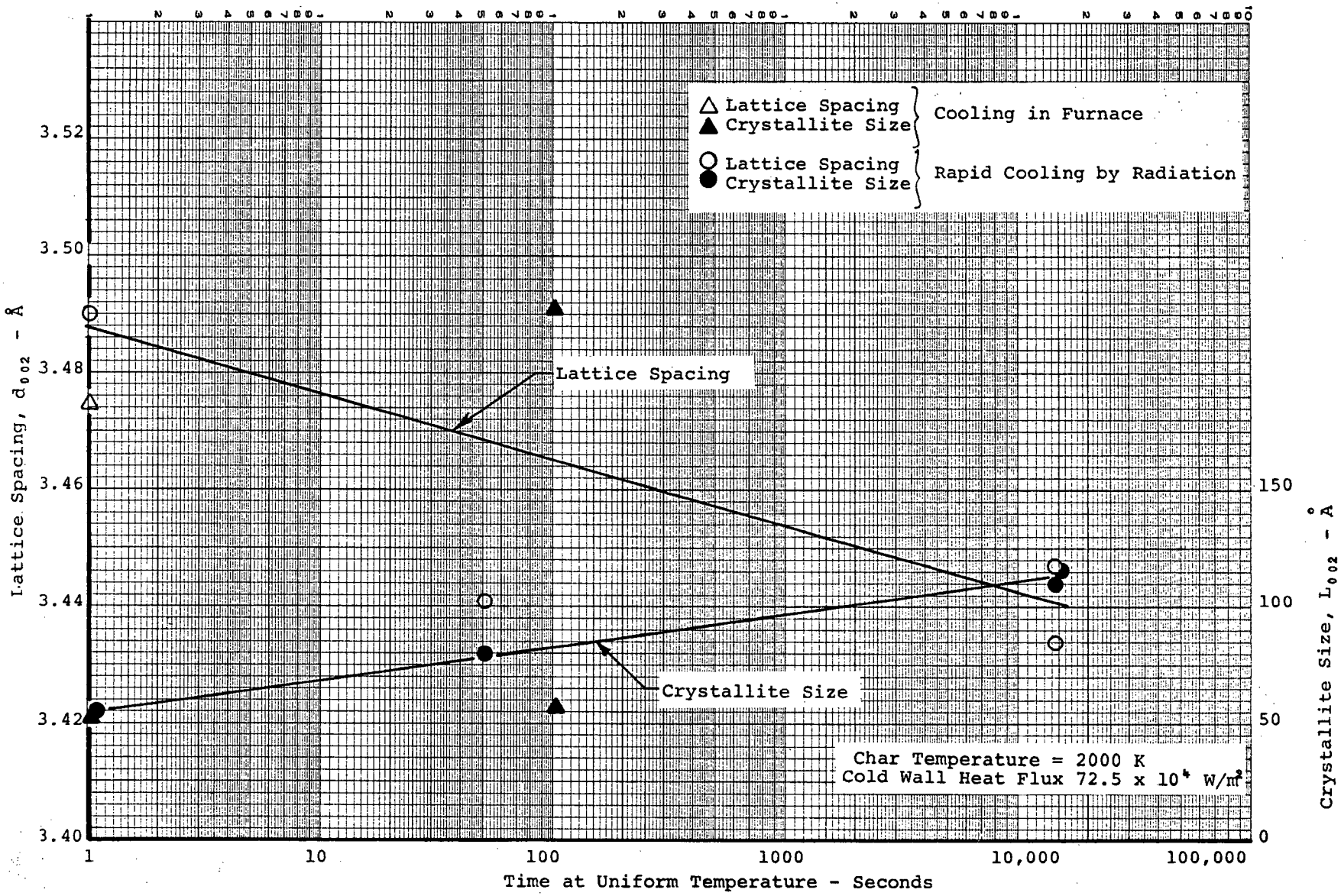

Figure 75. Effect of time-at-temperature on lattice spacing and crystallite size for chars prepared in the laboratory to 2000 K from low-density phenolic-nylon

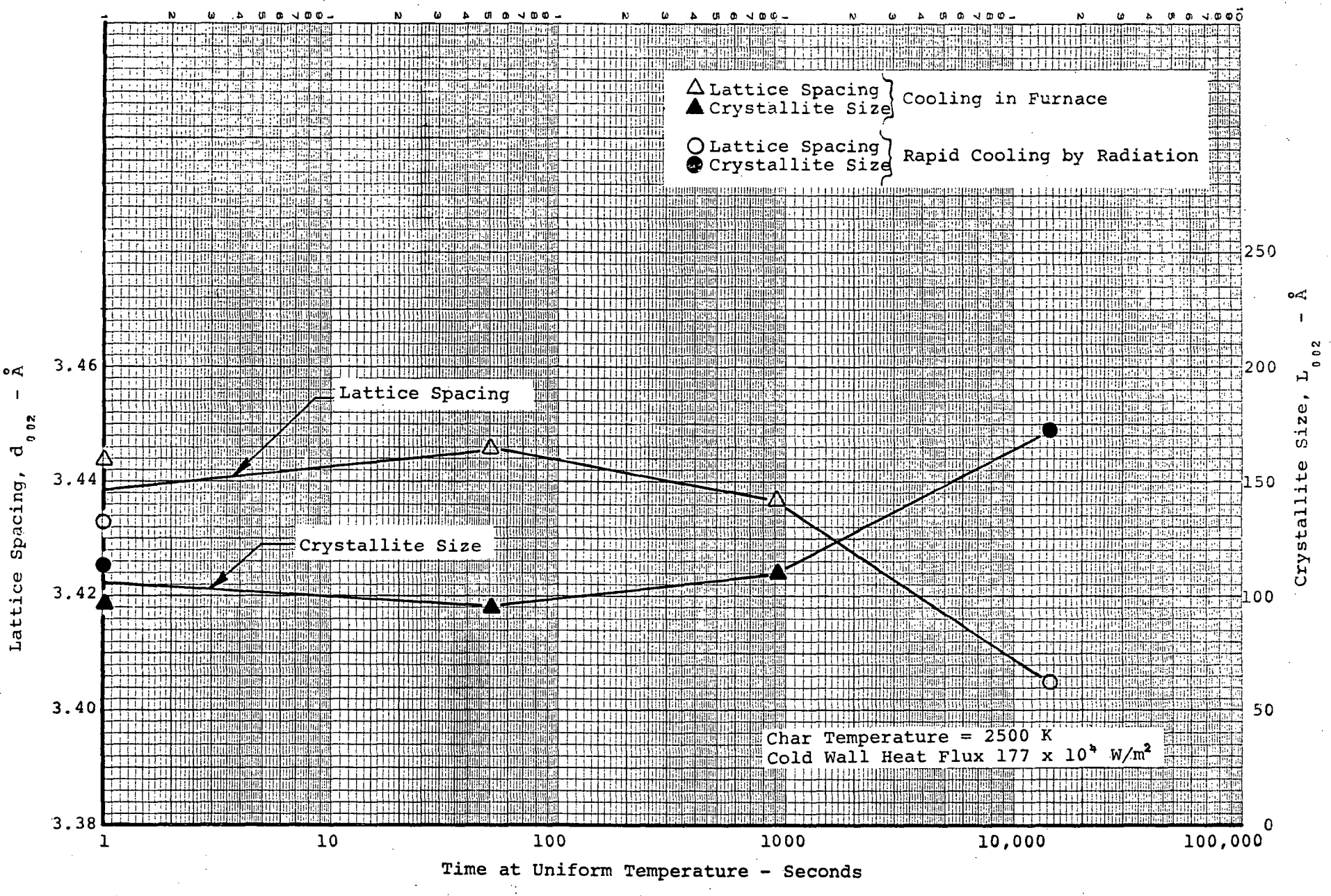

Figure 76. Effect of time-at-temperature on lattice spacing and crystallite size for chars prepared in the laboratory to 2500 K from low-density phenolic-nylon

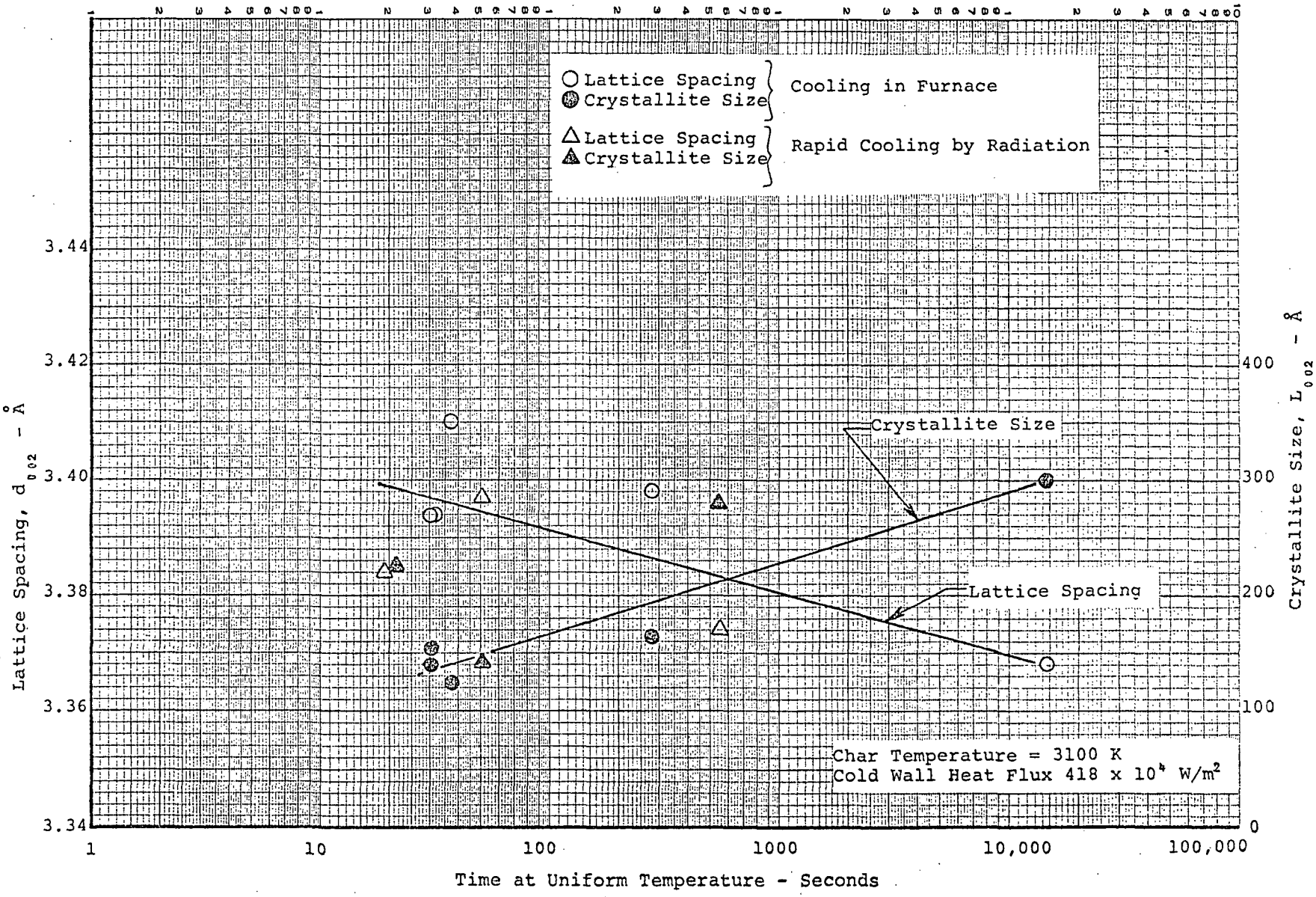

Figure 77. Effect of time-at-temperature on lattice spacing and crystallite size for chars prepared in the laboratory to 3100 K from low-density phenolic-nylon

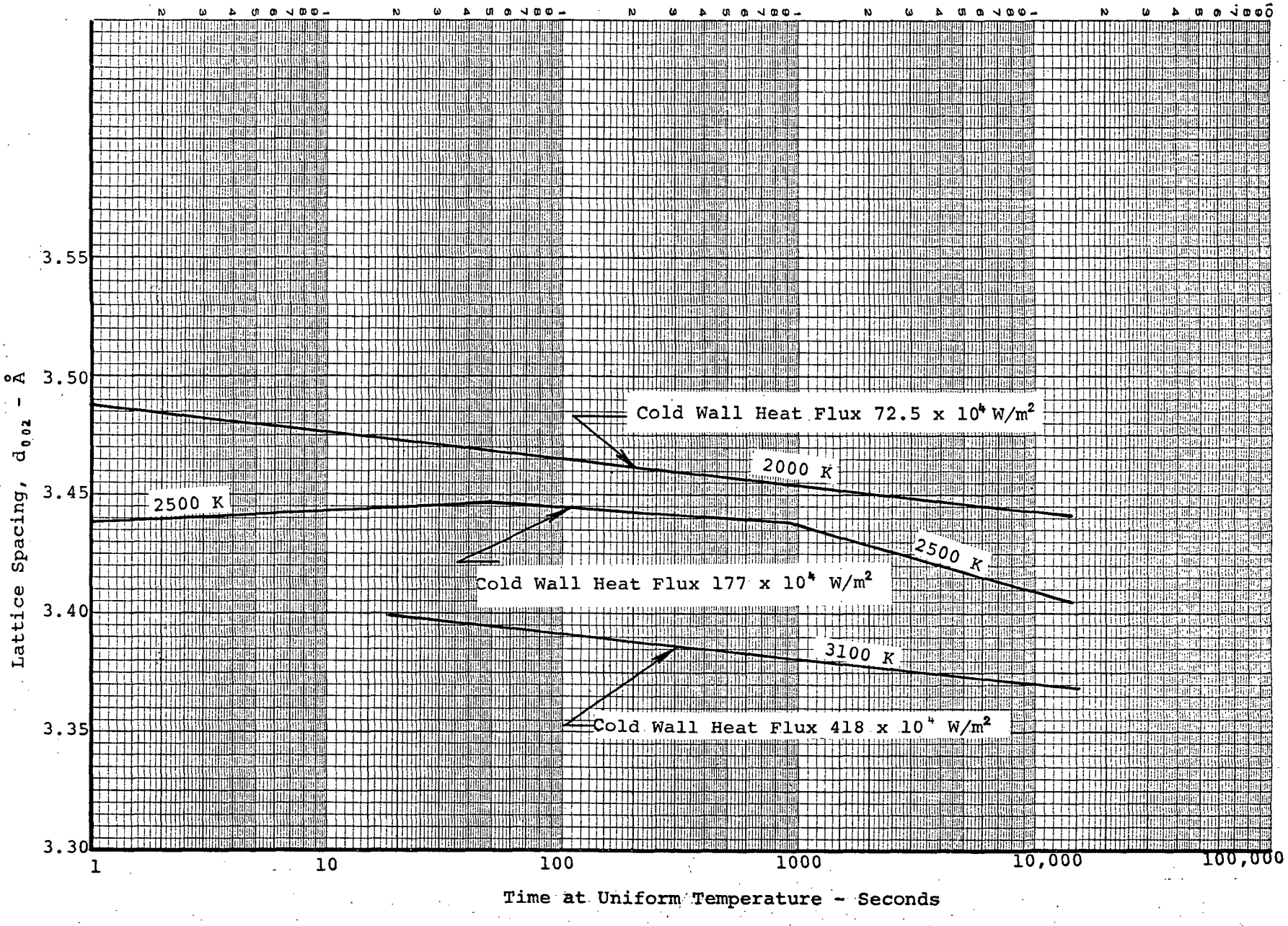

Figure 78. Composite plot of effect of time-at-temperature on lattice spacing for chars prepared in the laboratory to 2000, 2500 and 3100 K from low-density phenolic-nylon

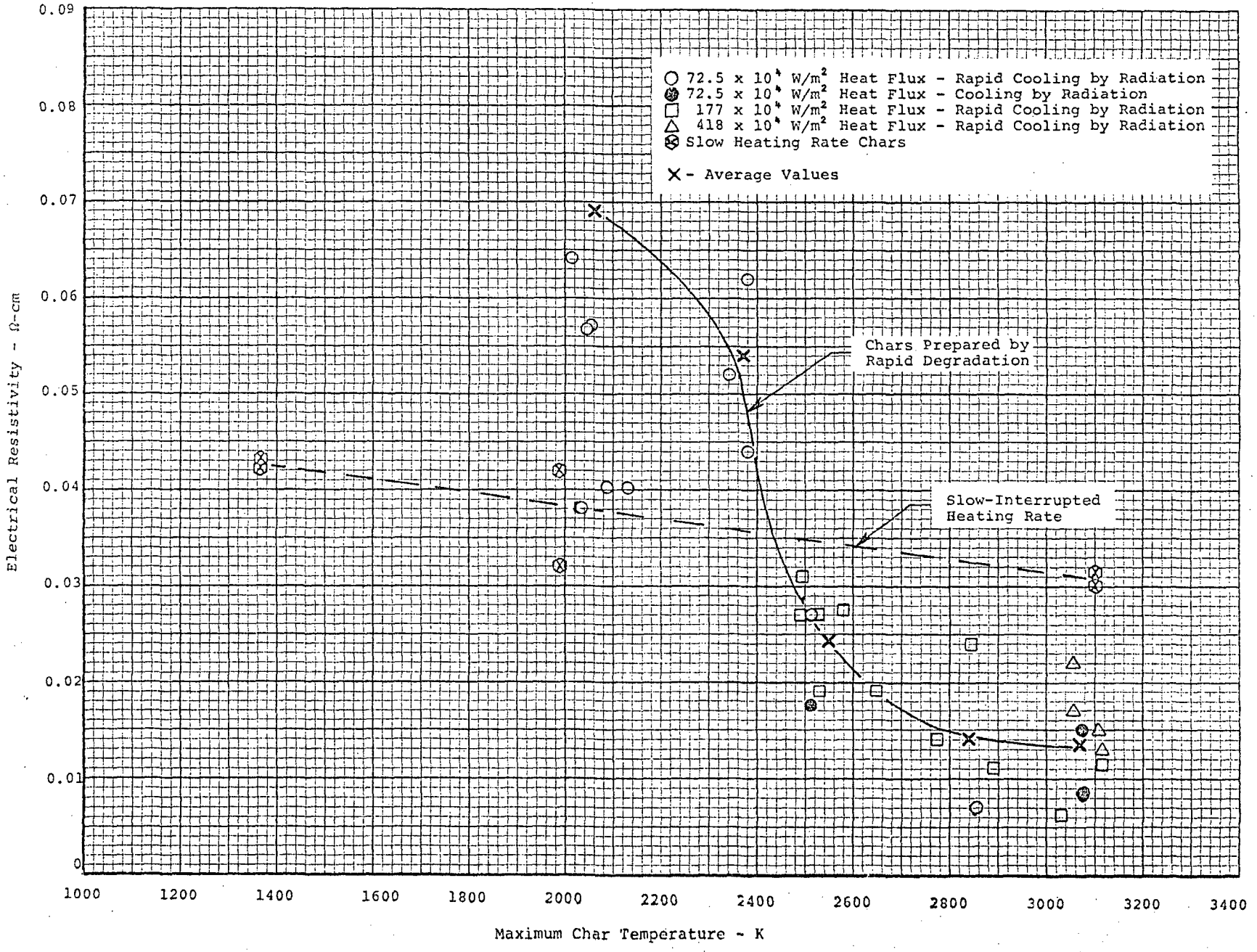

Figure 79. Effect of maximum char temperature on electrical resistivity for char prepared in the laboratory from low-density phenolic-nylon

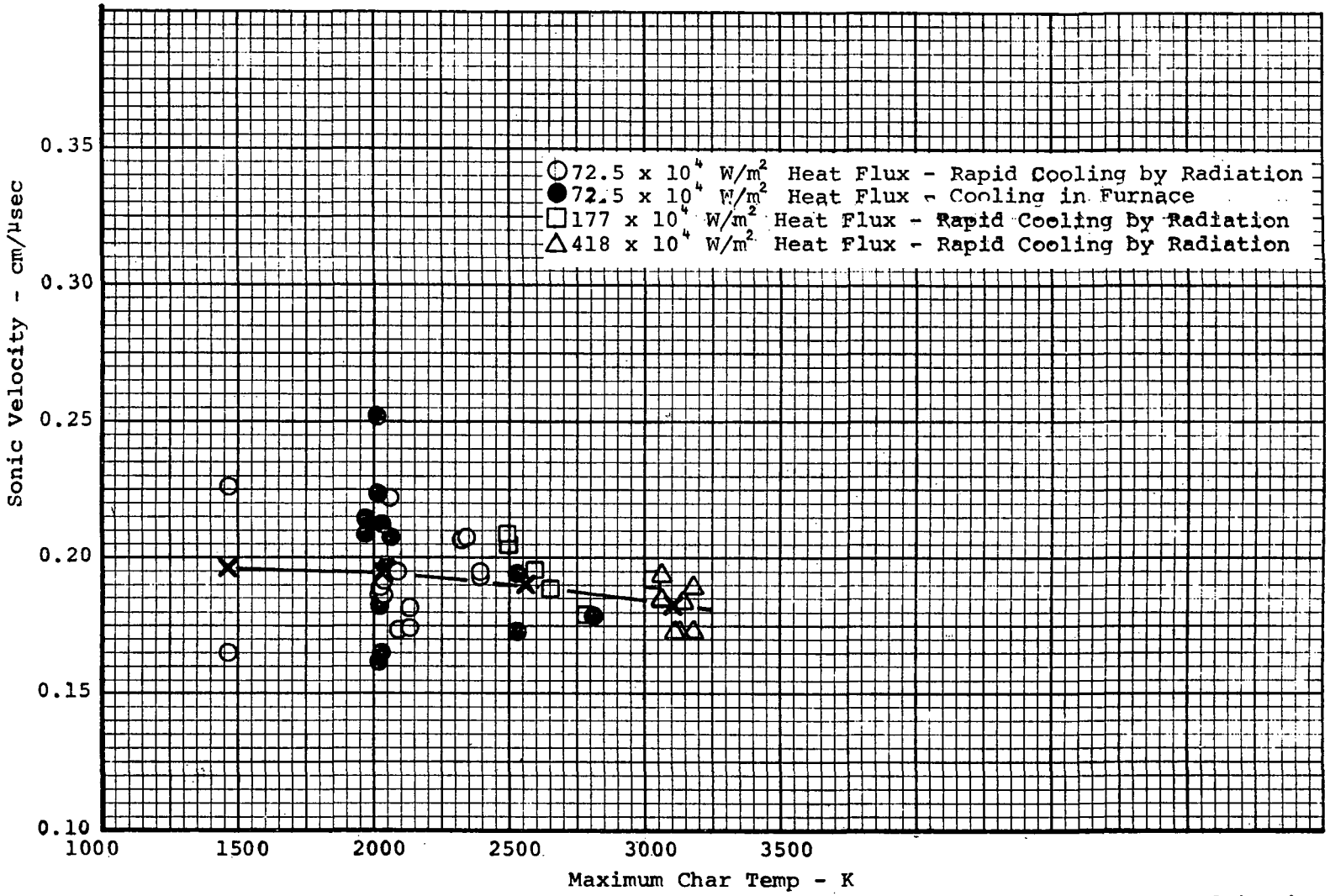

Figure 80. Effect of maximum char temperature on sonic velocity for char prepared in the laboratory from low-density phenolic-nylon

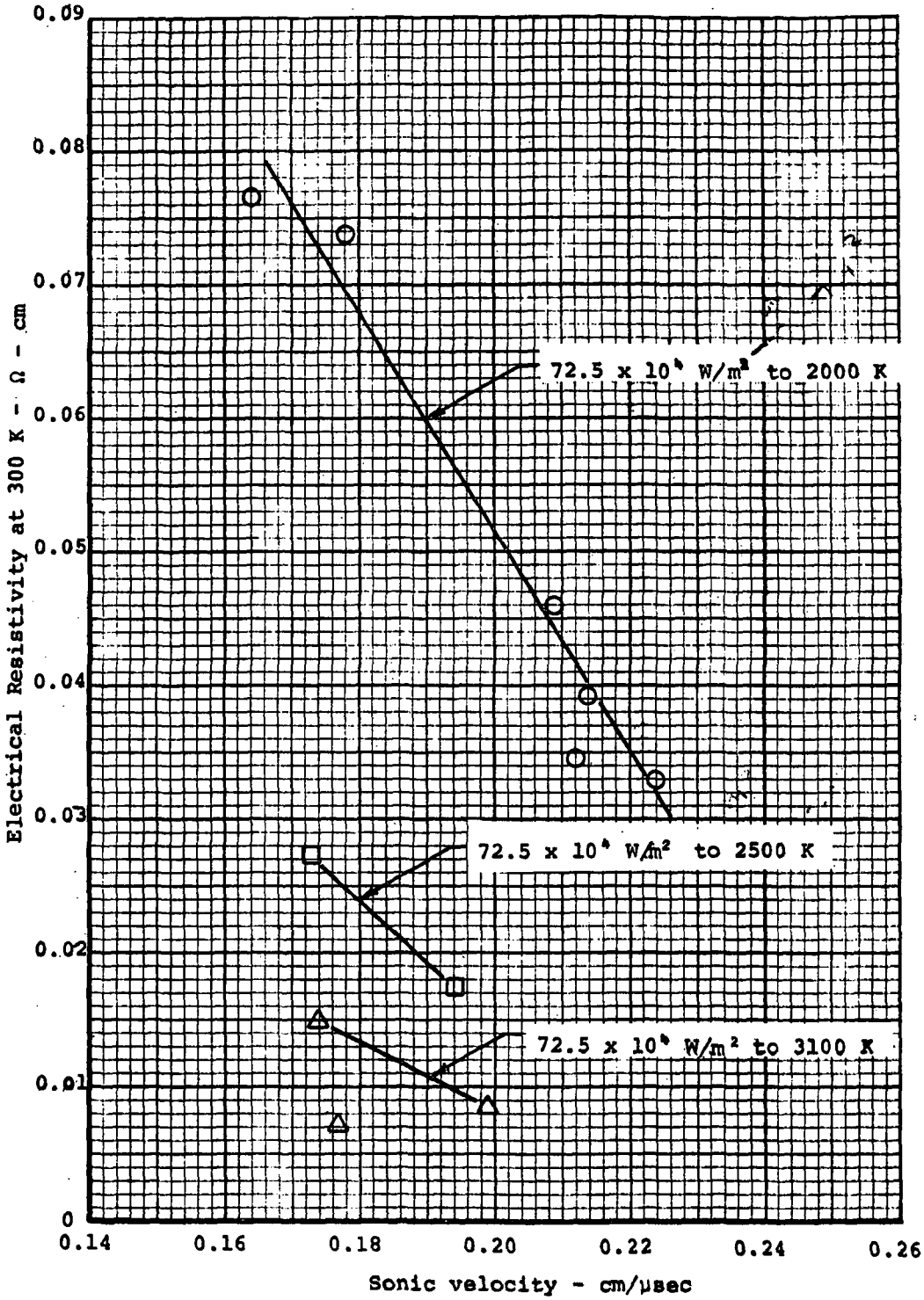

Figure 81. Electrical resistivity versus sonic velocity for charring of low-density phenolic-nylon at 72.5 x 10^4 W/m^2 cold wall heat flux

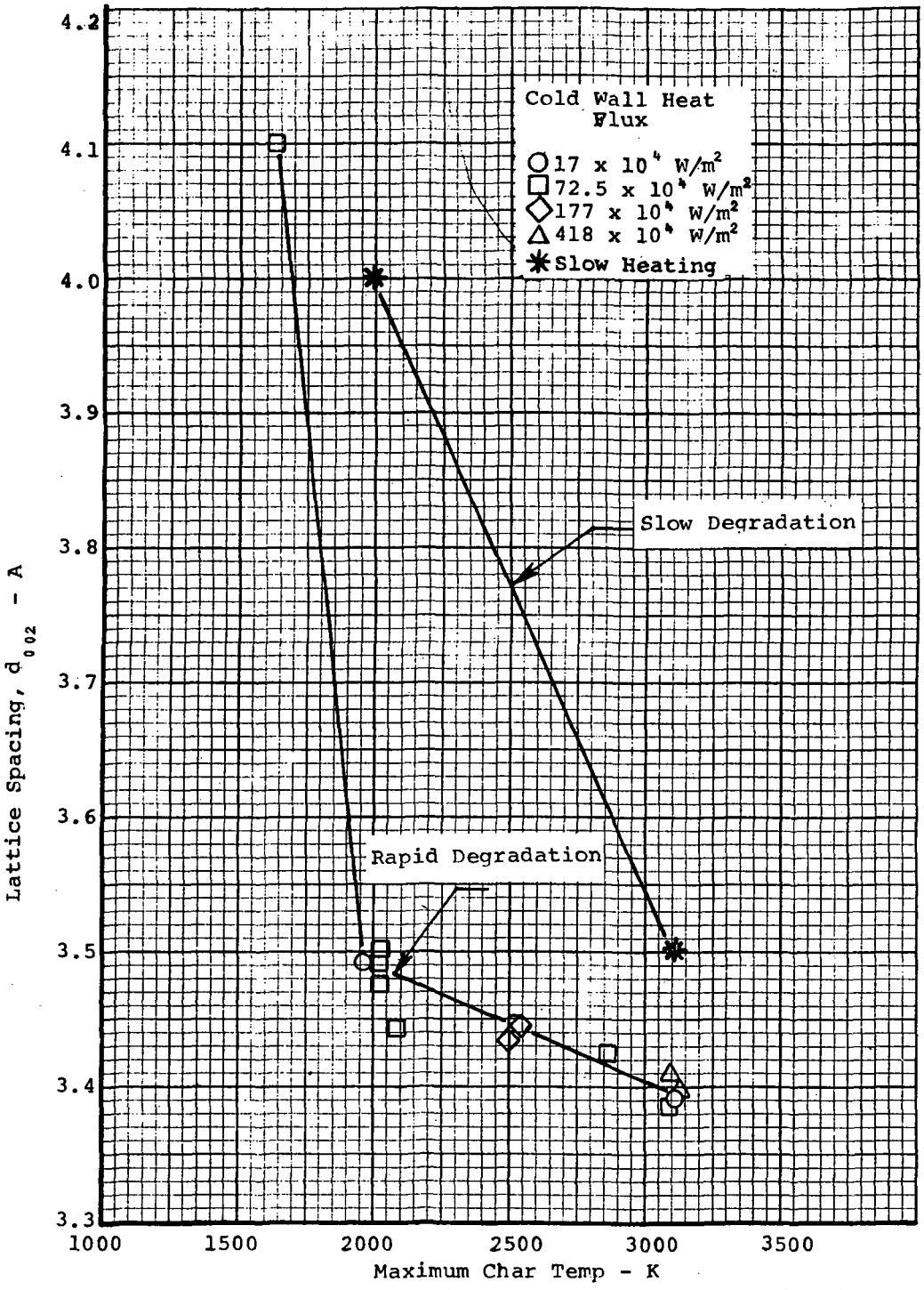

Figure 82. Effect of maximum char temperature on lattice spacing for char prepared in the laboratory from low-density phenolic nylon

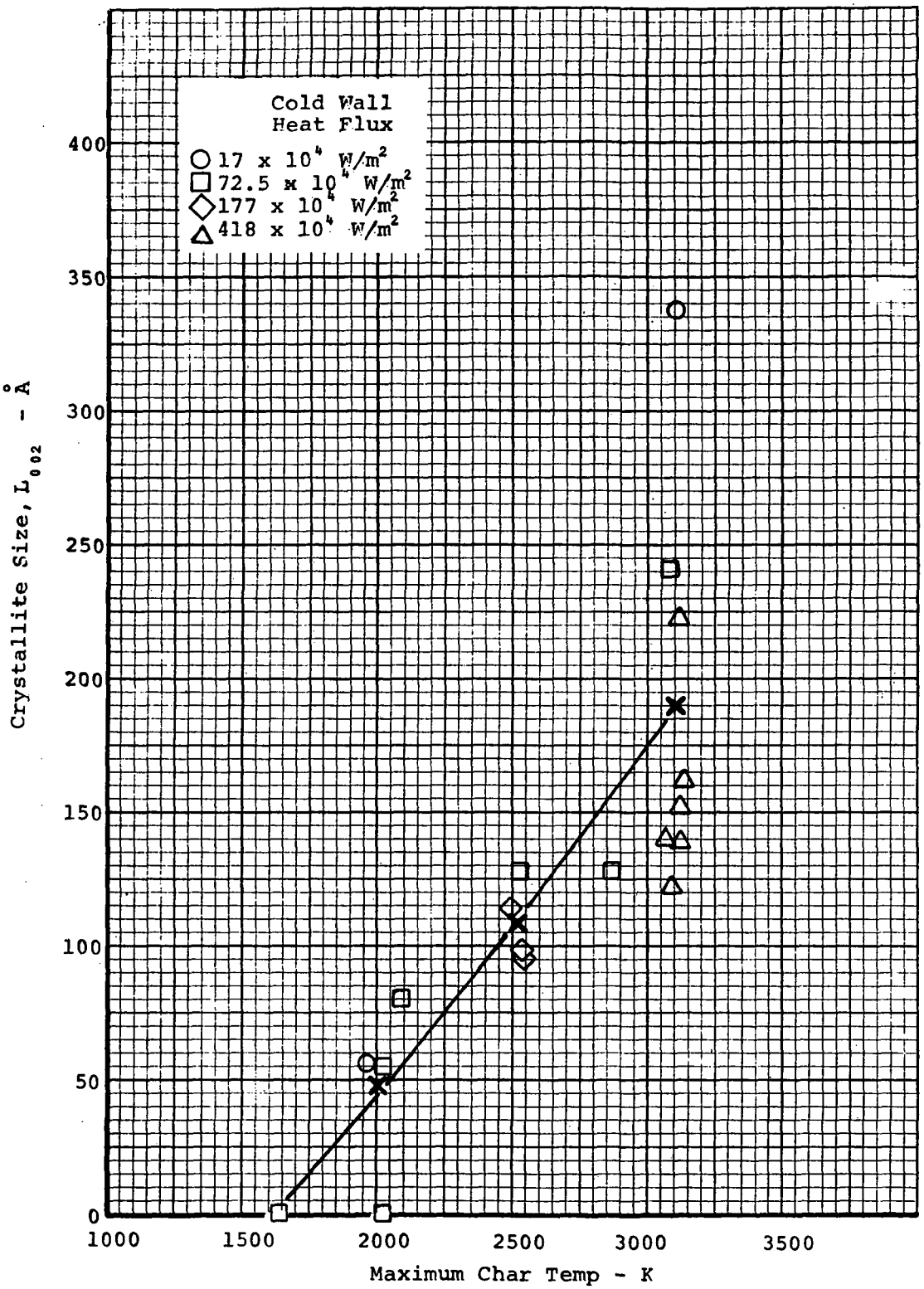

Figure 83. Effect of maximum char temperature on crystallite size for char prepared in the laboratory from low-density phenolic-nylon

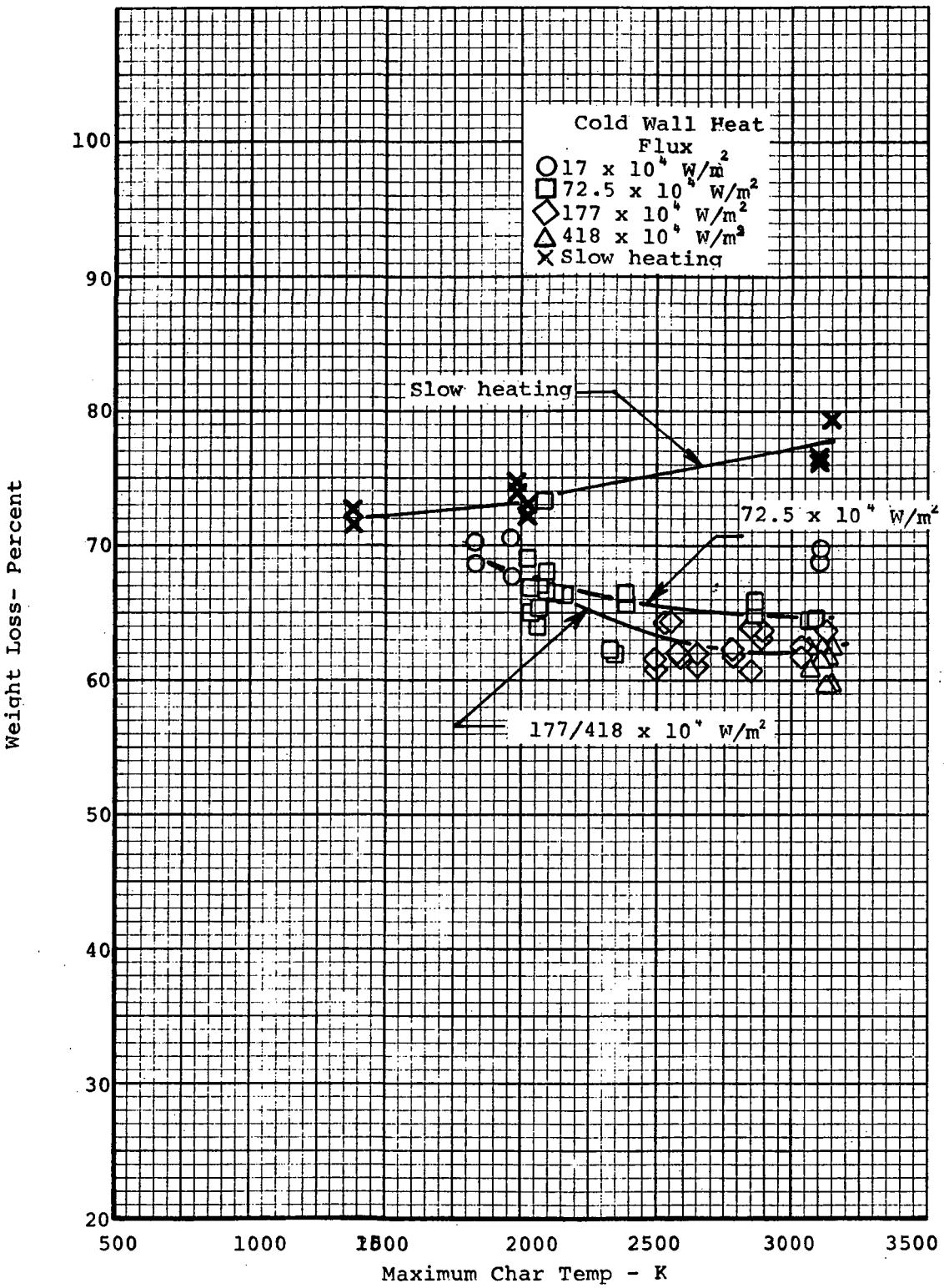

Figure 84. Effect of maximum char temperature on weight loss for char prepared in the laboratory from low-density phenolic-nylon

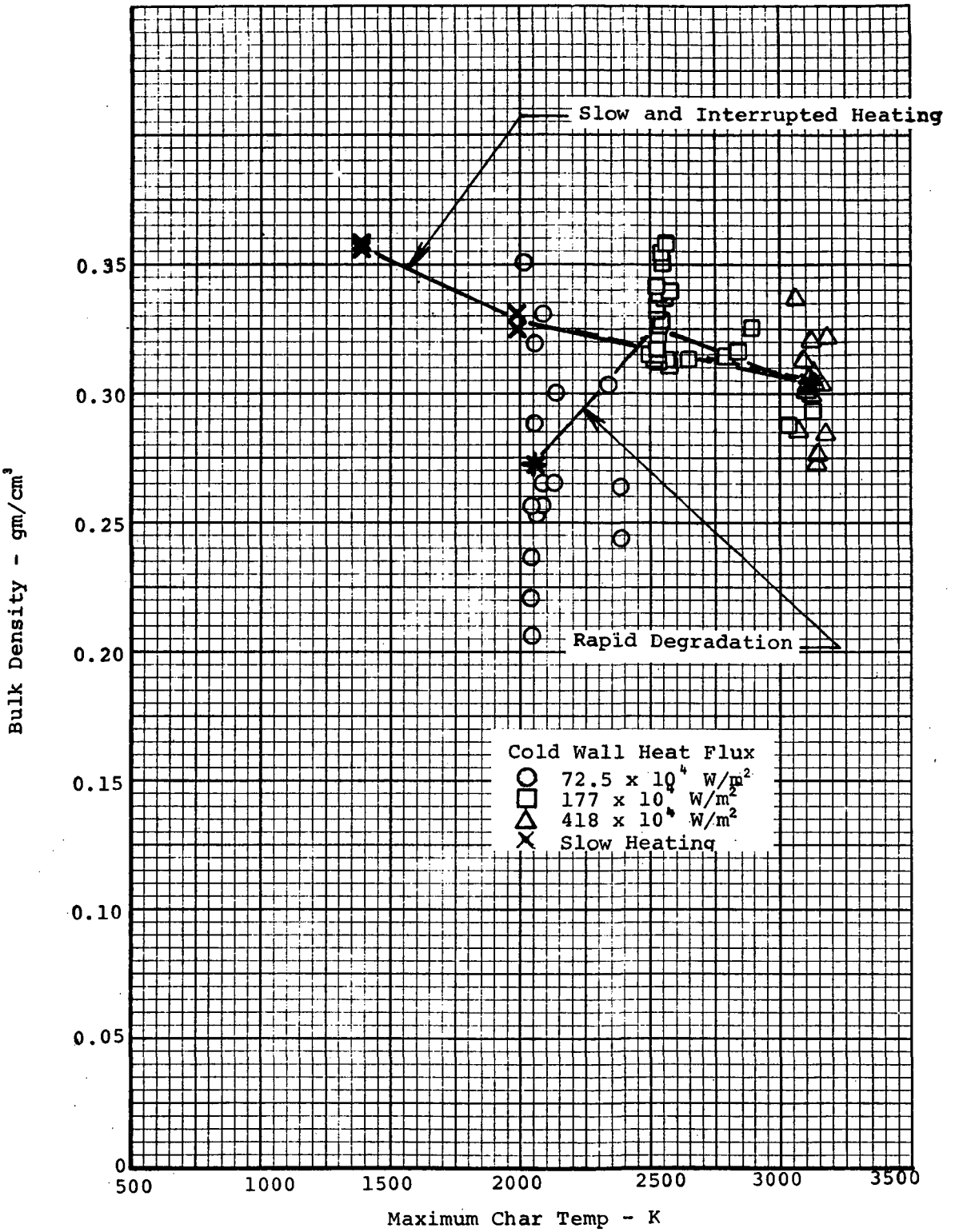

Figure 85. Effect of maximum char temperature on bulk density for char prepared in the laboratory from low-density phenolic-nylon

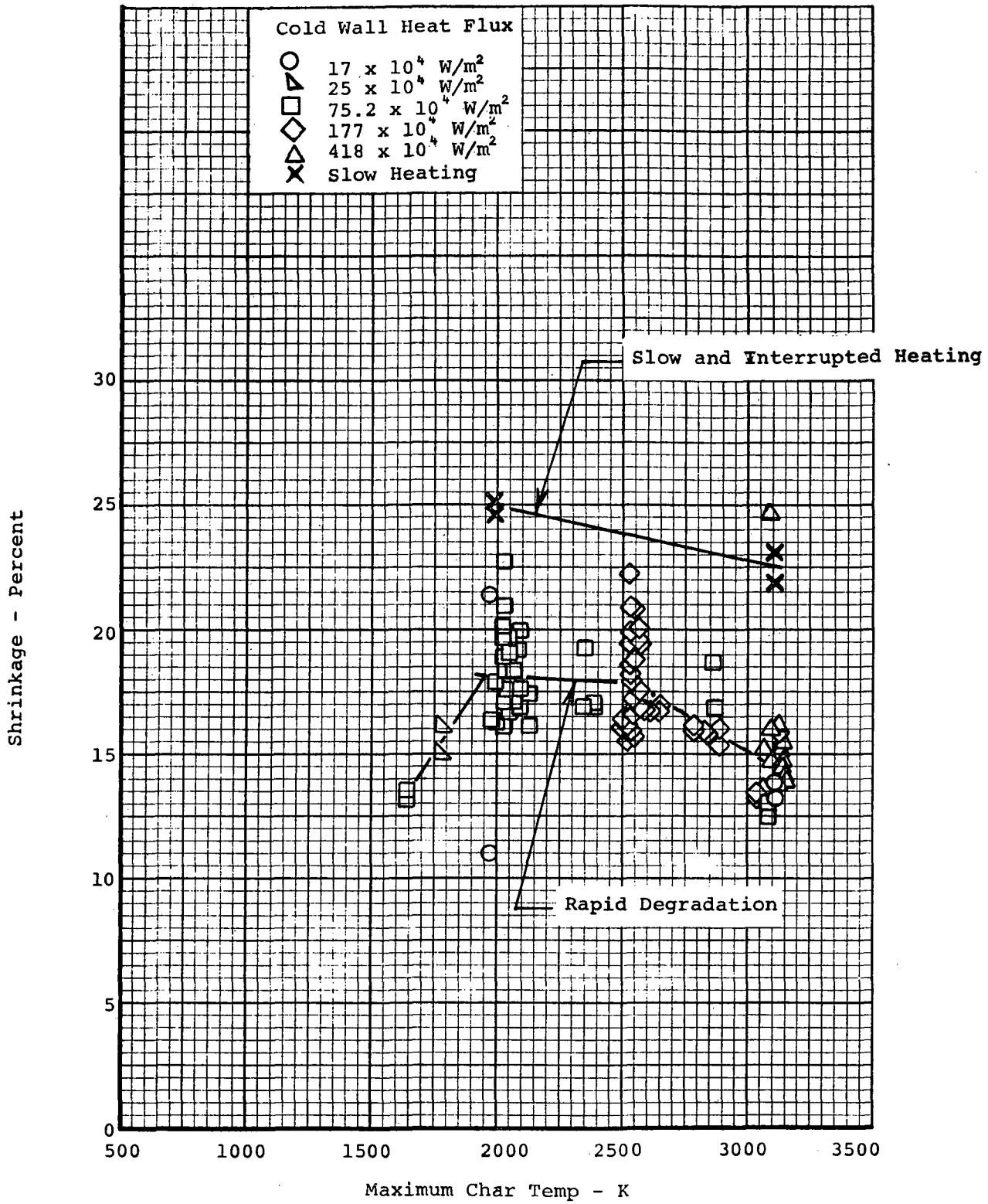

Figure 86. Effect of maximum char temperature on shrinkage in the charring direction for char prepared in the laboratory from low-density phenolic-nylon

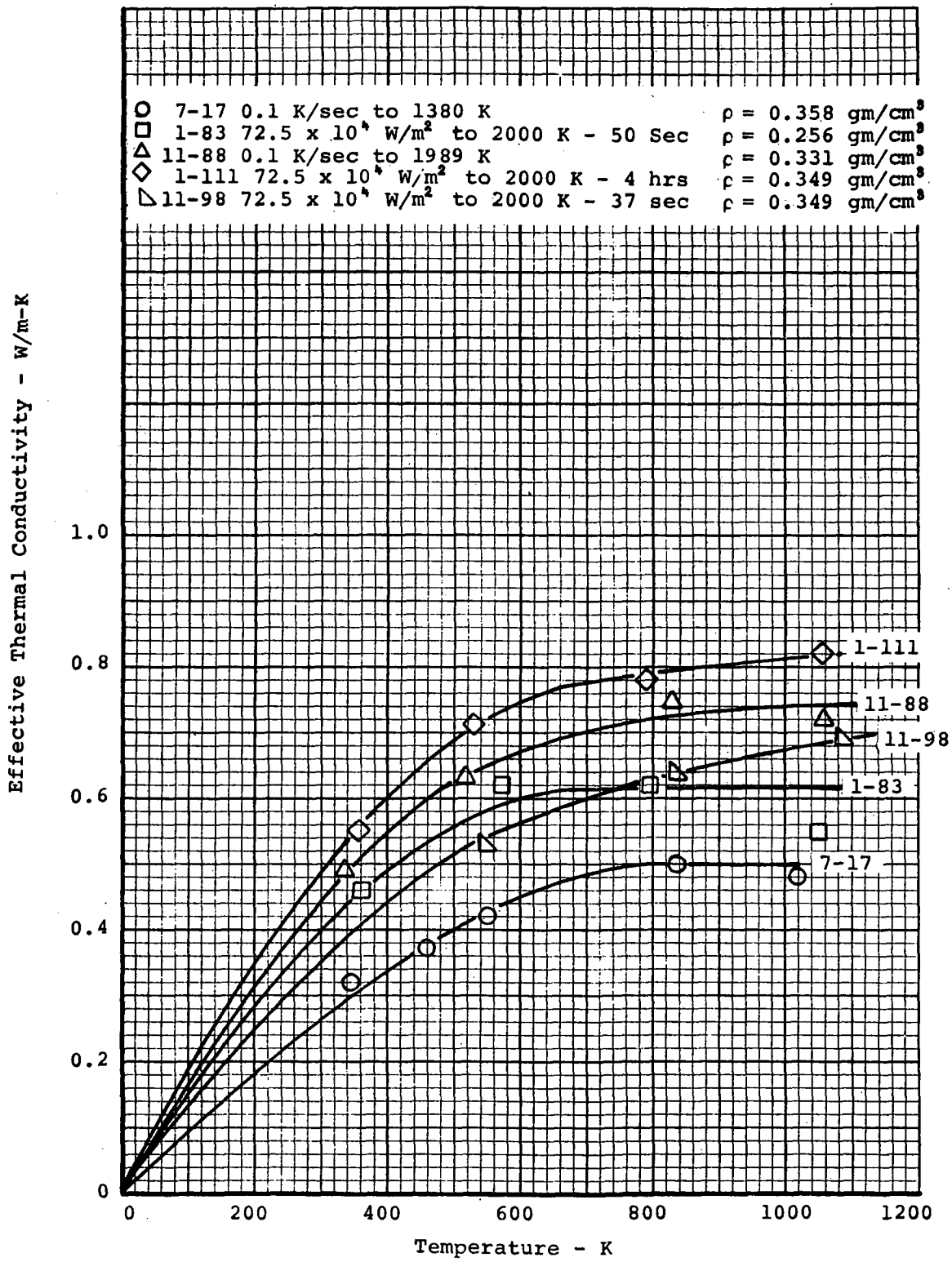

Figure 87. Effective thermal conductivity of low-density chars prepared in the laboratory to temperatures of 1366 K and 2000 K

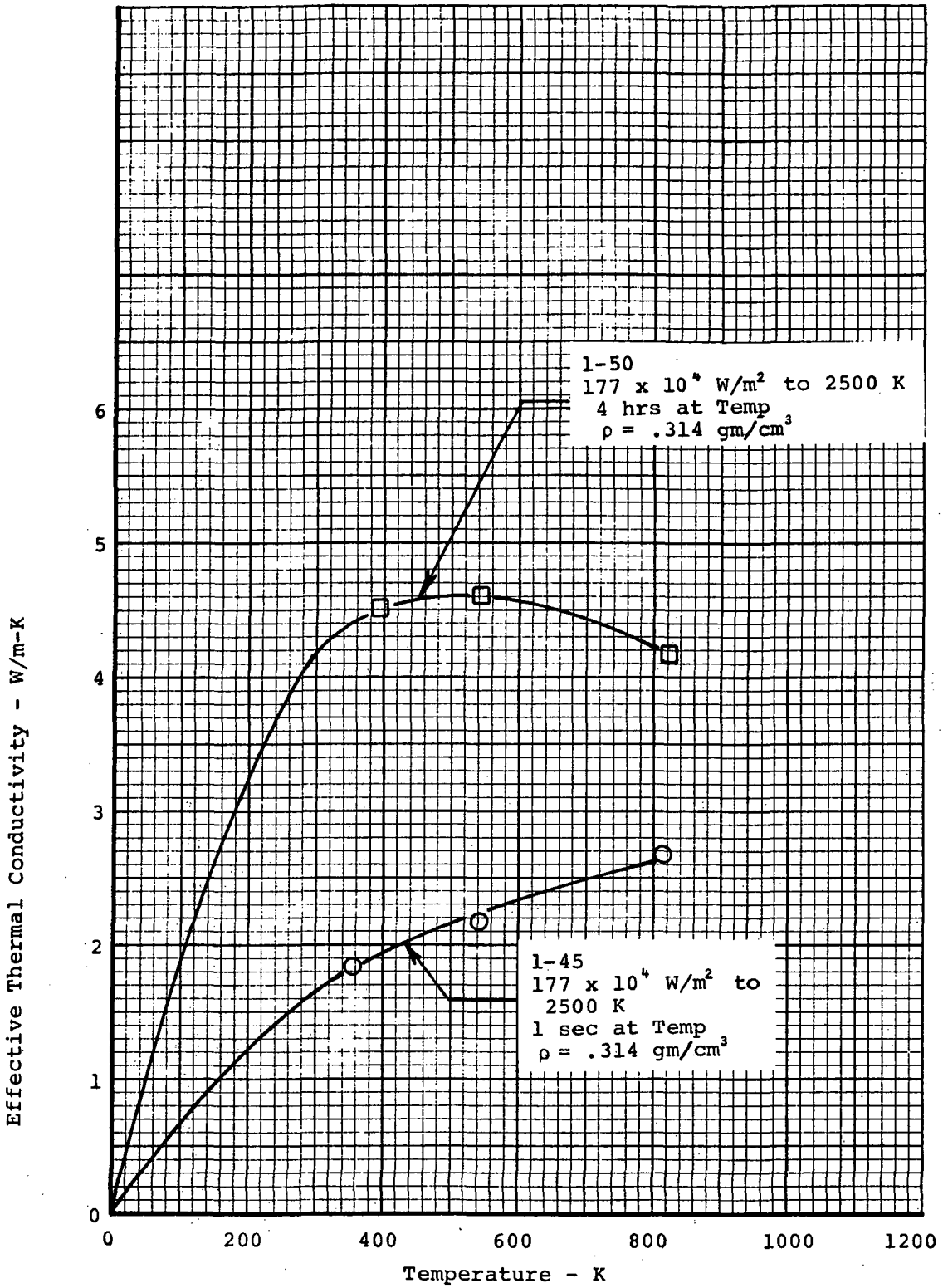

Figure 88. Effective thermal conductivity of low-density phenolic-nylon charred in the laboratory at 177 x 10^4 W/m^2 to 2500K

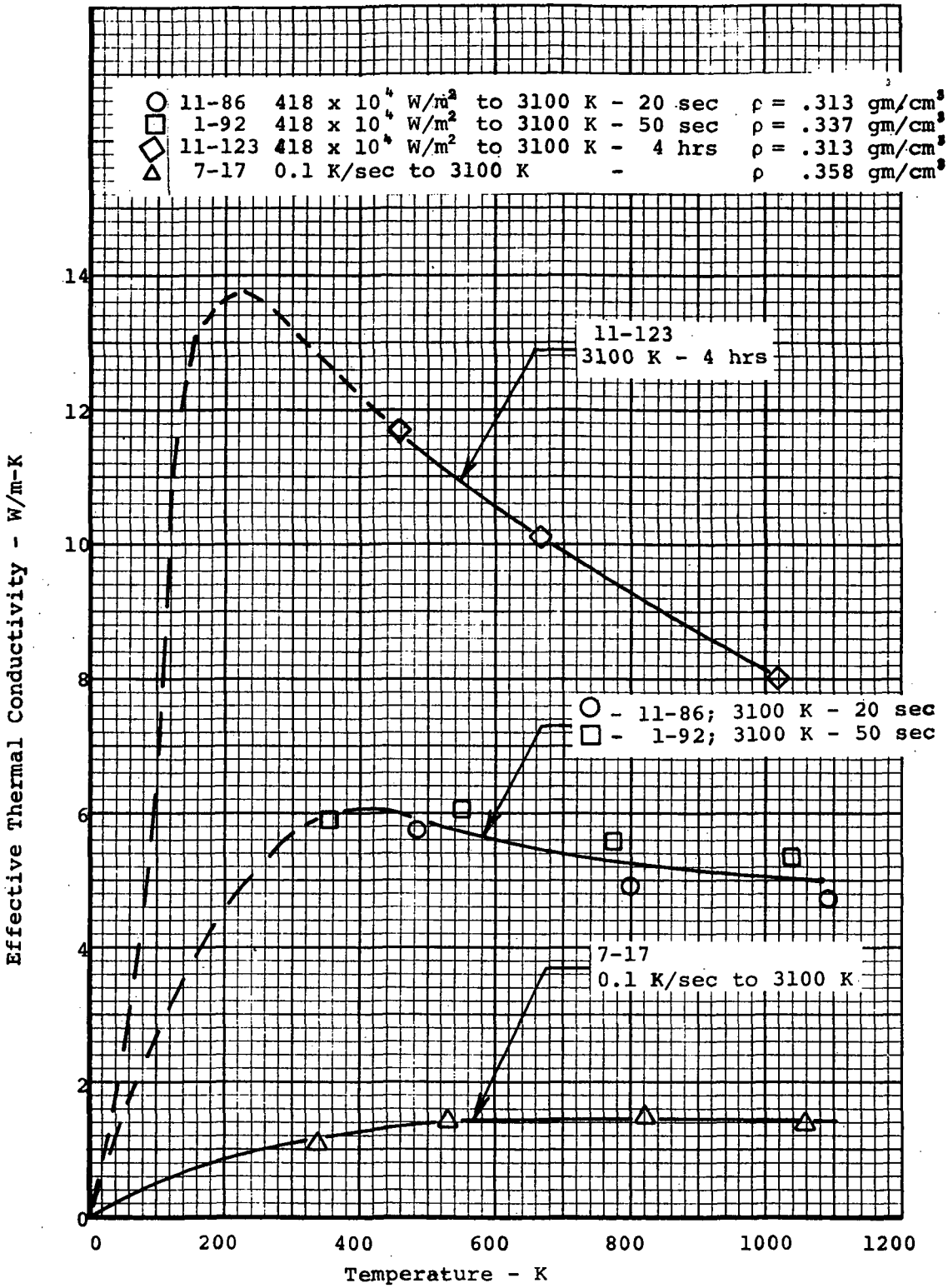

Figure 89. Effective thermal conductivity of low-density phenolic-nylon charred in the laboratory to 3100 K

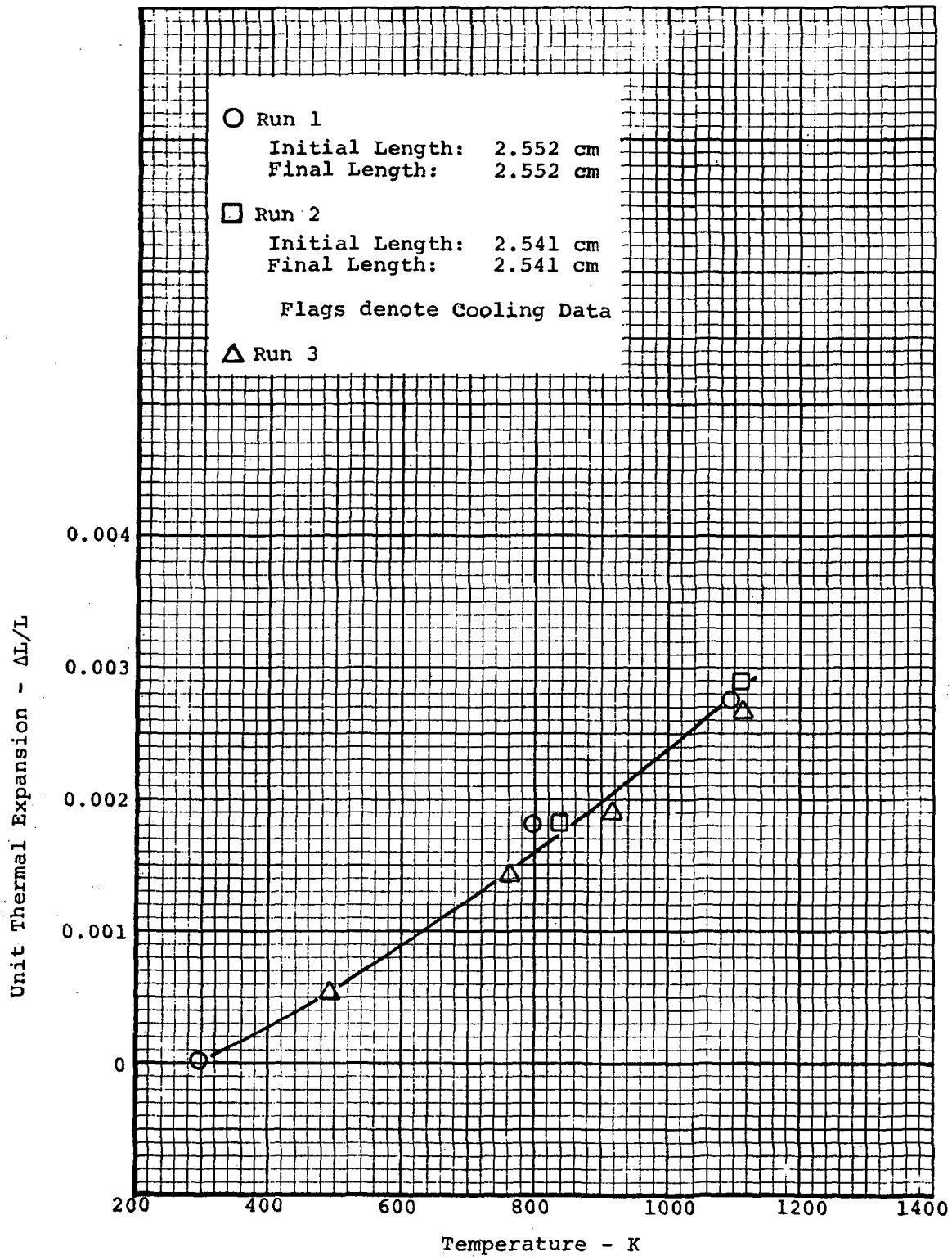

Figure 90. Thermal expansion of low-density phenolic-nylon char prepared in the laboratory specimen 7-18

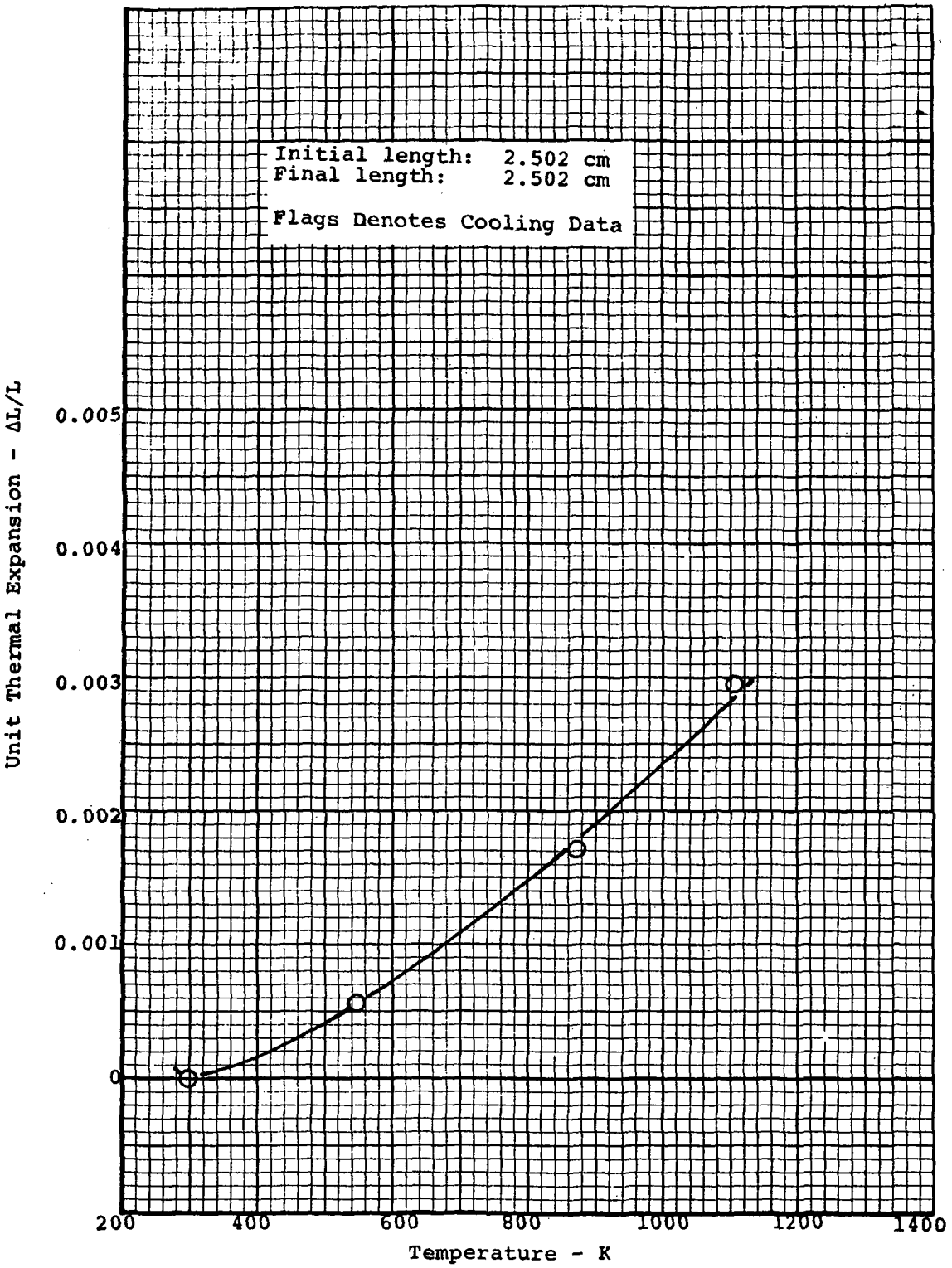

Figure 91. Thermal expansion of low-density phenolic-nylon char prepared in the laboratory specimen 11-78

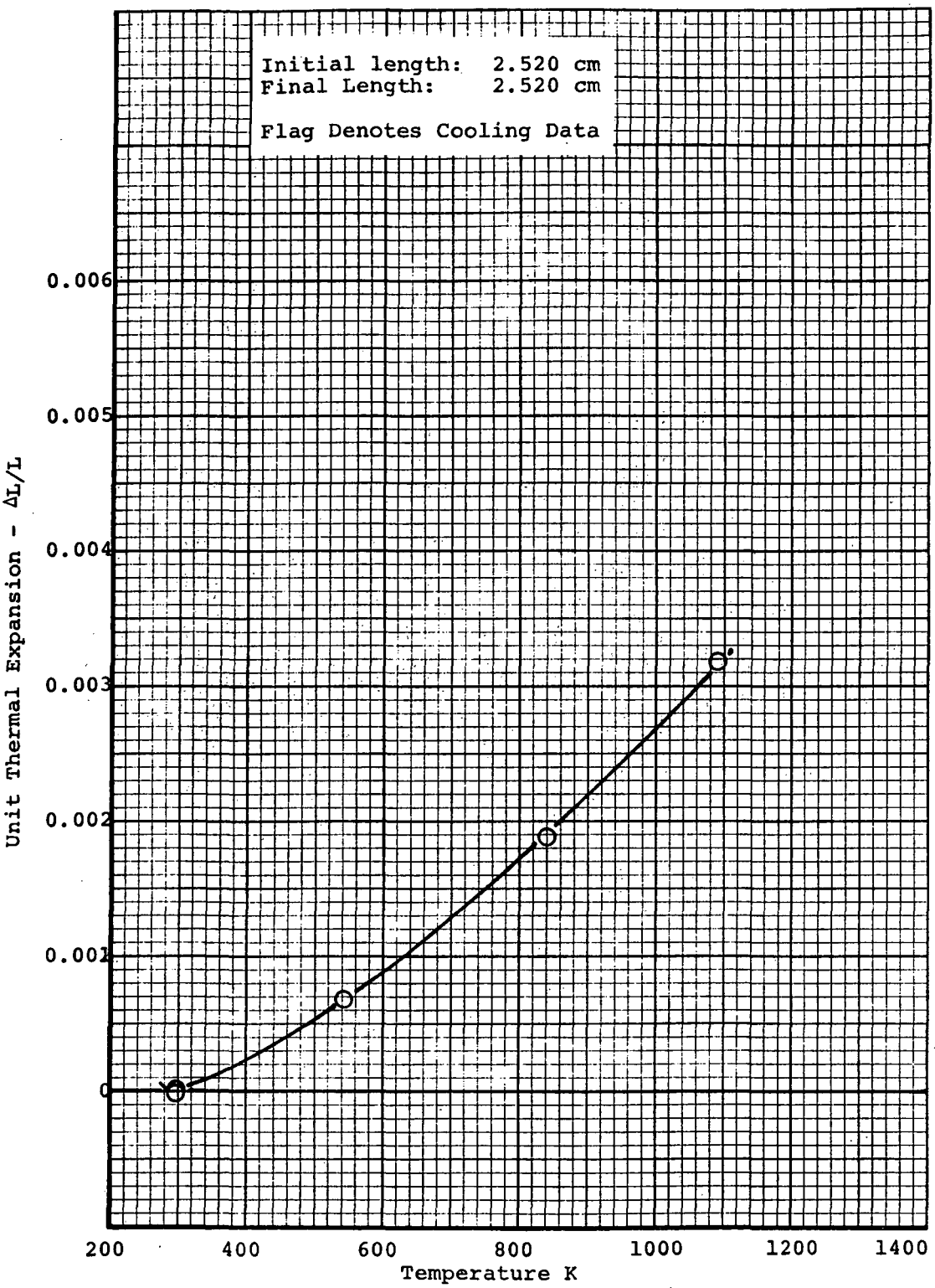

Figure 92. Thermal expansion of low-density phenolic-nylon char prepared in the laboratory specimen 11-123

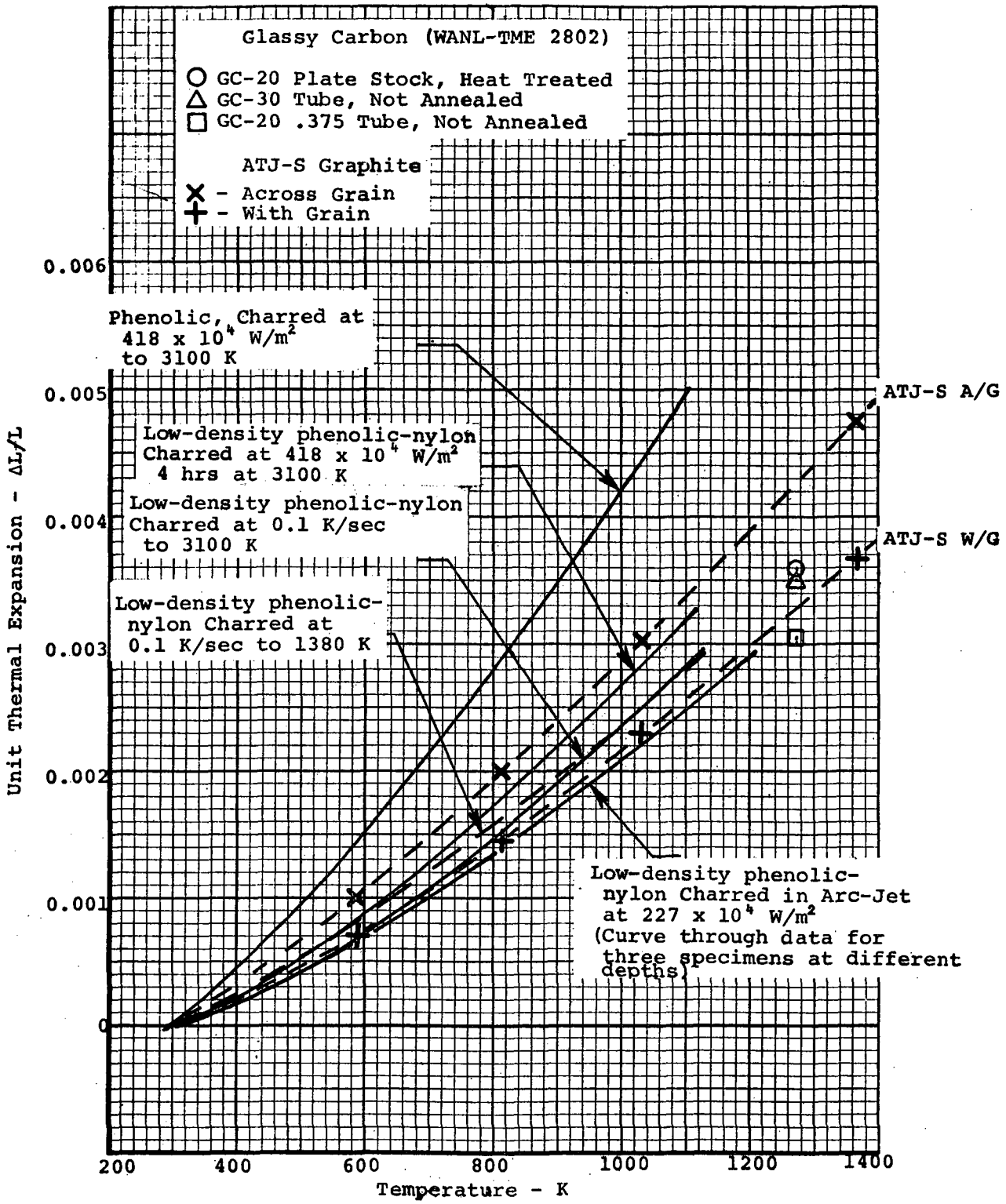

Figure 93. Thermal expansion comparison of phenolic and low density phenolic-nylon char prepared at different heating rates and temperatures to the thermal expansion of ATJ-S Graphite and glassy carbon

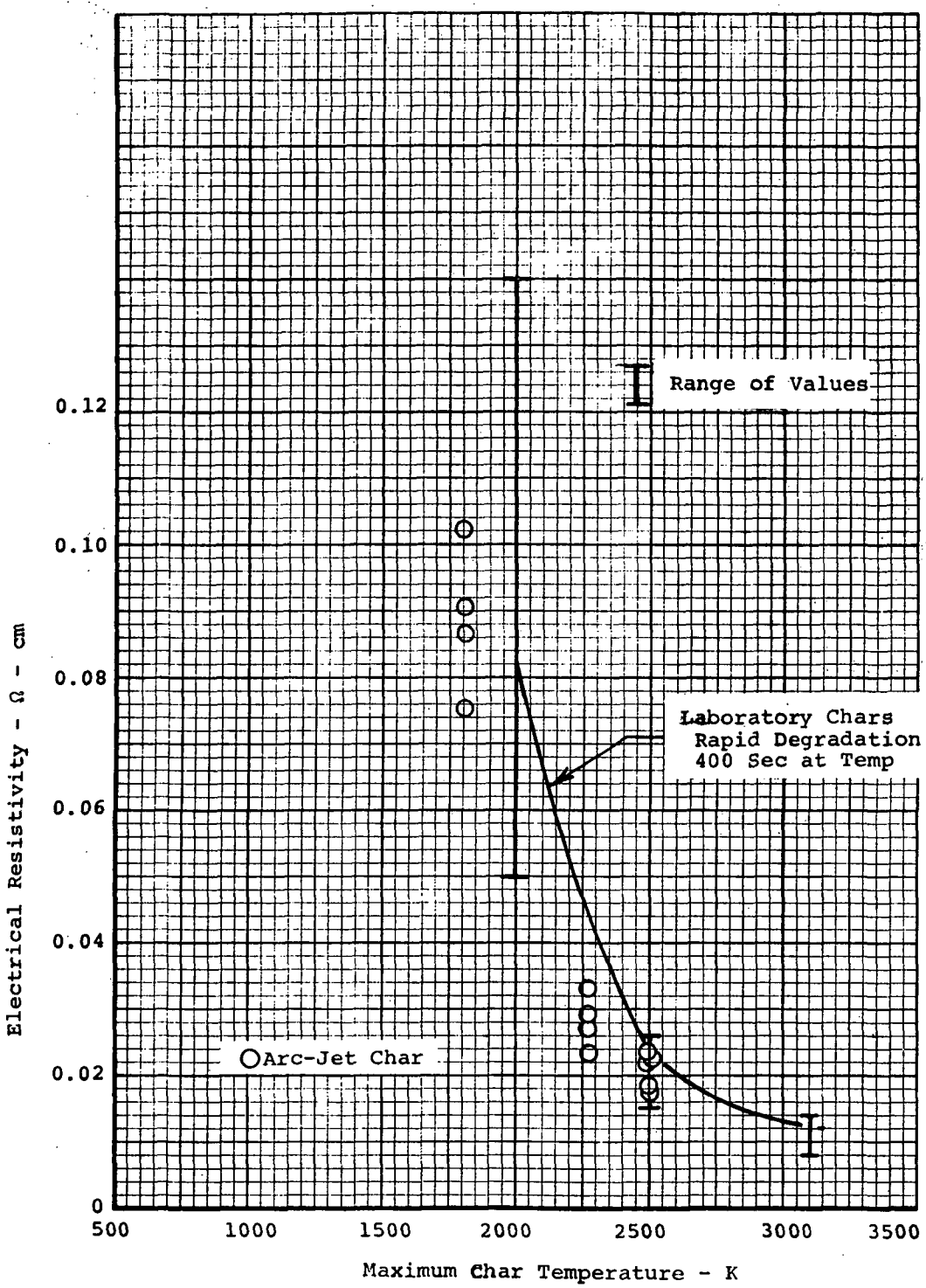

Figure 94. Effect of maximum char temperature on electrical resistivity for low-density phenolic-nylon charred in the arc-jet at 227 x 10^6 W/m^2

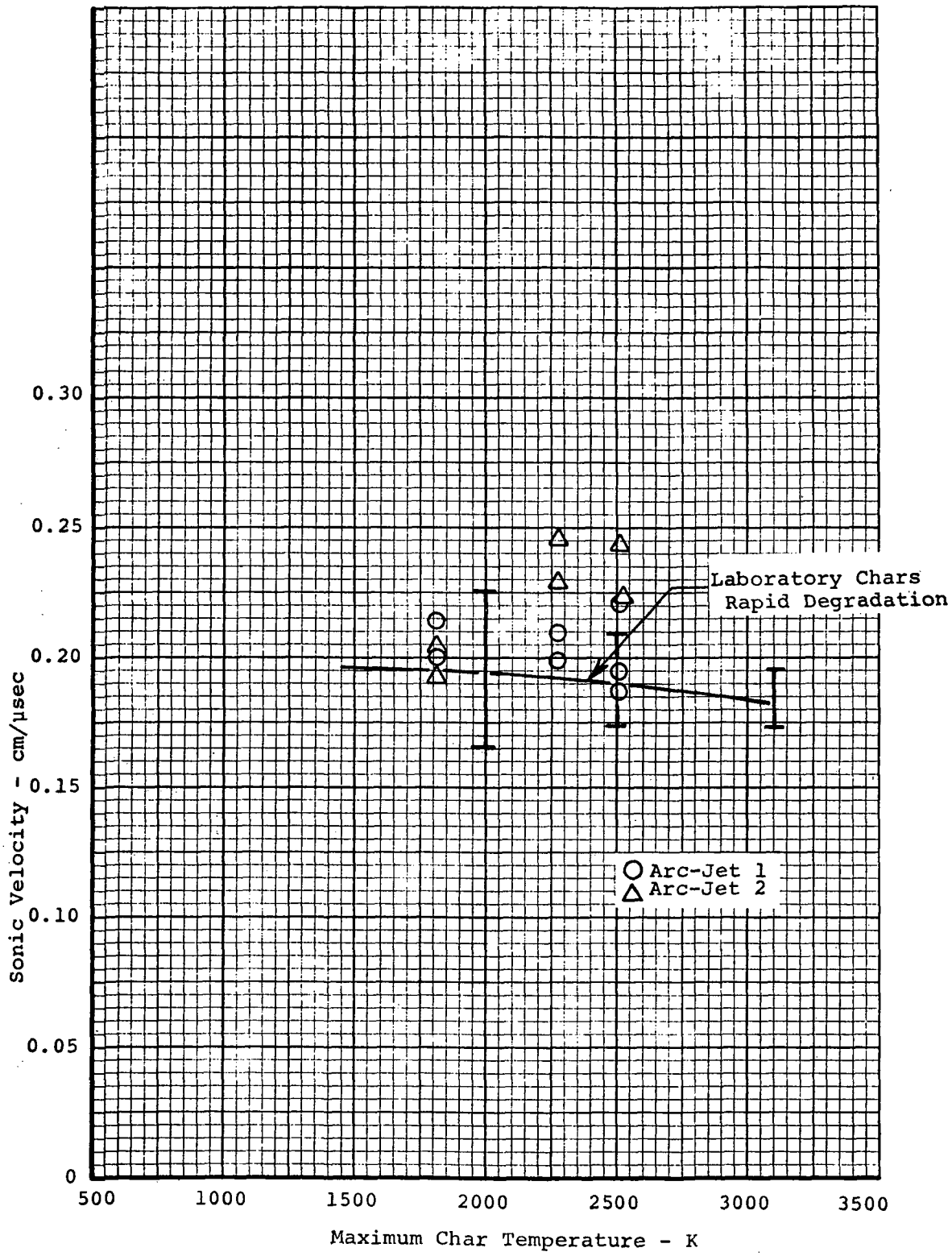

Figure 95. Effect of maximum char temperature on sonic velocity for low-density phenolic-nylon charred in the arc-jet at 227 x 10^4 W/m^2

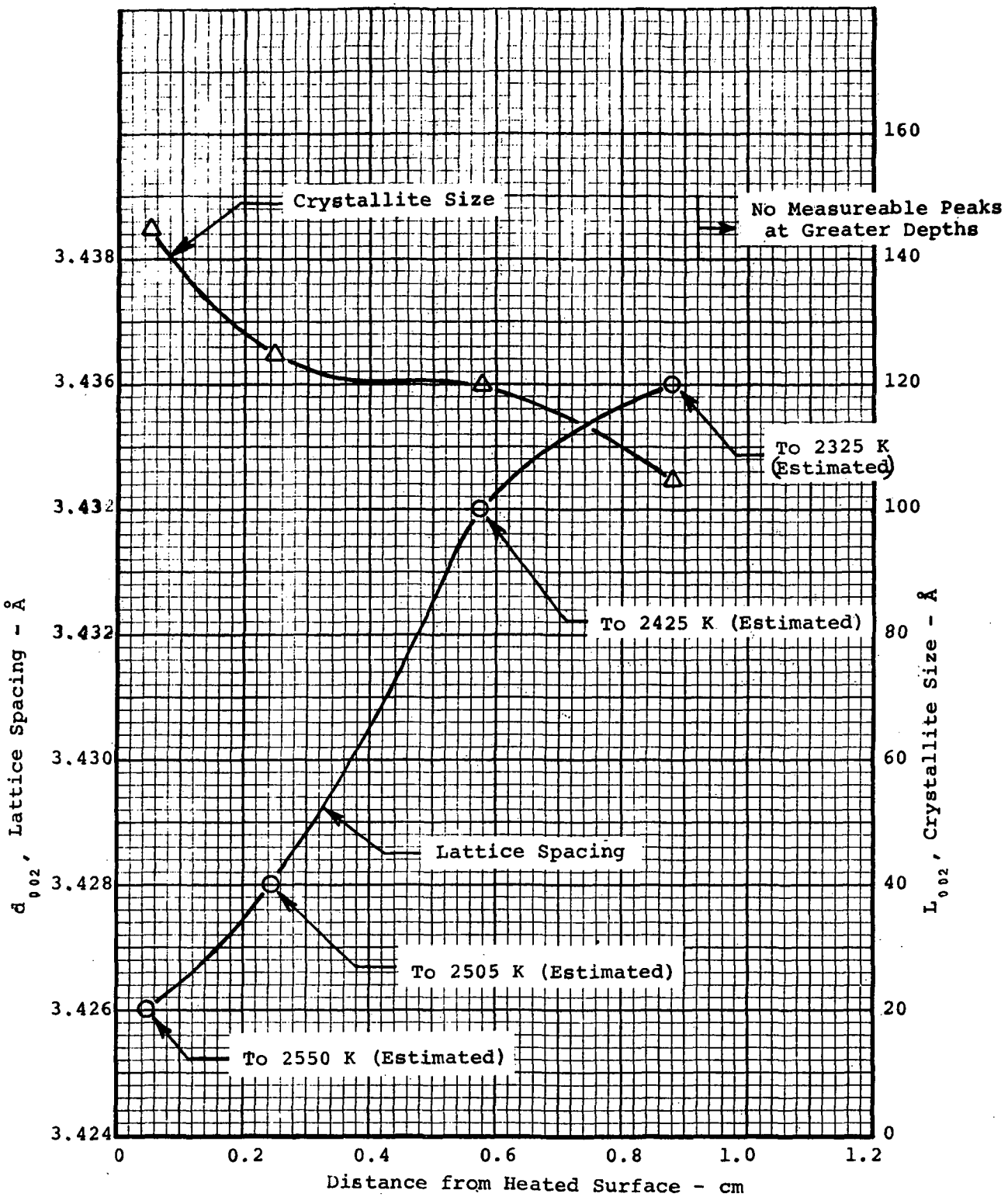

Figure 96. Variation of lattice spacing and crystallite size through low-density phenolic-nylon char prepared in the arc-jet at 227 x 10^4 W/m^2 in a nitrogen environment for 400-500 sec.

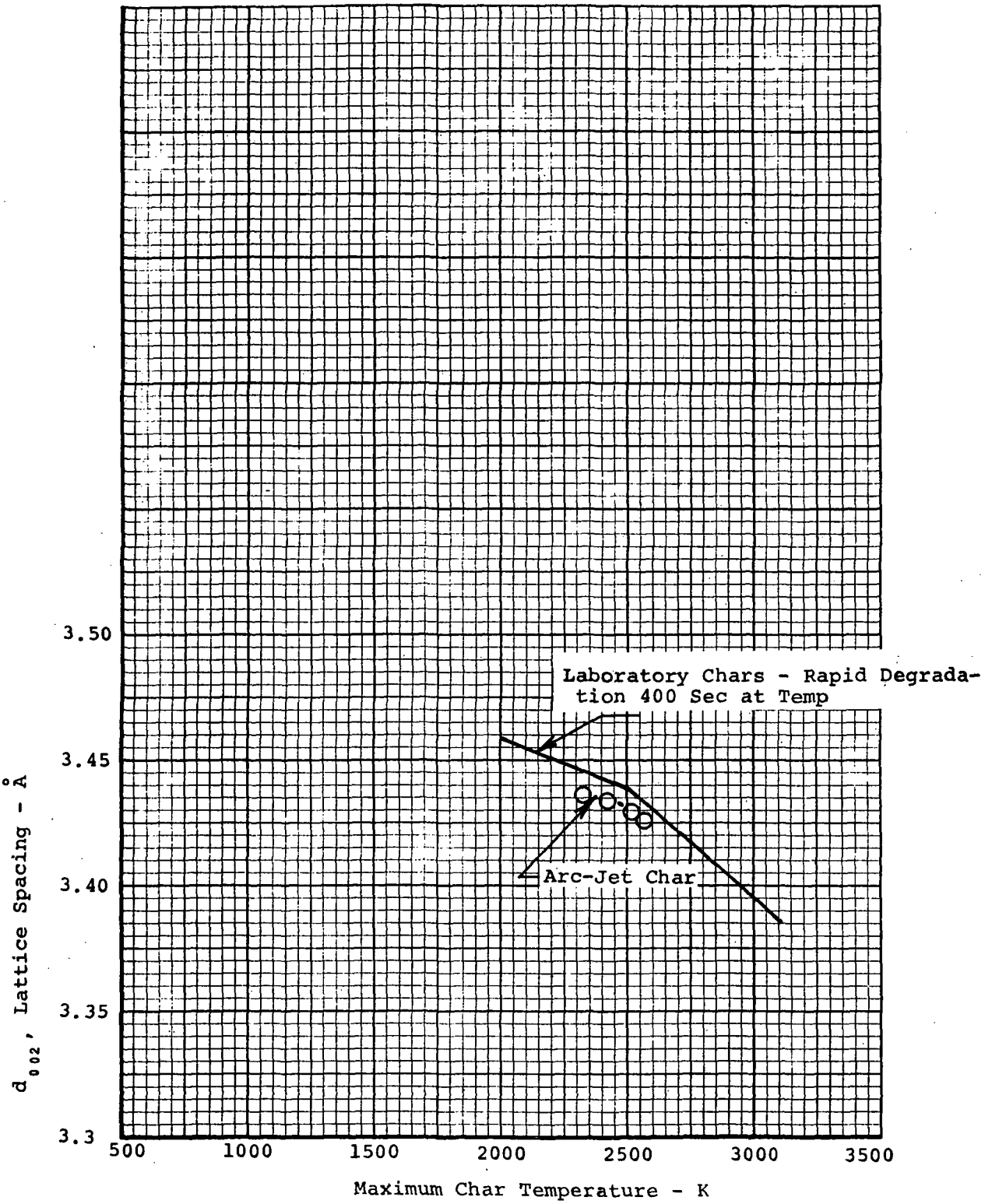

Figure 97. Effect of maximum char temperature on lattice spacing of low-density phenolic-nylon charred in the arc-jet at 227 x 10^4 W/m^2

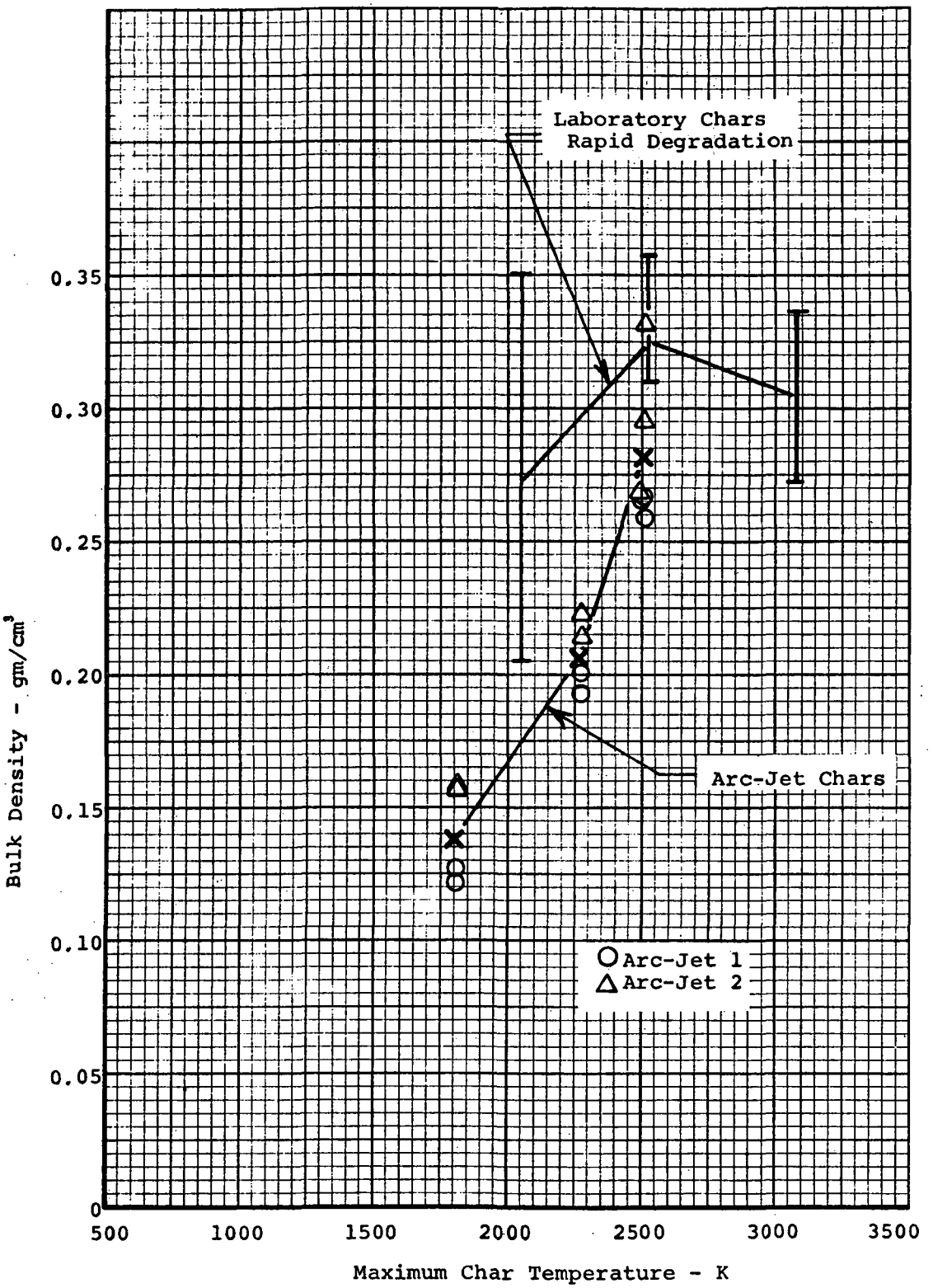

Figure 98. Effects of maximum char temperature on bulk density for low-density phenolic-nylon charred in the arc-jet

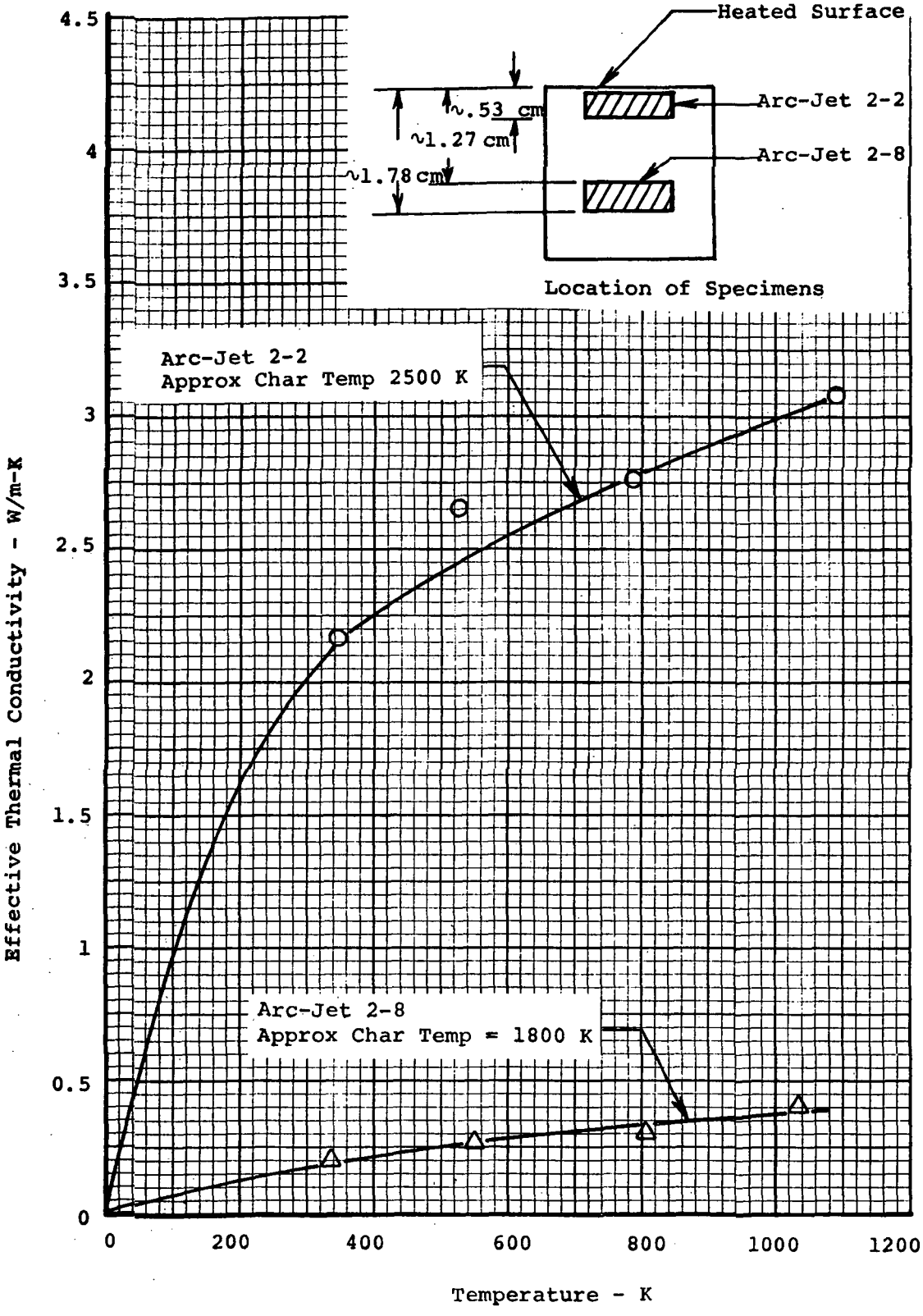

Figure 99. Effective thermal conductivity of low-density phenolic-nylon charred in arc-jet at 227 x 10^4 W/m^2 for 400-500 seconds

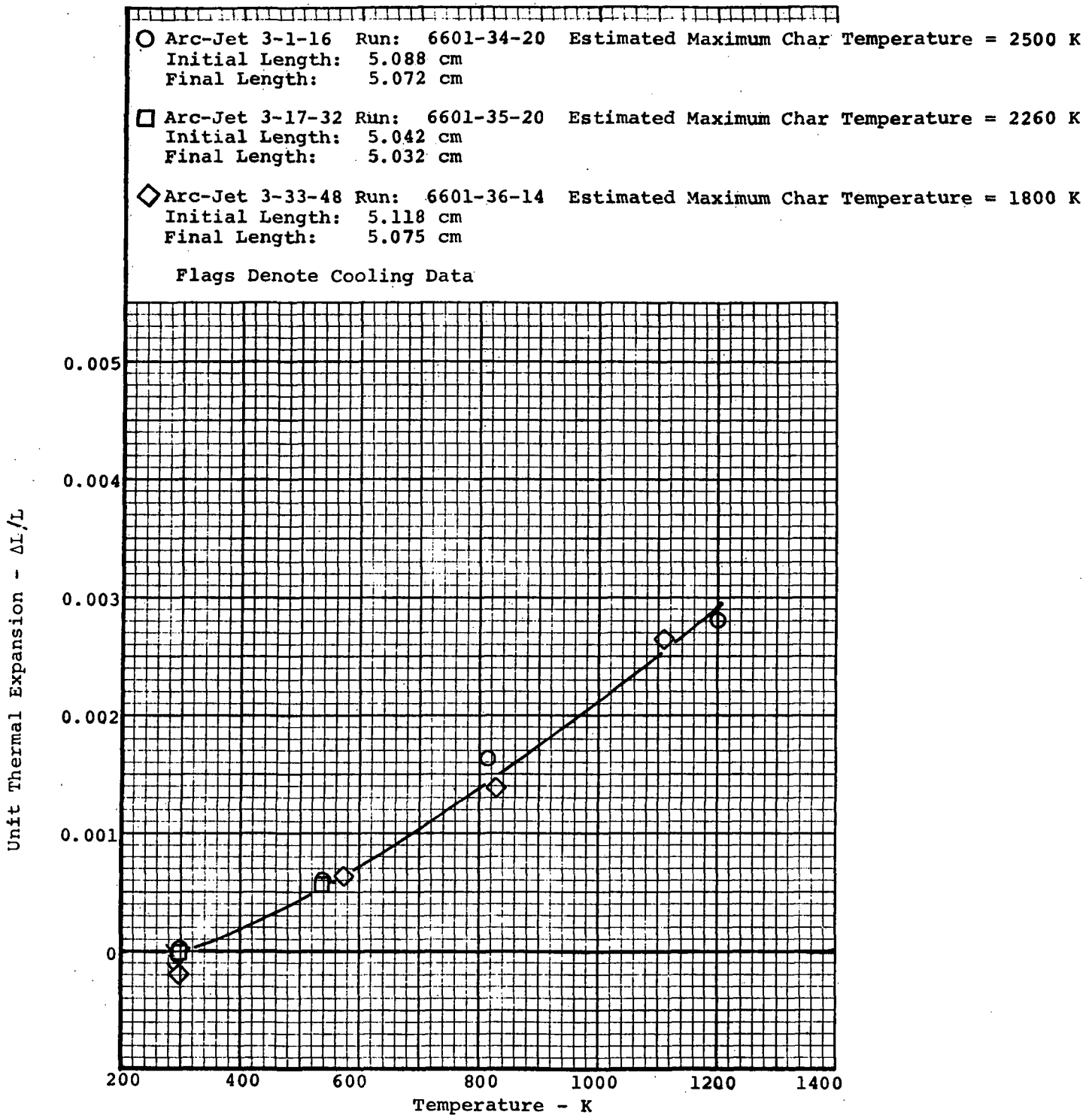

Figure 100. Thermal expansion of low-density phenolic-nylon charred in arc-jet at 227 x 10^4 W/m^2 cold wall heat flux

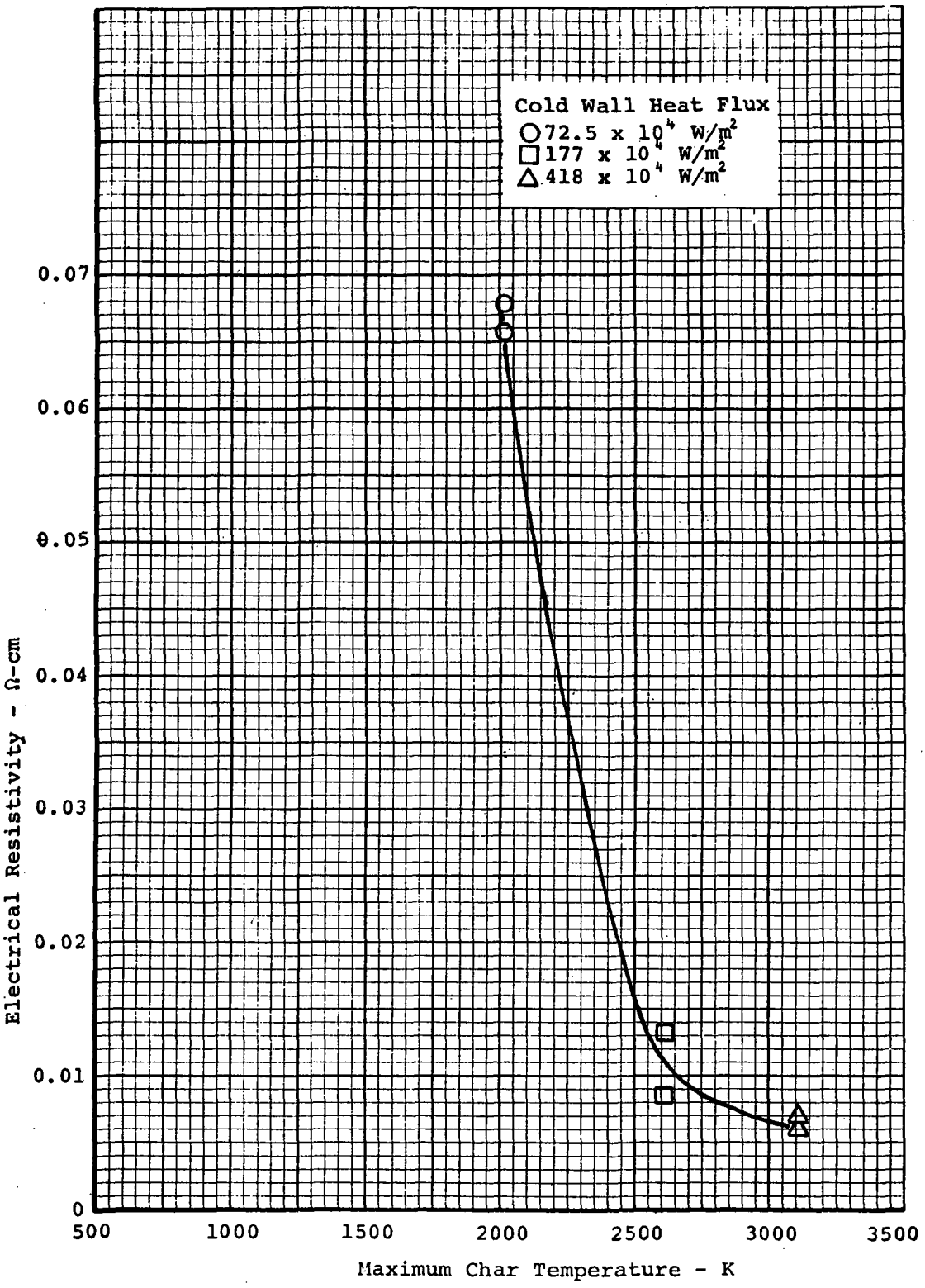

Figure 101. Effect of maximum char temperature on electrical resistivity for high-density phenolic-nylon charred in the laboratory

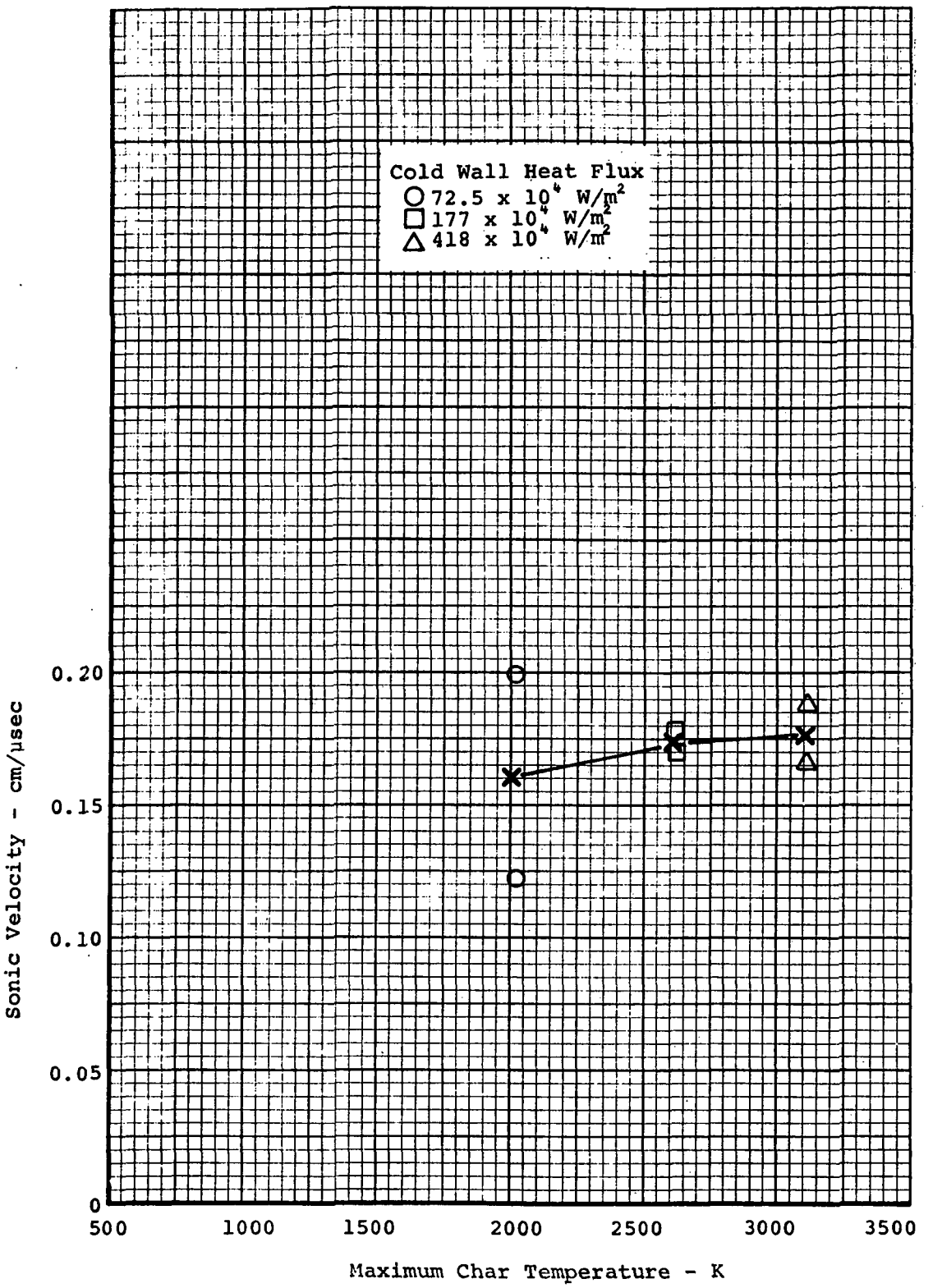

Figure 102. Effect of maximum char temperature on sonic velocity for high-density phenolic-nylon charred in the laboratory

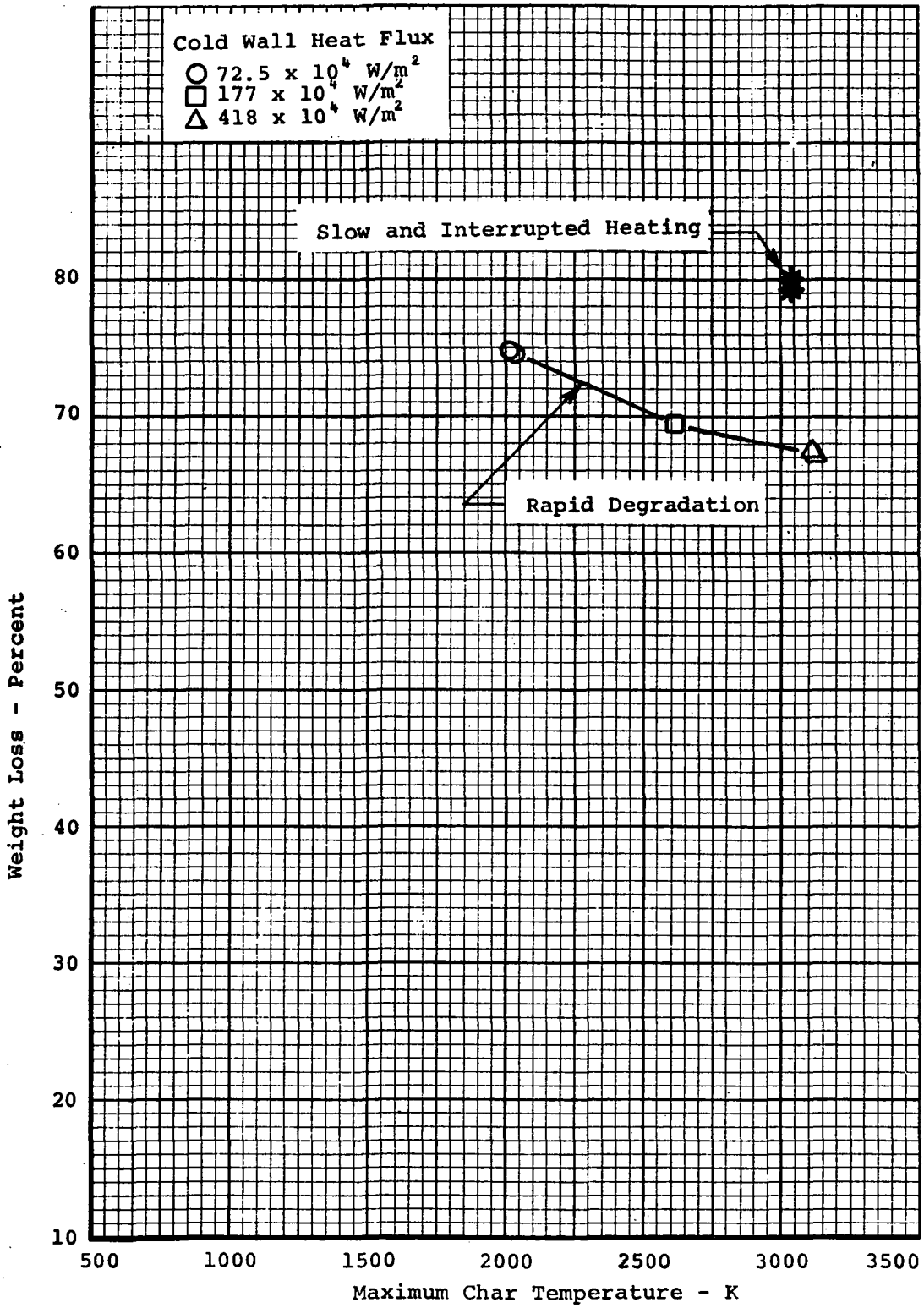

Figure 103. Effect of maximum char temperature on weight loss for high-density phenolic-nylon charred in the laboratory

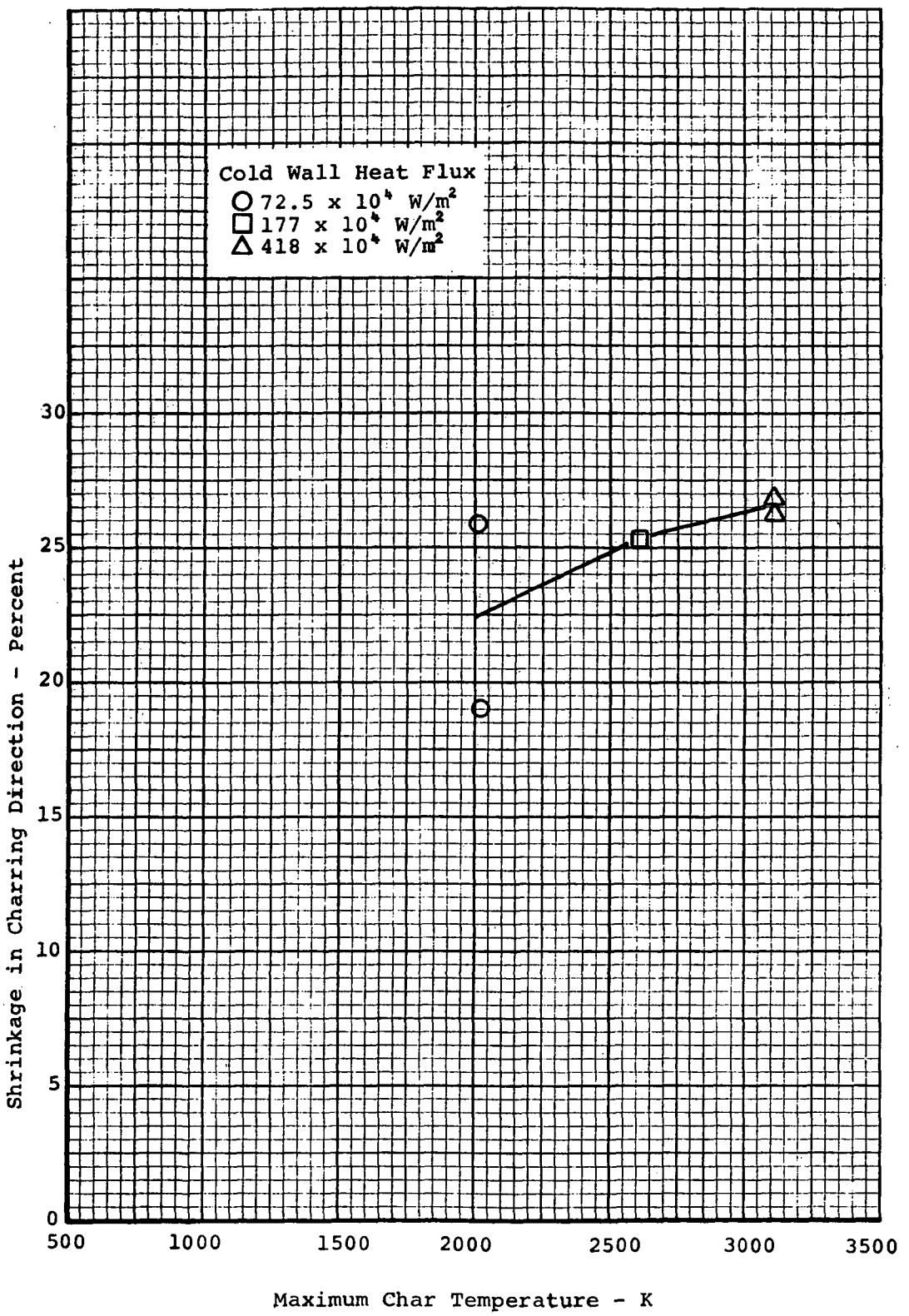

Figure 104. Effect of maximum char temperature on shrinkage in charring direction for high-density phenolic-nylon charred in the laboratory

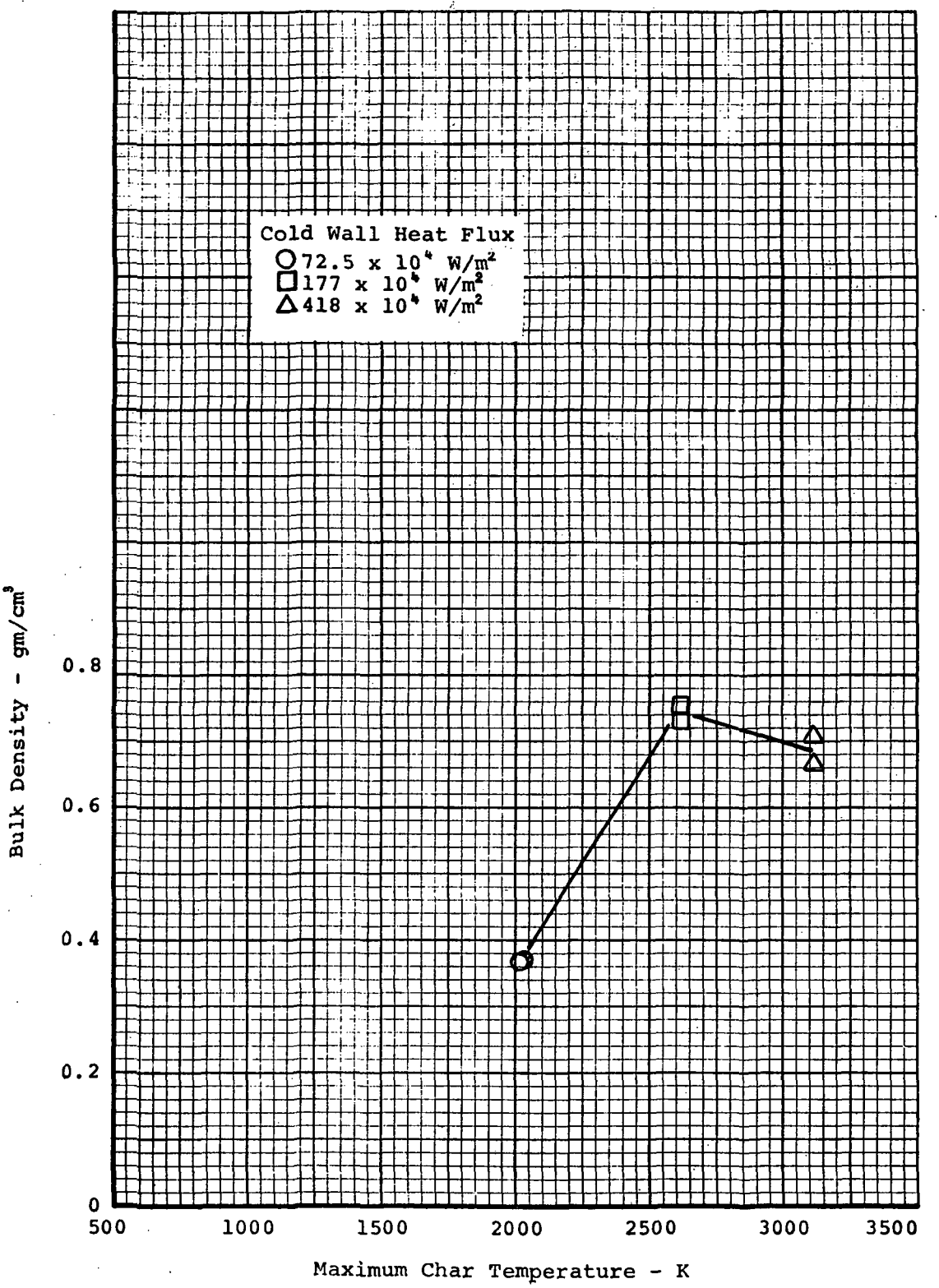

Figure 105. Effect of maximum char temperature on bulk density for high-density phenolic-nylon charred in the laboratory

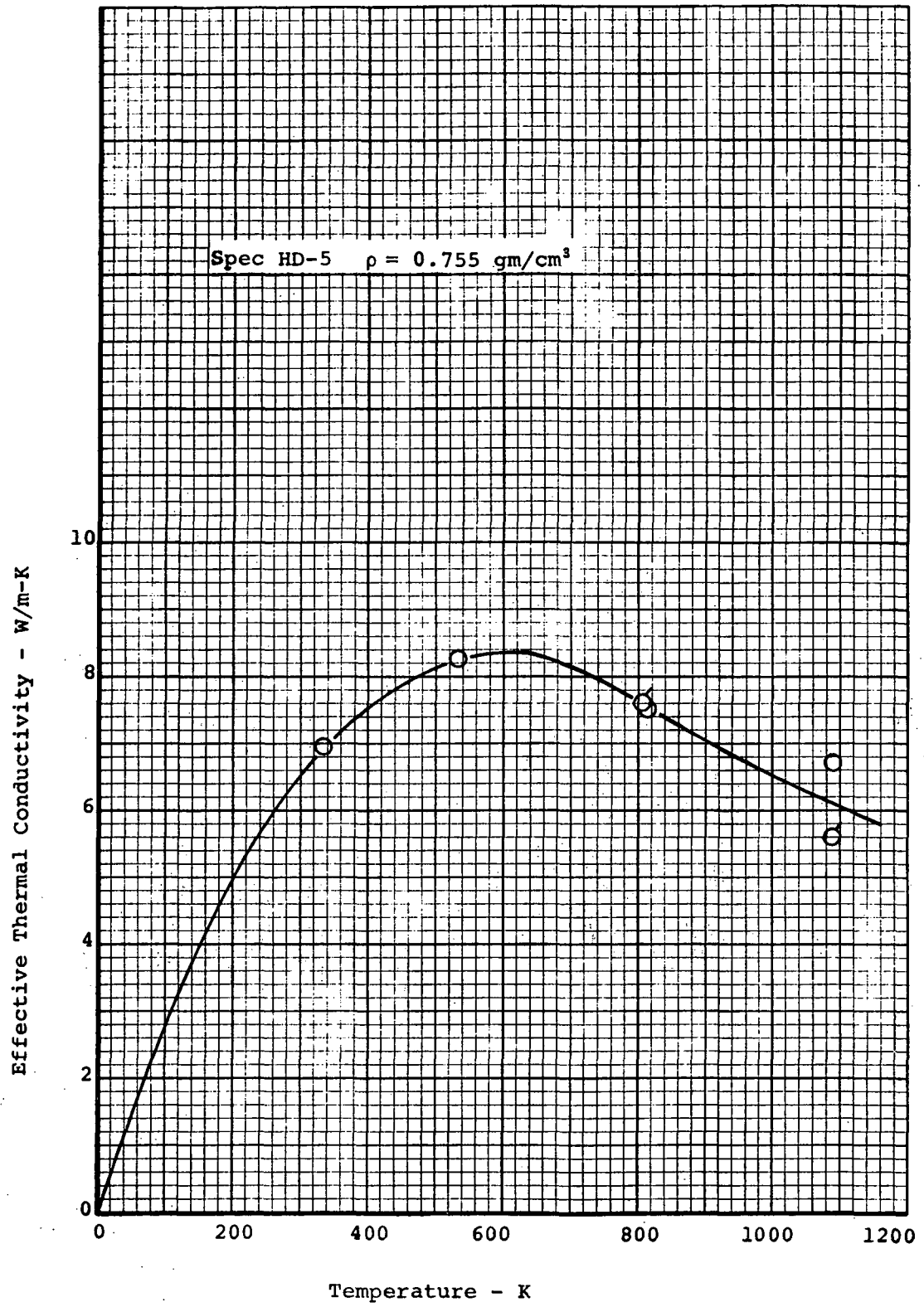

Figure 106. Effective thermal conductivity of high-density phenolic-nylon (1-2 gm/cm³) charred in furnace at 2600 K for 100 Sec

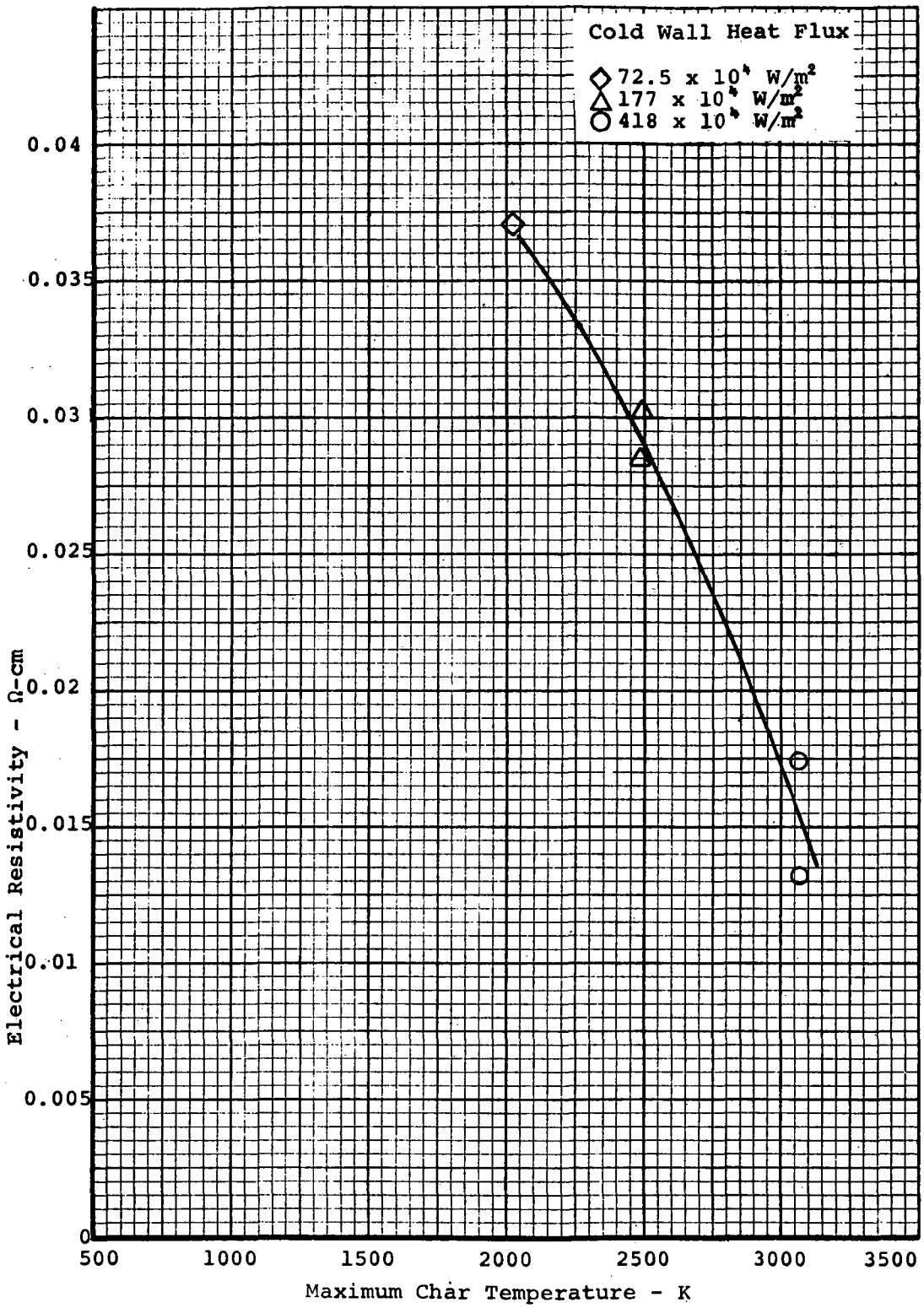

Figure 107. Effect of maximum char temperature on electrical resistivity for phenolic charred in in the laboratory

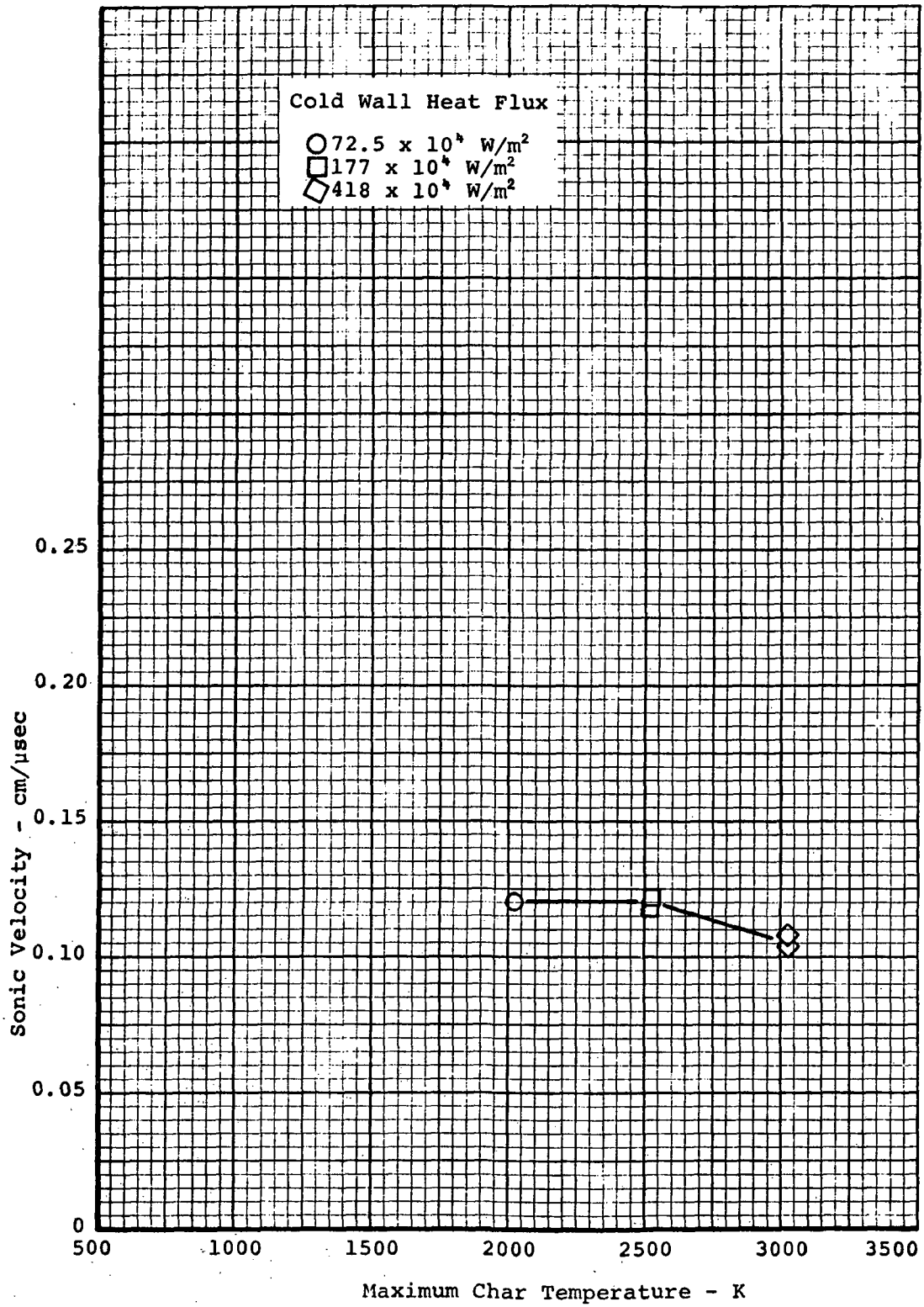

Figure 108. Effect of maximum char temperature on sonic velocity for phenolic charred in the laboratory

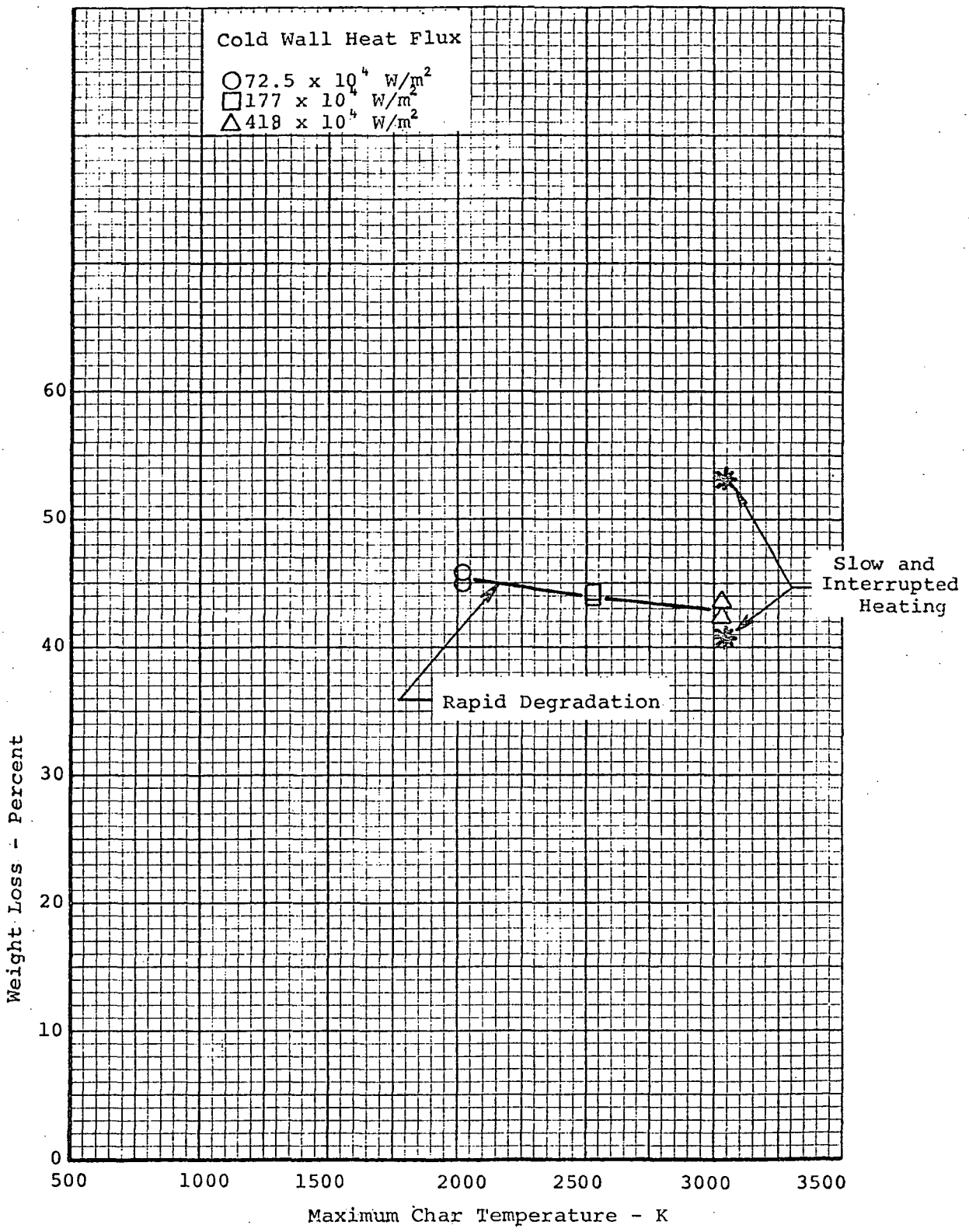

Figure 109. Effect of maximum char temperature on weight loss for phenolic charred in the laboratory

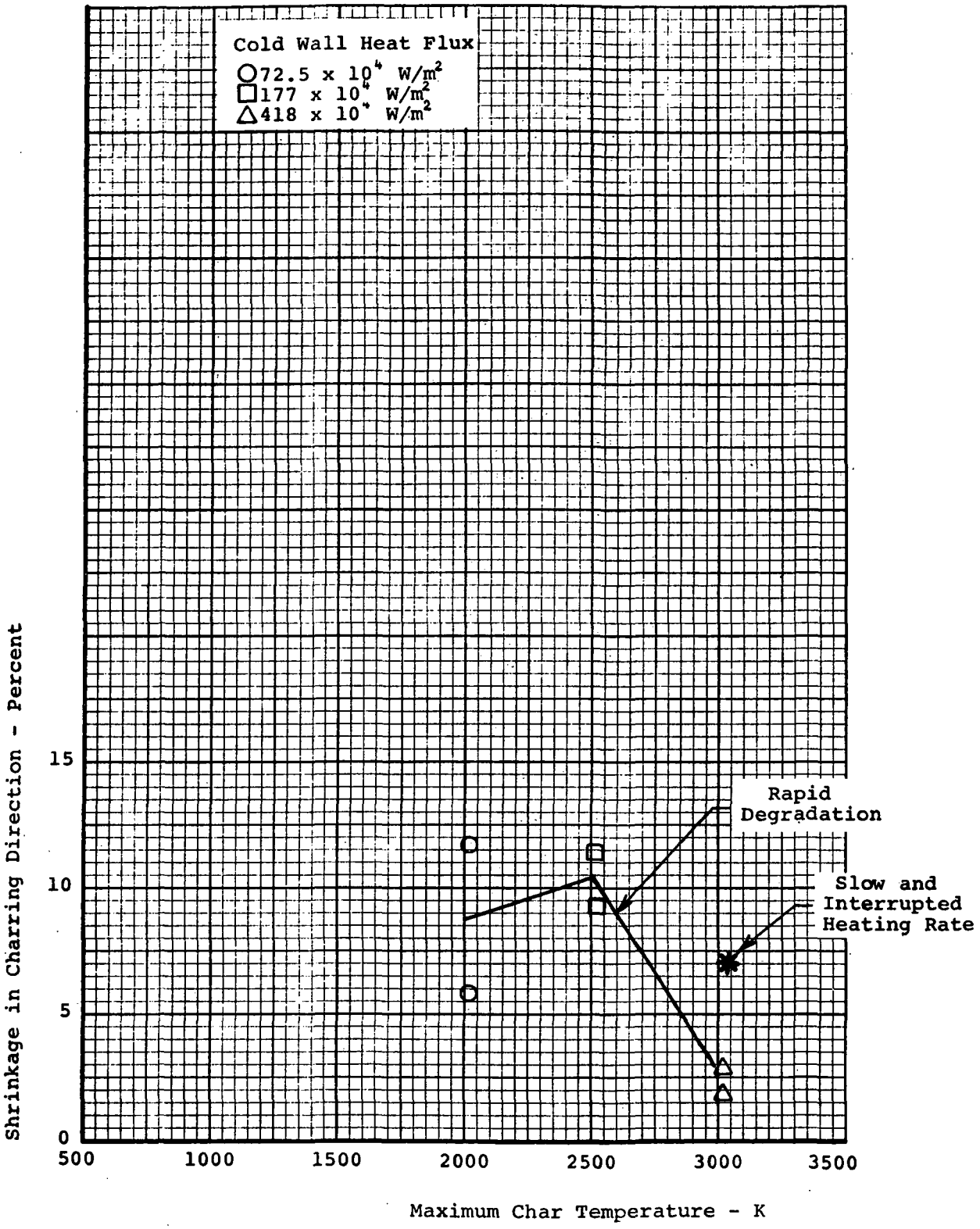

Figure 110. Effect of maximum char temperature on shrinkage in charring direction for phenolic charred in the laboratory

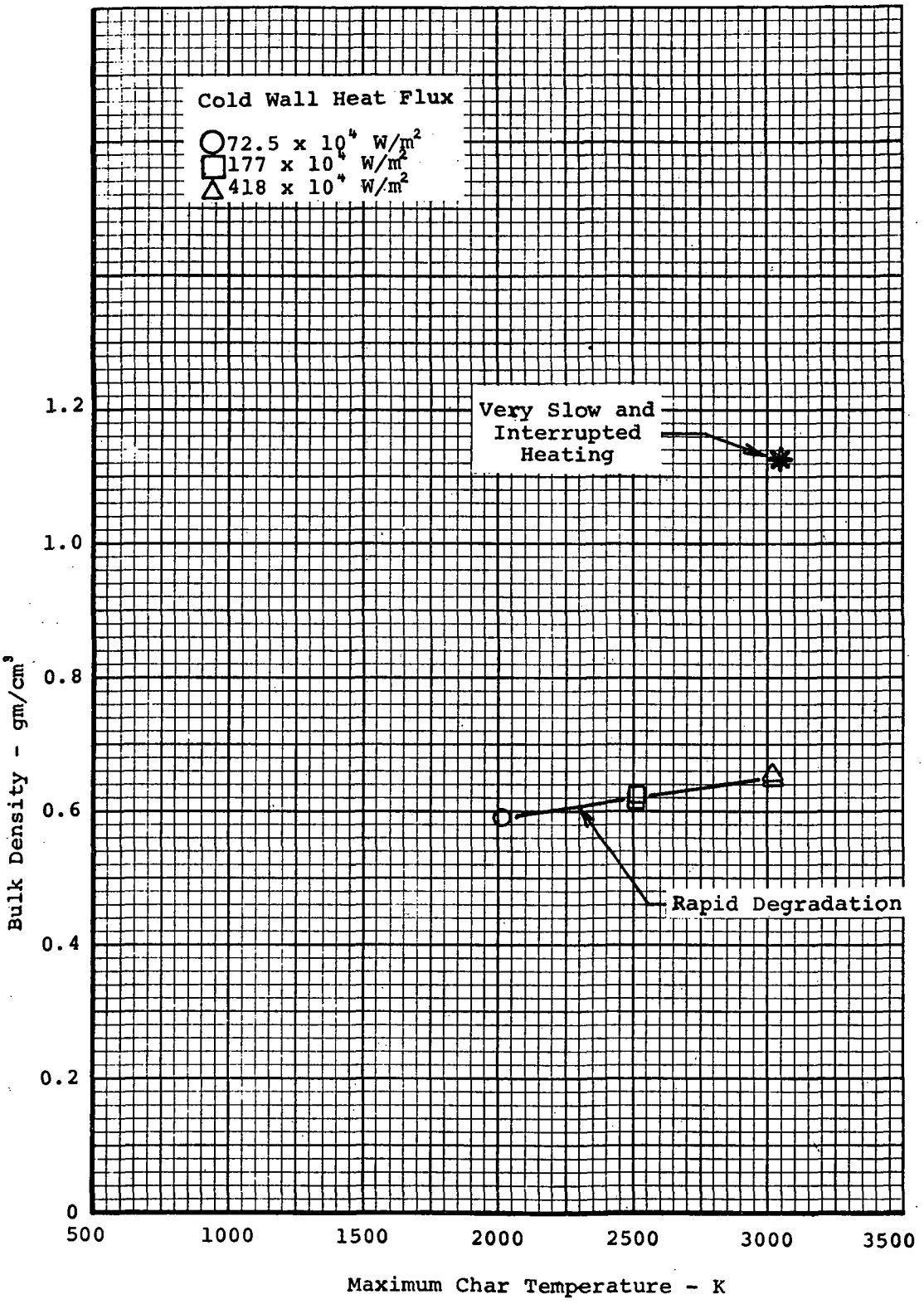

Figure 111. Effect of maximum char temperature on bulk density for phenolic charred in the laboratory

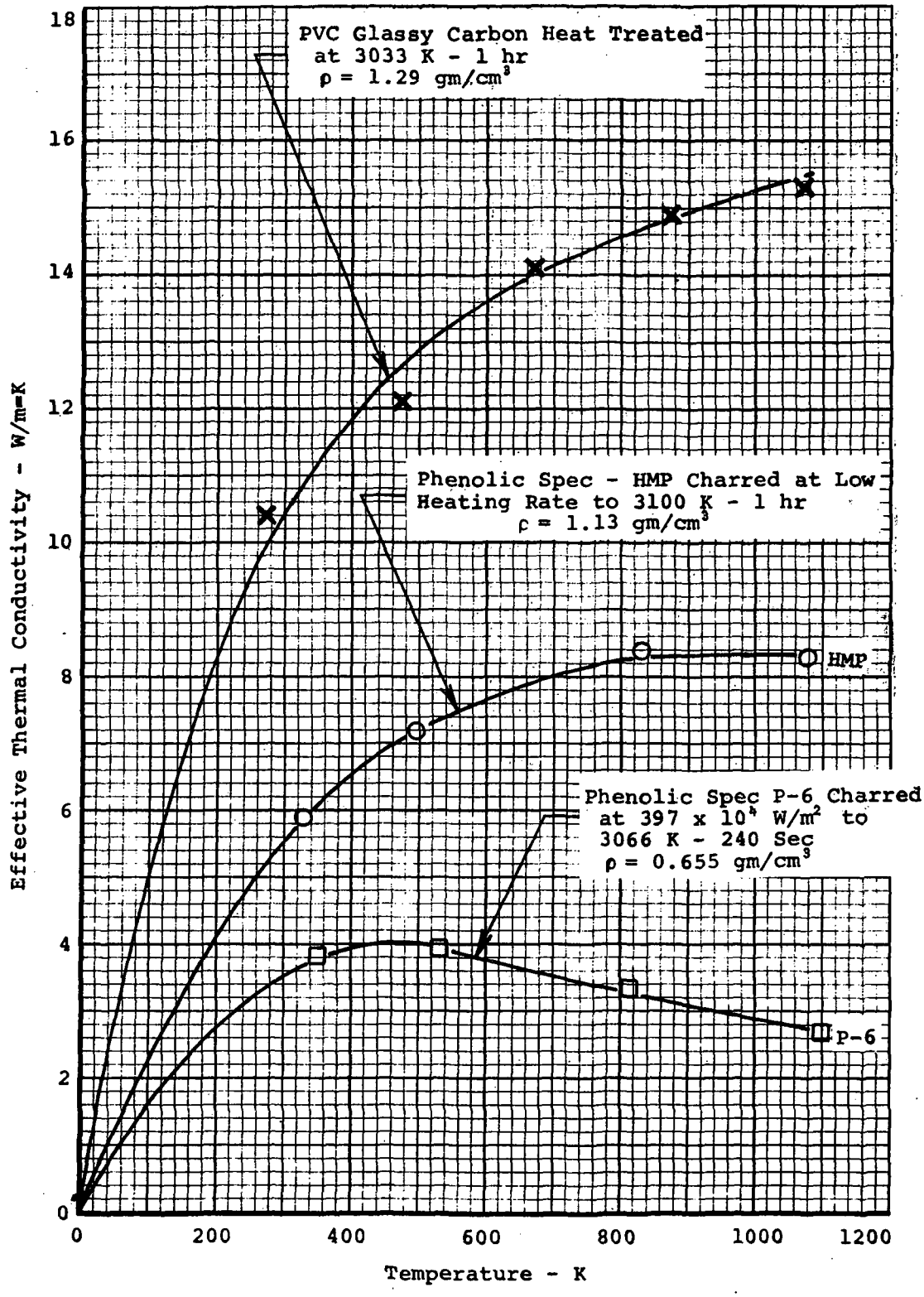

Figure 112. Effective thermal conductivity of charred phenolic and glassy carbon

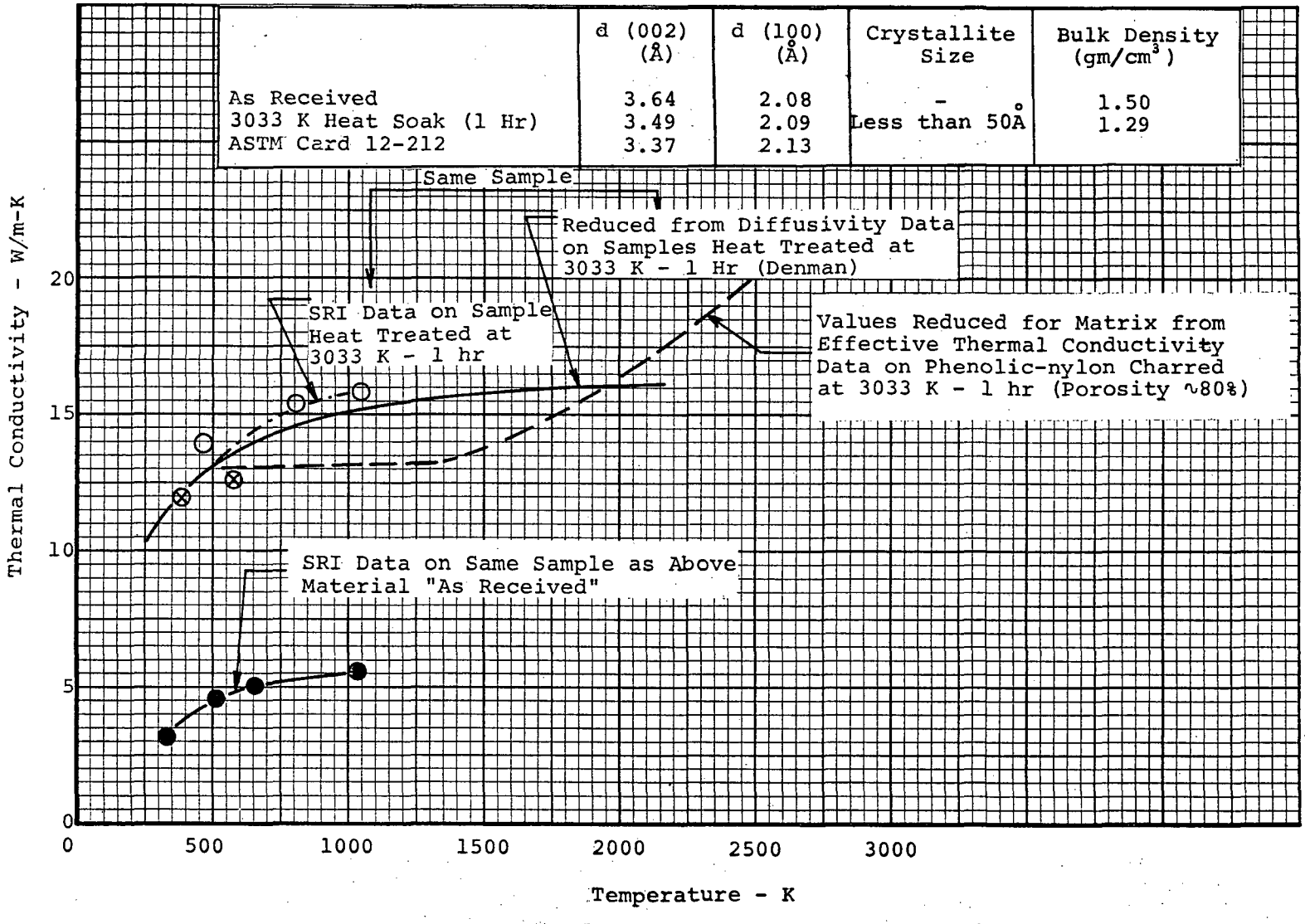

Figure 113. Thermal conductivity of dense PVC glassy carbon supplied by super temp

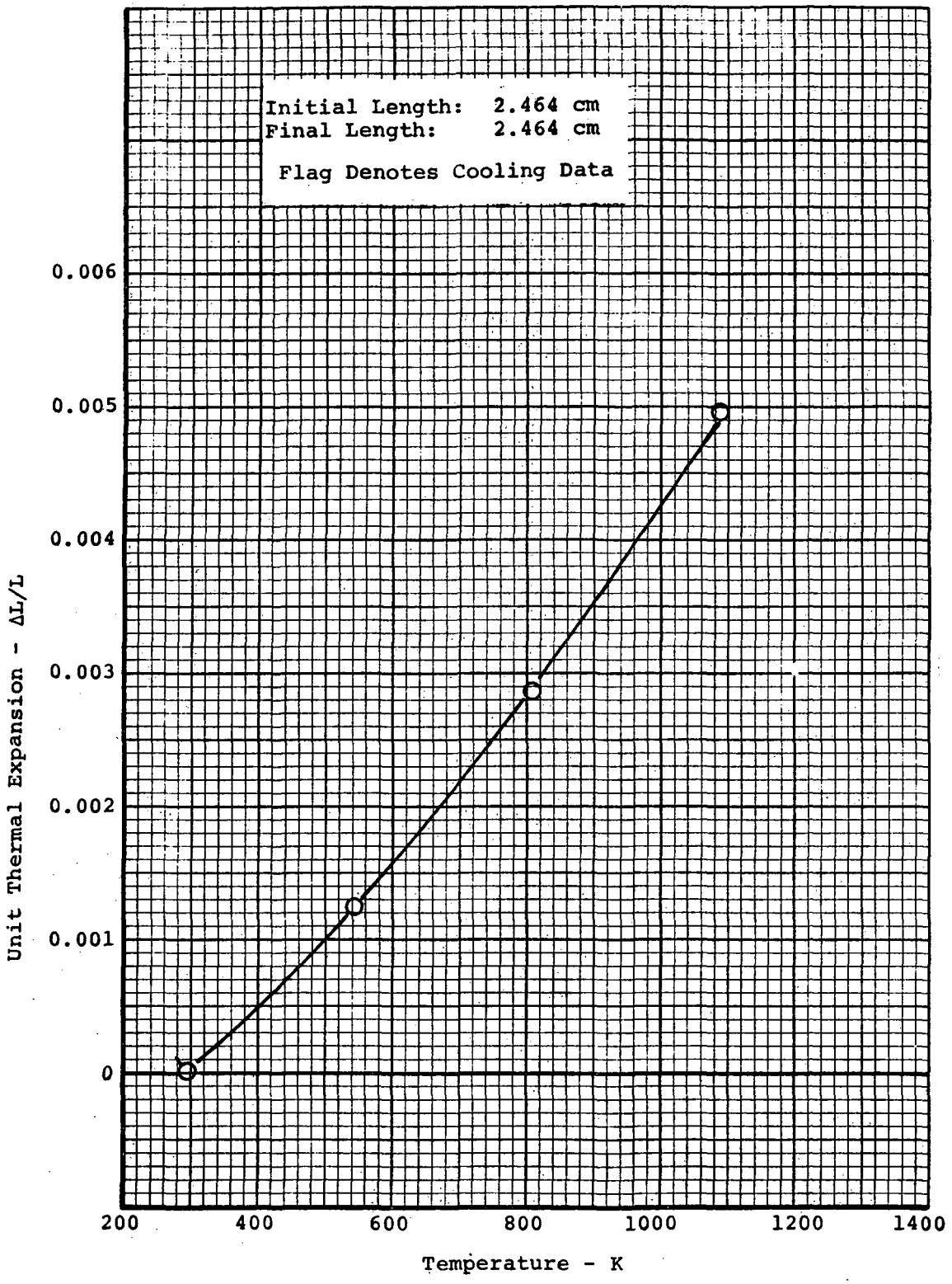

Figure 114. Thermal expansion of phenolic char prepared in the laboratory, specimen P-5

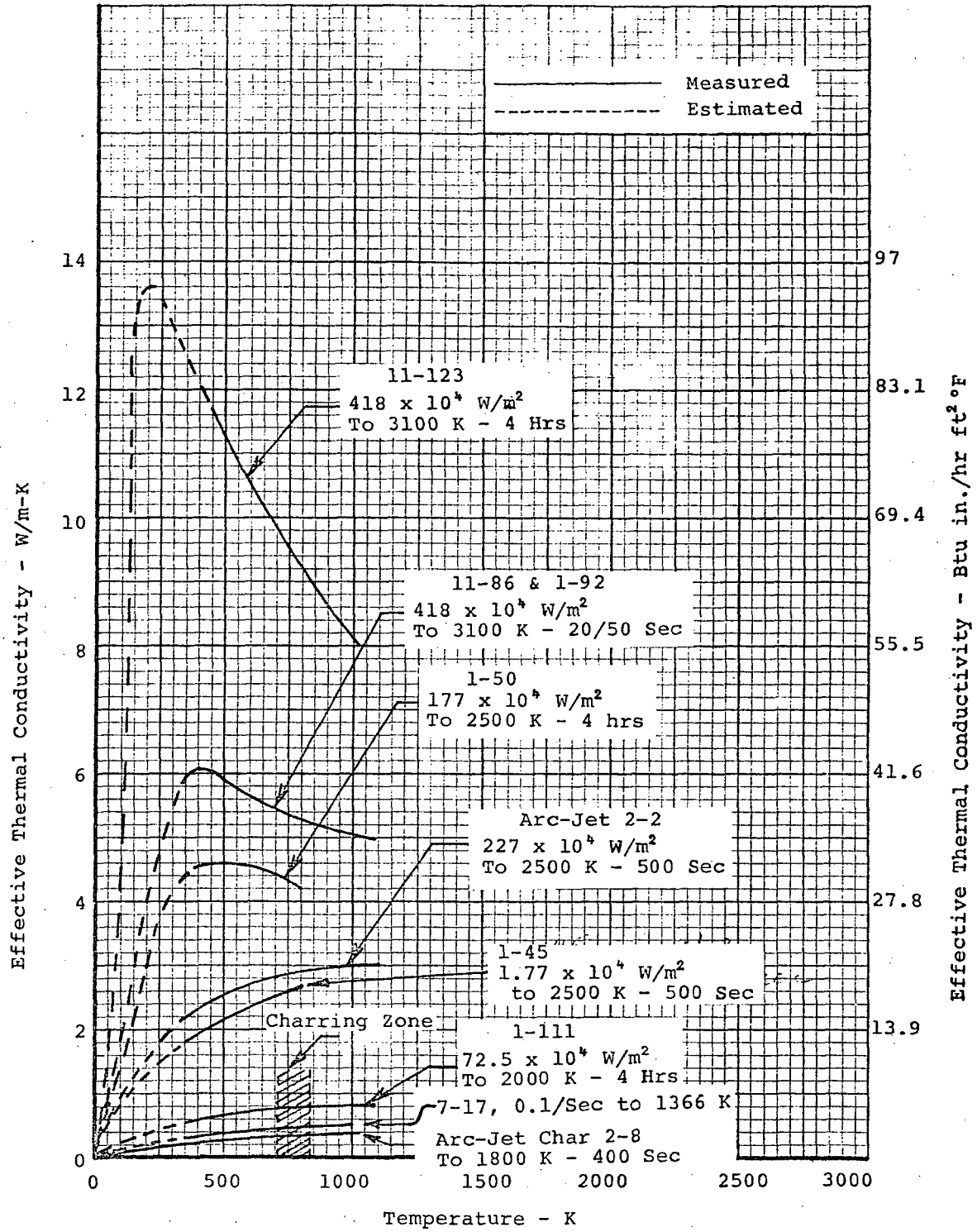

Figure 115. Effective thermal conductivities of low-density phenolic-nylon chars

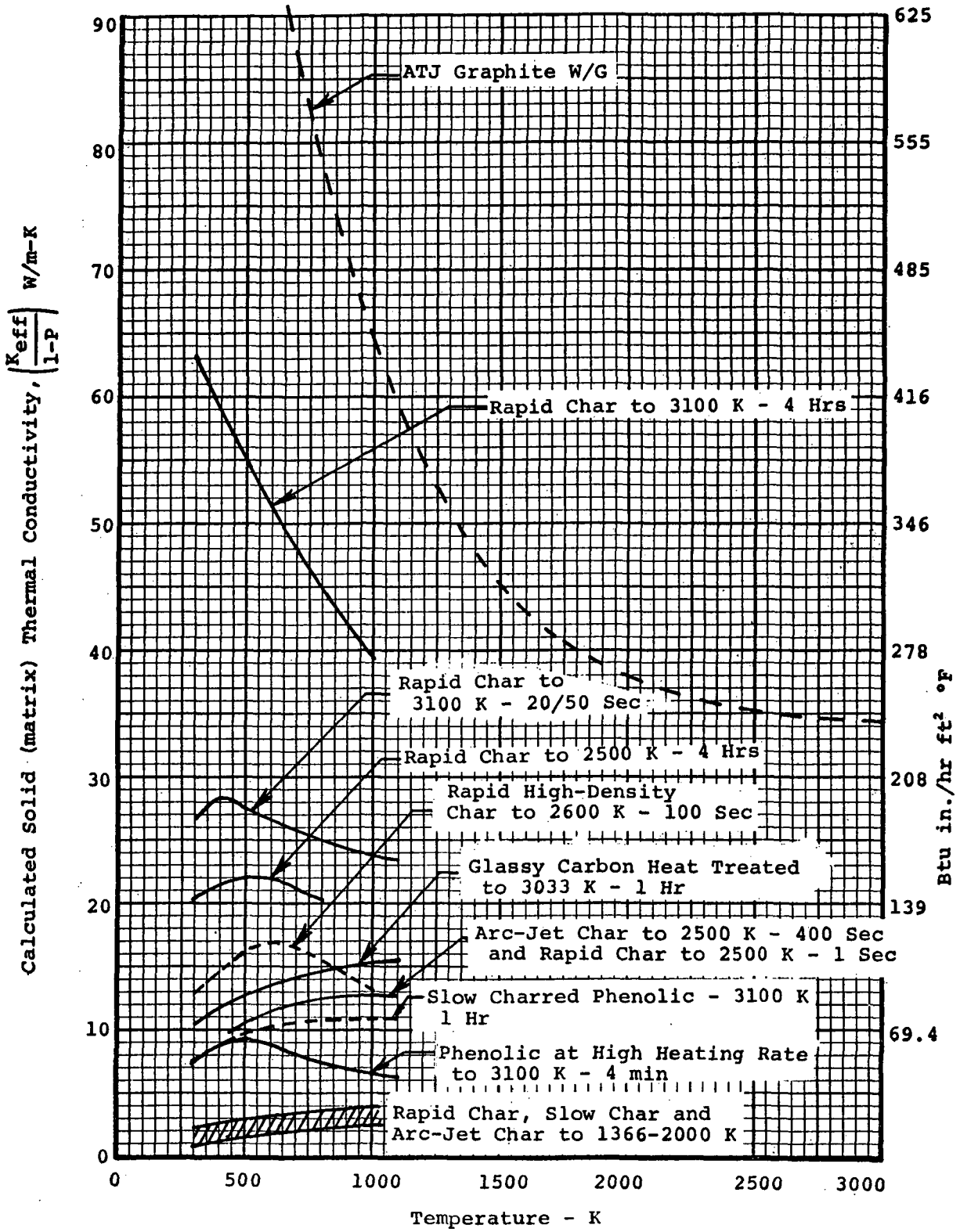

Figure 116. Composite plot of matrix conductivities of chars prepared from low-density phenolic-nylon, high-density phenolic-nylon, phenolic and glassy carbon at various conditions

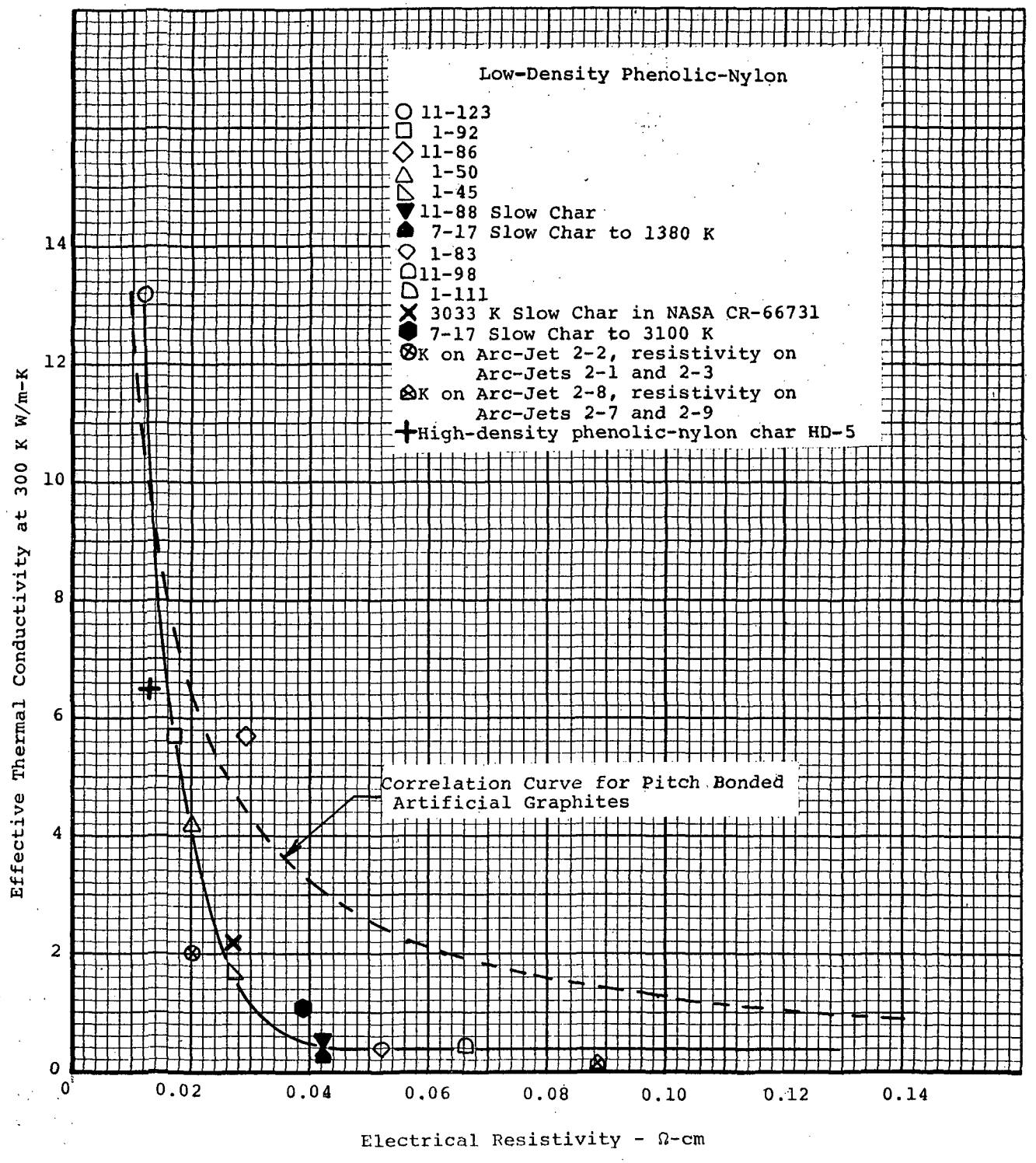

Figure 117. Correlation between effective thermal conductivity and electrical resistivity for various chars from low-density phenolic-nylon

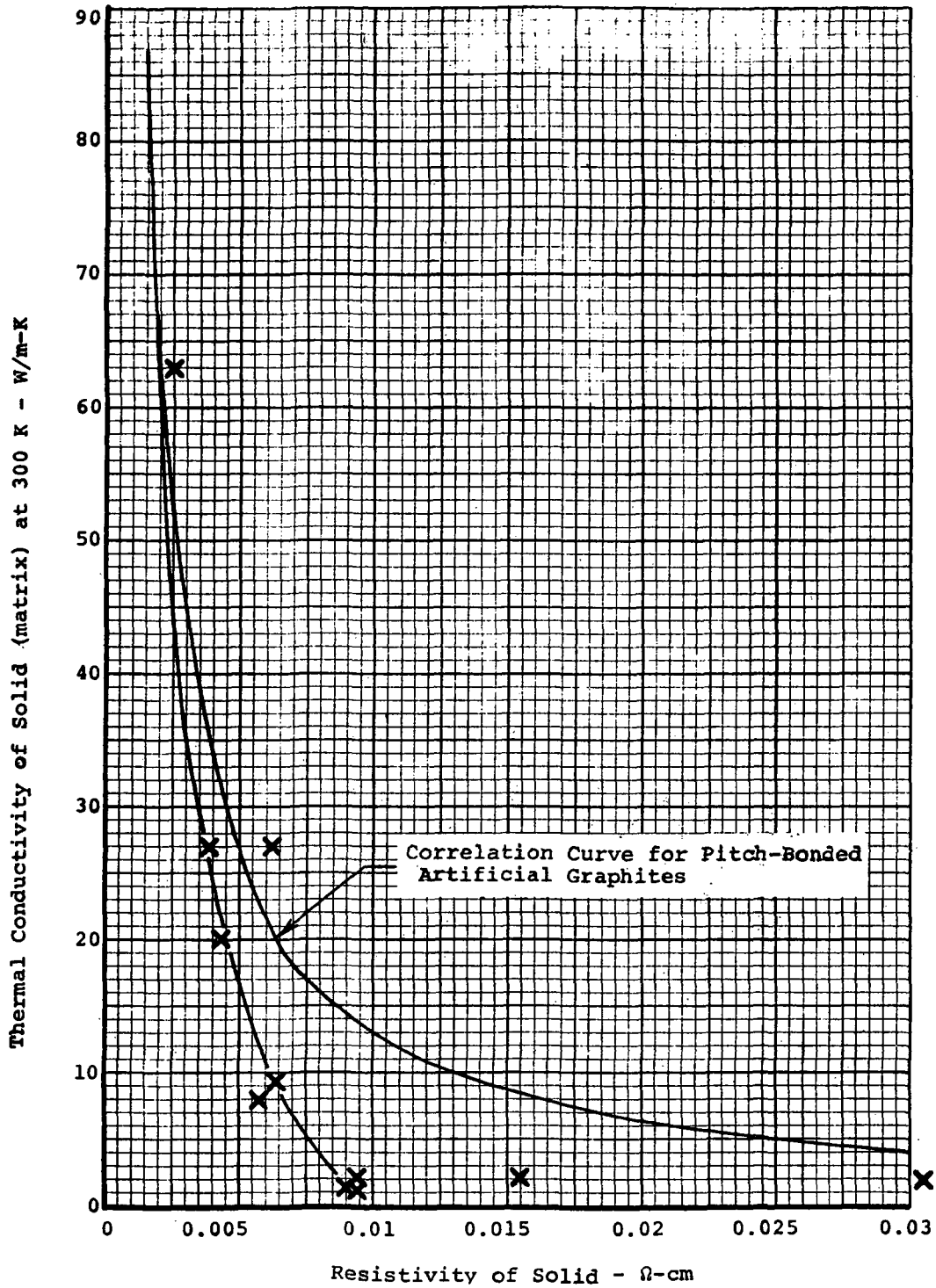

Figure 118. Correlation between thermal conductivity and electrical resistivity for solid (matrix) char

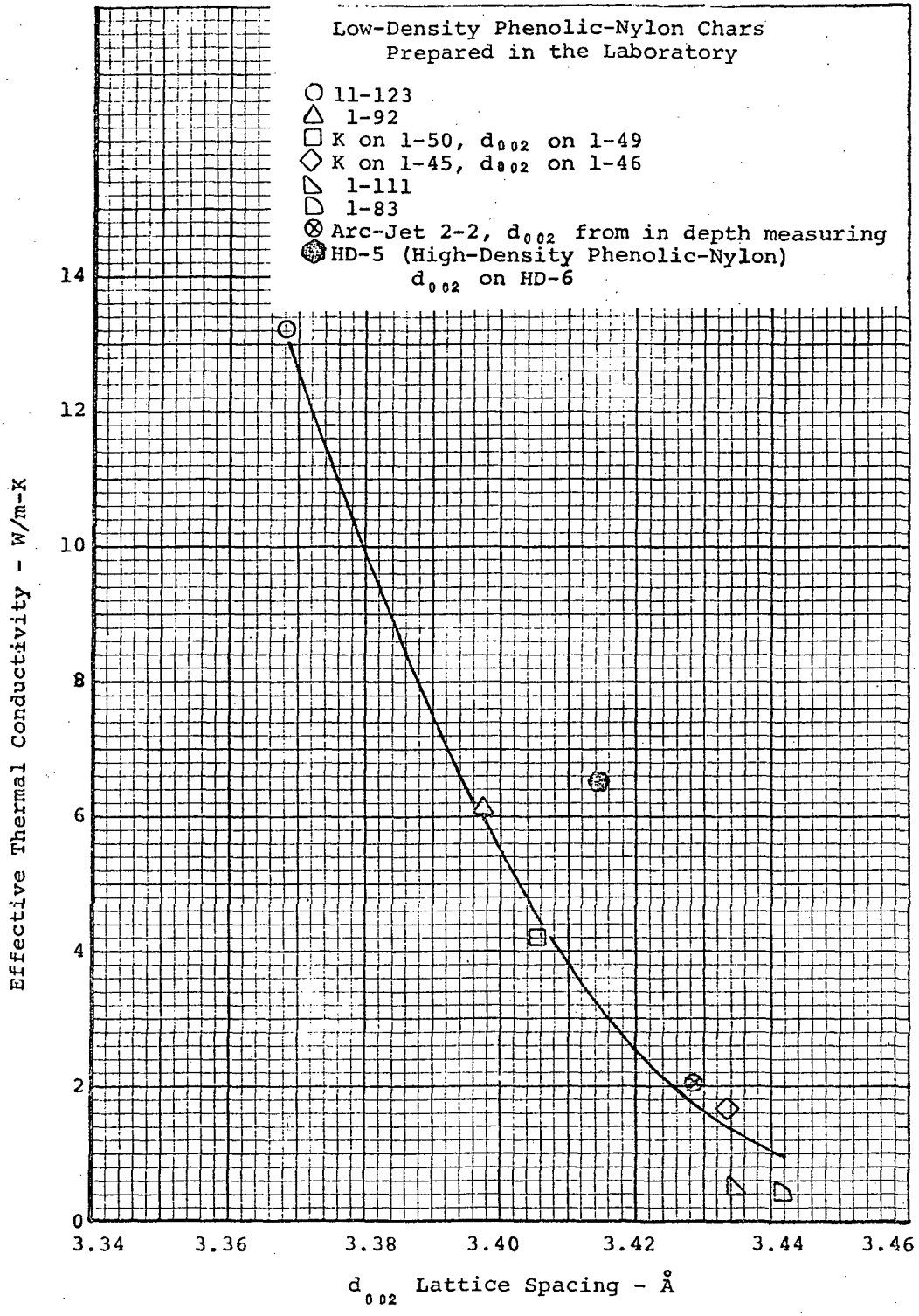

Figure 119. Correlation between effective thermal conductivity and d_{002} lattice spacing for chars prepared at rapid heating rates

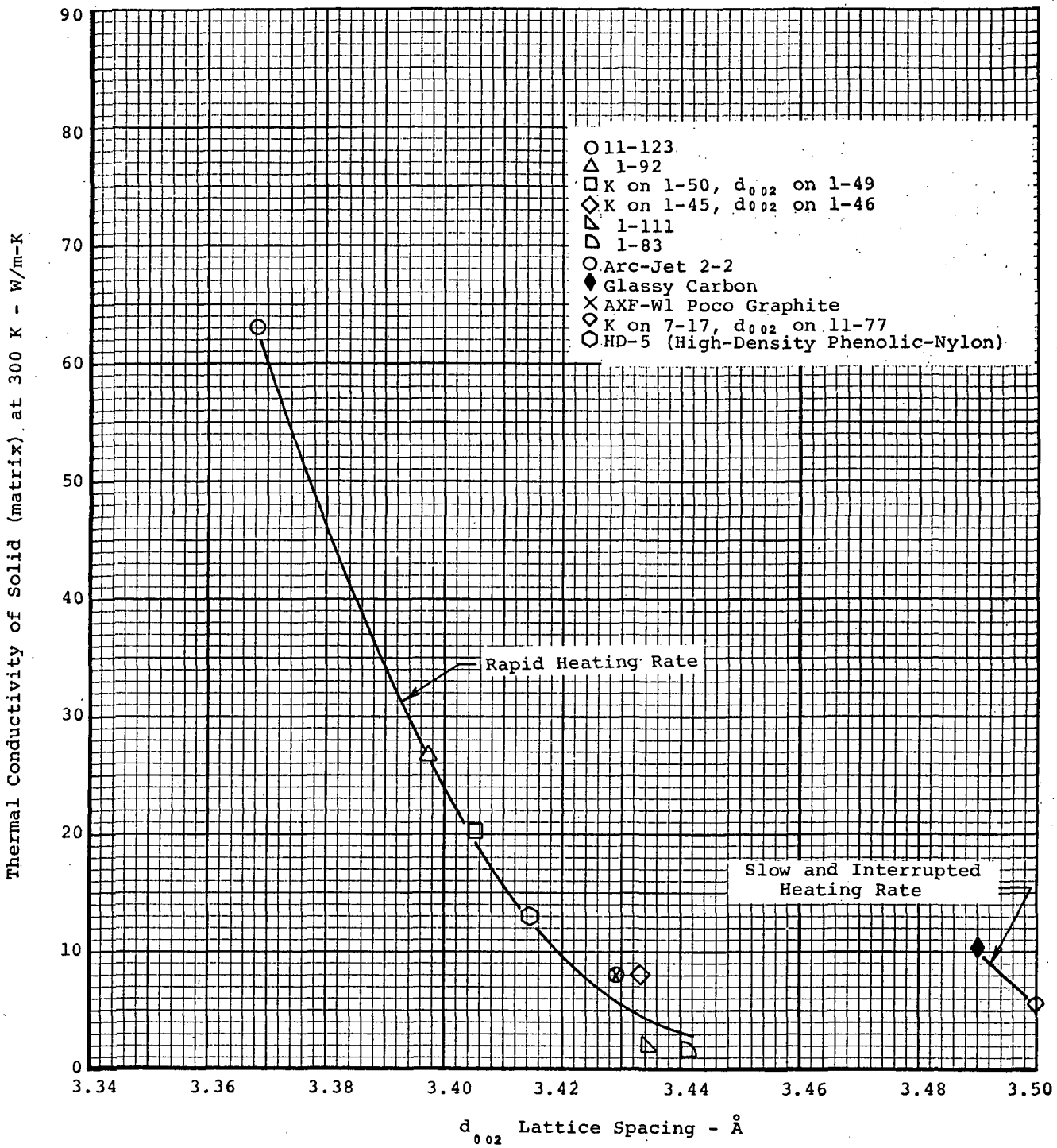

Figure 120. Correlation between calculated thermal conductivity of solid (matrix) and d_{002} lattice spacing for various chars

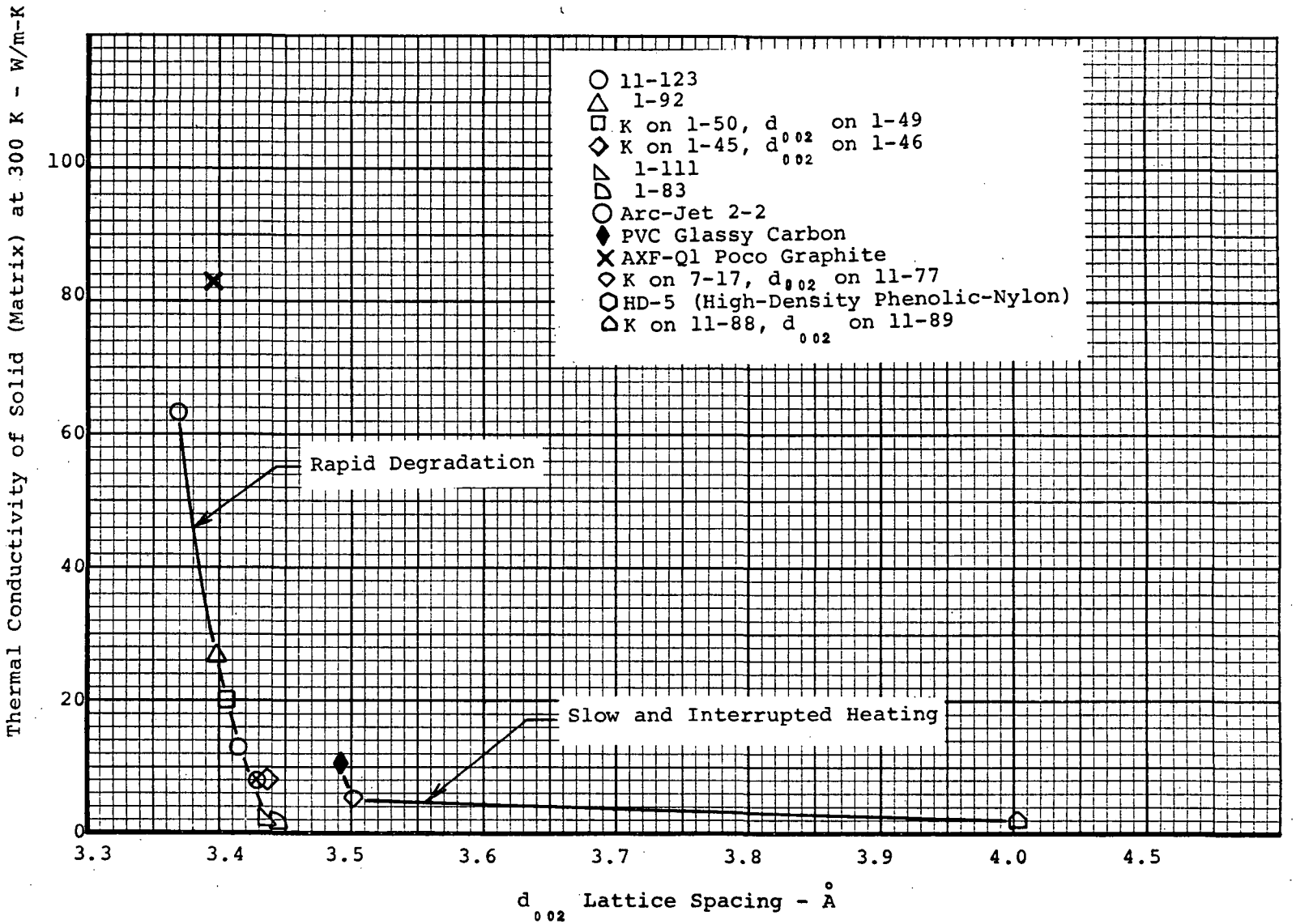

Figure 121. Correlation between calculated thermal conductivity of solid (matrix) and d_{002} lattice spacing for various chars

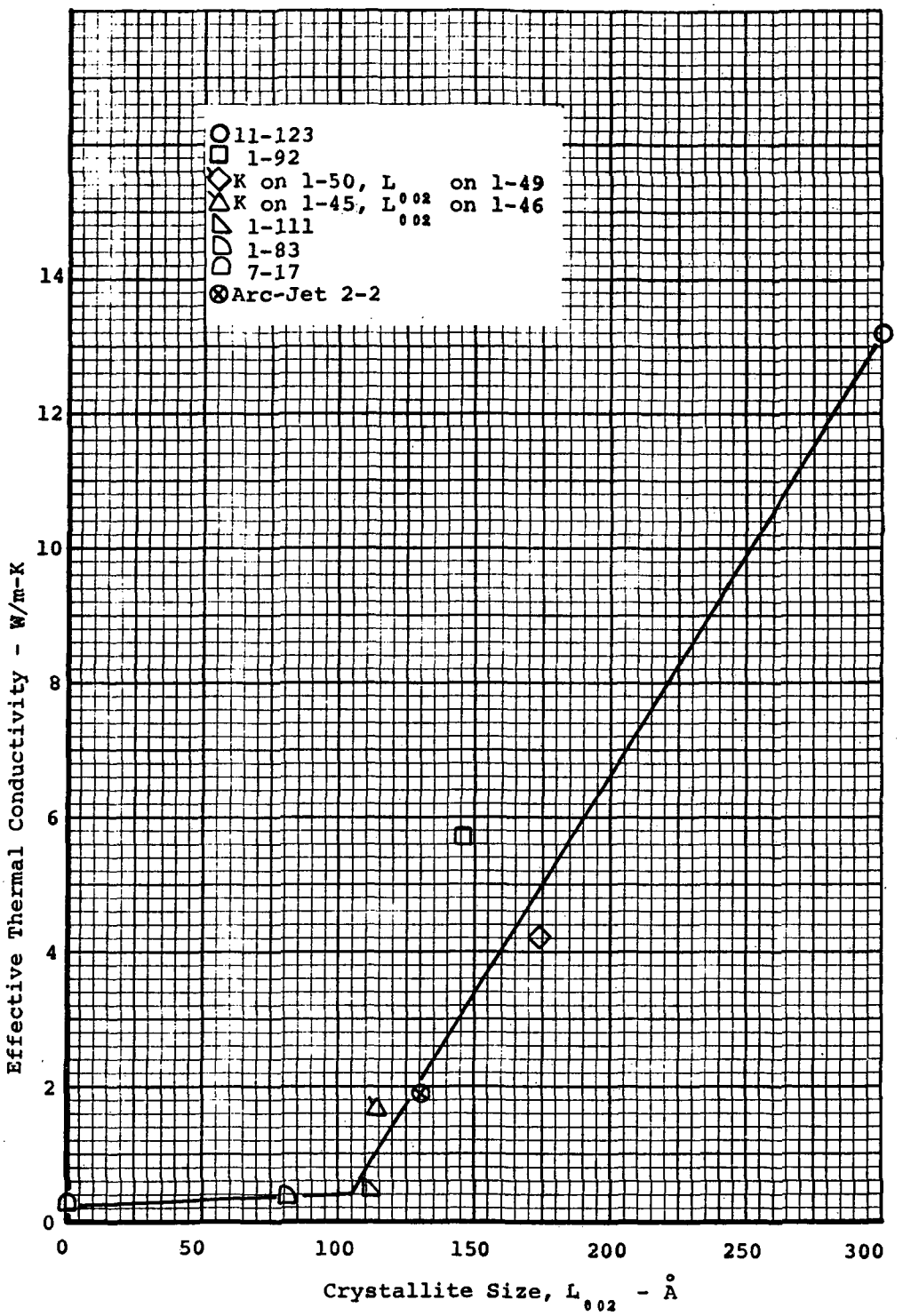

Figure 122. Correlation between effective thermal conductivity and crystallite size for char from low-density phenolic-nylon

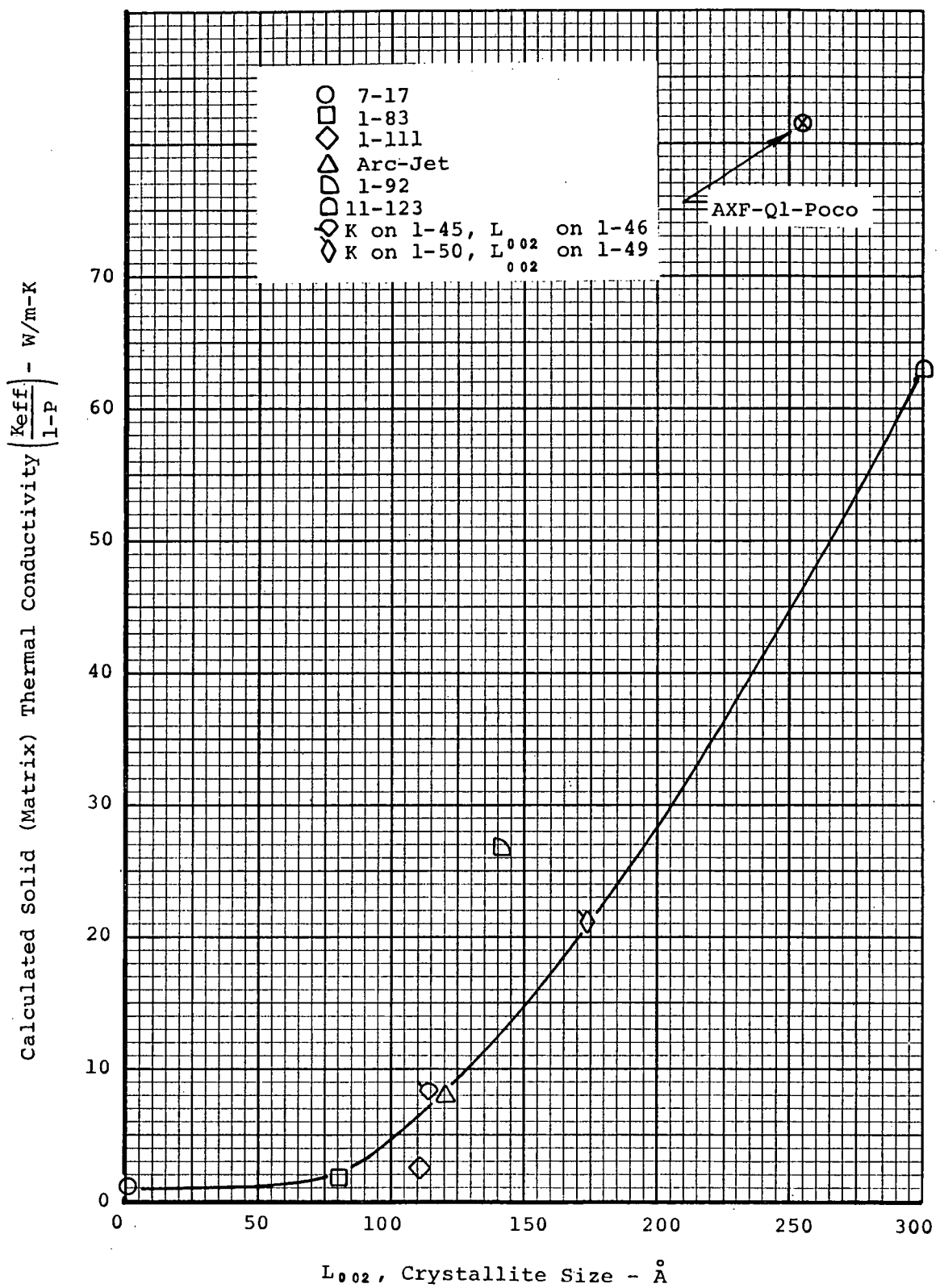

Figure 123. Correlation between calculated solid thermal conductivity and crystallite size for phenolic-nylon char

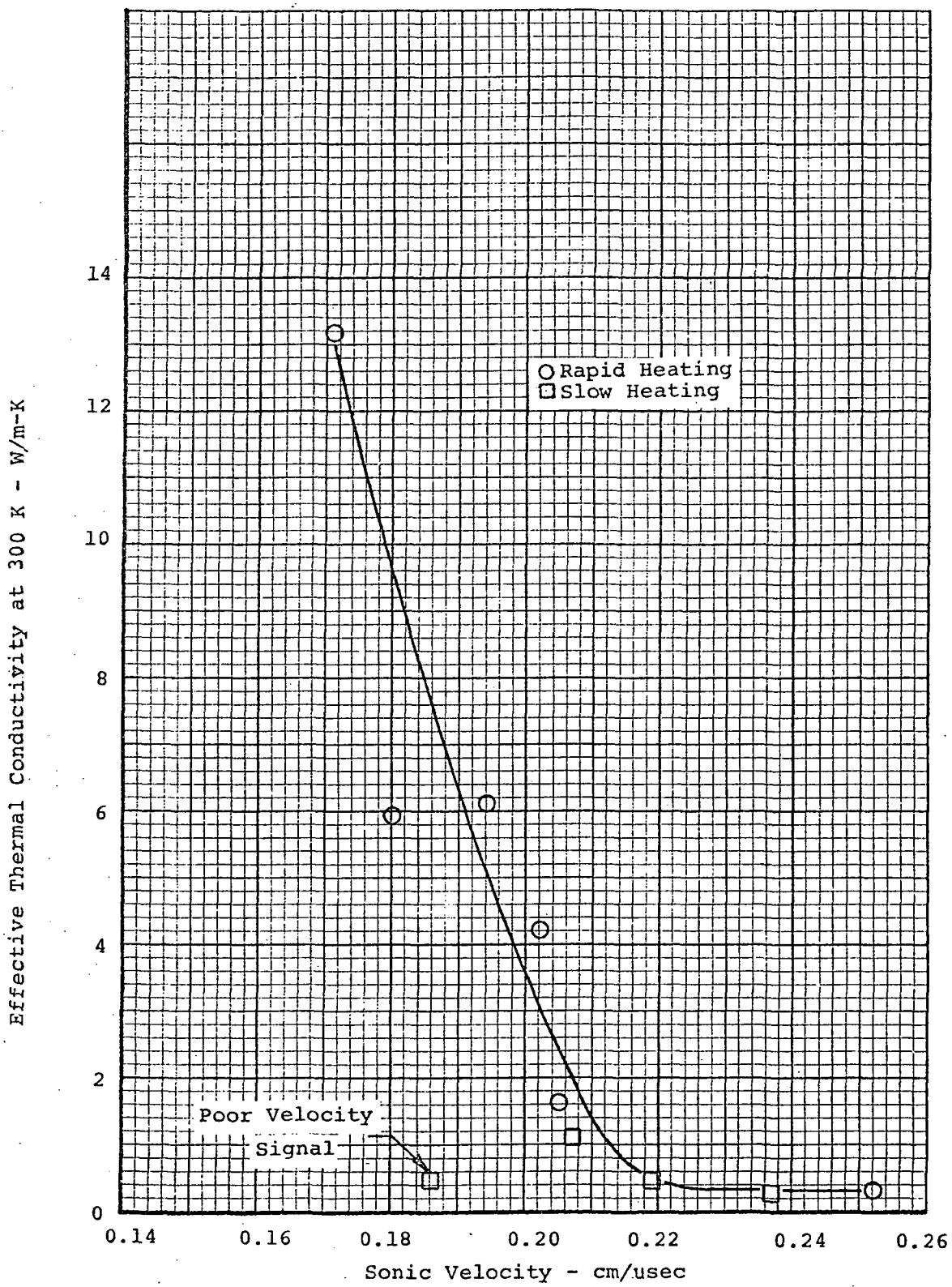

Figure 124. Correlation between effective thermal conductivity and sonic velocity for chars from low-density phenolic-nylon

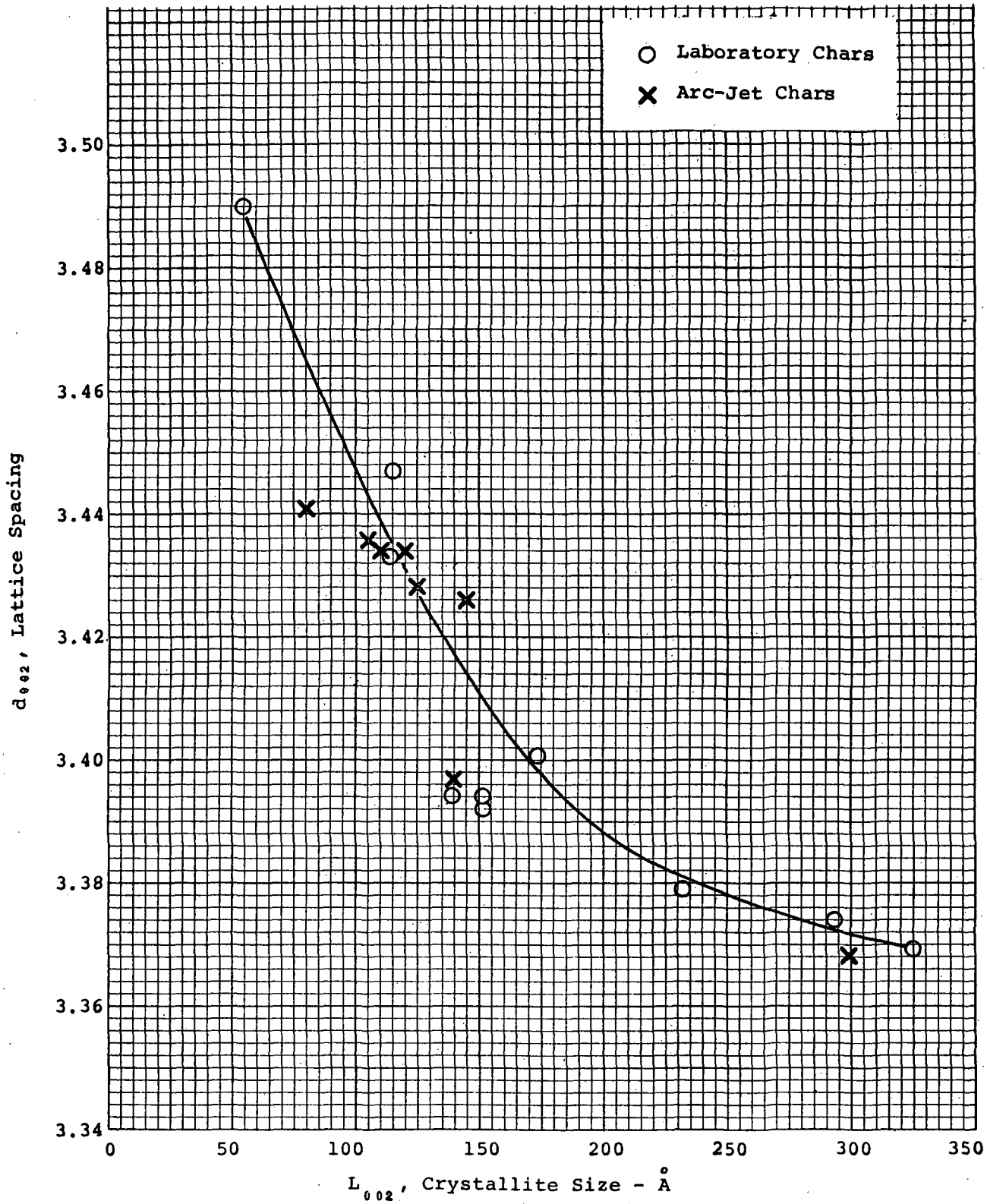

Figure 125. Correlation between lattice spacing and crystallite size for various chars

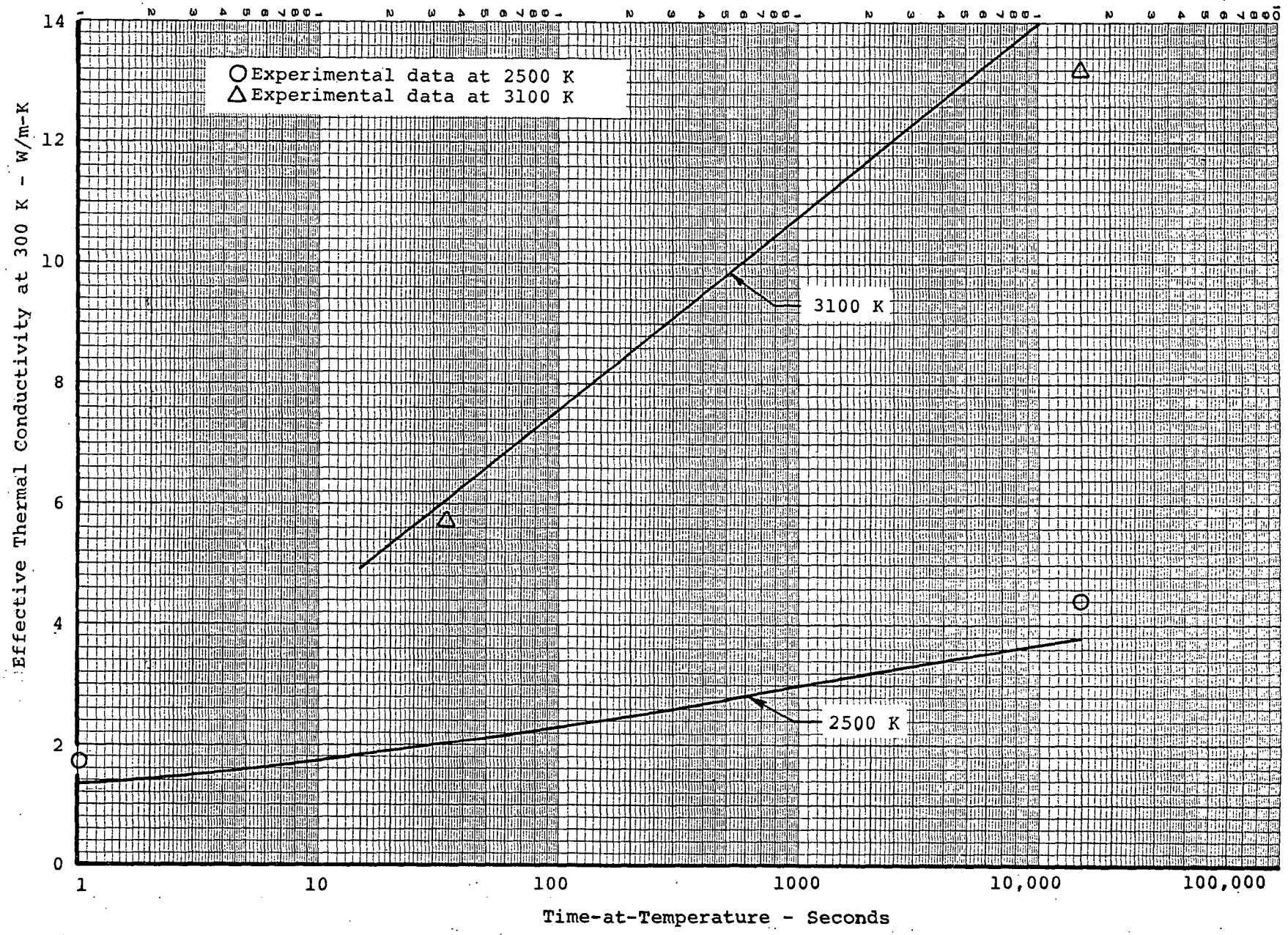

Figure 126. Effect of time-at-temperature on effective thermal conductivity as correlated from electrical resistivity versus time-at-temperature relationship

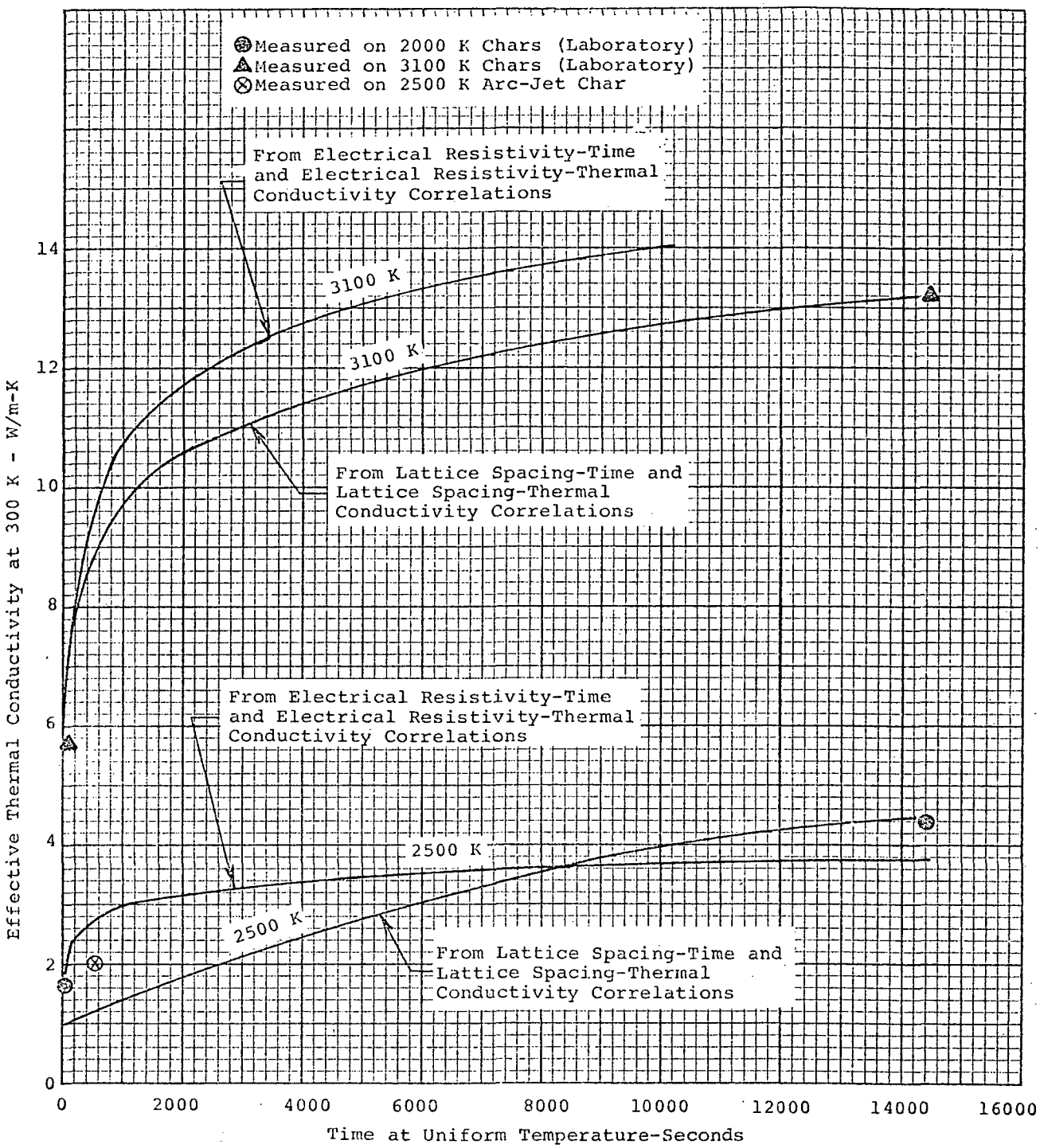

Figure 127. Effect of time-at-temperature on effective thermal conductivity for chars prepared in the laboratory at rapid heating rates from low-density phenolic-nylon

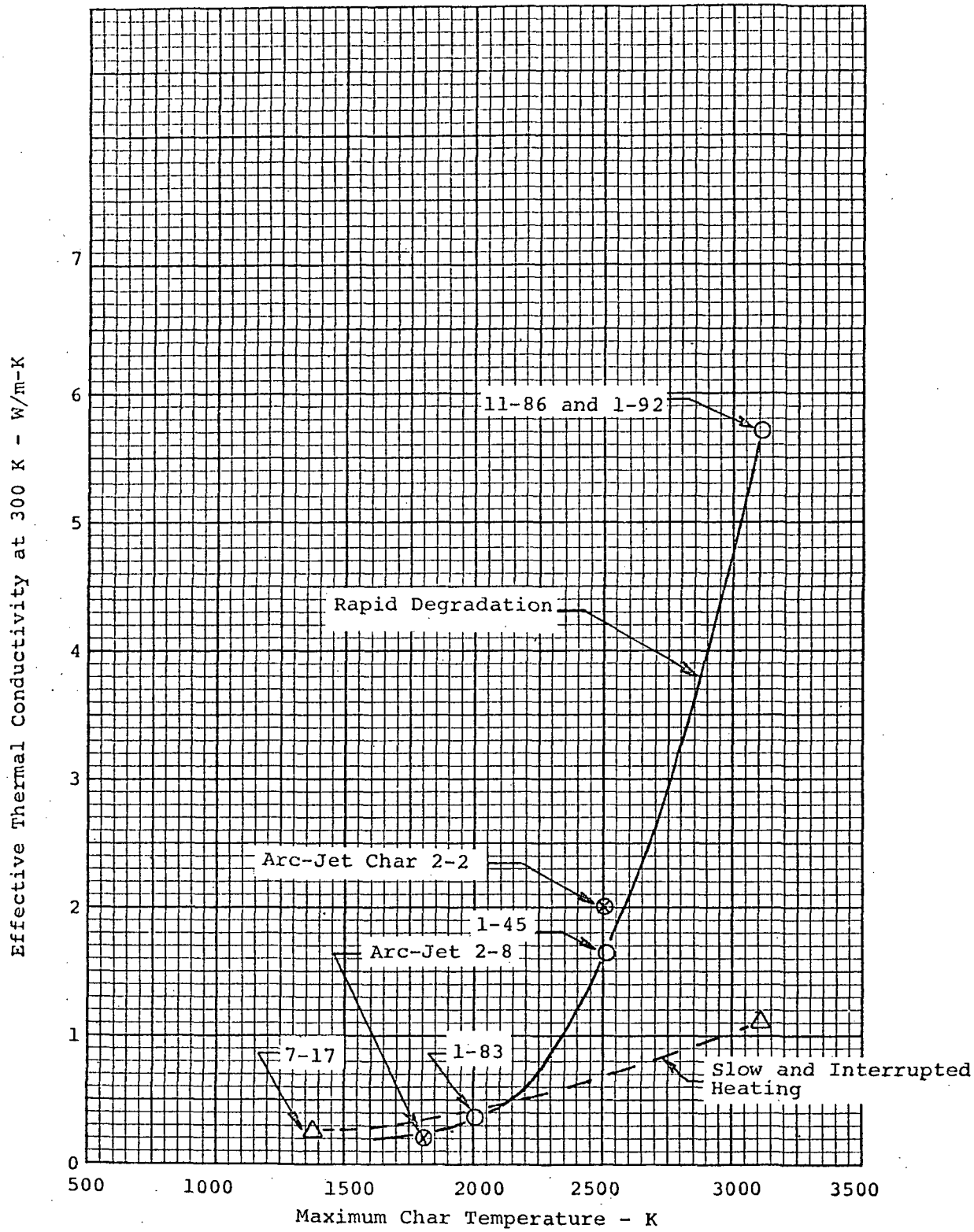

Figure 128. Effect of maximum char temperature on effective thermal conductivity for chars prepared in the laboratory at short times from low-density phenolic-nylon

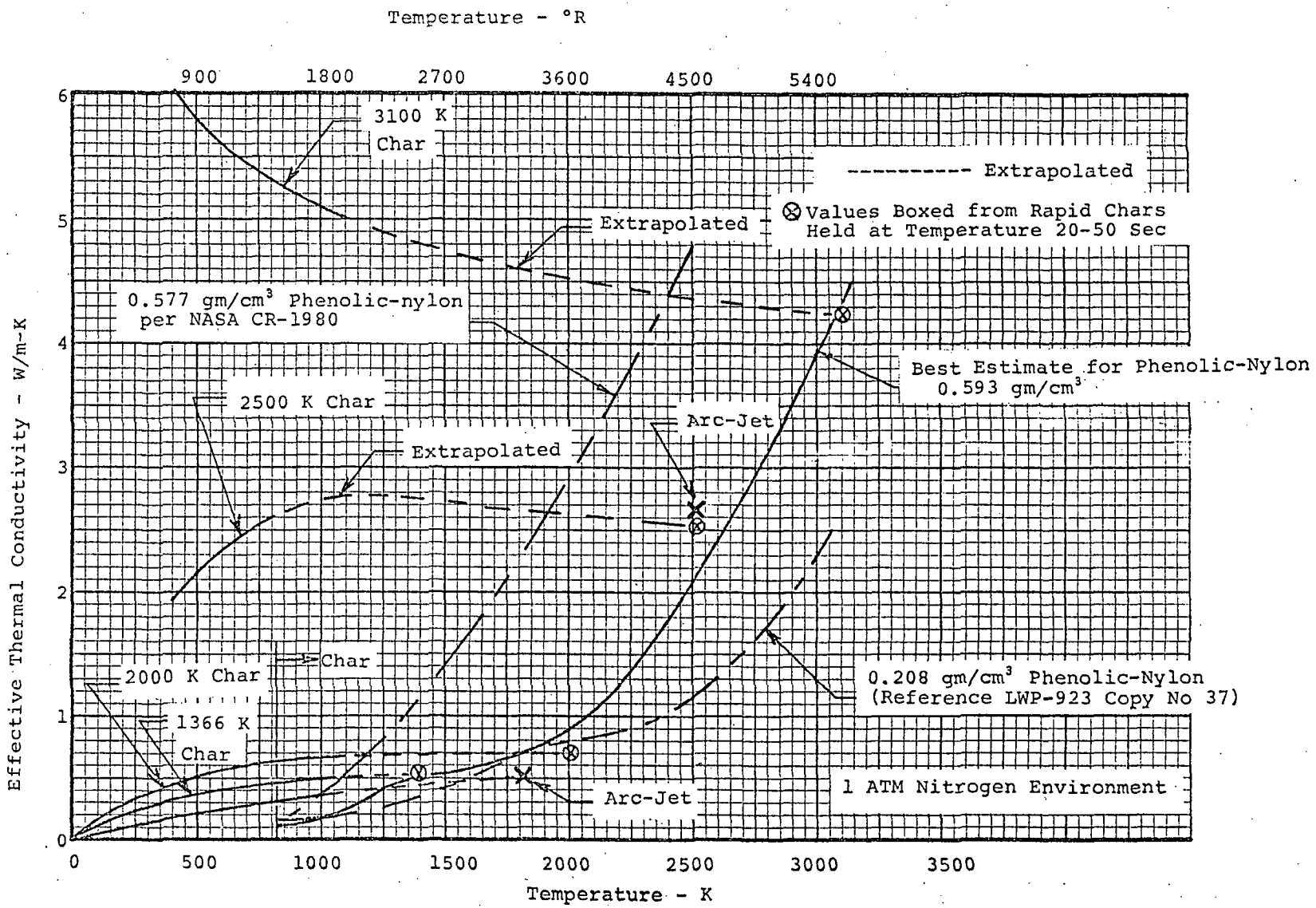

Figure 129. Best estimate of transient thermal conductivity of 0.593 gm/cm³ phenolic-nylon during degradation in a 1 ATM nitrogen environment - based on extrapolations of values measured on chars prepared by rapid heating for short times

REFERENCES

1. Flynn, D. R., "Thermal Guarding of Cut-Bar Apparatus", Conference on Thermal Conductivity Methods, Batelle Memorial Institute, 1961.

2. Flynn, D. R., "Thermal Conductivity of Ceramics", Mechanical and Thermal Properties of Ceramics, edited by J. B. Wachtman, Jr., NBS Special Publication 303, Washington, D.C., May 1969, pp. 63-123.

3. Gaal, P. S., Thermal Expansion of Glassy Carbon, WANL-TME-2802, Westinghouse Astronuclear Laboratory, February 1962.

4. Castle, J. G., "Heat Conduction in Carbon Materials", Proceedings of the First and Second Conferences on Carbon, University of Buffalo, Buffalo, New York, 1953 and 1955. P. 17.

5. Fair, F. V., and Collins, "Effect of Residence Time on Graphitization at Several Temperature", Proceedings of the Fifth Conference on Carbon. P. 503-508.

6. Jamieson, C. P. and Mrozowski, S.,"Thermal Conductivities of Polycrystalline Carbons and Graphites", Proceedings of the First and Second Conferences on Carbon, University of Buffalo, Buffalo, New York, 1953 and 1955, P. 159.

7. Ho, C. Y., Powell, R. W., and Liley, P. E., Thermal Conductivity of Selected Materials, Part 2, NSRDS-NBS 16, National Standard Reference Data Series - National Bureau of Standards - 16. U. S. Government Printing Office, Washington, D. C., February 1968.

8. Sanders, H. G., Smyly, E. D., and Pears, C. D., An Investigation of Some Thermal and Mechanical Properties of a Low-Density Phenolic-Nylon Ablation Material, NASA CR-66731, Southern Research Institute, February 1969.

9. Moyer, Carl B. and Green, Kenneth A., Demonstration of the Range over which the Langley Research Center Digital Computer Charring Ablation Program (CHAP) can be used with Confidence, NASA CR-1980, Aerotherm Corporation, February 1972.

10. Moss, James N., Olsen, George C., and Tompkins, S. S., Preliminary Thermophysical Property Data for very Low-Density Phenolic-Nylon and Elastomeric Ablators, LWP-923, Copy No. 37, Langley Research Center, Hampton, Virginia, December 22, 1970.